

THE JOURNAL OF PHYSICAL CHEMISTRY

(Registered in U. S. Patent Office)

M. Camp and K. Durham: The Foaming of Sodium Laurate Solutions—Factors Influencing Foam Stability.	993
Keihei Ueno and Arthur E. Martell: Infrared Study of Metal Chelates of Bisacetylacetonethylenediimine and Related Compounds.	998
S. E. S. El Wakkad, H. A. Rizk and I. G. Ebaid: The Electrochemical Behavior of the Tungsten Electrode and the Nature of the Different Oxides of the Metal.	1004
Eli S. Freeman and Saul Gordon: The Kinetics of the Underwater Corrosion of Powdered Magnesium.	1009
Paul Marx, C. W. Smith, A. E. Worthington and Malcolm Dole: Specific Heat of Synthetic High Polymers. IV. Polycaprolactam.	1015
Joseph J. Jasper and Elbert V. Kring: The Isobaric Surface Tensions and Thermodynamic Properties of the Surfaces of a Series of <i>n</i> -Alkanes, C ₅ to C ₁₅ , 1-Alkenes, C ₆ to C ₁₆ , and of <i>n</i> -Decylcyclopentane, <i>n</i> -Decylcyclohexane and <i>n</i> -Decylbenzene.	1019
W. H. Slabaugh: Heats of Immersion of Some Clay Systems in Aqueous Media.	1022
D. L. Hildenbrand and A. Greenville Whittaker: Burning Rate Studies. II. Variation of Temperature Distribution with Consumption Rate for Burning Liquid Systems.	1024
Henry G. Kuivila: Correlation of the Acidity Function, <i>H</i> ₀ , with Activities of Acid and Water.	1028
S. Z. Lewin: The Crystal Growth of Lead Chloride from Aqueous Solutions.	1030
Robert W. Phillips, Charles A. Orlick and Rudolph Steinberger: The Kinetics of the Thermal Decomposition of Nitrocellulose.	1034
R. G. Haldeman and P. H. Emmett: Specific Adsorption of Alkyl Orange Dyes on Silica Gel.	1039
Norman E. White and Martin Kilpatrick: Association of N-H Compounds. I. In Benzene.	1044
J. G. Aston, R. J. Tykodi and W. A. Steele: Tests of a Simplified General Model for Adsorption of Rare Gases on Solids.	1053
J. R. Dacey, J. F. Smelko and D. M. Young: The Sorption of Gases by Vacant Clathrate Compounds.	1058
Leon Wright, Sol Weller and G. A. Mills: Homogeneous Catalytic Hydrogenation. III. Cuprous and Silver Acetate in Pyridine and Dodecylamine.	1060
Terrell L. Hill: Corresponding States in Multilayer Step Adsorption.	1065
Hadden Clark: Vertical Discontinuities in the Adsorption Isotherm of Krypton on Graphitized Carbon Black.	1068
Sherwood F. West and L. F. Audrieth: Differential Thermal Analysis of Some Heteropoly Acids of Molybdenum and Tungsten.	1069
Clyde R. Simmons and Robert S. Hansen: Solvolysis of Hafnium and Zirconium Tetrachlorides in Methyl and Ethyl Alcohols.	1072
Melvin C. Baker, Philip A. Lyons and S. J. Singer: Some Physical Chemical Studies with Heteropoly Acids.	1074
F. K. Hassion, D. C. Thurmond and F. A. Trumbore: On the Melting Point of Germanium.	1076
Russell K. Edwards and James H. Downing: Mechanisms of Permeation of Silver, Copper and Mercury Gases of Solid Graphite Walls.	1079
Kenzi Tamaru: The Thermal Decomposition of Stibine.	1084
Russell S. Holland and Charles P. Smyth: Microwave Absorption and Molecular Structure in Liquids. X. The Relaxation Times of Nine Heterocyclic Molecules.	1088
B. J. Masters and G. E. Challenger: The Reduction of Ce(IV) in Solutions Irradiated by Au ¹⁹⁸ β-Particles.	1093
H. W. Fox, E. F. Hare and W. A. Zisman: Wetting Properties of Organic Liquids on High-Energy Surfaces.	1097
Note: P. L. Walker, Jr., and F. Rusinko, Jr.: Sorption-Hysteresis Properties of Gases on Carbonyl Iron Powder.	1106
Note: M. El Nadi and F. Abu Zeid: On the Sutherland Model for the Viscosity of Gases.	1107
Note: Donald S. MacIver and Paul H. Emmett: Surface Area Measurements on Carbon Black Produced by the Catalytic Decomposition of Carbon Monoxide over Iron.	1109

THE JOURNAL OF PHYSICAL CHEMISTRY

(Registered in U. S. Patent Office)

W. ALBERT NOYES, JR., EDITOR

ALLEN D. BLISS

ASSISTANT EDITORS

ARTHUR C. BOND

EDITORIAL BOARD

R. P. BELL

PAUL M. DOTY

S. C. LIND

E. J. BOWEN

G. D. HALSEY, JR.

H. W. MELVILLE

R. E. CONNICK

J. W. KENNEDY

W. O. MILLIGAN

R. W. DODSON

E. A. MOELWYN-HUGHES

Published monthly by the American Chemical Society at 20th and Northampton Sts., Easton, Pa.

Entered as second-class matter at the Post Office at Easton, Pennsylvania.

The *Journal of Physical Chemistry* is devoted to the publication of selected symposia in the broad field of physical chemistry and to other contributed papers.

Manuscripts originating in the British Isles, Europe and Africa should be sent to F. C. Tompkins, The Faraday Society, 6 Gray's Inn Square, London W. C. 1, England.

Manuscripts originating elsewhere should be sent to W. Albert Noyes, Jr., Department of Chemistry, University of Rochester, Rochester 3, N. Y.

Correspondence regarding accepted copy, proofs and reprints should be directed to Assistant Editor, Allen D. Bliss, Department of Chemistry, Simmons College, 300 The Fenway, Boston 15, Mass.

Business Office: Alden H. Emery, Executive Secretary, American Chemical Society, 1155 Sixteenth St., N. W., Washington 6, D. C.

Advertising Office: Reinhold Publishing Corporation, 430 Park Avenue, New York 22, N. Y.

Articles must be submitted in duplicate, typed and double spaced. They should have at the beginning a brief Abstract, in no case exceeding 300 words. Original drawings should accompany the manuscript. Lettering at the sides of graphs (black on white or blue) may be pencilled in, and will be typeset. Figures and tables should be held to a minimum consistent with adequate presentation of information. Photographs will not be printed on glossy paper except by special arrangement. All footnotes and references to the literature should be numbered consecutively and placed in the manuscript at the proper places. Initials of authors referred to in citations should be given. Nomenclature should conform to that used in *Chemical Abstracts*, mathematical characters marked for italic, Greek letters carefully made or annotated, and subscripts and superscripts clearly shown. Articles should be written as briefly as possible consistent with clarity and should avoid historical background unnecessary for specialists.

Symposium papers should be sent in all cases to Secretaries of Divisions sponsoring the symposium, who will be responsible for their transmittal to the Editor. The Secretary of the Division by agreement with the Editor will specify a time after which symposium papers cannot be accepted. The Editor reserves the right to refuse to publish symposium articles, for valid scientific reasons. Each symposium paper may not exceed four printed pages (about sixteen double spaced typewritten pages) in length except by prior arrangement with the Editor.

Remittances and orders for subscriptions and for single copies, notices of changes of address and new professional connections, and claims for missing numbers should be sent to the American Chemical Society, 1155 Sixteenth St., N. W., Washington 6, D. C. Changes of address for the *Journal of Physical Chemistry* must be received on or before the 30th of the preceding month.

Claims for missing numbers will not be allowed (1) if received more than sixty days from date of issue (because of delivery hazards, no claims can be honored from subscribers in Central Europe, Asia, or Pacific Islands other than Hawaii), (2) if loss was due to failure of notice of change of address to be received before the date specified in the preceding paragraph, or (3) if the reason for the claim is "missing from files."

Subscription Rates: to members of the American Chemical Society, \$8.00 for 1 year, \$15.00 for 2 years, \$22.00 for 3 years; to non-members, \$10.00 for 1 year, \$18.00 for 2 years, \$26.00 for 3 years. Postage free to countries in the Pan American Union; Canada, \$0.40; all other countries, \$1.20. \$12.50 per volume, foreign postage \$1.20, Canadian postage \$0.40; special rates for A.C.S. members supplied on request. Single copies, current volume, \$1.00; foreign postage, \$0.15; Canadian postage \$0.05. Back issue rates (starting with Vol. 56): \$15.00 per volume, foreign postage \$1.20, Canadian, \$0.40; \$1.50 per issue, foreign postage \$0.15, Canadian postage \$0.05.

The American Chemical Society and the Editors of the *Journal of Physical Chemistry* assume no responsibility for the statements and opinions advanced by contributors to THIS JOURNAL.

The American Chemical Society also publishes *Journal of the American Chemical Society*, *Chemical Abstracts*, *Industrial and Engineering Chemistry*, *Chemical and Engineering News*, *Analytical Chemistry*, and *Journal of Agricultural and Food Chemistry*. Rates on request.

(Continued from first page of cover)

Note: Leon M. Dorfman and F. J. Shipko: Radiation-Induced Exchange of Hydrogen Isotopes: Chain Inhibition	1110
Note: G. H. Cartledge and Wm. T. Smith, Jr.: Revision of the Electrode Potential Diagram for Technetium	1111
Note: C. S. Caldwell and A. L. Babb: Diffusion in the System Methanol-Benzene	1113
Note: Jui H. Wang: On the Role of Diffusion in Catalysis	1115
Note: E. Lee Purlee and Ernest Grunwald: A Reversible Silver-Silver Chloride Electrode for 95% (volume) Methanol-Water Solutions	1112
Note: L. H. Reyerson and Lowell Peterson: The Sorption of Gaseous Hydrogen Chloride by Crystalline Insulin	1117
Note: F. X. Hassion, A. J. Goss and F. A. Trumbore: On the Germanium-Silicon Phase Diagram	1118
Note: William C. Boyd: Table of Axial Ratios Calculated from the Perrin Equation	1119
Note: Karol J. Mysels and Horst W. Hoyer: Tracer Electrophoresis. IV. Modified Brady Method	1119

THE JOURNAL OF PHYSICAL CHEMISTRY

(Registered in U. S. Patent Office) (Copyright, 1955 by the American Chemical Society)

VOLUME 59

OCTOBER 25, 1955

NUMBER 10

THE FOAMING OF SODIUM LAURATE SOLUTIONS— FACTORS INFLUENCING FOAM STABILITY

By M. CAMP AND K. DURHAM

Research Department, Unilever Limited Port Sunlight, Cheshire, England

Received January 11, 1955

The effects of addition of electrolytes on the foam stability, surface tension and surface viscosity of 0.1% solutions of sodium laurate adjusted to pH 10 have been studied. The electrolytes employed had no significant effect on surface viscosity, but produced a progressive lowering in surface tension which is a function of cation concentration. The size and concentration of the hydrated cations were found to influence foam stability; thus the alkali metals increase foam stability in the order $\text{Li}^+ < \text{Na}^+ < \text{K}^+ < \text{Cs}^+$. Anions were also found to increase foam stability in the order, $\text{I}^- < \text{OH}^- < \text{SO}_4^{--} < \text{NO}_3^- < \text{CO}_3^{--} < \text{SiO}_3^{--} < \text{Cl}^-$. In addition Na_2HPO_4 , $\text{Na}_4\text{P}_2\text{O}_7$ and $\text{Na}_5\text{P}_3\text{O}_{10}$ are found to have a marked stabilizing effect on foams from sodium laurate solutions adjusted to pH 10. Factors influencing foam stability are enumerated and discussed and it is concluded that, although surface viscosity may not be very important, the rate of attainment of equilibrium surface tension is important in determining the stability of thin films.

Introduction

The effect of hydrogen ion concentration on the surface properties of sodium laurate solutions has been investigated by Powney¹ who found that if the pH of a 0.1% solution was increased from 7.5 to 9.5 the surface tension was increased by about 25 dynes/cm. This effect was attributed to the suppression of hydrolysis at the high pH with the consequent reduction in the concentration of the highly surface-active acid soap. Under similar conditions of suppressed hydrolysis Miles and Ross² found that the foaming power of sodium laurate solutions was negligible. It may be concluded from these results that the fatty acid acts as a foam stabilizer by packing between the adsorbed soap ions in the surface changing a tenuous surface film into one which is more coherent and more able to withstand disturbances.

Preliminary work in these laboratories confirmed the observations of Miles and Ross but revealed that 0.1% solutions of sodium laurate could have good foaming properties if the concentration of sodium ions in solution was increased to a relatively high value, even though this involved, in some cases, an increase in pH to considerably greater than 10. This paper describes the extension of the above experiments to include the effects of electrolytes on the stability of foams from sodium laurate solutions ad-

justed to pH 10 and also on the surface properties of the soap solutions.

Materials. Sodium Laurate.—The lauric acid used had an equivalent weight of 201.0 (theory 200.3) and a melting point of 43.95° (accepted value 43.8°). The fatty acid was neutralized with an alcoholic solution of NaOH; the neutral solution was evaporated to dryness and the soap was subsequently dried in a vacuum oven over P_2O_5 .

Inorganic Salts.—All the salts used as additives were analytical reagent grade with the exception of sodium metasilicate ("Metso," Crosfields, Warrington) and the sodium tripolyphosphate which was a commercial sample (Albright & Wilson).

Alcohols.—The dodecanol was B.D.H. laboratory reagent grade.

All solutions were made up using conductivity water prepared by passing distilled water through a monobed column.

Experimental

In all cases 100 ml. of a 0.1% sodium laurate solution was adjusted to pH 10 and the effects of progressive additions of electrolytes on the foaming and surface properties of the system were studied.

Foam stabilities were estimated by measuring the time taken for a column of foam to collapse to half its original height ($t_{1/2}$). The foam was produced by giving a 250-ml. graduated, stoppered cylinder containing 100 ml. of solution ten vigorous shakes. All the half-lives quoted are the mean values of three such experiments.

Surface tensions were measured using a Cambridge Instrument Co. Du Nouy Tensiometer and applying the corrections of Harkins and Jordan.³ The time taken for the measurement of surface tensions was kept small so as to minimize any influence of atmospheric carbon dioxide.

(1) J. Powney, *Trans. Faraday Soc.*, **31**, 1510 (1935).

(2) G. D. Miles and J. Ross, *This Journal*, **48**, 280 (1944).

(3) W. D. Harkins and H. F. Jordan, *J. Am. Chem. Soc.*, **52**, 1751 (1930).

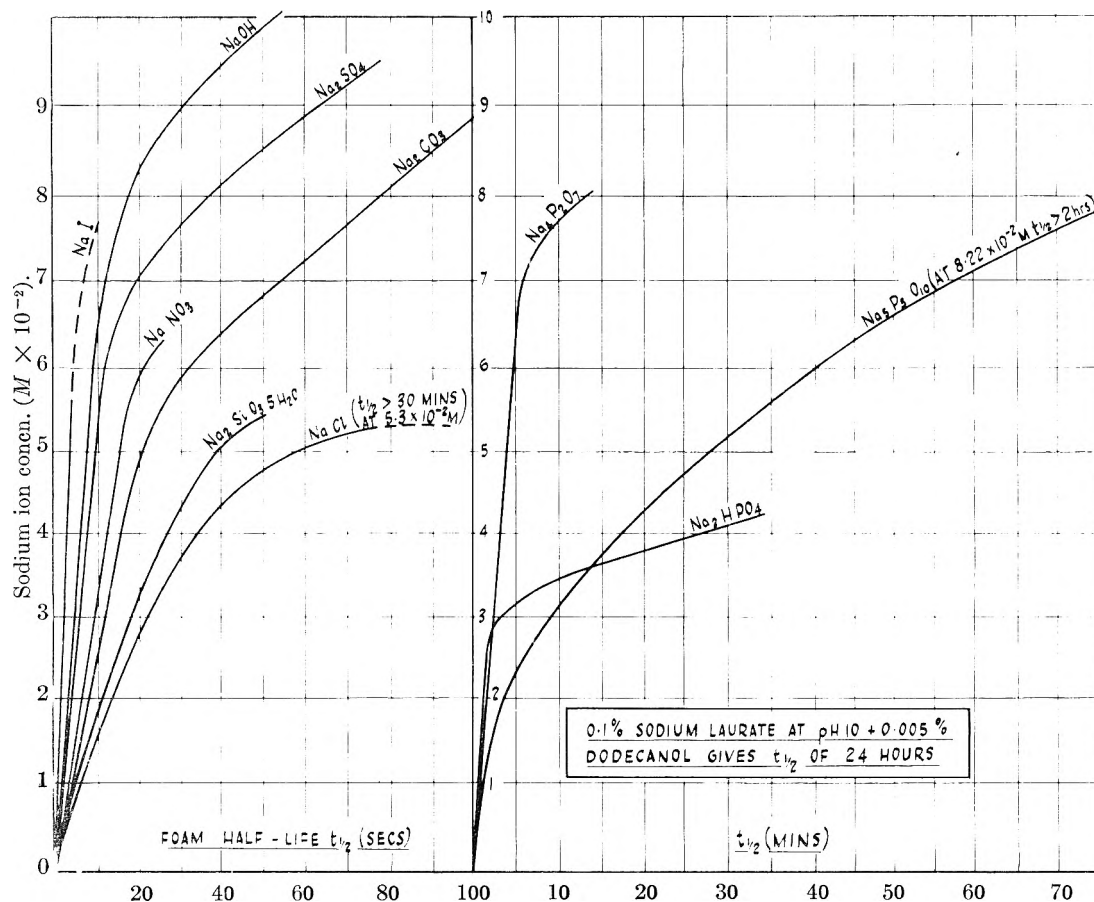


Fig. 1.—The effect of electrolytes on the foam stability of a 0.1% solution of sodium laurate after adjustment to pH 10.

It was found that if the measurements were made within 3 minutes of forming the surface, the effects of carbon dioxide could be ignored.

A constant speed, rotational surface viscometer was used to measure the surface viscosities of the solutions. This instrument is very similar to that described by Brown, *et al.*,⁴ but has the advantage that it can operate up to 11 r.p.m. Furthermore, the incorporation of electromagnetic damping enabled a lamp and scale to be used for measuring deflections with a consequent increase in sensitivity. The suspension wire was 36 s.w.g. with a torsional constant of 154 dynes/cm.; the solution was contained in a stainless steel pan radius 4.00 cm. and the polythene bob had a radius of 3.25 cm. Full details of the instrument will be published elsewhere.

All glassware used in these experiments was thoroughly cleaned by soaking in a 50/50 mixture of concentrated sulfuric and concentrated nitric acids. This was followed by rinsing in distilled water and then in conductivity water.

Results

Figures 1a and b show that the foam stability of the soap solution at high pH increases with sodium ion concentration. It is also apparent that $t_{1/2}$ varies considerably with the added anion—for similar sodium ion concentrations $t_{1/2}$ is a few seconds for NaI, but is several hours for $\text{Na}_5\text{P}_3\text{O}_{10}$. The phosphates clearly form a group of their own and have a much greater effect on the foam stability of the soap solution than the other anions. Table I which shows the effect of varying the added cation reveals that the alkali metals can be arranged, $\text{Li}^+ < \text{Na}^+ < \text{K}^+ < \text{Cs}^+$ in order of increasing effect on foam stability.

(4) A. G. Brown, W. C. Thuman and J. W. McBain, *J. Colloid Sci.*, **8**, 491 (1953).

Increasing the pH of the 0.1% sodium laurate solution to 10 results in a sharp rise in the surface tension of the solution and subsequent additions of electrolyte produce a lowering in surface tension but not to the value for the soap solution at its natural pH (Fig. 2). Although the different anions markedly influence the foam stability they do not significantly affect the surface tension lowering which appears to be a function of the cation concentration. The alkali metal ions affect the surface tension to different extents, lithium giving the smallest and cesium the greatest lowering in surface tension (Table I).

The results given in Table II show that none of the electrolytes produces any significant increase in the surface viscosity of the soap solution at high pH. The addition of dodecanol, however, does produce a definite increase in surface viscosity and gives high foam stability; a similar effect was found by Brown.⁴

Discussion of Results

(a) **Cation Effect.**—Cassie and Palmer⁵ showed that for ionized soluble monolayers

$$\sigma^2 = A \Sigma N_i (\exp.[-Z_i e \phi / kT] - 1) \quad (1)$$

where σ is the density of charge in the surface layer, A is a constant (at constant temperature), Z_i is the valency of ions of number N_i per ml. in the bulk of the solution, ϕ is the potential in the neighborhood of the ionized groups in the film, e is the charge on

(5) A. B. D. Cassie and R. C. Palmer, *Trans. Faraday Soc.*, **37**, 156 (1941).

TABLE I
THE EFFECT OF UNIVALENT CATIONS ON THE SURFACE PROPERTIES AND FOAM STABILITY
OF 0.1% SODIUM LAURATE AT pH 10
(All the salts used were chlorides)

Concn., (g. ions $\times 10^2$)	Li ⁺		Na ⁺		K ⁺		Cs ⁺	
	3.37	6.74	3.37	6.74	3.37	6.74	3.37	6.74
Surface tension (dynes/cm.)	48.6	49.2 ^a	48.2	44.8	44.6	41.7	41.0	36.9
Surface viscosity (surface poise $\times 10^3$)	1.5	1.5	2	2	2	2
Foam half-life $t_{1/2}$, sec.	20	20	26	30 min.	40	30 min.	Greater than 60 min. ^b	

^a The increase in surface tension was due to a salting out of the soap. ^b Even at approximately one half this concentration the foam half life was several hours.

an electron. The potential ϕ can be calculated from the following equation which Davies⁶ has shown to be applicable even at high ionic strength.

$$\phi = 2.303 \frac{kT}{e} \log \left(\frac{134^2 \times 4}{A^2 C} \right) \quad (2)$$

(A is the area per electronic charge in the film, C the concentration of electrolyte). Applying equation 2 to our work ($e\phi$) is found to be about $5-7kT$ and for the addition of univalent cations to a solution of an anionic detergent exp. $-Z_i e \phi / kT \approx 10^2$ so that the addition of salts should increase the adsorption of laurate ions. This increased adsorption is reflected in the progressive lowering in surface tension as more cation is added (Fig. 2) a factor which might increase foam stability.

The size of the cation governs its closest distance of approach to the film and should, therefore, influence its effect on the packing of the laurate ions in the monolayer. Aickin and Palmer⁷ have shown that the effect of univalent cations on the surface tension of anionic detergent solutions is inversely proportional to the size of the hydrated ion. Thus cesium with a small hydrated ion produces a greater surface tension lowering than the larger hydrated ion of lithium (Table I). A similar effect on the surface viscosities of positively charged films has been found by Davies and Rideal.⁸

This accounts for the different effects of the univalent cations on the surface tensions of the soap solutions, but the difference in the foam stabilizing effects between say lithium and cesium seems too great to be explained by relatively small differences in surface tension lowering (Table I).

(b) **Anion Effect (Excluding Phosphates).**—It will be seen from equation 1 that anions should have a much smaller effect than cations on the surface properties of anionic detergents. This prediction has been verified by several workers^{9,10} and is confirmed by Fig. 2 which reveals that anions have a very minor influence on the surface tension of the soap solutions. The various anions do, however, have slightly different effects on foam stability and may be arranged thus, $I^- < OH^- < SO_4^{--} < NO_3^- < CO_3^{--} < SiO_3^{--} < Cl^-$ (Fig. 1a). For example, there is an appreciable difference

(6) J. T. Davies, *Proc. Roy. Soc. (London)*, **A208**, 224 (1951).

(7) R. G. Aickin and R. C. Palmer, *Trans. Faraday Soc.*, **40**, 116 (1944).

(8) J. T. Davies and E. Rideal, *J. Colloid Sci.*, Supplement 1, 1 (1954).

(9) R. G. Aickin, *J. Soc. Dyers. Col.*, **60**, 36 (1944).

(10) E. D. Goddard, O. Harva and T. G. Jones, *Trans. Faraday Soc.*, **49**, 980 (1953).

between the effects of equimolar NaCl and NaNO₃ on the foam stability of 0.1% sodium laurate solutions, which cannot be explained by any marked differences in either surface tension (Fig. 2) or surface viscosity of the soap solutions (Table II).

TABLE II
THE EFFECT OF ELECTROLYTES ON THE SURFACE VISCOSITY
OF 0.1% SODIUM LAURATE AT pH 10^a

Compn. of soln.	Surface viscosity (surface poises $\times 10^3$)	
0.1% sodium laurate at natural pH	37.5	These results were calculated from a modified Reiner equation as used by Brown, <i>et al.</i> ⁴
0.1% sodium laurate at pH 10	1.5	
0.1% sodium laurate + NaOH	1.5	
0.1% sodium laurate + NaCl	1.5	
0.1% sodium laurate + NaNO ₃	1.5	
0.1% sodium laurate + NaI	1.5	
0.1% sodium laurate + Na ₂ SO ₄	1.5	
0.1% sodium laurate + Na ₂ CO ₃	1.5	
0.1% sodium laurate + Na ₂ SiO ₃	1.5	
0.1% sodium laurate + Na ₂ P ₂ O ₇	1.5	
0.1% sodium laurate + Na ₂ P ₃ O ₁₀	2	
0.1% sodium laurate + Na ₂ HPO ₄	1.5	
0.1% sodium laurate + 0.005% dodecanol	33.5	

^a In the table, the total cation concentration was always 5×10^{-2} g. ions when electrolyte was added.

It is clear that some effect other than surface tension lowering is necessary to explain the effects of different anions on foam stability; this point is discussed below.

(c) **Effect of Phosphates.**—The addition of phosphates to the soap solution produced marked increases in foam stability even with relatively low cation concentrations. Furthermore, the anion effect is considerably more marked than the cation effect—for similar sodium ion concentrations, $t_{1/2}$ is 15–20 sec. for sodium nitrate and 30 minutes for sodium tripolyphosphate. Figure 2 reveals that tripolyphosphate does not produce a greater lowering in the surface tension of the soap solution and it was thought that the enhanced foam stability might be due to the interlinking of the phosphate chains beneath the surface film of laurate ions and their associated sodium ions, the sodium ions acting as a bridge between the laurate ions and the phosphate ions. One would expect such interlinking considerably to increase the viscosity of the surface film with a resultant increase in film stability. No such increase in the surface viscosity of solutions containing tripolyphosphate was found (Table II).

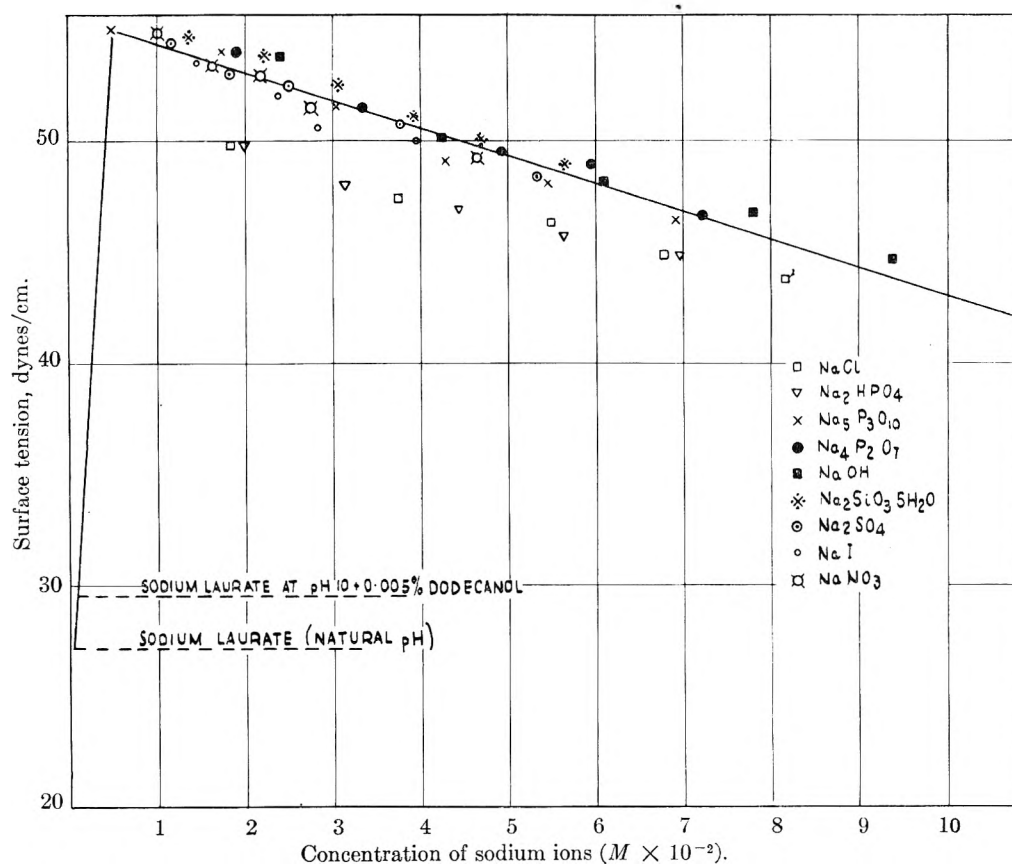


Fig. 2.—The effect of electrolyte on the surface tension of 0.1% solution of sodium laurate after adjustment to pH 10.

Furthermore it will be seen from the dimensions of the $-P-O-P-$ chain (Fig. 3¹¹) that the interlinking of such chains beneath the adsorbed laurate ions would give a condensed film with an area of less than 25 square ångströms for each laurate ion. The area of the adsorbed ions can be estimated from the surface tension results if we assume that for one

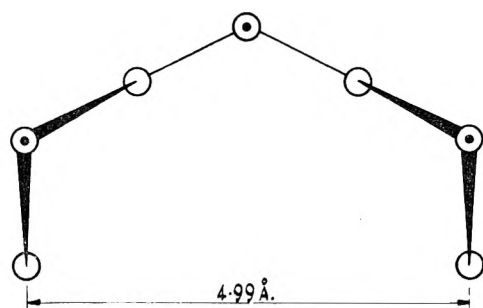


Fig. 3.—Dimensions of $-P-O-P-$ chain: ●, P; ○, O.

surface-active species the surface pressure is a function of Γ (the Gibbs surface excess) alone and is dependent on the ionic distribution below the surface film only through Γ . With this assumption it is possible to apply Brady's¹² results for the surface tensions of sodium dodecyl sulfate solutions to our work on sodium laurate. For a surface pressure of 26 dynes/cm. (the surface pressure of the soap-tripolyphosphate combination at maximum foam stability), Brady found the area per molecule of the

dodecyl sulfate ions to be 52 square ångströms. This is a reasonable area for adsorbed laurate ions so that the possibility of interlinking seems remote.

Finally, if we consider the distribution of added anions in the vicinity of the surface film the probability of phosphate ions being associated with the surface film can be deduced. Applying the Boltzmann principle we can write

$$\frac{C_s}{\gamma C_B} = \exp \frac{-Z_i e \phi}{kT} \quad (3)$$

where C_s is the concentration of ions in the region of the surface film, C_B is that in the bulk of the solution, ϕ is the potential in the region of the surface film, γ is the activity coefficient. From equation 2 it is seen that $(e\phi)$ may be assumed to be $> 5kT$. Therefore, for univalent anions

$$\frac{C_s}{\gamma C_B} < 10^{-2} \text{ and for } P_3O_{10}^{6-} \text{ ions, } \frac{C_s}{\gamma C_B} < 10^{-10}$$

The probability of tripolyphosphate or pyrophosphate ions being found in the immediate vicinity of the surface film appears therefore to be negligible unless they interact specifically. The mechanism whereby phosphates increase the foam stability of sodium laurate solutions at high pH is, therefore, obscure since they appear neither to increase exceptionally the adsorption of laurate ions nor to associate with the surface film to modify its mechanical properties.

General Requirements for Foam Stability

A possible explanation for the effects of phosphates can be obtained by considering the basic re-

(11) B. Raistrick, *Disc. Faraday Soc.*, No. 5, 234 (1949).

(12) A. P. Brady, *THIS JOURNAL*, 53, 56 (1949).

quirements for foam stability. Generally, any factor which reduces the rate of drainage from a film will increase the stability of the film. Such a factor is bulk viscosity and Henniker¹³ has shown that a viscous surface film may influence bulk viscosity by orienting layers of water molecules to a considerable depth below the surface. In addition a highly viscous film will offer a large resistance to any deformation tending to disrupt the film, thereby increasing the stability of the film.

The thinning of soap films will also be opposed by the repulsive forces between the electrical double-layers associated with the surfaces.¹⁴ The thickness of the double layer will thus influence the thinning of the film and, since this thickness is inversely proportional to (ionic strength)^{1/2}, the addition of electrolyte will tend to increase thinning and promote instability.

The electrolyte concentration was relatively high in many of our experiments and the surface and bulk viscosities were low. Furthermore, though all foams (except that stabilized by lauryl alcohol) drained rapidly immediately after formation, some were very stable. Clearly then only the operation of those factors which can stabilize a film thinned almost to rupture are important in this work. Gibbs¹⁵ first explained the stability of thin films against mechanical shock by showing that for stability the surface tension under film deformation should always change in such a way as to resist the deforming forces. Consider a given area of film divided into two segments one of which is expanded and the other contracted, the surface tension of the expanded element will increase and that of the contracted element decrease because the surface excess is reduced in the former and increased in the latter. The result of such unequal tensions is a force tending to restore the original conditions. Gibbs suggested that stable thin films thus possess elasticity due to the change of surface tension with area and he defined film elasticity (E) as

$$E = 2A \left(\frac{\partial \gamma}{\partial A} \right)_{N_1, N_2} \quad (4)$$

where A is the area of film, γ the surface tension, N_1 , N_2 are the total quantities of solvent and solute, respectively, per unit area of film.

Gibbs' treatment holds for an isolated element of film and for equilibrium values of surface tension,

(13) J. C. Henniker, *Rev. Mod. Phys.*, **21**, 322 (1949).

(14) W. E. Ewers and K. L. Sutherland, *Aust. J. Sci. Research*, **5**, 697 (1952).

(15) J. W. Gibbs, "Collected Works of J. W. Gibbs," Longmans, Green and Co., London, 1928, pp. 300-314.

but in practical systems the film is not isolated from the bulk of the solution which provides a reservoir of surface-active material. Furthermore, a foam is far from being an equilibrium system as evidenced by the turbulent motion of the interference colors in foam bubbles. Clearly the rate of adsorption and hence the rate of attainment of surface tension equilibrium must have an important influence on foam stability. According to Burcik¹⁶ this rate should be sufficiently high to produce a large lowering of surface tension under non-equilibrium conditions but not so high as to prevent restoring forces from coming into play. Burcik¹⁶ has summarized the facts which are important in foam stability thus: 1, low equilibrium surface tension; 2, a moderate rate of attainment of equilibrium surface tension; 3, high surface viscosity.

The addition of electrolytes to the sodium laurate solutions produces only a small reduction in the equilibrium surface tension, and the surface viscosity is hardly affected at the concentrations used in this work. At a high pH where foam stability is very poor Nutting and Long¹⁷ found, however, that the equilibrium surface tension of a sodium laurate solution is approached slowly; the addition of salts at this stage not only increases the foam stability but also the rate of adsorption.¹⁸ It is probable, therefore, that this increase in adsorption rate contributes considerably to the increase in the foam stability of the sodium laurate solutions at high pH. A possible confirmation of Burcik's view that a moderate rate of adsorption is necessary for foam stability can be found in the work of Posner and Alexander¹⁹ who found that lithium increases the rate of adsorption to a far greater extent than rubidium and it may well be that this large difference in rates is the reason that lithium ions are so poor and cesium ions so good in stabilizing the soap foams. The rate of adsorption thus appears to be important in determining foam stability, and a possible explanation of the enhanced stability with phosphate (Fig. 2 and Table II) is that they influence adsorption rates to a greater extent than do the other anions. Thus whilst low equilibrium surface tension and high surface viscosity may be desirable for foam stability they are not essential.⁴ It does, however, seem reasonable to conclude that the rate of attainment of surface tension equilibrium is an important factor in determining foam stability.

(16) E. J. Burcik, *J. Colloid Sci.*, **5**, 441 (1950).

(17) G. C. Nutting and F. A. Long, *J. Am. Chem. Soc.*, **63**, 84 (1941).

(18) E. J. Burcik, *J. Colloid Sci.*, **8**, 520 (1953).

(19) A. M. Posner and A. E. Alexander, *ibid.*, **7**, 585 (1952).

INFRARED STUDY OF METAL CHELATES OF BISACETYLACETONE-ETHYLENEDIIMINE AND RELATED COMPOUNDS¹

BY KEIHEI UENO^{2a} AND ARTHUR E. MARTELL^{2b}

Contribution from the Chemical Laboratories of Clark University,¹ Worcester, Mass.

Received February 1, 1955

Infrared absorption frequencies from 4000 to 400 cm^{-1} are reported for bisacetylaceton-ethylenediimine, bisacetylaceton-1,2-propylenediimine, bisbenzoylaceton-ethylenediimine, bisbenzoylaceton-1,2-propylenediimine, bisbenzoylaceton-1,3-propylenediimine, bistrifluoroacetylaceton-ethylenediimine, and many of the corresponding Cu(II), Ni(II), Co(II) and Pd(II) chelate compounds. Frequencies are assigned in most cases to bond or group vibrations, and shifts of frequencies resulting from replacement of enolic hydrogen of ligand by metal ions are discussed. Three bands in the frequency range 580–430 cm^{-1} are tentatively assigned to vibrations of covalent metal–ligand bonds.

Since the discovery by Tsumaki³ of the oxygen-carrying property of bisalicylaldehyde-ethylenediimine–Co(II), this substance and similar metal chelate compounds have been investigated extensively as models of the naturally occurring oxygen carrying compounds. However, a systematic study of the infrared absorption spectra of these compounds has not been reported. This paper is the first of a series dealing with an infrared study of the structures of metal chelates resembling both the synthetic and natural oxygen carriers. The work reported here is restricted to nineteen compounds related to bisacetylaceton-ethylenediimine, and which differ from the synthetic oxygen carriers mainly in the absence of the aromatic ring.

The ligands chosen for this investigation—bisacetylaceton-ethylenediimine, bisacetylaceton-1,2-propylenediimine, bisbenzoylaceton-ethylenediimine, bisbenzoylaceton-1,2-propylenediimine, bisbenzoylaceton-1,3-propylenediimine and bistrifluoroacetylaceton-ethylenediimine—form neutral, tetradentate chelates of the transition metals. The metals chosen for investigation, Co(II), Ni(II), Cu(II) and Pd(II), are known to form square-planar coordination compounds and were selected in order to provide a series of related metal chelates having analogous structures, no residual charges, and having no coordinated groups beyond the four provided by the ligand.

Experimental Part

The composition and structures of the ligands employed in this investigation are summarized in Table I. The preparation of these compounds will be reported elsewhere.⁴ As indicated by the footnotes to Table I, most of these ligands and metal chelates have not been reported previously.

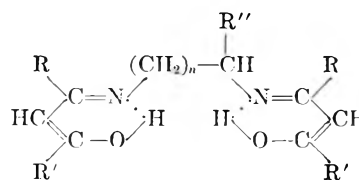
The infrared absorption spectra were measured with the aid of a Perkin-Elmer Model 21 double beam recording infrared spectrophotometer. Sodium chloride optics were used in the region from 4000 to 650 cm^{-1} , and an interchangeable potassium bromide prism assembly was substituted for measurements in the region from 650 to 400 cm^{-1} .

Infrared absorption in carbon tetrachloride or chloroform was investigated as a function of concentration for some compounds soluble in these solvents. No significant shifts were found over the spectra obtained by the potassium bromide pellet method. Therefore all the spectra reported

were obtained by the latter technique. The significant spectral lines found for the compounds studied are reported in Tables II and III, together with the assignments that were possible in each case.

TABLE I

LIGANDS



	R	R'	R''	n
1	CH ₃	CH ₃	H	1
2	CH ₃	CH ₃	CH ₃	1
3	C ₆ H ₅	CH ₃	H	1
4	C ₆ H ₅	CH ₃	CH ₃	1
5	C ₆ H ₅	CH ₃	H	2
6	CH ₃	CF ₃	H	1

^a A. Combes and C. Combes, *Compt. rend.*, **108**, 1252 (1889).

^b Ni(II), Cu(II) and Pd(II) chelates reported by G. Morgan and J. Smith, *J. Chem. Soc.*, 918 (1926).

^c Co(II) chelate reported by G. Morgan and J. Smith, *ibid.*, 2034 (1925).

^d The structural proof of these compounds will be given in a later publication.

^e Ligand and Cu chelate reported by R. L. Belford, A. E. Martell and M. Calvin *Journal of Inorganic and Nuclear Chemistry*, in press.

Discussion

For convenience the infrared absorption spectra of the compounds investigated have been divided into three regions with the frequency ranges: 4000–2800 cm^{-1} , 1700–900 cm^{-1} and 900–400 cm^{-1} . These three regions will be discussed separately.

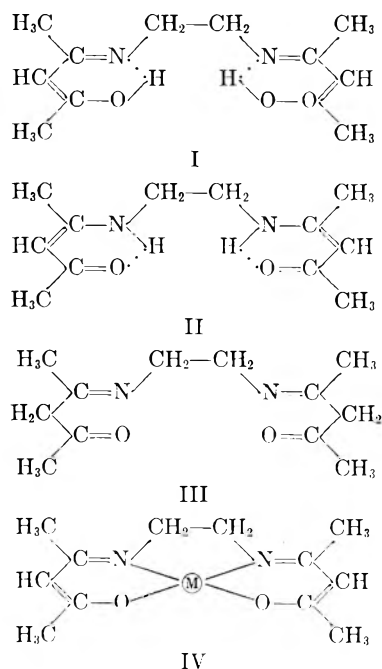
3200–2800 cm^{-1} Region.—The three possible structures of bisacetylaceton-ethylenediimine are illustrated by formulas I, II and III. It is reasonable to expect hydrogen bonding between hydroxyl hydrogen and imino nitrogen (I), or between imino hydrogen and carbonyl oxygen (II). Structure III is the non-hydrogen-bonded form with free carbonyl groups. The infrared spectra of bisacetylaceton-ethylenediimine, and of its Pd(II), Ni(II) and Cu(II) chelates are illustrated in Fig. 1.

(1) This research was supported by a grant from National Institutes of Health, U. S. Public Health Service.

(2) (a) Postdoctoral Research Fellow, Clark University; on leave, Dojindo & Co., Ltd., Kumamoto, Japan, 1953–55; (b) Clark University, Worcester, Mass.

(3) T. Tsumaki, *Bull. Chem. Soc., Japan*, **13**, 252 (1938).

(4) P. J. McCarthy, R. J. Hovey, K. Ueno and A. E. Martell, unpublished work; P. J. McCarthy, Clark University, Ph.D. Dissertation, September, 1954.



It is apparent that the ligand has a broad absorption band at about 3150 cm^{-1} , which may be due to the stretching vibration of either an O-H group in accordance with formula I or of a N-H groups of the type indicated by formula II. This assignment is strengthened by the disappearance of the band in the metal chelates shown in Fig. 1. Evidence for strong hydrogen bonding is found in the broadening of the band, and the extent of the shift from the normal position ($3730\text{--}3520\text{ cm}^{-1}$ for free O-H and $3400\text{--}3300\text{ cm}^{-1}$ for free N-H). Although there is no positive proof that this absorption is due to the vibration of the hydrogen-bonded O-H group in I, it is the opinion of the authors that this is the case, since the hydrogen-bonded N-H vibration is often too weak to be observed. Since this ligand does not absorb in the region around 1700 cm^{-1} , as will be discussed later, it cannot have a free carbonyl group. Hence III is eliminated and the ligand is believed to be a tautomeric equilibrium mixture of structures I and II.

Absorption bands in $3000\text{--}2800\text{ cm}^{-1}$ which are observed both in the ligand and in the chelates are assigned to C-H stretching vibrations of CH, CH₂ and CH₃ groups. Since absorption bands of the other compounds investigated have characteristics similar to those of bisacetylacetonethylenediimine, similar structures involving hydrogen-bonding are proposed for all ligands.

It seems, therefore, that the six-membered ring systems containing hydrogen bonds (structures I and II) are greatly stabilized by conjugated double bond systems, as in the case of β -diketones and salicylaldehyde.⁵ Because of valence-bonded resonance in these ring systems, it is necessary that each ring have a planar structure. However, both hydrogen-bonded rings of the molecule cannot be in the same plane because of the steric hindrance and electrostatic repulsions of O-H-N or O-H-N

(5) (a) R. S. Rasmussen, D. D. Tunnicliff and R. R. Brattain, *J. Am. Chem. Soc.*, **71**, 1068 (1949); **71**, 1073 (1949); (b) M. Tsuboi, *Bull. Chem. Soc. Japan*, **25**, 385 (1952).

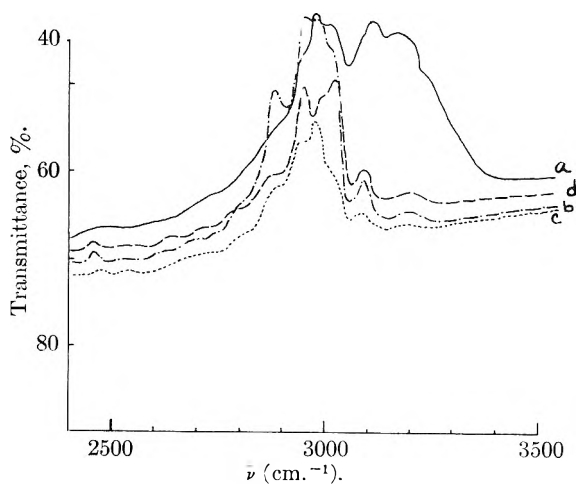


Fig. 1.—Absorption spectra of bisacetylacetonethylenediimine (a), and its Cu(II) (b), Ni(II) (c), and Pd(II) (d) chelates in 3000 cm^{-1} region.

groups. Consequently the actual structure is believed to be such that each ring system is rotating about the axis of the C-C bond of ethylenediimine, a proposition which is also confirmed by dipole moment measurement.⁴ However, in the metal chelate compounds, both rings are fixed in the same plane without steric hindrance by the central metal atom as shown in the formula IV. This conclusion concerning coplanarity of the metal chelate rings is further supported by the demonstration through X-ray studies that the analogous compound, bisalicylaldehyde-ethylenediimine-Co(II) is also coplanar.⁶

1700-900 cm.⁻¹ Region.—There is no significant absorption band between 2800 and 1700 cm^{-1} , the first absorption band being observed around 1600 cm^{-1} ; however, many absorption bands are found in $1700\text{--}900\text{ cm}^{-1}$ region, which are summarized in Table II and III.

If, as suggested above, the ligands are tautomeric mixtures of structures I and II, observed infrared absorption spectra may be considered to be the result of the superposition of spectra corresponding to both structures. According to the tautomeric forms I and II of the ligand, and structure IV of the metal chelates, we can expect strong absorptions in the double bond region corresponding to C=C, C=N, and hydrogen-bonded C=O stretching vibrations for the ligand, and absorptions arising from C=C and C=N bonds for the metal chelate compounds. However, since these double bonds are conjugated, and since we can expect resonance in the ring systems involving hydrogen bonding, these double bonds have considerable single-bond character and would have lower than normal frequencies. Thus it is fairly certain that the first absorption band at $1615\text{--}1600\text{ cm}^{-1}$, which is always very strong and is found only in the ligands, can be assigned to a C=O stretching vibration in the hydrogen-bonded ring systems.⁷

(6) E. W. Hughes, C. H. Barkislaw and M. Calvin, OMSr-279, March 15, 1944.

(7) (a) For instance, the absorption band corresponding to the hydrogen-bonded carbonyl group is shifted to $1639\text{--}1538\text{ cm}^{-1}$ in the conjugated chelate system of acetylacetonone (cf. ref. 5b). (b) Bellamy and Branch have also assigned the chelated carbonyl absorption of β -diketones to this region, *J. Chem. Soc.*, 4487 (1954).

TABLE II (Continued)

Ligand	Compound 1 Metal chelate			Ligand	Compound 2 Metal chelate		Ligand	Compound 6 Metal chelate		Assignments
	Cu	Ni	Pd		Cu	Ni		Cu	Cu	
554vw				544w	562vw	561vw	543w			} Metal-ligand vibration
522w				515w			530w	528w		
	454m	480m	477w		479w	489w	513vw	514w		
			469m		454w	473vw		455m		
				458w			433vw			
418vw	419vw	419vw	419vw	418vw	419vw	418vw	420vw	420vw		

* The number of compound refers to Table I. ^b Definite absorption peak cannot be found; broad band in the range specified (*e. g.*, between 1460 and 1430 cm.^{-1}).

TABLE III

INFRARED ABSORPTION SPECTRA OF COMPOUNDS 3, 4, 5 AND THEIR METAL CHELATE COMPOUNDS

Ligand	Compound 3 Metal chelate			Ligand	Compound 4 Metal chelate			Ligand	Compound 5 Metal chelate		Assignments
	Cu	Ni	Co		Cu	Ni	Co		Cu	Cu	
1603vs				1605vs				1600vs			C=O... in H bonded rings
1586s	1600s	1598s	1591m	1592vs	1597s	1590s	1590s	1596vs	1597s	} C=C stretching and phenyl	
1577s	1578s	1579s	1568s	1579vs	1574m	1571m	1558s	1585vs	1576m		
1547s			1550m	1548s				1546vs			
1522s	1518vs	1519vs	1517s	1522s			1511s	1525m	1514vs	} C=N stretching	
	1509vs		1505s	1513m	1509vs	1508vs	1500vs	-10°	1507vs		
1490m	1488vs	1491vs	1490vs	1486m	1485vs	1484s	1485vs	1487vw	1485vs	} Phenyl	
1474s	1471s	1466s	1460s	1469w	1462vs	1460vs	1453s	1470m	1468vs		
1465m	1462s			1436s	1440s	1440s	1436s	1437s	1440s	} CH ₃ and CH ₂ deformations	
						-35°					
1444s											
	1431s	1432s	1432s		1422s	1417s	1406vs		1422vs		
			1417s								
1383w	1358m	1363m	1362m	1365w	1368m	1367w	1370m	1380m	1353m	} CH ₃ deformation	
1341s	1303w	1308m	1310w	1322s	1338w	1337w	1341w	1329vs	1326m		
	1288m	1300m	1300w					1310s	1308m		
1287s				1287s				1289s		} O—H... in H bonded rings	
					1298vw	1295vw	1295vw				
					1271w			1266s	1286m		
1234m	1240w	1240w	1238w	1246m	1242m	1241w	1242w	1251m	1247m		
	1233w	1231w	1232w	1221w	1235m	1230w	1232w	1225w	1208vw		
1176w	1177w	1178w	1178w	1175vw	1178vw	1175vw	1176vw	1178w	1173vw	} Phenyl	
	1163vw	1161vw	1158vw								
1159vw				1148m				1139w		} C—O— in H bonded rings	
					1127w	1137w	1133w		1114w		
	1120w	1120w	1117vw								
	1085w	1091w	1088vw		1190w	1093w	1092w	1084w	1093w	} C—O— in metal chelate rings	
1087s				1085w					1082w		
1065m	1073m	1075m	1074m	1062m	1057w	1063w	1063w	1065m	1070w	} Phenyl	
1027w	1030w	1029w	1027w	1024m	1021w	1020w	1022w	1025w	1024w		
	1015w	1020w	1020w					998vw	999vw		
									973vw		
922w	892w	906w	904w	922vw	907w	915w	913w	932w	919vw		
									894vw		
					876vw	887vw			883w		
878w	854w	860w	858w	855vw	853w	862vw	860vw		854vw		
844m				843vw	835vw			846m			
				837vw							
				825vw							
				814w							
805m				797w				804w			
	798w	810w	810vw								
		795w	795vw								
776w		785w	786vw		787vw	786vw	787vw	787w	791w		

TABLE III (Continued)

Ligand	Compound 3 Metal chelate			Ligand	Compound 4 Metal chelate			Ligand	Compound 5 Metal chelate		Assignments
	Cu	Ni	Co		Cu	Ni	Co		Cu		
753vs	737vs	735vs	746vs	728s	731s	736m	743m	743s	745m	} Phenyl	
								731s	732s		
								708m	708m		
709s	696s			701w		707m	707m	686m	696m	} Phenyl	
690s	685m	691s	691s	685w	690s	693s	692s	676m	686m		
669w				674w		684m	684m				
								616vw	619vw		
576w				561w				565w			
567w											
	535m	557m	557w		543vw	565w	564w		538w	Metal-ligand vibration	
504vw											
	467m	493m	493w		479vw	498vw	495w			Metal-ligand vibration	
				478vw				497vw			
	450vw	451vw	451vw		465vw	480w	481w		463vw	} Metal-ligand vibration	
				458vw					438w		
417vw	419vw	418vw	419vw	418vw	419vw	418vw	418vw	418vw	418vw		

^a Same as footnote *b*, Table II.

If the methyl group which is directly attached to the carbonyl carbon in structure II, is replaced by the strongly negative group, such as trifluorocarbon, one would expect a decrease in the polarizability of the carbonyl group, and a corresponding shift of the absorption band to the higher frequency. This seems to be the case in bistrifluoroacetylaceton-ethylenediimine (compound 6), for which hydrogen-bonded C=O absorption shifts to 1614 cm^{-1} , the highest carbonyl frequency observed for the compounds studied.

The next strong absorption at 1596–1580 cm^{-1} in the ligands, which is usually accompanied by a weaker absorption of 1565–1560 cm^{-1} , can be assigned to a C=C stretching vibration in the hydrogen-bonded rings. In the case of benzoylacetone derivatives, the absorptions due to skeletal vibrations of phenyl rings are also expected in this region; however, these absorptions may overlap each other and each absorption cannot be identified separately. The main absorption band at 1596–1580 cm^{-1} is usually shifted to a slightly higher frequency by metal chelation, while the second absorption band shifts to a lesser extent or is missing in some compounds.

The next set of fairly intense bands, which consists of two bands in most cases, can be assigned to C=N stretching vibration in the hydrogen-bonded rings. These bands shift to a slightly higher frequency and become more intense by metal chelation. In trifluoroacetylaceton-ethylenediimine, the assigned C=N bands becomes very weak, while the bands due to hydrogen-bonded C=O and C=C bonds have the same intensities as was observed for bisacetylaceton ethylenediimine. This indicates that the strong negativity of trifluorocarbon group probably stabilizes the carbonyl structure II rather than I, so that the contribution of C=N to the spectra becomes less than in bisacetylaceton compound.

It is also probable that the hydrogen-bonded N-H deformation vibration in structure II absorbs

in these region; however the intensity of this band is usually too weak to be observed. Although one additional absorption band of intermediate intensity at 1450–1445 cm^{-1} is found in the ligand, it is doubtful whether this band can be assigned to N-H deformation.

All benzoylacetone derivatives have a sharp absorption band of intermediate intensity at 1490–1485 cm^{-1} , the frequency of which remains almost unchanged from ligand to metal chelate compounds. This band can be assigned, without doubt, to the skeletal vibration of phenyl ring. Weak absorption bands at around 1176 and 1027 cm^{-1} in these compounds can also be assigned to vibrations of the monosubstituted phenyl ring.

It is known that CH_2 deformation gives rise to absorption at around 1465 cm^{-1} and asymmetrical CH_3 deformations to absorption at around 1450 cm^{-1} .⁸ Two absorption bands of varying intensities in this region, which are found in all of the compounds, can be assigned to these modes or vibration. Although the symmetrical deformation of hydrogen in the CH_3 group is known to give an absorption band in the range of 1385–1370 cm^{-1} , which is very stable in position,⁸ these compounds reported here do not always give clear absorption bands which can be assigned to this mode of vibration.

The next fairly strong absorption band is observed at 1290–1280 cm^{-1} in all ligands except the trifluoro compound, which shows absorption at 1242 cm^{-1} . Since no band with comparable intensity can be found in this region in the metal chelate compounds, it is believed to be due to O-H deformation vibration in hydrogen-bonded rings. Although it is known that alcohol gives rise to two bands in the region 1410–1050 cm^{-1} , it is not made clear which of these bands is due to C-O stretching, and which corresponds to the O-H deformation vibration. However, another absorption

(8) L. J. Bellamy, "The Infrared Spectra of Complex Molecules," John Wiley and Sons, Inc., New York, N. Y., 1954, p. 19.

band at around 1150 cm.^{-1} is fairly stable in position from one ligand to the other, and is therefore assigned to the C–O stretching vibration. Although the intensity of this band is not so strong, and is very weak in bisbenzoylacetone-ethylenediimine, the frequency is shifted to the lower values by metal chelation. This shift may be due to the increased mass of metals attached to oxygen, as well as to a weakening of the C–O linkage.

In the trifluoro compound, O–H deformation and C–O stretching vibrations are assigned to the absorptions at 1242 and 1078 cm.^{-1} , respectively, both being shifted in the direction opposite to that which would be expected as a result of the inductive influence of the trifluoromethyl group.

Carbon-fluorine stretching vibrations are known to give rise to very strong bands in the 1400 – 1000 cm.^{-1} region. By comparing the spectra of bisacetylacetone-ethylenediimine, bistrifluoroacetylacetone-ethylenediimine and its Cu(II) chelate, along with bisacetylacetone–Cu(II) and bistrifluoroacetylacetone–Cu(II), the following five strong absorption bands, which are fairly stable in position, can be assigned to C–F stretching vibrations; 1282 , 1222 , 1187 , 1130 and 1118 cm.^{-1} for the ligand and 1293 , 1223 , 1178 , 1147 and 1126 cm.^{-1} for the Cu(II) chelate.

900–400 cm.^{-1} Region.—The main absorption bands in this region occur at 780 – 650 cm.^{-1} in the spectra of both the ligands and the metal chelate compounds. There are also ligand absorption bands of intermediate intensities around 840 cm.^{-1} , and several characteristic absorption bands of weak or intermediate intensities in the spectra of the metal chelate compounds.

Bisacetylacetone-ethylenediimine and bisacetylacetone-1,2-propylenediimine as well as their metal chelate compounds, give very sharp absorption bands of intermediate intensities at around 750 and 740 cm.^{-1} which shift slightly with metal chelation. Bistrifluoroacetylacetone-ethylenediimine also gives similar absorption bands at 779 and 773 cm.^{-1} . While two bands are always observed in the ligands, one of these bands is missing in some metal chelate compounds. These absorptions are assigned to C–H out-of-plane deformation vibrations. The C–H out-of-plane deformations in analogous compounds of the type $\text{R}'\text{R}''\text{C}=\text{CHCH}_3$ are in the general frequency range of 840 – 800 cm.^{-1} , which is 30 – 60 cm.^{-1} higher than the values assigned in the present investigation. However, the aromatic nature of the six-membered rings including hydrogen bonding in the ligands, and of the same ring system including the metal ion in the metal chelate compounds, is believed to be the reason for the shift of these bands from their normal position.

The compounds which have phenyl groups give rise to sharp absorptions at around 750 and 690 cm.^{-1} , both of which occur as doublets or triplets in certain cases. These bands are assigned to C–H out-of-plane deformation of the phenyl ring.

In all ligands additional absorption bands are observed in the range of 850 – 800 cm.^{-1} . These are more intense in bisacetylacetone-ethylenediimine, -1,2-propylenediimine, and bistrifluoroacetylacetone-ethylenediimine, and less strong in benzoyl-

acetone derivatives. Since each six-membered ring system of the ligands can rotate freely to some extent about the axis of the C–C bond of alkylene bridge, it is expected that the ligand will have absorptions which are due to such skeletal deformation of the alkylenediimine bridge. However, the energy corresponding to the frequency range under discussion is probably too high to warrant assignment to these modes of vibration. Thus these bands are not assigned to any definite mode of vibration at present time.

The absorptions due to metal–oxygen and metal–nitrogen vibrations are also expected in this region. Some absorptions resulting from metal–oxygen vibrations in metallic acetylacetonates were observed at 700 – 600 cm.^{-1} by Morgan⁹ and more extensively by Lecomte.¹⁰ Also the nature of bonding between the metal and oxygen of these compounds was found by magnetic moment measurements¹¹ to be essentially ionic. On the other hand, the metal–oxygen and metal–nitrogen bonds in the bisacetylacetone-ethylenediimine chelates are believed to be essentially covalent because of the great difference of the ultraviolet and visible absorption spectra between the ligand and its metal chelate compounds.¹² Also bisalicylaldehyde-ethylenediimine–Ni(II) and –Co(II), which have a similar skeletal structure, were found by magnetic moment measurements to have covalent metal–ligand bonds.¹¹ The relationship between the polarity of the coordination bond and the bond strength has been stated by Cottrell and Sutton¹³ to involve a decrease in the covalent contribution to the bond strength with increasing polarity up to a certain difference in polarity, as was pointed out by Walsh.¹⁴ Thereafter, according to Pauling,¹⁵ increasing polarity should increase the ionic contribution to bond strength. Although there are many uncertainties in applying these ideas to the chelate compounds under discussion, it seems that the more covalent metal–ligand bonds in bisacetylacetone-ethylenediimine–metal chelates will be stronger than ionic metal–ligand bonds in metal chelates of acetylacetone.

Now returning to the experimental results, we can assign the following three bands, at 688 , 609 and 480 cm.^{-1} , to the metal-specific absorptions of bisacetylacetone-ethylenediimine–Ni(II). These bands shift slightly with the kind of metals chelated: in the Cu(II) chelate to a slightly lower frequency, and in the Pd(II) chelate to a slightly higher frequency. Similar bands observed in the metal chelates of the other ligands are shown in the Tables II and III. These metal–ligand absorption bands are usually not very strong, and in some compounds it is possible that they are overlapped

(9) H. Morgan, U. S. Atomic Energy Commission, 1949; AECD, 12659.

(10) J. Lecomte, *Disc. Faraday Soc.*, **9**, 108 (1950); C. Duval, R. Freymann and J. Lecomte, *Bull. soc. chim. France*, 106 (1952).

(11) A. E. Martell and M. Calvin, "Chemistry of the Metal Chelate Compounds," Prentice-Hall, Inc., New York, N. Y., 1952, p. 214.

(12) Ultraviolet and visible absorption spectra will be reported in a later publication.

(13) T. L. Cottrell and L. E. Sutton, *Proc. Roy. Soc. (London)*, **A207**, 49 (1951).

(14) A. D. Walsh, *J. Chem. Soc.*, 398 (1948).

(15) L. Pauling, "The Nature of the Chemical Bond," Cornell University Press, Ithaca, N. Y., 1945, p. 48.

by other strong absorptions, such as those resulting from C-H deformation of the phenyl ring. It is interesting to note that the observed metal-ligand bands are spread over a wide frequency region, while the metal specific bands of bisacetylacetonate metal chelates are observed in the range of 700-600 cm.^{-1} .¹⁰

If metal-specific absorptions of both types of compounds are due to the similar mode of metal-ligand vibrations, we could expect the absorptions of bisacetylacetonate-ethylenediamine metal chelates to occur in a higher frequency region than those of bisacetylacetonate metal chelates, since the covalent metal-ligand bonds of the former compounds have the higher bond energies. At present, however, it is difficult to compare the absorption bands of these compounds, because there are many modes of vibration, such as metal-oxygen and -nitrogen stretching, in-plane and out-of-plane deformation vibrations, all of which result in change of dipole moment, and hence are responsible for infrared absorptions.

In general, the order of decreasing frequency of bands of each set of metal-specific absorptions in the

metal chelates of a given ligand is: Pd > Ni and Co > Cu. On the other hand, the stability of complexes of these bivalent metal ions usually follows the order Pd > Cu > Ni > Co.¹⁶ The relationship between the metal-ligand stretching force constant and the metal-ligand bond strength, which is a measure of the stability of complexes, might be expected to lead one to predict Pd > Cu > Ni > Co as the order of decreasing frequency.¹⁷ However the greater mass of Pd might also be expected to shift its absorption frequencies to lower values. The irregularity of the Cu-ligand frequencies reported indicates that the absorptions may arise from a complicated, rather than a simple mode of vibration. For all the metals investigated, it is possible that other factors, such as resonance effects involving the d-orbitals of the metal ion, may also influence the metal-ligand vibrations.

(16) D. P. Mellor and L. Maley, *Nature*, **159**, 370 (1947); **161**, 436 (1948).

(17) Bellamy and Branch recently reported the linear relationship between the stability of salicylaldehyde metal chelates and the shift of the chelate carbonyl frequency in 1600 cm.^{-1} region. However, no attempt has been made in lower frequency region, *J. Chem. Soc.*, 4491 (1954).

THE ELECTROCHEMICAL BEHAVIOR OF THE TUNGSTEN ELECTRODE AND THE NATURE OF THE DIFFERENT OXIDES OF THE METAL

BY S. E. S. EL WAKKAD, H. A. RIZK AND I. G. EBAID

*Department of Chemistry, Faculty of Science, Cairo University, Cairo, Egypt, and
John Harrison Laboratory of Chemistry, University of Pennsylvania, Philadelphia, Pa.*

Received February 7, 1955

The limited results previously reported on the behavior of the tungsten electrode in solutions of different pH values are conflicting. This is clarified here by calculating the potentials of the different oxides of tungsten and comparing them with the experimental results. It is found that the behavior of the tungsten electrode depends upon whether it is massive or in the powdered form. From this study it has been found possible to define clearly the pH range over which the tungsten electrode can function properly as an indicator electrode for hydrogen ion activity. The anodic oxidation of tungsten at very low current density is studied and the nature of the different oxides of tungsten which are apt to be formed on the electrode surface has been revealed. From all these studies it is shown that the tungsten electrode is far better than the antimony electrode as an indicator electrode for the hydrogen ion activity since a calibration curve can stand for much longer period without any of the appreciable drift characteristic of the antimony electrode.

Quite recently the electrochemical behavior of the antimony electrode was studied by El Wakkad^{1,2} and the factors which govern the electrode behavior were defined. The present investigation deals with the tungsten electrode which has been the subject of a limited amount of experimental work.³⁻⁶ The results obtained by different workers are conflicting and the pH range over which the electrode can give correct measurements for the hydrogen ion activity as well as the time during which a calibration curve can give satisfactory values are obscure. The precise determination of these factors is complicated not only for the different types of oxides given by tungsten but also by the great variety of compounds with bases given by these oxides, especially the trioxide. In this investigation, however, the

potentials of the different oxides of tungsten are calculated and compared with the experimental results. It is shown that the behavior of the tungsten electrode depends upon whether it is in the massive or in the powdered form. From this study it has been found possible to define clearly the pH range over which the tungsten electrode can function properly as an indicator electrode for the hydrogen ion activity. The anodic oxidation of tungsten at very low current density is studied and the nature of the different oxides of tungsten which can be formed on the surface of the electrode has been revealed. From these studies it is concluded that this electrode in its behavior as an indicator electrode for the hydrogen ion activity is far better than the antimony electrode. A calibration curve in case of the tungsten electrode can stand for a much longer period without the characteristic drift of the antimony electrode.

Experimental

I. The Tungsten Electrodes.—The tungsten electrodes used were of the following types:

- (1) S. E. S. El Wakkad, *J. Chem. Soc.*, 2894 (1950).
- (2) S. E. S. El Wakkad and A. Hickling, *THIS JOURNAL*, **57**, 203 (1953).
- (3) J. E. Baylis, *Ind. Eng. Chem.*, **15**, 852 (1923).
- (4) H. C. Parker, *ibid.*, **17**, 737 (1925).
- (5) A. L. Holven, *ibid.*, **21**, 965 (1929).
- (6) H. T. S. Britton and E. N. Dodd, *J. Chem. Soc.*, 829 (1931).

(A) **Massive Tungsten Rod or Filament.**—The rod electrode was of pure tungsten (B.D.H.) 4.2 cm. long and 0.4 cm. in diameter, while the filament was one cm. long and 0.40 mm. in diameter. The electrodes were sealed directly to Pyrex glass tubes. Each electrode before use was refreshed by immersing it several times in concentrated solution of sodium hydroxide, rubbing it with filter paper, washing thoroughly with a stream of redistilled water, and finally washing with the solution in which it would be examined.

(B) **Aged Tungsten Rod or Filament.**—This was the same as (A) but in this case the same electrode was used throughout without being refreshed.

(C) **Powdered Tungsten.**—This was a B.D.H. sample which had been shaken with the solution for sometime and then used directly to cover a platinum contact for electrical measurements.

II. The Tungsten-Tungsten Trioxide Electrodes.—As most previous authors have attributed the behavior of the tungsten electrode as an indicator electrode for hydrogen ion activity to the formation of tungsten trioxide,⁷ the behavior of the following electrode also was examined.

(D) **Powdered Tungsten-Tungsten Trioxide.**—In this case the powdered metal was mixed thoroughly with the trioxide prepared as described by Archibald.⁸ The mixture was shaken with the solution for some time, and then allowed to settle on a platinum contact for electrical measurements.

III. The Solutions.—The solutions in which the electrodes were examined were buffers, except in the extreme alkaline range of pH where sodium hydroxide solutions were used.

From pH 0.65 to 5.00 we used the sodium acetate-hydrochloric acid buffer mixtures. A buffer solution of pH 5.79 was prepared from succinic acid and borax. From pH 7.05 to 9.25, boric acid-borax buffer mixtures were used, while for pH values 10.15, 10.85 and 11.03, sodium carbonate-hydrochloric acid mixtures were prepared.⁹

For the extreme alkaline range, sodium hydroxide solutions of concentrations 0.01, 0.05, 0.10, 0.50, 1.00 and 2.50 *M* were used. All the solutions were prepared from highly purified materials and their pH values were carefully checked with the hydrogen electrode and when possible with the quinhydrone electrode.

Electrical Measurements.—The electrical measurements were performed in the usual manner in an air thermostat fixed at $25 \pm 0.02^\circ$. These measurements were carried out in duplicate with differently prepared stock solutions using a saturated calomel electrode as the reference half cell. The e.m.f. measurements were carried out using a calibrated meter bridge on which accurate readings could be taken to 0.02 cm. A cadmium cell calibrated by the National Physical Laboratory and an Onwood Mirror galvanometer having a sensitivity of 190 mm./micro-ampere were used.

Results and Discussion

I. The Behavior of the Tungsten Electrodes in Solutions of Different pH Values.—Consideration of the variation of potential with time as well as with the pH of the solution for the different types of tungsten electrodes revealed the following.

(1) **Electrodes of Type A.**—Equilibrium potentials were recorded in all solutions after 1–2 hours from the time of immersion in unstirred solutions. The equilibrium values remained constant for 48 hours which was the time limit for our experiments. Both the tungsten rods and the filaments were found to give the same equilibrium potentials in the same solutions.

(2) **Electrodes of Type B.**—The steady-stage potential values were reached in all solutions directly after immersion and remained quite con-

stant for the next 48 hours. In this case also, the aged tungsten rod and filament electrodes gave approximately the same equilibrium potentials in the same solutions.

(3) **Electrodes of Type C.**—The potentials after immersion decreased to less positive values with time. Moderately constant potentials were obtained after about 24 hours which remained fairly constant for 48 hours.

(4) By plotting the steady-state potential values against pH for the electrodes of types A, B and C the three curves shown in Fig. 1 were obtained. These curves reveal that the potentials of the electrodes A and B are linear function of the logarithm of the hydrogen ion activity from \sim pH 0 to \sim pH 4 and then from \sim pH 5 to the extreme alkaline solutions. In case of the powdered tungsten electrodes the potentials are linear function of the pH from \sim pH 0 to \sim pH 6 and then from \sim pH 7 to the extreme alkaline solutions. The E_0 values (potential values at pH 0) were 0.26, 0.27 and 0.15 v. for the electrodes A, B and C before the break and 0.30, 0.31 and 0.30 v. after the break.

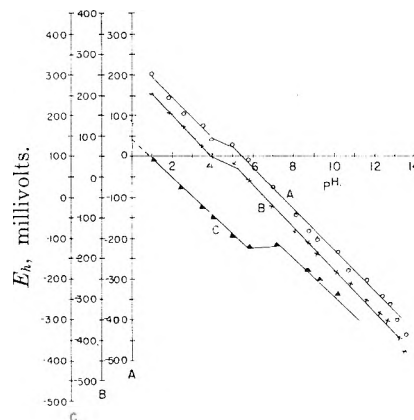


Fig. 1.—A, massive tungsten rod or filaments; B, aged tungsten rod or filament; C, powdered tungsten.

II. The Behavior of the Tungsten-Tungsten Trioxide Electrode in Solutions of Different pH Values.—In this case the following was observed.

(1) The potentials of the electrodes of the type D decreased to less positive values with time. Equilibrium potentials were obtained after about 24 hours which remained fairly constant for 48 hours.

(2) Figure 2, curve I, represents the plot of the equilibrium potentials against the pH of the solutions for the electrodes of type D. One must expect that the saturation of the solutions (specially with higher pH values) with WO_3 changes the pH values of such solutions. When buffer solutions of known pH values were saturated with WO_3 , the following variations in their pH values were noticed

Original pH	Final pH	Original pH	Final pH
1.03	0.90	5.82	5.45
1.93	1.96	7.10	5.65
3.04	3.03	8.05	6.15
3.98	4.01	9.10	6.65
5.02	5.13	10.15	7.14

Curve I in Fig. 2 was therefore corrected for such variations, in the pH values to curve II. From

(7) O. Gatty and E. C. R. Spooner, "The Electrode Potential Behavior of Corroding Metals in Aqueous Solutions," Oxford Press, New York, N. Y., 1938, p. 372.

(8) E. H. Archibald, "The Preparation of Pure Inorganic Substances," John Wiley and Sons, Inc., New York, N. Y., 1932, p. 285.

(9) H. T. S. Britton, "Hydrogen Ions," 2nd Edition, Chapman and Hall Ltd., London, 1932, p. 217.

this curve it can be noticed that the potentials of the electrodes of type D vary linearly with the pH of the solution from the extreme acid to the extreme alkaline solutions with a small break from pH 5 to 6. The E_0 value for this type of electrode was 0.24 v. before the break and 0.35 v. after the break.

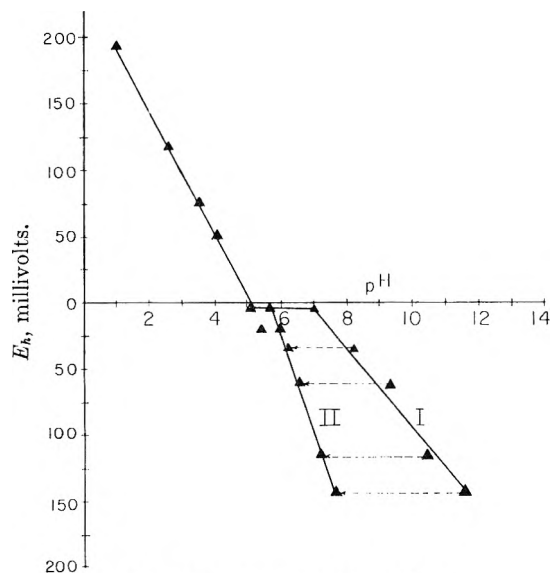
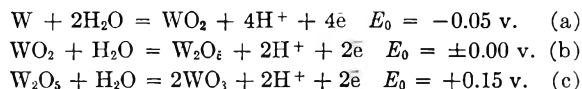


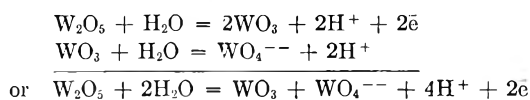
Fig. 2.—W powdered + WO_3 .

From the above results it can be noticed that both the fresh and aged tungsten rod electrodes gave quite similar potential- pH curves which were on the average similar to those of the powdered tungsten with the tungsten trioxide. In the case of the powdered tungsten electrode without the trioxide the potentials in comparatively acid solutions were always less positive. The agreement between the results obtained with the rod electrodes and the powdered tungsten-tungsten trioxide electrodes suggests that the behavior of the massive rod electrodes is governed by the formation of WO_3 . The free energy of such an oxide at 25° is $-171,400$ cal.¹⁰ and by taking the free energy of water at the same temperature as $-56,690$ cal.,¹⁰ then the free energy change in the reaction: $W + 3H_2O = WO_3 + 6H^+ + 6e$ will be at 25° $\Delta F = -1330$ cal. From this result the E_0 of the tungsten-tungsten trioxide electrode will be equal to -0.01 v. This value does not agree with the E_0 values obtained in any type of our electrodes and shows clearly that the idea of considering the behavior of the tungsten electrode as indicator electrode for hydrogen ion activity to its functioning as W/WO_3 electrode⁷ must be discarded. In order to clarify this point, the possibility of formation of other oxides than WO_3 over the electrode must be taken into consideration. The potentials registered in the different buffer solutions may represent the oxidation-reduction potentials between the higher and lower oxides. The free energies of the oxides WO_2 and W_2O_5 are $-118,300$ and $-293,000$ cal., respectively.¹⁰ From these free energy values the E_0 values for the different oxidation-reduction systems can be calculated as



From these results it can be noticed that the E_0 value of our powdered tungsten electrode in comparatively acid solutions agrees with that obtained from reaction (c) which indicates that the behavior of this electrode in such solutions is due to such a process.

In the comparatively alkaline solutions in all types of electrodes the E_0 values are, however, more positive than this value. If we take into consideration in such solutions, the formation of the tungstate ion WO_4^{--} , the electrode process will be



Now taking the free energy of formation of the WO_4^{--} at 25° as $-220,000$ cal. by comparison with the chromate,¹⁰ the free energy change in this process $\Delta F = 14,980$ cal. and hence E_0 will be equal to $+0.32$ v. This value agrees quite satisfactorily with the E_0 values obtained with all different types of electrodes in comparatively alkaline solutions. Calculations for the formation of two WO_4^{--} instead of one were found to lead to E_0 value which does not agree with the experimental results.

The fact that the E_0 value of powdered tungsten electrode in comparatively acid solutions agrees with the thermodynamically calculated value for the reaction $W_2O_5 + H_2O = 2WO_3 + 2H^+ + 2e$, while the E_0 values for all types of electrodes in comparatively alkaline solutions agree with that for the reaction $W_2O + 2H_2O = WO_3 + WO_4^{--} + 4H^+ + 2e$ is very interesting. As previously shown in the case of the antimony electrode,¹ one must expect that under certain comparable conditions the rate with which a certain type of oxide is formed at the surface of an electrode in aerated aqueous solutions will depend upon the surface of the metal exposed as compared with the supply of oxygen. Thus at any electrode surface under these conditions two processes are operating, the first is the action of atmospheric oxygen to give the higher oxide and the second is the effect of the metallic surface exposed which tends to reduce the higher oxide to the lower form. In the case of the powdered tungsten electrode the metallic surface exposed is comparatively larger than in the case of the massive rod electrode. This tends to reduce the higher oxide WO_5 to the lower form. It is known that the reduction of the hexavalent tungsten to the pentavalent state takes place in comparatively strong acid solutions; in weak acid solutions the reduction is incomplete and the intermediate reduction product tungsten blue is obtained.¹¹ This tungsten blue is usually considered as a compound between the penta- and hexavalent forms and can be represented by analogy with molybdenum blue either as $W_3O_8(WO_3 + W_2O_5)$ or $W_4O_{11}(2WO_3 + W_2O_5)$.¹² In neutral or alkaline solutions such re-

(10) W. M. Latimer, "The Oxidation States of the Elements and their Potentials in Aqueous Solutions," Prentice-Hall, Inc., New York, N. Y., 1938, p. 236.

(11) S. E. S. El Wakkad and H. A. Rizk, *The Analyst*, **77**, No. 912, 161 (1952).

(12) O. Glemser and H. Sauer, *Z. anorg. Chem.*, **252**, 144 (1943).

duction of the hexavalent tungsten cannot take place.¹³

These facts can explain quite clearly the behavior of the different types of tungsten electrodes. Thus in the case of the powdered tungsten electrode, owing to the comparatively larger metallic surface exposed, one must expect that the reduction of the hexavalent tungsten can take place but as the solutions are not very strong acid the reduction can proceed only to the intermediate stage the tungsten blue. Further evidence for this view has been obtained by preparing the tungsten blue according to the method recommended by Fridman¹⁴ and the oxidation-reduction potentials existing in solutions of different pH values were measured with a platinum electrode. The results obtained are shown in Fig. 3. This curve indicates that the potentials are linear function of the pH value and that E_0 is +0.14 v. in satisfactory agreement with the expected value according to our view.

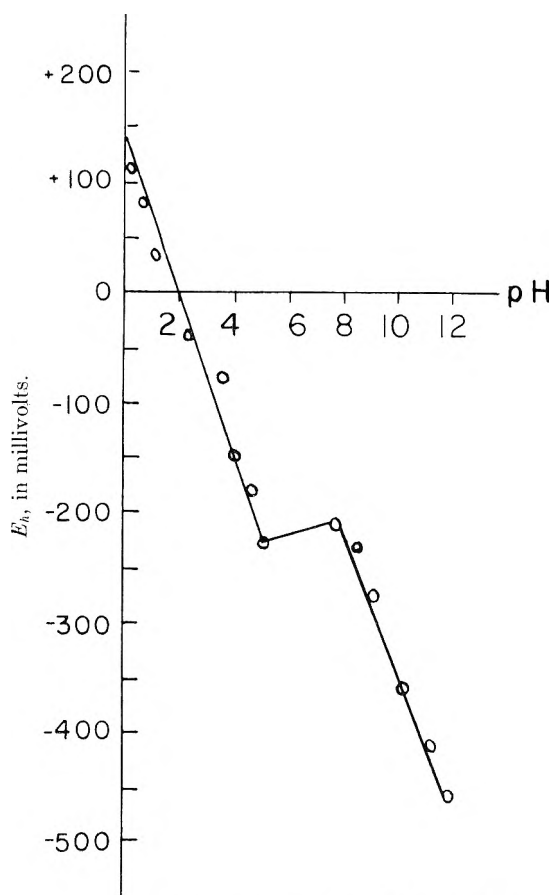


Fig. 3.—The behavior of tungsten blue electrode.

In the case of all types of tungsten electrodes in comparatively alkaline solutions, which are also similar to the powdered tungsten-tungsten trioxide electrode, no reduction is expected to occur in such medium and the WO_3 is not completely masked within the tungsten blue and thus the existence of the tungstate ions must be taken into consideration.

(13) S. Glasstone and A. Hickling, "Electrolytic Oxidation and Reduction," London, 1935, p. 134.

(14) D. Fridman, *Zhur. Obshchei Khimi. (J. Chem. U.S.S.R.)*, **18**, 1027 (1948).

Thus the electrode reaction in this case corresponds to $\text{W}_2\text{O}_6 + 2\text{H}_2\text{O} = \text{WO}_3 + \text{WO}_4 + 4\text{H}^+ + 2\text{e}$ and the E_0 values obtained experimentally agree with the one calculated from the free energy change in such reaction.

In comparatively acid solutions with massive rod electrodes and with powdered tungsten electrodes to which excess of WO_3 has been added we have seen that the potentials are not in agreement with any of the above given reactions. Two factors can be suggested as responsible for such behavior; the first is that in such comparatively less alkaline solutions, and in addition as WO_3 is not masked within the tungsten blue, the simple WO_4^{--} cannot exist as such. Thus, as will be shown in a following publication, the change from the para to the meta tungstate can take place between pH 6-4 and as the acidity increases several polytungstates are formed. The second factor, as was shown before in the case of antimony, is that there are two processes on the electrode surface; the first is the formation of the higher oxide WO_3 which tends to displace the potential to the more positive value and the second is the reduction of this oxide in such comparatively acid solutions leading to more negative potentials. The electrode is expected, therefore, to take an intermediate position between the two extremes. Against this view, however, is the fact that there is no appreciable drift in the potentials with time as in the case of the antimony electrode. This may suggest that the lower oxide film is comparatively more protective and thus the reduction process is exceedingly slow while as was shown in the case of antimony, the oxide film is not protective² leading to the continuous drift in potential with time. In order to clarify this point the anodic behavior of the tungsten electrode in the massive form was examined in 2.1 N NaOH and 8 N H_2SO_4 solutions following the same procedures developed by El Wakkad, *et al.*,¹⁵ in the anodic oxidation of metals at very low current density. Figure 4 is the charac-

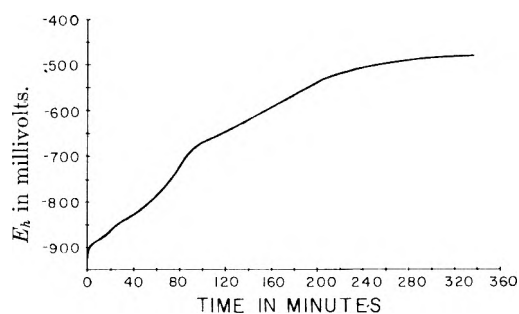


Fig. 4.

teristic anodic polarization curve of the tungsten electrode, with a polarizing current equal to 0.5 μ a. in 2.1 N NaOH and Fig. 5 is the curve in case of 8 N H_2SO_4 with a polarizing current equal to 5 μ a. From these curves it can be seen that at first there is a very short rapid initial build up of potential ascribable to the charging of the double layer as in previous studies¹⁵ which is followed by clear

(15) S. E. S. El Wakkad and S. H. Emara, *J. Chem. Soc.*, 461 (1952); 3504 (1953); 3508 (1953); S. E. S. El Wakkad and A. M. Shams Eldin, *ibid.*, 3094 (1954); 3098 (1954); S. E. S. El Wakkad, A. M. Shams Eldin and Abd. Elsayed, *ibid.*, 3103 (1954).

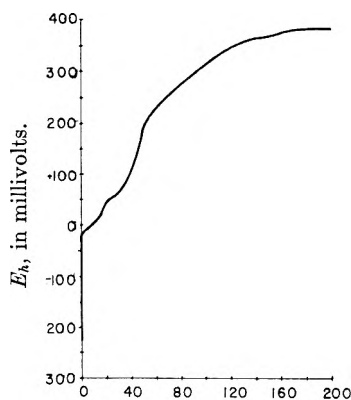


Fig. 5.

three steps before a constant potential was reached. Measurements from a large number of polarization curves in the 2.1 *N* NaOH gave an average value for the double layer capacity of about 200 μ F. per apparent sq. cm. and about 250 μ F. per apparent sq. cm. in 8 *N* H₂SO₄. The first arrest after the charging of the double layer appears to start at a potential of -0.89 v. in the sodium hydroxide solution and at a potential of -0.01 v. in the sulfuric acid solution. The second arrest appears to start at a potential of -0.84 v. and of $+0.05$ v. whereas the third step at -0.68 v. and $+0.20$ v. in these two solutions, respectively. The final constant potential recorded was at about -0.52 v. in the sodium hydroxide solution and at about $+0.035$ v. in the sulfuric acid solution. In Table I are shown the starting potentials for the three arrests in the sodium hydroxide solution as compared with the equilibrium potentials of the systems W/WO₂, WO₂/W₂O₅ and W₂O₅/WO₃ which are calculated at the corresponding pH from the thermal data as shown in eq. a-c.

TABLE I

Obsd. steps	Starting potential, v.		Oxidation system	Equilibrium potential, v.	
	NaOH	H ₂ SO ₄		NaOH	H ₂ SO ₄
1st	-0.89	-0.01	W-WO ₂	-0.89	0
2nd	-0.84	$+0.05$	WO ₂ -W ₂ O ₅	-0.83	$+0.06$
3rd	-0.68	$+0.20$	W ₂ O ₅ -WO ₃	-0.68	$+0.21$

The agreement between the equilibrium potentials calculated for the different systems of tungsten oxides and the starting potentials of the different steps experimentally observed in the anodic polarization curves strongly suggests that these steps correspond to the consecutive formation of the oxides WO₂, W₂O₅ and WO₃ on the surface of the tungsten anode. The latter oxide must be expected to dissolve in the strongly alkaline hydroxide solution to give the tungstate ion WO₄²⁻. It is interesting to

remark here that the constant potential recorded after the third step in the strong alkali hydroxide solution, *viz.*, -0.43 v., is in good agreement with the potential of the system (W₂O₅-WO₃)/WO₄²⁻ which is -0.51 v. at the corresponding pH as calculated from the thermal data. Also, in the case of the strongly acid solution the constant potential recorded after the third step as can be seen from Fig. 5 is at a potential equal to $+0.37$ v. as compared with $+0.32$ v. for the calculated value of the system (W₂O₅-WO₃)/WO₄²⁻. In such strongly acid solutions one must expect that the simple WO₄²⁻ ions cannot exist as such and the dissolution of the trioxide must be in the form of the tungstate ion WO₂²⁺. The isoelectric point of the tungsten trioxide as will be seen in another publication lies at about pH 0.43.

By calculating the thickness of the oxide films from the quantity of the electricity passed in each step and the capacity of the double layer,¹⁵ it was found that WO₂ formed in the strongly alkaline solution was less than unimolecular layer while in the strong acid solution it was 1-2 molecules thick. The quantity of electricity passed in the formation of W₂O₅ indicated that the oxide film in this case was also less than unimolecular in the sodium hydroxide solution and 2-3 molecules thick in the strong acid solution. At such extreme ranges of pH one must expect that the oxides of tungsten possess higher solubility and the estimated thickness of their films is higher than it should be.¹⁵

Trials were made to carry out the anodic polarization of tungsten in 0.1 *M* borax solution of pH 9.2 and 0.1 *N* sulfuric acid solution using polarizing currents of 1×10^{-6} or 5×10^{-7} a. per electrode but unfortunately the changes in the potential were too rapid to be recorded by the direct potentiometric method indicating the very small thickness of the oxides formed on the anode under these conditions. In this case, it was found that the potential of the anode reached a very high positive value and it increased very much with the increase of the polarizing current being about 4 volts when a polarizing current equal to 100 μ a. was applied and about 20 volts when the current was increased to 200 μ a. per electrode. Hence it can be concluded that the oxides of tungsten must be very protective and of highly non-conducting nature.

These facts explain satisfactorily that the tungsten rod electrodes do not show any appreciable drift with time and thus give this type of electrode an advantage over the antimony electrode for use as an indicator electrode for the hydrogen ion activity. A calibration curve for a tungsten electrode is expected to last for longer period of time.

THE KINETICS OF THE UNDERWATER CORROSION OF POWDERED MAGNESIUM¹

BY ELI S. FREEMAN AND SAUL GORDON

Pyrotechnics Chemical Research Laboratory, Picatinny Arsenal, Dover, N. J.

Received February 9, 1955

The kinetics of the underwater corrosion of atomized and ground magnesium powder was investigated in the presence of nitrogen, helium, carbon dioxide, hydrogen and oxygen. The course of the reaction was followed by observing changes in volume and pressure due to the hydrogen formed, as a function of time. Factors such as pH, nature of the film coating the particles, specific surface, gaseous atmosphere, pressure and temperature were found to affect the rate process. The kinetics appear to be determined by two rate-controlling mechanisms: (1) a non-diffusion controlled mechanism which may involve the neutralization of protons or the combination of hydrogen atoms on the surface of the metal to form molecular hydrogen, and (2) the diffusion of water through the hydrated magnesium hydroxide film coating the metal particles. The former mechanism predominates during the initial stages of the reaction; whereas the latter is important when films of sufficient thickness are formed. The kinetics of the initial stage of the reaction may be expressed by the logarithmic rate law: $t = Ae^{n/k}$ (see Appendix 1 for definition of symbols). The ensuing diffusion controlled stage of the reaction follows a general parabolic law, which in differential form may be expressed as $dN/dt = BN^{-k}$. The activation energies based upon the logarithmic and parabolic rate laws were calculated to be 7.48 kcal. per mole and 6.39 kcal. per mole, respectively, over the temperature range of 30.0 to 65.0°.

Introduction

The reaction of magnesium and water in the absence of oxygen may be considered from the point of view of a galvanic cell having Mg, Mg(OH)₂ and H₂, H₃O⁺ electrodes. The metal is oxidized and reacts with hydroxyl ions to form magnesium hydroxide, which coats each magnesium particle. The protons act as oxidizing agents and are reduced to hydrogen. Since gas is evolved as a reaction product, a convenient and simple method used to study the rate process involves measuring pressure or volume changes, at constant volume and pressure, respectively, as a function of time.

The effect of factors such as surface treatment, specific surface, temperature, pressure and the nature of the gases in the system were studied, since they may affect the kinetics of the reaction and contribute to an interpretation of the reaction mechanism.

Experimental

The magnesium powders used in the experimental work were obtained from the Dow Chemical Company, the Golvynne Chemical Corp. and the American Magnesium Company, as indicated in Table I. The atomized samples were very closely screened fractions (95+%) and were found to be of uniform shape and size, by microscopic examinations. The particle sizes of the samples were ascertained by the air permeability method using the Picatinny Arsenal particle size apparatus,² and the chemical composition was determined by spectroscopic and chemical analyses. The results are presented in Table I.

The apparatus for measuring pressure changes at constant volume consists of a 100-ml. two-neck round-bottom Pyrex flask (reaction vessel) connected to an open end manometer (2 mm. bore) containing dibutyl phthalate as the manometric fluid, and a 10-ml. buret.

For measuring changes in volume at constant pressure, the manometer is replaced by a gas buret and compensating tube, separated by a manometer. Two platinum wires are sealed in the intervening manometer and connected to an electronic relay³ used to operate a solenoid valve.⁴ An increase in pressure breaks the contact between the wire and the mercury on the buret side of the manometer, opening the solenoid valve. The mercury level in the gas buret

drops until the original pressure is restored, at which point the mercury-wire contact is again made, and the solenoid valve closes. The pressure of the system is controlled by varying the length of the wire. The response time for the apparatus is four milliliters per second. Changes in volume as small as 0.05 ml. are measured in this manner.

A weighed sample of magnesium powder is placed in the reaction vessel, and immersed in a thermostatically controlled water-bath in which the temperature is maintained to $\pm 0.2^\circ$. The reaction vessel is then connected to the appropriate apparatus for measuring volume or pressure changes. Two and five gram samples were used for the experiments at constant volume and pressure, respectively. The desired gas or mixture of gases was passed through the system until all the air was displaced, whereupon 10 ml. of water (saturated with magnesium hydroxide and the gas under study) was added to the flask by means of the buret. This solution, which was prepared by the reaction between ground magnesium and distilled water at the experimental temperature, had a pH of 10.7 (except in CO₂) and was used in all the experimental work in order to maintain a constant pH during the initial phase of the corrosion reaction. The gases used in this investigation ranged in purity from 99.6 to 99.9% and were purchased from the Matheson Company Inc. Prior to use the gases were passed through concentrated sulfuric acid and a concentrated solution of sodium hydroxide.

Blank determinations were carried out simultaneously with the experiments at constant volume in order to correct for variations in ambient pressure and temperature during the course of the reactions. The volumetric data obtained at constant pressure were reduced to standard conditions. The values for the rate of change in volume and pressure were determined by dividing the difference in volume or pressure between two successive times, by the difference in the corresponding times. All experimental determinations, with the exception of the temperature dependency series, were conducted at 30.0°.

Results

An indication of the effect that depolarization by oxygen⁵ may have on the kinetics of the reaction is obtained by observing the rate of corrosion in an oxygen atmosphere. The results are shown in Fig. 1, which is a log-log graph of the rate of change in pressure vs. time, for the reaction between atomized magnesium powder (specific surface 176 cm.² per g.) and water in oxygen and nitrogen environments. Also included in this figure is the reaction between ground magnesium (specific surface 10,700 cm.² per g.) and water in an atmosphere of nitrogen. The points fall along straight lines indicating that

(1) This paper was presented in part at the Meeting-in-Miniature of the American Chemical Society's New York Section before the Division of Physical and Inorganic Chemistry, February, 1954.

(2) B. Dubrow and M. Nieradka, *Anal. Chem.*, **27**, 302 (1955).

(3) A thyatron operated relay similar to the Emil Greiner Co. Model E-2.

(4) Automatic Switch Co. Valve #826212.

(5) S. Glasstone, "Introduction to Electrochemistry," D. Van Nostrand Co., Inc., New York, N. Y., 1942, p. 501.

TABLE I
 POWDERED MAGNESIUM SAMPLES

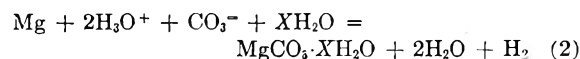
Screen fraction U. S. S. sieves	Particle size (μ)	Specific surface, cm. ² /g.	% compn.						
			Mg ^a	Al	Mn	Ni, Cu, Zn	Pb, Cd, Cr, Sn, Si, Ag	Fe	
60/80	196 ^a	176	99.1	0.02	0.09	0.02	0.03	0.05-0.06	
100/120	124 ^b	278	99.8	.2-0.3	.07	.02	.03	.05-.06	
120/140	115 ^b	299	99.5	.2-0.3	.07	.02	.03	.05-.06	
140/170	904 ^b	360	98.5	1.5	.07	.02	.03	.05-.06	
	53.9 ^c	650	97.4	0.02	.09	.02	.03	.05-.06	
		10,700 ^d							

^a Dow (atomized, disc method). ^b Golwynne Chemicals Corp. (atomized, jet method). ^c American Magnesium Co. (ground). ^d Specific surface as determined by krypton adsorption isotherms. ^e Metallic magnesium.

the rate of reaction may be expressed as a hyperbolic function of time

$$(dP/dt)_v = Ft^{-a} \quad (1)$$

In a carbon dioxide atmosphere, the initial pH of the solution is decreased, and hydrated magnesium carbonate rather than magnesium hydroxide is formed



The existence of magnesium carbonate as well as the basic carbonate was confirmed by X-ray studies in this Laboratory and by others.⁶ A rapid de-

crease in pressure occurs during the initial 25 minutes there is a rapid increase in pressure and the film coating the particles does not appear to exhibit inhibiting properties, since the rate of change in pressure is approximately constant. However, a parabolic type of corrosion follows. This is illustrated in Fig. 2, a graph of the log of the rate of change in pressure at constant volume vs. the log of time, which shows that the rate of change in pressure is a hyperbolic function of time during the latter period.

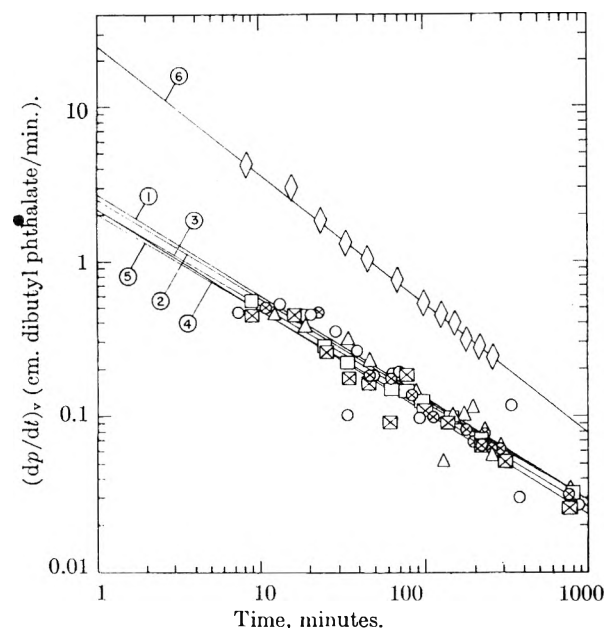


Fig. 1.—The rate of reaction of two grams of atomized and ground magnesium powders at constant volume; 30.0°; initial pressure 75.0 cm.; least square plot; $\log (dP/dt)_v$ vs. $\log t$.

- 1 ○ { atomized magnesium, specific surface 176 cm.²/g.,
- 2 △ { nitrogen atm.
- 3 □ {
- 4 ⊗ { atomized magnesium, specific surface 176 cm.²/g.,
- 5 ⊠ { oxygen atm.
- 6 ◇ { ground magnesium specific surface 10,700 cm.²/g.,
- { nitrogen atm.

crease in pressure occurs during the initial 25 minutes of the reaction. This is attributed to the dissolution of CO₂ due to the addition of a solution saturated with CO₂ in air into a system having a

(6) J. E. Regan and M. S. Silverstein, Frankford Arsenal, Tech. Report No. R-1092, 1952.

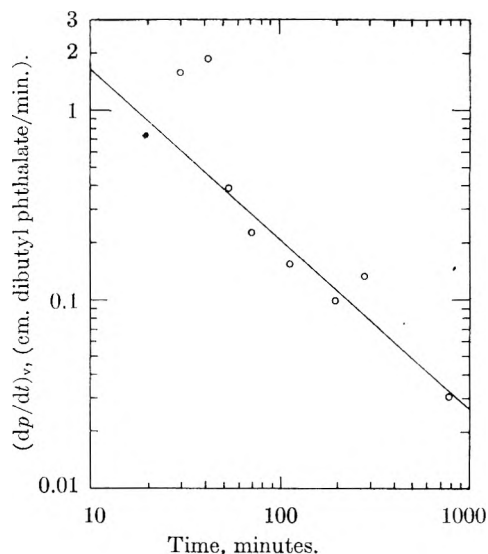


Fig. 2.—The rate of corrosion of 2 g. of atomized magnesium in the presence of carbon dioxide. Specific surface 176 cm.²/g.; initial pressure 75.0 cm.; 30.0°; $\log (dP/dt)_v$ vs. $\log t$.

The effect of hydrogen on the rate of corrosion is shown in Fig. 3, a graph of the log of the rate of change in pressure vs. the log of time. It is apparent that the velocity of the reaction has decreased significantly (see Table II). In a hydrogen atmosphere, F is 60% smaller than in nitrogen. However, the exponent, a , remains essentially unchanged.

The influence of pressure on the corrosion kinetics was studied in a nitrogen environment by varying the total pressure in the system from 43.0 to 74.9 cm. of mercury. An increase in the reaction rate was observed with increasing pressure.

It has been known for some time that forces acting on the surface of particles change with particle size and surface area. Therefore, this investigation included a study of this effect on the kinetics

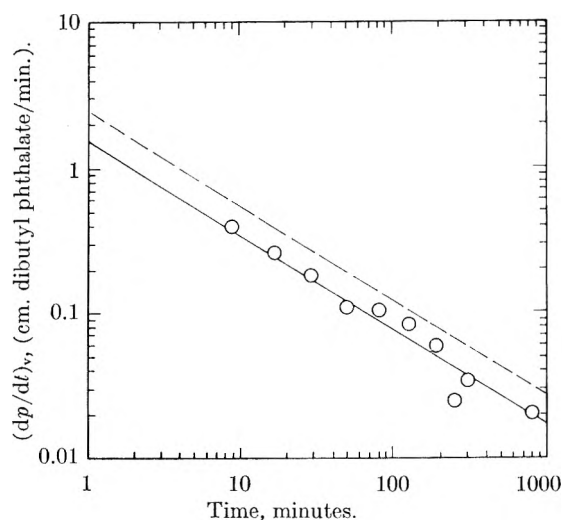


Fig. 3.—The influence of hydrogen on the rate of corrosion of two grams of atomized magnesium at constant volume; specific surface 176 cm.²/g., 30.0°; nitrogen diluent; initial pressure 75.0 cm., least square plot; log (dP/dt)_p vs. log *t*.

Partial hydrogen pressure
 - - - 0 (av. value)
 O 1.00

of the reaction. The results are shown in Fig. 4, a graph of the log of the rate of change in volume at constant pressure vs. the log of the volume. A series

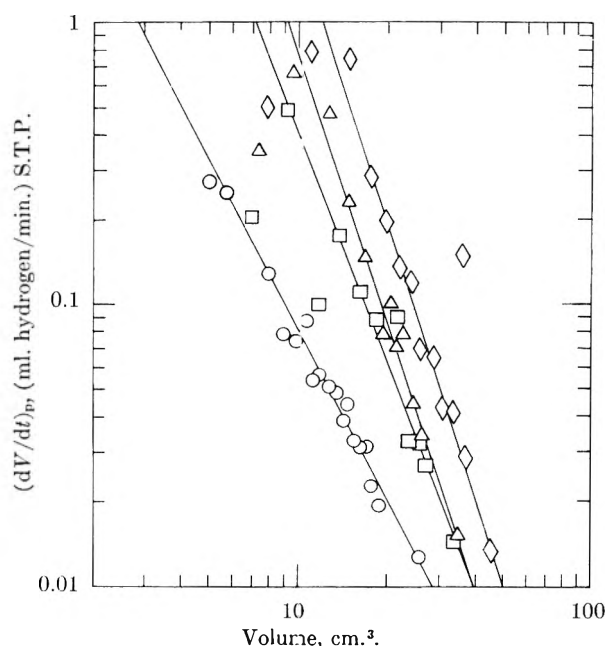


Fig. 4.—The effect of specific surface on the rate of reaction at constant pressure; five grams atomized magnesium; 30.0°, pressure 75.0 cm.; nitrogen atmosphere except for the sample of specific surface 176 cm.²/g., in helium atmosphere; pressure 74.9 cm. log (dV/dt)_p vs. log *V*.

TABLE II
 RATE PARAMETERS—RATE OF REACTION AT CONSTANT VOLUME, 30.0°

$$(dP/dt) = Ft^{-a}, k = a(1 - a)^{-1}$$

Gasous environment	$F,^b$ cm. dibutyl phthalate, g. ⁻¹ min. ⁻¹	a	k
Atomized magnesium, specific surface 176 cm. ² per g.			
N ₂ ^a	1.30	0.657	1.92
	1.08	.628	1.68
	1.28	.649	1.85
Average	1.22	.645	1.82
O ₂	1.03	0.628	1.68
	1.06	.645	1.82
Average	1.05	.637	1.75
CO ₂	6.50	0.894	8.54
H ₂	0.755	0.645	1.82
Ground magnesium, ^c specific surface 10,700 cm. ² per g.			
N ₂	12.3 ^d	0.832	4.95

^a $F = 6.94 \times 10^{-3}$ cm. dibutyl phthalate cm.⁻² min.⁻¹.
^b F is defined as the value of rate of change in pressure per gram at a time of one minute. ^c $B = 255$ moles H₂ cm.⁻² min.⁻¹. ^d $F = 1.15 \times 10^{-3}$ cm. dibutyl phthalate cm.⁻² min.⁻¹.

ies of straight lines are obtained, whose slopes increase in magnitude with particle size. The general equation for these lines is

$$(dV/dt)_p = BV^{-k} \quad (3)$$

A graph of the rate at which water reacts with atomized magnesium powder, (specific surface 176 cm.² per g.), vs. the concentration gradient across the film, results in curved lines showing that the diffusion coefficient is continually changing (see Fig. 5). The concentration gradient was obtained by considering that the concentration at the outer

	Specific surface cm. ² /g.
1	176
2	278
3	299
4	360

periphery of the film is that of pure water, and at the metal-film interface is zero.⁷ The curves are shown for reactions carried out over the temperature range of 30 to 65°. Initially a sharp decrease is observed which tapers off and approaches zero as the concentration gradient approaches zero and time approaches infinity.

A plot of the log of the rate of reaction at constant pressure vs. the log of the volume at 30.0, 40.0, 50.0, 60.0 and 65.0°, Fig. 6, yields a series of straight lines. At 50.0 60.0 and 65.0° deviations from parabolic behavior are observed during the initial stage of the reaction. Using the portion of the curve which is linear, the values of the constants k and B are determined (Table III). These vary from 2.00 to 5.62 for k , and 1.62 to 1.05 $\times 10^7$ ml. of hydrogen per gram per minute, for the coefficient, B . From an Arrhenius plot showing the temperature dependency of the rate constant, k , (Fig. 7) the activation energy was calculated to be 6.39 kcal. per mole.

It may be seen in Fig. 8, a graph of the log of the time vs. volume, that the deviations from the parabolic rate law at higher temperatures can be accounted for by the logarithmic rate law⁸

$$t = Ae^{cV} \quad (4)$$

At a temperature of 30.0° the logarithmic

(7) The calculation of the film thickness was based upon the formation of a magnesium hydroxide film (density 2.38 g./cm.³) equivalent to the volume of hydrogen evolved.

(8) G. Tammann and W. Koster, *Z. anorg. allgem. Chem.*, **123**, 196 (1922).

TABLE III
RATE PARAMETERS-RATE OF REACTION AT CONSTANT PRESSURE (ATMOSPHERIC)

Temp., °C.	Gaseous atm.	Specific surface, cm. ² /g.	$t = Ae^{v/k'}$		$\left(\frac{dv}{dt}\right)_P = BV^{-k}$		k	k'^a
			A , ^a min.	Ml. H ₂ , ^b g. ⁻¹ min. ⁻¹	Ml. ^a H ₂ , ^b cm. ⁻² min. ⁻¹	Moles H ₂ , ^b cm. ⁻² min. ⁻¹		
30.0	N ₂	278	...	3.74×10^1	1.34×10^{-1}	5.97×10^{-6}	2.68	.
		299	...	2.24×10^2	7.52×10^{-1}	3.35×10^{-6}	3.16	...
		360	...	6.32×10^2	1.76	7.75×10^{-6}	3.25	...
40.0	He	176	5.63×10^{-3}	1.62	9.20×10^{-3}	4.10×10^{-7}	2.00	0.200
			5.70×10^{-4}	1.91×10^1	1.08×10^{-1}	4.82×10^{-6}	2.66	.290
			5.70×10^{-4}	1.26×10^3	7.16	3.20×10^{-4}	3.50	.510
60.0			3.16×10^{-4}	5.05×10^6	2.86×10^3	1.28×10^{-1}	5.08	.630
65.0			2.00×10^{-4}	1.05×10^7	5.97×10^4	2.66	5.62	.750

^a First logarithmic branch. ^b B is defined as the rate of reaction when the volume per g., volume per unit surface area or number of moles of hydrogen per unit surface area is equal to unity.

branches are not well defined and the points appear to fall along a smooth curve. At 40.0° the first logarithmic branch extends to a period of ten minutes, and is increased to 35 minutes at a temperature of 65.0°.

For the first logarithmic branch, from a graph of the log of k' ($k' = C^{-1}$) vs. the reciprocal of the absolute temperature, Fig. 7, the activation energy was calculated to be 7.48 kcal. per mole.

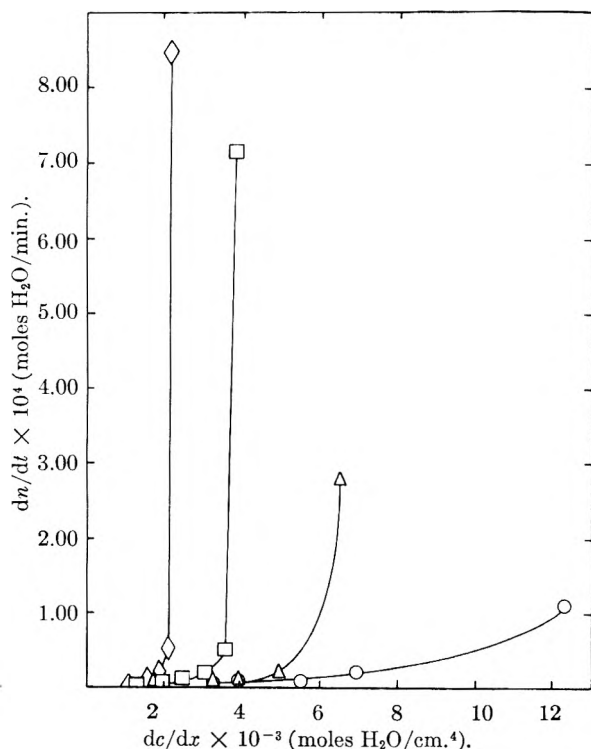


Fig. 5.—The diffusion of water through the magnesium hydroxide film as a function of the concentration gradient at constant pressure; five grams atomized magnesium; specific surface 176 cm.²/g.; helium atmosphere; dn/dt vs. dc/dx .

Pressure, cm.	Temp., °C.
74.9	○ 30.0
74.9	△ 40.0
74.5	□ 50.0
74.9	◇ 65.0

Discussion

Figure 1 demonstrates that in oxygen and nitrogen the underwater corrosion of magnesium powder

is a hyperbolic function of time (equation 1), a modified form of the general parabolic rate law.

$$P_v^2 = Kt + b \quad (5)$$

The intercept values are slightly smaller for the reaction in oxygen than in a nitrogen atmosphere (Table II). This may be due to the formation of magnesium oxide, which would increase the density and impermeability of the film. The lack of a

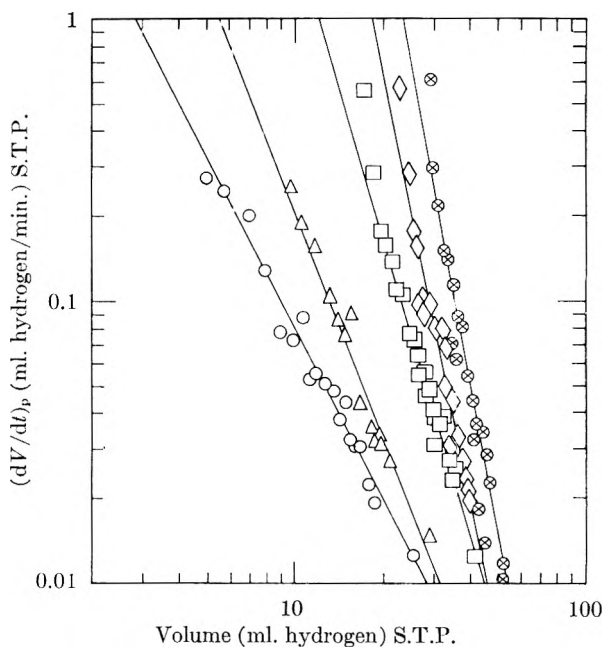


Fig. 6.—Log of the rate of change in volume vs. log of volume at constant pressure; 5 g. atomized magnesium; specific surface 176 cm.²/g.; helium atmosphere.

Pressure cm.	Temp., °C.	Symbol
74.9	30.0	○
74.9	40.0	△
74.5	50.0	□
75.1	60.0	◇
74.9	65.0	⊗

depolarizing effect by oxygen indicates that the rate of depolarization is not of primary importance as far as the kinetics of the reaction is concerned, at 30.0°, and the rate of the over-all reaction may be attributed to a diffusion mechanism. The integral form of equation 1 (equation 5) has been observed by others for reactions in which the rate-controlling step is that of a material transported

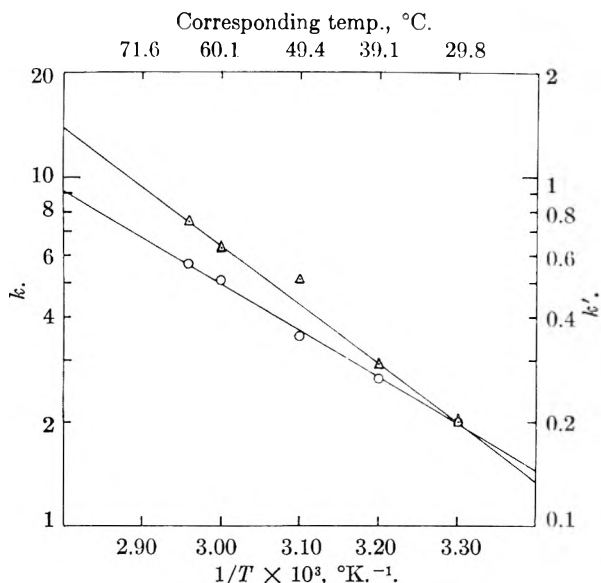


Fig. 7.—Temperature dependency of the corrosion of atomized magnesium powder at atmospheric pressure; specific surface 176 cm.²/g.; helium atmosphere: O, $\log k$ vs. $1/T$ ($^{\circ}\text{K.}^{-1}$); Δ , $\log k'$ vs. $1/T$ ($^{\circ}\text{K.}^{-1}$).

through a film, such as in the high temperature oxidation of metals.⁹

The rate of reaction of ground magnesium powder (specific surface 10,700 cm.² per g.) per unit weight is considerably greater than that of atomized magnesium powder (specific surface 176 cm.² per g.), as shown in Fig. 1. The constant, a , increases from 0.645 to 0.832 and the constant, F , which is numerically equal to the rate of reaction after a period of one minute, increases from 1.22 to 12.3 cm. of dibutyl phthalate per gram per minute. In terms of the increase in pressure per unit surface area, the results are reversed and the constant, F , is greater for atomized magnesium than for the ground powder. The values are 6.94×10^{-3} and 1.15×10^{-3} cm. dibutyl phthalate per cm.² per minute, respectively. The significance of these results is discussed further under the effect of particle size.

In a carbon dioxide atmosphere the constant, F , is from five to six times greater than that in oxygen and nitrogen environments, the value being 6.5 cm. of dibutyl phthalate per gram per minute. The constant, a , is increased from 0.645 to 0.894 (Table II). From the point of view of the permeability of the film coating the magnesium, the results may seem anomalous since hydrated magnesium carbonate and the basic carbonate have greater densities than magnesium hydroxide. This effect, however, is apparently small, compared to the influence of the greater proton concentration.

The rate of reaction in an atmosphere of hydrogen is less than in oxygen or nitrogen. This inhibiting effect is not attributed to a reversal of the reaction, since it is not thermodynamically feasible under the experimental conditions, but rather to an increase in the extent of polarization due to the hydrogen environment. This effectively causes an increase in hydrogen-bound surface and consequently a decrease in the amount of magnesium available for reaction.

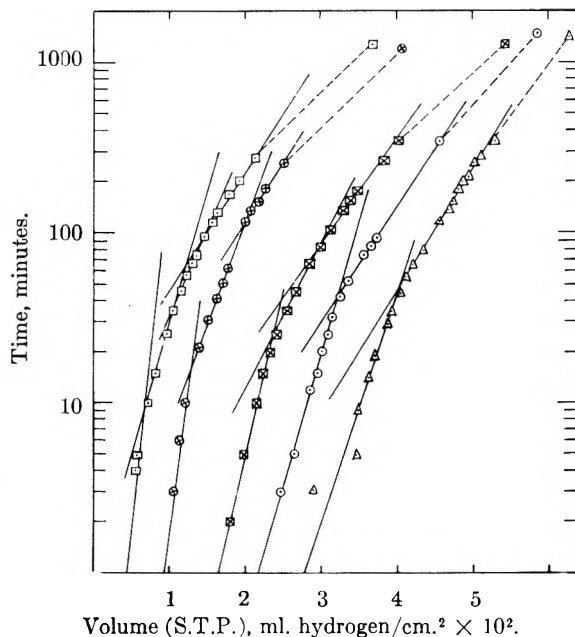


Fig. 8.—Log time vs. volume of hydrogen evolved per cm.² of surface; same legend as Fig. 6.

By increasing the pressure (43.0 to 74.9 cm.) the reaction rate is increased. This is attributed to an acceleration in the rate of diffusion of water. It is of interest to point out that in the dry oxidation of metals, electrons and cations are thought to diffuse from the metal-metal oxide interface to the outer periphery of the protective film, where the metal oxide is formed.¹⁰ In the underwater corrosion of magnesium, the outward diffusion of magnesium ions may take place over short distances. However, since the cation is hydrated, this process is slow compared to the rate of diffusion of water into the film. Therefore, as a consequence of the greater size and weight of the hydrated cations the film growth probably occurs at the metal-film interface.

In studying the effect of particle size, a differential form of equation 5 was used, *i.e.*, equation 3. A broader understanding of the significance of this relationship may be obtained by converting the equation to its logarithmic form

$$\log (dV/dt)_P = \log B - k \log V \quad (6)$$

By differentiating and solving for k , it is evident that although k is dimensionless it expresses a rate: the ratio of the change in the log of the rate of change in volume to the change in the log of the increase in volume

$$\frac{d \log (dV/dt)_P}{d \log V} = -k \quad (7)$$

Since the volume is a measure of the increase in film thickness, k may be looked upon as a rate parameter expressing the change in the log of the rate of reaction per unit change in the log of the increase in film thickness. While both constants are necessary to define the system, the constant k , a measure of the effect of film thickness, would appear to be of greater fundamental significance than the co-

(9) B. Lustman, *Trans. Electrochem. Soc.*, **83**, 313 (1943).

(10) (a) N. F. Mott, *Trans. Faraday Soc.*, **36**, 472 (1940); (b) C. Wagner and K. Grunewald, *Z. physik. Chem.*, **40B**, 455 (1938).

efficient B , which in physical terms refers to the reaction rate at a specific film thickness.

As the specific surface of the atomized magnesium powder was increased from 176 to 360 cm.² per g., there was an increase in k from 2.00 to 3.25. B , which is numerically equal to the number of moles of hydrogen formed per cm.² of surface per minute, increased from 4.10×10^{-7} to 7.75×10^{-5} . In the case of ground magnesium, specific surface 10,700 cm.² per g., the corresponding values of k and B are 4.95 and 2.55×10^2 ml. of hydrogen per cm.² per minute (see Table III). These values are calculated from the constants, F and a , in equation 1, which are related to k and a , by equations 8 and 9¹¹

$$k = a(1 - a)^{-1} \quad (8)$$

$$B = (1 - a)(F/(1 - a))^{1/(1-a)} \quad (9)$$

Previously it was pointed out that although the constant a was greater for ground than atomized magnesium powder, the reverse was true for the value of F , in terms of the rate of reaction per unit surface area. When considering that the reaction rate is diffusion controlled, these results may be expected, since the value of F refers to a rate of reaction at a time of one minute, when the film thickness on the ground magnesium particles is greater than that formed on the less reactive atomized magnesium powder. The results show that the rate of reaction per unit surface area increases with increasing specific surface. This may be attributed to forces acting on the diffusing molecules and/or the protective film, thusly affecting its structure and permeability.

In Fig. 5, it is observed that the diffusion coefficient is continually changing. These results are attributed to an aging of the magnesium hydroxide film. In the same figure it may be seen that the diffusion of water is rate controlling only after a certain minimum or critical film thickness has been attained. As the temperature is increased, the critical film thickness increases, as indicated by the limiting values of the concentration gradient, when the diffusion coefficient approaches infinity.

The value of the energy of activation for parabolic corrosion was calculated to be 6.39 kcal. per mole. This value is in the range expected for reactions in which the diffusion of water is rate determining. It was previously shown (see Results, Fig. 8) that the initial stages of the reaction which deviate from parabolic behavior obey a logarithmic rate law.

From the logarithmic form of equation 4, which upon differentiation yields

$$dv/d \ln t = C^{-1} \quad (10)$$

it is evident that C^{-1} is a rate constant referring to the change in volume per unit change in the logarithm of time

$$\text{rate constant, } k' = C^{-1} \quad (11)$$

Incorporating the rate constant into equation 4, the final form of the rate equation is obtained

$$t = Ae^{v/k'} \quad (12)$$

The constant A has the dimensions of time and may perhaps be considered as an induction period.

The logarithmic deviation from parabolic be-

havior is of interest since it indicates the possibility of an additional rate-determining mechanism prior to the formation of a protective film. Another indication of two rate mechanisms may be seen in Fig. 5 from which it is evident that an additional rate mechanism is operative prior to the attainment of a certain minimum film thickness, beyond which the reaction rate is diffusion controlled. An analogy may be drawn between the underwater corrosion of magnesium powder and the electrolysis of many aqueous solutions, for which a rate mechanism involving the discharge of protons by electrons or the recombination of hydrogen atoms on the surface of the metal to form molecular hydrogen is postulated.¹² The activation energy during this initial period, based upon logarithmic behavior (7.48 kcal. per mole), is in the range expected for this mechanism.

Acknowledgment.—The authors wish to express their appreciation to J. J. Campsis and S. Weisberger for the X-ray diffraction and spectroscopic analyses reported in this study, and to B. Dubrow, M. Nieradka and A. Tomicsek for the particle size analyses and preparation of the powdered metal samples. We also wish to thank M. Katz of the Chemical Physics Branch, Squier Signal Laboratory, Fort Monmouth, New Jersey for the krypton adsorption studies. In addition, the authors express their gratitude to D. Hart, H. Cohen, G. Weingarten and B. Werbel for their discussions and review of this manuscript.

Appendix I

A = a constant	t = time
K = a constant	P = pressure
B = a constant	V = volume
F = a constant	N = moles of hydrogen formed
a = a constant	P_v = change in pressure at constant vol.
n = a constant	$(dP/dt)_v$ = rate of change in pressure at constant vol.
b = a constant	$(dV/dt)_P$ = rate of change in vol. at constant pressure
k = rate constant	
k' = rate constant	

Appendix II

Evaluation of the Constants k and B in Terms of a and F .—The rate of corrosion obeys the general parabolic rate law

$$N^n = Kt \quad (1)$$

where N may equal pressure, volume or number of moles of hydrogen formed per unit surface area. Differentiating implicitly and explicitly

$$\frac{dN}{dt} = \frac{K}{n} N^{1-n} \quad (2)$$

$$\frac{dN}{dt} = \frac{K^{1/n}}{n} t^{1/n-1} \quad (3)$$

The experimental rate equations are

$$\frac{dN}{dt} = BN^{-k} \quad (4)$$

$$\frac{dN}{dt} = Ft^{-a} \quad (5)$$

By comparing equations 2 with 4, and 3 with 5 the following relationships are obtained

$$B = K/n \quad (6)$$

(12) S. Glasstone, K. J. Laidler and H. Eyring, "The Theory of Rate Processes," McGraw-Hill Book Co., New York, N. Y., 1941, p. 583.

(11) See Appendix II for derivation.

$$F = \frac{K^{1/n}}{n} \quad (7)$$

$$(1/n) - 1 = -a; \quad n = (1 - a)^{-1} \quad (8)$$

Solving for K in equation 7

$$K = (Fn)^n \quad (9)$$

K and B may be related by substituting equation 6 in the above expression

$$B = (Fn)^n/n \quad (10)$$

Substituting equation 8 in equation 10 results in the final relationship

$$B = (1 - a) \left(\frac{F}{1 - a} \right)^{(1-a)^{-1}} \quad (11)$$

By comparing the exponents of equations 2 and 4

$$k = n - 1 \quad (12)$$

Substituting equation 8 in equation 12

$$k = a(1 - a)^{-1} \quad (13)$$

SPECIFIC HEAT OF SYNTHETIC HIGH POLYMERS: IV. POLYCAPROLACTAM

BY PAUL MARX, C. W. SMITH, A. E. WORTHINGTON AND MALCOLM DOLE

Contribution from the Chemical Laboratory of Northwestern University, Evanston, Illinois

Received March 11, 1955

Polycaprolactam, or 6 Nylon, has been studied with respect to its specific heat using a new calorimetric system over the temperature range -20 to 280° in flake, drawn, undrawn filament and annealed forms. The results are compared with similar measurements on 6-6 Nylon. Apparently, depolymerization in the melt on annealing lowers the glass transition temperature about 15° . The undrawn filaments exhibit irreversible recrystallization effects from 90 to 160° . The crystallinity of 6 Nylon is slightly less than that of 6-6 Nylon, but exhibits a maximum in the case of the drawn and undrawn fibers at 190° . At room temperature the crystallinity of the drawn fibers is less than that of the undrawn.

I. Introduction

Polycaprolactam or 6 Nylon is chemically identical with polyhexamethylene diamine, 6-6 Nylon, except for head-to-tail arrangement of its imine and carbonyl groups as compared to the head to head arrangement of the imine or carbonyl groups in 6-6 Nylon. For this reason it appeared to be of interest to measure the specific heat of 6 Nylon for comparison with previous measurements on 6-6 Nylon.¹ Such measurements include the measurement of heats of fusion, heats of transition, heats of crystallization and heats associated with second order or glass² transitions. As far as we are aware there have been no previously published data for the specific heat of 6 Nylon.

Brill³ made an X-ray study of 6 and 6-6 Nylon as a function of temperature. He demonstrated that the 020 and 220 lattice spacings increased more rapidly with temperature in the case of the 6-6 Nylon than in the case of 6 Nylon and equalled the 200 spacing at 165° giving to the 6-6 Nylon a pseudo hexagonal structure at that temperature. This hexagonal structure exists in cross-section only. In the case of 6-6 Nylon the breaking of hydrogen bonds followed by the shifting of adjacent chains and a rotational oscillation of about 60° of the chain segments permits the formation of new hydrogen bonds and the establishment of the pseudo hexagonal structure. In 6 Nylon the segmental rotation does not result in conditions favorable for hydrogen bond formation, hence 6 Nylon does not make the transition to pseudo hexagonal symmetry.

Mikhailov and Klesman⁴ studied the effect of ex-

tent of crystallization on the thermal properties of 6 Nylon. Making a thermographic and X-ray analysis of samples prepared from an evaporation of a formic acid solution or by slow cooling and samples prepared by rapid cooling, they concluded that 6 Nylon could exist in two forms, an imperfect, unstable crystalline form, and a glassy amorphous form. The slowly cooled form exhibited a single endothermic effect at 206 – 216° , while the amorphous form showed two endothermic effects, at 120 – 158° and at 216 – 222° . The 120 – 150° range is also referred to as a range of temperatures where vitrification occurs. They speak of a "heat of fusion" of the crystalline form as 12.4 cal./g., and of the glassy modification as 9.4 cal./g.

II. Experimental Details

The following samples of 6 Nylon⁵ were studied:

1. Extracted 6 Nylon flake containing approximately 1.7% water extractables having a number average molecular weight on an extracted basis of about 20,000.

2. Undrawn 6 Nylon yarn (1050 denier, 34 filaments) containing about 4% water extractables and having a number average molecular weight on an extracted basis of about 18,500.

3. Drawn 6 Nylon yarn (210 denier, 34 filaments) containing about 4% water extractables, and having a number average molecular weight on an extracted basis of about 18,500.

The above samples were used as received from the du Pont Company except that the samples were dried to constant weight by evacuation before each specific heat measurement. "Melt annealed" samples were prepared by slowly cooling the 6 Nylon while still in the calorimeter after the 6 Nylon had been heated above the melting point. It was assumed that due to depolymerization in the melt the melt annealed samples contained 11% of monomer (caprolactam) when heated⁶ to 282° , and 7% monomer if heated⁶ to 235° . Other annealed samples were prepared by slow cooling from a temperature somewhat below the melting point. These were called "210 or 190° annealed" Nylon.

(5) Generously forwarded to us by Dr. J. Zimmerman of the Nylon Research Division, E. I. du Pont de Nemours and Co.

(6) Information received from Dr. R. E. Wilfong, Nylon Research Division, E. I. du Pont de Nemours and Co.

(1) R. C. Wilhoit and M. Dole, *THIS JOURNAL*, **67**, 14 (1953).

(2) P. J. Flory, "Principles of Polymer Chemistry," Cornell University Press, Ithaca, N. Y., 1953, p. 56; and W. Kauzmann, *Chem. Revs.*, **43**, 219 (1948), have reviewed the subject of second order and glass transitions.

(3) R. Brill, *J. prakt. Chem.*, **161**, 49 (1942).

(4) N. V. Mikhailov and V. O. Klesman, *Doklady Akad. Nauk. U.S.S.R.*, **91**, 99 (1953); *C.A.*, **48**, 20 (1954); **48**, 13359 (1954).

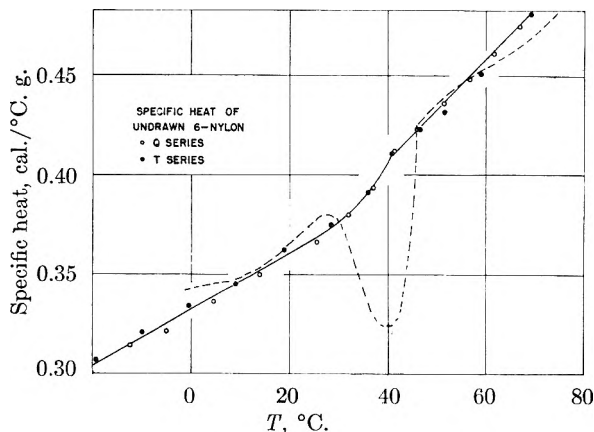


Fig. 1.—Comparison of the specific heat of undrawn 6 Nylon (solid line) with that of undrawn 6-6 Nylon (dotted line) over the temperature range -20 to 80° .

A new improved calorimeter and bimetallic adiabatic jacket⁷ were used for the specific heat measurements on 6 Nylon. The watt-hour meter for the measurement of the electrical energy input previously described⁸ was calibrated⁷ by measuring the energy required to melt a known weight of ice in the calorimeter. The heat capacity of the empty calorimeter was found by calibration⁷ using synthetic sapphire, Al_2O_3 , whose specific heat has been accurately determined by Ginnings and Furukawa.⁹ The technique of applying corrections for temperature unbalance between the calorimeter and adiabatic jacket previously described¹⁰ was considerably simpler in this research as compared to that on 6-6 Nylon,¹ because of the improved design of the calorimeter and the use of heat shields to close the top and bottom ends of the adiabatic jacket.⁷ Only one correction factor was applied instead of two or more. In one calibration experiment using Al_2O_3 sixteen heat capacity results for the total system of calorimeter plus contents deviated

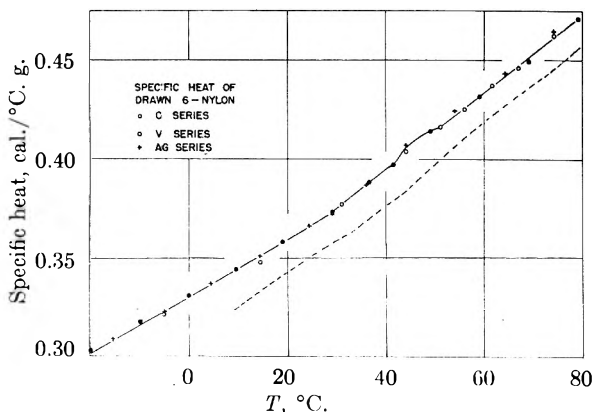


Fig. 2.—Comparison of the specific heat of drawn 6 Nylon (solid line) with that of drawn 6-6 Nylon (dotted line) over the temperature range -20 to 80° .

from a smooth curve to an average extent of 0.07%. The specific heat data for the high polymers are less accurate, however. The uncertainty depends partly on the experimental methods and technique, but also on the reproducibility of the behavior of the polymers themselves, as previously noted.¹ As an example, let us consider the undrawn fibers which represent the most rapidly quenched and the least reproducible samples. Over the temperature range from -20 to $+40^{\circ}$, which covers the glass transition range,

(7) A. E. Worthington, Paul Marx and M. Dole, paper submitted for publication.

(8) M. Dole, N. R. Larson, J. A. Wethington, Jr., and R. C. Wilhoit, *Rev. Sci. Instrum.*, **22**, 818 (1951).

(9) D. C. Ginnings and G. T. Furukawa, *J. Am. Chem. Soc.*, **75**, 522 (1953).

(10) M. Dole, W. P. Hettinger, Jr., N. Larson, J. A. Wethington, Jr., and A. E. Worthington, *Rev. Sci. Instrum.*, **22**, 812 (1951).

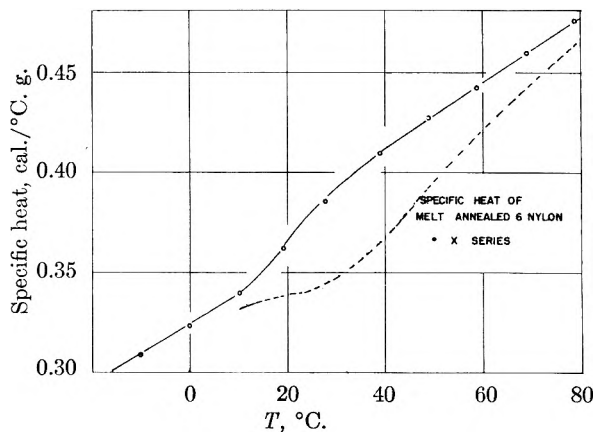


Fig. 3.—Comparison of the specific heat of melt annealed 6 Nylon (solid line) with that of 6-6 Nylon (dotted line)

the data obtained in two independent series of measurements fluctuated on the average $\pm 0.4\%$ from a smooth curve; over the temperature range 40 to 80° , the fluctuations decreased to an average of $\pm 0.33\%$, but over the range 80 to 160° where probably some recrystallization took place in the polymer, the average fluctuations rose to $\pm 0.93\%$. In the liquid range, 240 to 270° , where strains and irregularities similar to those of the solid state would not be expected to exist, the average fluctuations fell to $\pm 0.25\%$ for the data of three series despite the higher temperatures and the greater difficulty of carrying out specific heat measurements at such temperatures. The uncertainty in the absolute values at the high temperatures may be as high as $\pm 0.5\%$.

III. Experimental Results and Discussion

A. Second Order or Glass Transition Effects.—

Both 6 and 6-6 Nylon exhibit changes of specific heat with temperature suggestive of second order or glass transitions. By a second order or glass transition we mean a discontinuity in the specific heat-temperature curve, the specific heat suddenly increasing with the slope of the specific heat-temperature curve usually being greater at temperatures above the second order transition than below. The transitions are not sharp, nor are they transitions between two phases in thermodynamic equilibrium.¹¹ Because they are probably kinetic effects with the magnitude of the effect depending on the time of observation, these transitions should more properly be called glass transitions.² The glass transitions occur probably only in the amorphous regions of the polymer, inasmuch as they seem to be far more pronounced and definite in polyvinyl chloride¹² and polyethylene terephthalate¹³ which are much more amorphous than the polyamides. Another indication of the importance of the amorphous regions for the glass transitions is the fact that the glass transition temperatures for 6 and 6-6 Nylon are the same (at least for the flake form) despite the fact that their maximum melting points (determined by the crystalline regions) differ by 40° .

Examples of glass transitions in this research are shown in Fig. 1, undrawn 6-Nylon at 30 – 40° ; and Fig. 3, melt-annealed 6-Nylon at 15 – 20° . Granular 6 Nylon also shows a glass transition at 40 – 50° .

The lowering of the glass transition temperature on melt-annealing the 6 Nylon is probably the re-

(11) J. E. Mayer and S. F. Streeter, *J. Chem. Phys.*, **7**, 1019 (1939).

(12) Unpublished data of S. Alford and M. Dole.

(13) Unpublished data of C. W. Smith and M. Dole.

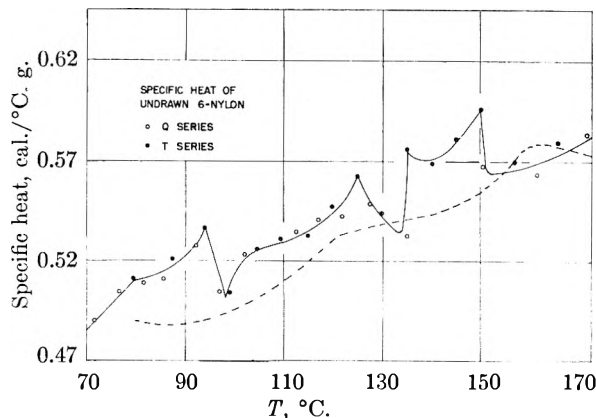


Fig. 4.—Comparison of the specific heat of undrawn 6-Nylon (solid line) with that of 6-6 Nylon (dotted line) over the temperature range 70 to 170°.

sult of the depolymerization of the material that occurs at high temperatures, the monomer and dimer content rising to 11 from 4 weight per cent.⁶ Table I contains data that illustrate the relationship between monomer content and the glass transition temperature. The glass transition temperature given is the temperature at which the slope of the specific heat temperature curve is a maximum.

TABLE I

GLASS TRANSITION TEMPERATURE AND MONOMER CONTENT

Form	Transition temp., °C.	Approx. % of cyclic monomer present
Flake	45-48	1.7
Undrawn filaments	37	4
Pre-melt annealed	38	4
Melt annealed	20	11

The monomer possibly acts as a plasticizer¹⁴ in the amorphous regions of the polymer, thus permitting the onset of the molecular vibrations responsible for the appearance of the glass transition at 20 instead of 40°. Conversely drawing the fibers produces a peculiar peak in the specific heat curve at 115° in the case of 6 Nylon, Fig. 5, and a less pronounced peak at 135° in the case of 6-6 Nylon. There is a definite slight "hump" in the specific heat curve of drawn 6 Nylon at 42°. When the drawn fibers are annealed just below their melting point, the pre-melt annealing, the effect at 115° disappears and the glass transition reappears at 40°. We interpret these observations on the supposition that drawing the polymer produces mechanical strains in the amorphous regions which raise the activation energy required for the onset of the molecular motion responsible for the glass transition; annealing eliminates the strains and permits the molecular motions to commence at their normal temperature of 40°.

B. Recrystallization in the Solid State.—Much more pronounced than the glass transition effects are the unusual fluctuations in specific heat of the undrawn 6 Nylon over the temperature range 90 to 160° as illustrated in Fig. 4. As these effects are

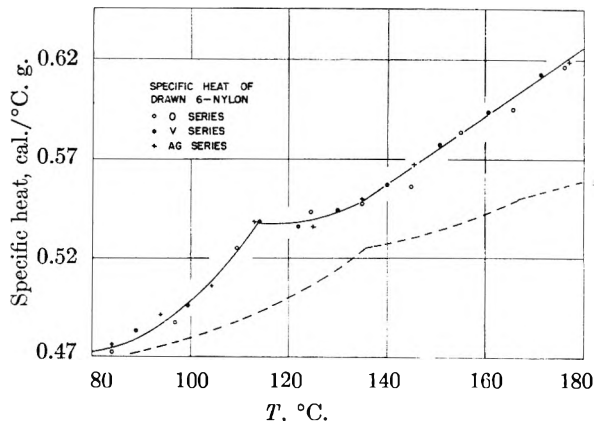


Fig. 5.—Comparison of the specific heat of drawn 6 Nylon (solid line) with that of 6-6 Nylon (dotted line) over the temperature range 80 to 180°.

not reproduced by the annealed samples, they undoubtedly represent irreversible transitions of segments of the chains from metastable states to states of lower energy. The transitions might also represent small crystallizations taking place. Three fairly well defined minima seem to exist over this range. Drawing the undrawn filaments eliminated these fluctuations. In the case of the melt annealed sample, Fig. 6, the specific heat rose smoothly with temperature over the temperature interval, 80 to 180°. Neither the pre-melt annealed nor the granular 6 Nylon exhibited any unusual specific heat effects in this temperature range.

It should be noted that the specific heat data are sensitive indications of transformations within the solid. Thus, the area between a straight line connecting the peaks of the specific heat temperature curve for the undrawn sample at 125 and 144° and the curve itself is equal to 0.5 cal./g. The evolution of this quantity of heat could be produced by the crystallization of only about 1% of the polymer.

In the case of 6-6 Nylon, the annealed polymer exhibited a well defined maximum in the specific heat curve at a temperature of 165° where the crystal structure of 6-6 Nylon changes from triclinic to a pseudo hexagonal type lattice as discovered by Brill.³ There was no indication from the X-ray investigation of a crystal structure change at 165° in the case of 6 Nylon, nor was there anything peculiar in the specific heat in this temperature range. Brill first considered the possibility that the inability of 6 Nylon to make the crystal structure transition resulted from a hindering of rotation or rotational vibrations in 6 Nylon as compared to 6-6 Nylon, but he then rejected this explanation in favor of one in which he postulated that in the case of 6-6 Nylon a rotation of the chains through an angle of about 60° as well as a shift of neighboring chains of molecules relative to each other in the direction of the long axis made possible further hydrogen bonding between the chains. In 6 Nylon a similar rotation is not favorable for the formation of hydrogen bonds. The specific heat data favor this second interpretation of Brill's rather than the first, inasmuch as if the first were true, one might expect a higher specific heat at 165° for 6-6 Nylon than for 6 Nylon, but the opposite is true.

(14) Th. Gast, *Kunststoffe*, **43**, 15 (1953), measured the specific heat of polyvinyl chloride as a function of plasticizer content and demonstrated that the glass transition range broadens out to lower temperatures as the content of plasticizer increases.

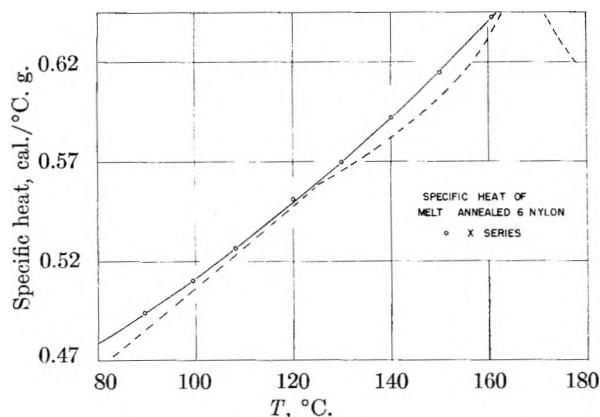


Fig. 6.—Comparison of the specific heat of melt annealed 6 Nylon (solid line) with that of 6-6 Nylon (dotted line) over the temperature range 80 to 180°.

C. The Percentage Crystallinity of 6 Nylon.—

In Fig. 7 the percentage crystallinity of undrawn, drawn and melt annealed 6 Nylon is given. These curves were calculated from the following assumptions: (1) the enthalpy of the amorphous 6 Nylon down to 160° is given by the equation for the enthalpy, H_L , of liquid 6 Nylon as deduced from measurements of the specific heat in the liquid range, or

$$C_p(\text{liquid}) = 0.577 + 3.36 \times 10^{-4}T$$

$$H_L = H_{L, 280^\circ} + 0.577(T - 280) + 1.68 \times 10^{-4}\{T^2 - (280)^2\}$$

where T is the temperature in degrees centigrade.

(2) The enthalpy of the amorphous 6 Nylon from zero to 160° is given by adding the heat of fusion to the estimated enthalpy of perfectly crystalline 6 Nylon, H_s , or

$$C_p(\text{solid}) = 0.325 + 1.5 \times 10^{-3}T$$

$$H_s = H_{s, 160^\circ} + 0.325(T - 160) + 7.5 \times 10^{-4}\{T^2 - (160)^2\}$$

(3) The entropy of fusion of 6 Nylon, ΔS_f , is equal to the estimated entropy of fusion of 6-6 Nylon at 225°, the maximum melting temperature of 6 Nylon.

(4) The heat of fusion of 6 Nylon at 225° is given by $T_m \Delta S_f$ where T_m is 498°K. and ΔS_f is 0.09 e.u./g.

(5) The heat of fusion of 6 Nylon below the maximum melting point is given by the heats of fusion of 6-6 Nylon multiplied by the ratio 45/46.5 which is the calculated heat of fusion of 6 Nylon, 45 cal./g., obtained as explained under assumption (4) and 46.3 is the estimated heat of fusion of 6-6 Nylon at 225°. It is interesting to note that the lowering of the melting point in going from 6-6 Nylon to 6 Nylon can be brought about by such a small change in the heat of fusion.

(6) The percentage of crystallinity of melt annealed 6 Nylon remains constant with temperature up to 190°.

When the curves of Fig. 7 are compared with similar curves of 6-6 Nylon,¹ it will be seen that the crystallinity of 6 Nylon is slightly less than that of 6-6 Nylon, that the crystallinity of the drawn and undrawn filaments does not rise to such high val-

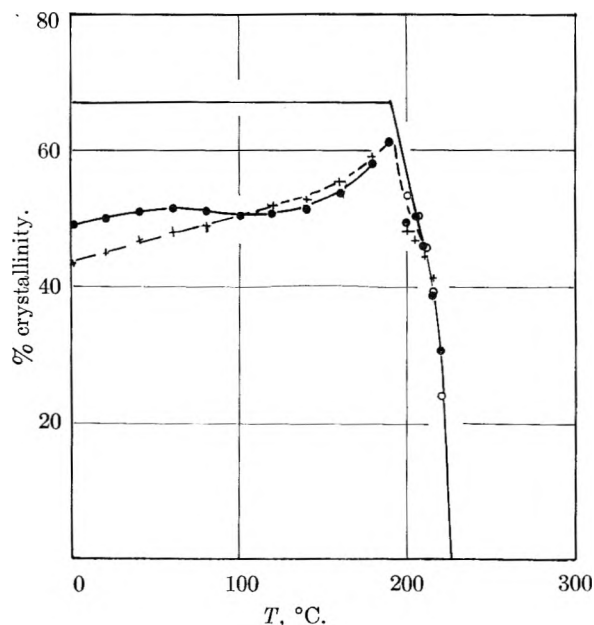


Fig. 7.—Comparison of the percentage of crystallinity of different forms of 6 Nylon: O, melt annealed; ●, undrawn filaments; +, draw. filaments.

ues, and that in contrast to 6-6 Nylon the crystallinity of the drawn filaments is slightly less than that of the undrawn at room temperature. This latter observation was also noted in the case of drawn and undrawn polyethylene.¹⁵ The decreased crystallinity of annealed 6 Nylon with respect to annealed 6-6 Nylon may be the result of the presence of monomer and dimer produced by the annealing.

Between 190 and 225° the actual heat of fusion would be approximately 0.67×44 or 29 cal./g. This is considerably more than the estimate of 12.4 cal./g. due to Mikhailov and Klesman.⁴ At zero degrees C. the heat of fusion might be as low as 0.67×32 , or 21 cal./g., but as this is below the glass transition temperature, any estimate of the enthalpy of the amorphous component and from this the true heat of fusion at 0° would be most speculative.

D. Comparison of 6 and 6-6 Nylon.—In Figs. 1 to 6 the specific heat of 6-6 Nylon in its various forms is shown by the dotted lines. Above the glass transition temperature the specific heats of the two types of Nylon in the annealed form are strikingly similar until 165° is reached where the 6-6 Nylon undergoes a slight crystal structure modification, and the specific heat levels off before rising in the melting range. The specific heats of the two types in the undrawn filament form are also closely similar, except that the 6-6 Nylon does not exhibit the considerable fluctuations in specific heat over the 90-160° temperature range.

The most marked differences in the specific heat seem to be in the drawn form. Possibly this difference results from the fact that drawn 6-6 Nylon is considerably more crystalline than drawn 6 Nylon according to our estimates. Thus at 190° drawn 6-6 Nylon is about 75% crystalline as compared to an estimate of 60% for drawn 6 Nylon.

(15) M. Dole, W. P. Hettlinger, Jr., N. Larson and J. A. Wethington, Jr., *J. Chem. Phys.*, **20**, 781 (1952).

Acknowledgments.—Grateful appreciation is expressed for support of this project by the Office of Ordnance Research, U. S. Army. The gift of

materials and technical information from the Nylon Research Division, E. I. du Pont de Nemours and Co., is also acknowledged.

THE ISOBARIC SURFACE TENSIONS AND THERMODYNAMIC PROPERTIES OF THE SURFACES OF A SERIES OF *n*-ALKANES, C₅ TO C₁₈, 1-ALKENES, C₆ TO C₁₆, AND OF *n*-DECYLCYCLOPENTANE, *n*-DECYLCYCLOHEXANE AND *n*-DECYLBENZENE

BY JOSEPH J. JASPER AND ELBERT V. KRING

Department of Chemistry, Wayne University, Detroit, Michigan

Received March 30, 1955

This is the third of a series of three papers on the surface tension measurements of a series of *n*-alkanes and 1-alkenes made available by the American Petroleum Institute Research Project 44. In the following there is described the procedure for measuring the surface tensions of the hydrocarbons isobarically under nitrogen saturated conditions. The method of least squares was applied to the data and linear equations obtained. The equations were used to calculate the surface tension values which are presented in two tables together with the constants of the least square equations. A third table presents least square constants for the latent heat equation, and also the enthalpy of the surface formation of the hydrocarbons.

The surface tension is a fundamental thermodynamic property of the liquid surface region and serves as an accurate index of the relative magnitudes of other properties of the liquid state. This property, which has its origin in intermolecular attraction, constitutes an important source of data for evaluating certain extensive properties of the transition region between the liquid phase and the vapor contiguous with it. These data become all the more important if they are obtained over a temperature range since most of the extensive properties are functions of the temperature. The surface tension is very sensitive to the presence of capillary-active impurities; therefore, accurate and reproducible data can be obtained only from very pure compounds.

An examination of the literature shows that the orthobaric and the isobaric surface tensions obtained at the same temperature differ quite appreciably for most liquids. The orthobaric surface tensions for the *n*-alkanes, C₅ to C₁₈, the 1-alkenes, C₆ to C₁₆, and *n*-decylcyclopentane, *n*-decylcyclohexane and *n*-decylbenzene have been reported.^{1,2} The purpose of this investigation was to obtain isobaric surface tensions of these 26 hydrocarbons over an appreciable temperature range. With the aid of these data it was possible to formulate empirical equations relating the variables and to calculate the values of a number of thermodynamic properties of the liquid surfaces. The authors wish to acknowledge their appreciation to the Research Corporation for the grant-in-aid which they kindly awarded us, and to the American Petroleum Institute for the loan of the pure hydrocarbons which made this investigation possible. The compounds were made available by the API project 44 at the Carnegie Institute of Technology from the research samples of hydrocarbons purified by research

project 6 from source materials supplied as follows: *n*-tridecane, *n*-pentadecane and *n*-heptadecane from the research project 42 at Pennsylvania State College; *n*-pentane, *n*-hexane, *n*-heptane, *n*-octane, *n*-nonane, *n*-decane, *n*-undecane, *n*-dodecane, *n*-tetradecane, *n*-hexadecane, *n*-octadecane from the API research project 6; 1-hexene, 1-heptene, 1-nonene, 1-undecene, *n*-decylcyclopentane, *n*-decylcyclohexane and *n*-decylbenzene by the API research project 45 at the Ohio State University; 1-octene, 1-decene, 1-dodecene, 1-tetradecene, and 1-hexadecene by the API research project 6 at the Carnegie Institute of Technology.

Experimental

Description of the Apparatus.—In this investigation it was desired to obtain surface tension data with a precision of 0.01 erg cm.⁻² and calculations based upon this degree of precision served as a guide in the selection of the essential parts of the capillarimeter and the final design. Since limited volumes of the hydrocarbons were available it was necessary to design the capillarimeter to conform with the structural and dimensional requisites of a high precision instrument but which, however, required a relatively small volume of liquid. This was successfully accomplished, and the description of the method used to test the essential parts of the resulting instrument have been described in earlier papers.^{3,4} The measurements were made under isobaric conditions in an atmosphere consisting of dry nitrogen and the vapor of the hydrocarbon under consideration. The total pressure, which could be varied at will, was maintained at 760 ± 5 mm. over the entire temperature range with the aid of a special manometer. The latter was equipped with a side arm through which nitrogen could be introduced or the mixture of nitrogen and vapor withdrawn as the temperature condition required. To maintain a constant temperature during the measurements, a specially designed and constructed glass-wool insulated water-bath was used which was equipped with non-distorting heat resistant plate glass windows. Efficient stirring was accomplished with a turbine stirrer, and the temperature variation was no greater than 0.08° up to the boiling point of water. Temperatures were measured with a NBS certified Leeds and Northrup resistance thermometer used in conjunction with a NBS certified C-2 Mueller bridge made by the same company. The galvanometer used in the bridge circuit was an HS

(1) J. J. Jasper, E. R. Kerr and F. Gregorich, *J. Am. Chem. Soc.*, **75**, 5252 (1953).

(2) J. J. Jasper and E. R. Kerr, *ibid.*, **76**, 2659 (1954).

(3) J. J. Jasper and K. D. Herrington, *ibid.*, **68**, 2142 (1946).

TABLE I
THE SURFACE TENSION AND LEAST-SQUARE FACTORS a AND b FOR THE n -ALKANES C_5 TO C_{18} TEMPERATURE, $^{\circ}C$.

Compound	Temperature, $^{\circ}C$.											a	b
	0	10	20	30	40	50	60	70	80	90	100		
n -Pentane	18.25	17.15	16.05	14.94	18.25	0.11021
n -Hexane	20.44	19.42	18.40	17.38	16.36	15.34	14.32	20.44	0.1022
n -Heptane	22.10	21.12	20.14	19.17	18.18	17.20	16.22	15.24	14.26	13.28	...	22.10	0.0980
n -Octane	23.52	22.57	21.62	20.67	19.71	18.77	17.81	16.86	15.91	14.96	14.01	23.52	0.09509
n -Nonane	24.72	23.79	22.85	21.92	20.98	20.05	19.12	18.18	17.24	16.31	15.37	24.72	0.09347
n -Decane	25.67	24.75	23.83	22.91	21.99	21.07	20.15	19.23	18.31	17.39	16.47	25.67	0.09197
n -Undecane	26.46	25.56	24.66	23.76	22.86	21.96	21.05	20.15	19.25	18.35	17.45	26.46	0.09010
n -Dodecane	27.12	26.24	25.35	24.47	23.58	22.70	21.81	20.93	20.05	19.16	18.28	27.12	0.08843
n -Tridecane	27.73	26.86	25.99	25.11	24.24	23.37	22.50	21.63	20.75	19.88	19.01	27.73	0.08719
n -Tetradecane	...	27.43	26.56	25.69	24.82	23.96	23.09	22.22	21.35	20.48	19.61	28.30	0.08688
n -Pentadecane	27.07	26.21	25.35	24.50	23.64	22.78	21.93	21.07	20.21	28.78	0.08565
n -Hexadecane	27.47	26.62	25.76	24.91	24.06	23.20	22.35	21.49	20.64	29.18	0.08540
n -Heptadecane	27.06	26.22	25.38	24.52	23.68	22.83	22.00	21.14	29.60	0.08460
n -Octadecane	27.45	26.61	25.77	24.92	24.08	23.24	22.39	21.55	29.98	0.08428

TABLE II
THE SURFACE TENSION AND LEAST-SQUARE FACTORS a AND b FOR THE SERIES OF 1-ALKENES AND FOR n -DECYLCYCLOPENTANE, n -DECYLCYCLOHEXANE AND DECYLBENZENE

Compound	Temperature, $^{\circ}C$.											a	b
	0	10	20	30	40	50	60	70	80	90	100		
1-Hexene	20.47	19.44	18.42	17.39	16.36	15.33	14.31	20.47	0.10271
1-Heptene	22.28	21.29	20.30	19.31	18.32	17.33	16.34	15.34	14.35	22.28	0.09908
1-Octene	23.68	22.72	21.76	20.81	19.85	18.89	17.93	16.97	16.02	15.06	14.10	23.68	0.09581
1-Nonene	24.90	23.96	23.02	22.09	21.15	20.21	19.27	18.33	17.40	16.46	15.52	24.90	0.09379
1-Decene	25.84	24.92	24.00	23.08	22.16	21.24	20.33	19.41	18.49	17.57	16.65	25.84	0.09190
1-Undecene	26.67	25.77	24.86	23.96	23.05	22.15	21.24	20.34	19.43	18.53	17.62	26.67	0.09048
1-Dodecene	27.38	26.49	25.63	24.71	23.82	22.92	22.03	21.14	20.25	19.36	18.47	27.38	0.08911
1-Tetradecene	28.56	27.68	26.80	25.92	25.04	24.16	23.29	22.41	21.53	20.65	19.77	28.56	0.08791
1-Hexadecene	...	28.61	27.75	26.89	26.03	25.16	24.30	23.44	22.58	21.72	20.86	29.47	0.08612
n -Decylcyclopentane	31.11	30.22	29.34	28.45	27.57	26.68	25.80	24.91	24.02	23.14	22.25	31.11	0.08862
n -Decylcyclohexane	31.49	30.63	29.77	28.92	28.06	27.20	26.34	25.49	24.63	23.77	22.91	31.49	0.08579
n -Decylbenzene	32.73	31.85	30.97	30.08	29.21	28.32	27.44	26.55	25.67	24.79	23.91	32.73	0.08822

ballistic type with shielded leads. A brass frame, which was hung in the bath, carried a vertically adjustable brass plate with a narrow horizontal slit. This was placed between the fluorescent light source and the capillarmeter and when the slit was adjusted to a position tangent to the reference meniscus the latter appeared in sharp silhouette and its exact position readily determined. A precision Gaertner cathetometer, which could be read to 0.0001 cm., was used to measure the capillary heights.

Procedure.—The hydrocarbons were supplied in sealed glass ampoules and to avoid contamination it was necessary to transfer them to and from the capillarmeter in a dry inert atmosphere. This was accomplished in a gas-tight steel chamber within which there was maintained an atmosphere of dry nitrogen. Under these conditions the ampoules were opened and the compounds transferred to the reservoir bulb of the capillarmeter through a side arm which carried a mercury cup-seal. The pressure-regulating manometer was then connected to the capillarmeter through the mercury seal. During subsequent manipulations the total pressure upon the liquid within the capillarmeter was maintained at 760 ± 5 mm. at all temperatures. At each temperature at least 30 minutes were allowed for the capillarmeter and contents to reach thermal equilibrium with the surrounding bath. Since a receding contact angle approaches more closely to zero than the advancing angle⁴ the capillarmeter was frequently tilted to an angle approximately 60° from the vertical. This forced the liquid to flow to a higher point in the capillary and upon resumption of the vertical position the liquid meniscus dropped to its normal equilibrium position. Readings were taken at each temperature until ten consecutive capillary heights were obtained which varied no more than 0.01 cm.

Results

The data were applied in the following form of the capillary height equation

$$\gamma = \frac{r(h + r/3)(d_1 - d_v)g}{2 \cos \theta}$$

where r is the radius of the capillary (0.012299 cm.), $(h + r/3)$ the corrected capillary height^{5,6} d_1 and d_v the densities of the liquid and vapors, respectively, and g the gravitational factor (980.316 in Detroit). Since the solid-liquid contact angle was very close to zero (the upper meniscus appeared to be a true hemisphere in shape) the cosine factor was equal to unity. The effective density ($d_1 - d_v$) was determined for each compound at the various temperatures with the aid of the density data of the liquid hydrocarbons, the Antoine constants which were tabulated in the tables of selected values of properties of hydrocarbons published by the American Petroleum Institute, Project 44, and the density of nitrogen. Thus, the total d_v consisted of contributions from both the hydrocarbon vapors and of dry nitrogen. For those hydrocarbons having high boiling points the d_v consisted almost entirely of the nitrogen contribution. The probable error of the derived results of the surface

(4) W. D. Harkins, "The Physical Chemistry of Surface Films," Reinhold Publ. Corp., New York, N. Y., 1952, p. 66.

(5) T. W. Richards and L. S. Coombs, *J. Am. Chem. Soc.*, **37**, 1656 (1915).

(6) Lord Rayleigh, *Proc. Roy. Soc. (London)*, **A92**, 184 (1915).

tension calculations were determined and these proved to be never greater than 0.01 erg cm.⁻²

The principle of least squares was applied to the measured surface tension-temperature data and the resulting equations were of the linear form $\gamma = a - bt$. The surface tension values together with the *a* and *b* factors of the least square equation are shown in Tables I and II.

Discussion

The enthalpy, *h*, of formation of each cm.² of surface is the sum of the free surface energy, γ , required to extend the surface by unit area, and the latent heat, *q*, required to maintain isothermal conditions. The thermodynamic equation of Clapeyron takes the following two-dimensional form when applied to liquid surfaces

$$-(\partial\gamma/\partial T) = q/T = s \quad (1)$$

From the application of this equation the entropy, *s*, and the latent heat, *q*, can be calculated. By rearranging equation 1 and combining with the free surface energy, the enthalpy can be calculated. Thus

$$h = \gamma + q = \gamma - T(\partial\gamma/\partial T) \quad (2)$$

For most liquids *q* increases with the temperature at precisely the same rate that the free surface energy decreases. Consequently, the value of the enthalpy is independent of the temperature. It is to be noted that the *b* factors of Tables I and II are the entropies of surface formation for the different hydrocarbons, and these, likewise, are independent of the temperature. The entropies decrease with increasing chain length of the hydrocarbons and appear to be approaching a constant value.

The temperature-latent heat relations takes the linear form $q = c + dt$ and the *c* and *d* factors for this equation are tabulated in Table III. For a given temperature the value of *q* decreases with increasing chain length in an homologous series, and, since *q* is a measure of the work done in bringing the molecules from the interior to the surface, it is evident that the energy required to overcome intermolecular attraction decreases with increasing chain length for the hydrocarbons.

An interesting fact, observed and reported by several investigators, is the difference between the orthobaric and isobaric surface tensions of liquids at the same temperatures. Richards and Carver⁷

(7) T. W. Richards and E. K. Carver, *J. Am. Chem. Soc.*, **43**, 827 (1921).

TABLE III
THE ENTHALPY, AND THE *c* AND *d* FACTORS OF THE LATENT HEAT EQUATION FOR THE *n*-ALKANES, 1-ALKENES, AND FOR *n*-DECYLCYCLOPENTANE, *n*-DECYLCYCLOHEXANE AND *n*-DECYLBENZENE

Compound	<i>c</i>	<i>d</i>	<i>h</i> , ergs/cm. ²	Range, °C.
<i>n</i> -Pentane	30.10	0.1102	48.30	0-30
<i>n</i> -Hexane	27.91	.1022	48.36	0-60
<i>n</i> -Heptane	26.77	.0980	48.87	0-90
<i>n</i> -Octane	25.98	.0951	49.50	0-100
<i>n</i> -Nonane	25.53	.0935	50.26	0-100
<i>n</i> -Decane	25.12	.0920	50.79	0-100
<i>n</i> -Undecane	24.61	.0901	51.07	0-100
<i>n</i> -Dodecane	24.16	.0884	51.28	0-100
<i>n</i> -Tridecane	23.82	.0872	51.55	0-100
<i>n</i> -Tetradecane	23.73	.0869	52.03	10-100
<i>n</i> -Pentadecane	23.40	.0857	52.18	20-100
<i>n</i> -Hexadecane	23.33	.0854	52.51	20-100
<i>n</i> -Heptadecane	23.11	.0846	52.71	30-100
<i>n</i> -Octadecane	23.02	.0843	53.00	30-100
1-Hexene	28.06	.1027	48.53	0-60
1-Heptene	27.06	.0991	49.34	0-80
1-Octene	26.17	.0958	49.85	0-100
1-Nonene	25.62	.0938	50.52	0-100
1-Decene	25.10	.0919	50.94	0-100
1-Undecene	24.72	.0905	51.39	0-100
1-Dodecene	24.34	.0891	51.72	0-100
1-Tetradecene	24.01	.0879	52.57	0-100
1-Hexadecene	23.52	.0861	52.99	10-100
<i>n</i> -Decylcyclopentane	24.21	.0886	55.32	0-100
<i>n</i> -Decylcyclohexane	23.43	.0858	54.92	0-100
<i>n</i> -Decylbenzene	24.10	.0882	56.83	0-100

tested the effects of air on the capillary height and found that these values varied between zero and 0.5% lower than the orthobaric values. Rice⁸ attributes this effect in part to gas adsorbed on the liquid surface. In the present study pure dry nitrogen was used to maintain a constant pressure within the capillarimeter and the surface tension measurements were made, therefore, under nitrogen saturated conditions. Between 0 and 30° the average surface tension values of the *n*-alkanes and 1-alkenes varied between 0.4 and 0.5% lower than the orthobaric values at the same temperatures. This difference gradually increased to an average difference of 0.7% as the boiling points of the liquids were approached.

(8) O. K. Rice, *J. Chem. Phys.*, **15**, 333 (1947).

HEATS OF IMMERSION OF SOME CLAY SYSTEMS IN AQUEOUS MEDIA

By W. H. SLABAUGH

*Department of Chemistry, Oregon State College, Corvallis, Oregon**Received April 4, 1955*

Heats of immersion are given for raw, centrifuged, and sodium and calcium bentonite in water, butylamine, butylamine hydrochloride and alkyltrimethylbenzylammonium chloride solutions for the purpose of seeking data that permit the development of a reaction mechanism. The data indicate that there is a definite difference between the reaction of an amine and an amine hydrochloride with a clay system.

Introduction

The present study was made for the purpose of providing more information concerning the interactions among clay surfaces, water, amines and amine salts. In reacting with the reagents the clay acts in a twofold capacity—these reagents may react with the clay surfaces through hydration and adsorption, or these reagents may react with the base exchangeable ions on the clay. Because of the low level of energy involved in either of these processes, a detector of high sensitivity is required in studying the heats of these interactions. For this study a calorimeter was designed using a thermistor whose temperature coefficient of resistance was measured in a manner similar to that of Zettle-moyer and co-workers.¹

The work by Jordan² has shown that amine salts react with the base exchange ion of the clay, with the resulting attachment of the amine ion at the base exchange site. More recent work by the author³ has shown that the reaction of amine salts with sodium bentonite is accompanied by an equivalent replacement of sodium ion from the clay micelle. The present work is an attempt to gain a more complete understanding of these reactions.

Method and Materials

The calorimeter used in this study consists of a wide-mouth pint Dewar flask containing a 38.11 ohm standardizing heating coil, a sample tube holder with a screw-type breaking device, a thermistor,⁴ and a stirrer, driven by a constant speed motor at 110 r.p.m. The flask, clamped by means of a Lucite collar to a plate of similar material and sealed by a rubber gasket, is immersed in a 10-gallon tank of water, the whole of which, except for the extensions to the stirrer and tube breaker, is housed in a constant temperature air-bath. The air-bath is thermostated at $30.0 \pm 0.1^\circ$. This holds the water-bath at $28.000 \pm 0.005^\circ$ and provides an environment wherein the internal part of the calorimeter undergoes no more than a constant drift of 0.0001° per minute during an observation.

The change in temperature produced by the immersion of a sample is measured by the deflection on a one meter scale of a Leeds and Northrup Type HS galvanometer which indicates the off-balance of a Leeds and Northrup Type G-2 Mueller resistance bridge. The sensitivity of this detector system permits the observation of temperature changes of 0.00002° . An observation is made by first providing conditions that produce a constant drift of less than 0.0001° per minute. After 5 minutes of constant drift the heat capacity of the system is evaluated by means of the standardizing heater. With total contents of the calorimeter weighed to ± 0.1 g., the response of the detector produces a scale deflection of 2.71 ± 0.02 cm. per calorie of heat released in the

calorimeter. During a single determination the temperature of the calorimeter is rated about 0.005° . This small change does not appreciably affect the standardization of the instrument.

The sample tube, containing 0.2000 g. of material, is made of 7 mm. i.d. Pyrex tubing 55 mm. in length. The samples are outgassed at 52° and 0.01 mm. pressure for 24 hours. The tube is broken by a rod which is forced against the tube by an external screw. The correction for the heat of breaking the tube is attributed to the heat of wetting of the inside surfaces of the glass tube, the kinetic energy of the aqueous medium which rushes into the tube upon breaking and the heat of wetting of a cotton plug which is needed to prevent loss of sample during outgassing. The tube breaking correction, applied to all measurements, is 0.23 cal., 0.03 cal. of which is attributed to the kinetic energy of entry of aqueous media into the tube. The results, expressed in calories, are based upon the relationship: 1 cal. = 4.186 joules.

Measurements in this study were made on Wyoming bentonite which was treated prior to the heat of immersion observations in the following manner:

Raw bentonite: 200 mesh clay, as received in a sample supplied by the Baroid Division, National Lead Company. Base exchange capacity is 82 meq./100 g.

Raw centrifuged bentonite: clay containing less than 0.1% quartz whose base exchange capacity is 92 meq./100 g. of clay. In both samples of raw bentonites, only 50% passed through a 230-mesh sieve, 100% passing through a 100-mesh sieve.

Sodium bentonite was prepared from the raw centrifuged bentonite by passing a 1.5% suspension of it through an Amberlite IR 120 column charged with sodium ion. Calcium bentonite was similarly prepared in a column charged with calcium ion. These clays were recovered from the aqueous media by either removing the water in a 105° oven (hereafter called an oven-dried clay) followed by grinding with a mortar and pestle to 200 mesh, or by a freeze-drying method described by Call.⁵ These clays are believed to be converted to homoionic systems that are at least 98% pure in the specified ion. All clays were oven-dried one hour at 95° prior to weighing into the sample tubes. A so-called hydrogen bentonite was prepared in a similar fashion, using an acid-charged resin column.

Solutions of butylamine and butylamine hydrochloride were prepared from Eastman Kodak Company butylamine, the salt being made by neutralizing the amine with HCl to pH 5.90. A 0.1 M solution of B.T.C. (alkyltrimethylbenzylammonium chloride, Onyx Oil and Chemical Co., where the alkyl radical is principally $C_{12}H_{25}$) was prepared. Freshly distilled water was used in all cases.

Another series of measurements was made in which 0.2 M solutions of butylamine and butylamine hydrochloride were added to 200 ml. of a 1% raw centrifuged bentonite suspension. Because the concentrations of the various components of these reaction systems were not strictly comparable to the concentrations involved in the immersion of the dry clay samples, only qualitative comparisons between these two kinds of determinations can be made.

Experimental Results and Discussion

The heats of immersion of the various clay systems were determined, the results being expressed in Table I. Standard deviations are given for each system on each of which at least three determinations were made. These deviations reflect the total accuracy of the determinations, which involves

(1) A. C. Zettle-moyer, G. J. Young, J. J. Chessick and F. H. Healey, *THIS JOURNAL*, **57**, 649 (1953).

(2) John W. Jordan, B. J. Hook and C. M. Finlayson, *ibid.*, **54**, 1196 (1950).

(3) W. H. Slabaugh, *ibid.*, **58**, 162 (1954).

(4) The Thermistor, No. 15A, was supplied by Western Electric Co., New York.

(5) F. Call, *Nature*, **172**, 126 (1953).

TABLE I
HEATS OF IMMERSION OF CLAYS IN VARIOUS MEDIA AT 28.0° (CAL. PER G. CLAY)

Sample	Water	0.1 M C ₄ H ₉ NH ₂	0.1 M C ₄ H ₉ NH ₂ ·HCl	0.1 M B.T.C.
Raw bentonite (50% 200 mesh)	9.99 ± 0.05	11.68 ± 0.04	11.33 ± 0.04
Centrifuged bentonite (oven-dried) (50% 200 mesh)	12.88 ± 0.02	14.51 ± 0.05	12.62 ± 0.05	18.84 ± 0.05
Centrifuged bentonite (freeze-dried)	11.56 ± 0.05
Sodium bentonite (oven-dried) (200 mesh)	14.29 ± 0.02	15.16 ± 0.03	14.36 ± 0.06	19.57 ± 0.04
Sodium bentonite (freeze-dried)	12.04 ± 0.04
Calcium bentonite (oven-dried) (200 mesh)	21.28 ± 0.06	21.36 ± 0.05	20.06 ± 0.10	24.13 ± 0.10
Hydrogen bentonite (oven-dried) (200 mesh)	21.02 ± 0.05	25.85 ± 0.01	20.67 + 0.10

weighing, outgassing, heat of breaking and calorimeter performance.

In Table II, the heats of reaction of three clay systems with amine reagents is given. These values are obtained from Table I by subtracting the heat of immersion in water from the heat of immersion in the reagent for each of the amine reagents.

TABLE II
HEATS OF REACTION OF CLAYS WITH AMINE REAGENTS
(CAL. PER G. CLAY)

Sample ^a	0.1 M C ₄ H ₉ NH ₂	0.1 M C ₄ H ₉ NH ₂ ·HCl	0.1 M B.T.C.
Centrifuged bentonite	1.63	-0.26	5.96
Sodium bentonite	0.87	0.07	5.28
Calcium bentonite	0.08	-1.22	3.85
Hydrogen bentonite	4.82	0.24	...

^a All samples were oven-dried.

Table III gives the heats of reaction between amine reagents and a 1% bentonite suspension. The calorimeter is designed so that the reagent may be added in stepwise fashion in ml. portions.

TABLE III
HEATS OF INTERACTION BETWEEN AMINE REAGENTS AND
200 ML. OF 1% RAW CENTRIFUGED BENTONITE SUSPENSIONS

Reagent	Total vol. of reagent added, ml.	Total heat evolved per mmole of reagent added, cal.
0.2 M C ₄ H ₉ NH ₂	2	1.25
	4	1.53
	6	1.71
	8	1.71
0.2 M C ₄ H ₉ NH ₂ ·HCl	2	-0.36
	4	-0.62
	6	-0.75
	8	-0.75

In general, the magnitude of certain of the heats of immersion measured in this study agree well with those of Ovcharenko and Bykov,⁶ and with the results of Siefert.⁷ The present measurements extend both the accuracy of the determination and

(6) F. D. Ovcharenko and S. F. Bykov, *Kolloid Zhur.*, **16**, 134 (1954).

(7) A. C. Siefert, Ph.D. Thesis, Pennsylvania State College, 1942.

the effect of various reagents upon the heats of immersion of these materials.

An examination of the data for the heats of immersion listed in Tables I and II permits the following deductions:

(1) The heats of immersion increase from raw clay to Na-clay to H-clay to Ca-clay.

(2) The removal of the non-clay fraction from raw clay gives a clay that has a higher heat of immersion.

(3) A freeze-dried clay shows a heat of immersion in water which is 2 to 3 cal. less than for an oven-dried clay.

(4) More heat is evolved by immersing a clay in butylamine than in butylamine hydrochloride. This difference is most notable with the H-clay.

(5) The mechanisms of the reactions of the clay with an amine and with an amine hydrochloride are considerably different.

(6) The immersion of a clay in a high molecular weight amine salt evolves a large quantity of heat.

A brief consideration of these deductions follows.

The differences in the heats of immersion of these clay systems are attributed to at least two factors: the wetting of the clay surfaces and the hydration of the ion in the base-exchange position. In a raw clay, which contains similar amounts of sodium, calcium and magnesium ions, along with 12% non-clay impurities (quartz, cristobalite and feldspar), there is less heat evolved because there is less clay mineral, more non-clay material than in the centrifuged samples. The heats of immersion are higher for divalent ions; they increase in the order Na < H < Ca, an order in agreement with measurements on kaolinites by Siefert⁷ and others.

A freeze-dried clay, as reported by Call,⁵ may have similar surface areas to an oven-dried clay. However, the consistently smaller amount of heat evolved by the freeze-dried clays indicates that there is a considerable difference in the physical constitution of these two clays.

In a previous study³ it was found that for the lower amine salts, an equivalent amount of exchangeable cation was released for a certain amount of amine ion picked up by the clay. The 0.07 cal. per g. of clay released by the Na clay-amine hydrochloride reaction agrees with these earlier results.

In contrast the Ca clay-amine salt reaction shows a negative heat value, (-1.22 cal.) indicating that considerable energy is used up in replacing the Ca ion on the clay by an amine ion.

When the amine hydrochloride reacts with a clay it is conceivable that the process is primarily an exchange. However, the interaction of an amine with a clay introduces the possibility of adsorption of the amine to the clay without appreciable exchange. The resulting differences in the energy changes of these two processes are reflected in the data observed above. The 4.82 cal. per g. of H-clay, released when immersed in butylamine, are equivalent to 7300 cal. per mole of hydrogen ion on the H-

clay. This amount of heat is essentially the heat of neutralization between the amine and the H-clay. In an earlier study⁸ an entirely different method gave $9,400$ cal. for the heat of neutralization of a similar H-clay by NaOH.

In addition to exchange and adsorption, there are other factors which undoubtedly contribute to the heats of reaction—the dissociation of the exchangeable ion from the clay, the desolvation of the amine and amine ion upon reacting with the clay surfaces, and the orientation of the hydrocarbon chain of the amine on the clay surface.

(8) W. H. Stabaugh, *J. Am. Chem. Soc.*, **74**, 4462 (1952).

BURNING RATE STUDIES. II. VARIATION OF TEMPERATURE DISTRIBUTION WITH CONSUMPTION RATE FOR BURNING LIQUID SYSTEMS

BY D. L. HILDENBRAND AND A. GREENVILLE WHITTAKER

Chemistry Division, U. S. Naval Ordnance Test Station, Inyokern, China Lake, California

Received April 5, 1955

The thermocouple method has been used on several burning liquid systems to study variations in the temperature distribution brought about by changing the consumption rate. Data are presented showing the effect on surface and maximum gas temperatures and the results are discussed with respect to their possible significance. A thermal model for the combustion process appears to be compatible with the data and, in particular, a radiation and conduction model can be used to describe all or part of the temperature distribution in the condensed phase.

Introduction

Previously a method was developed for obtaining a reproducible and reasonably accurate measurement of the temperature distribution in the condensed phase of a liquid system burning in an inert atmosphere.¹ The method has been used to study the variation in temperature distribution as the result of changing consumption rate.² Of principal interest were variations in liquid surface temperature and maximum gas phase temperature, results for which are reported herein. It is hoped that work of this type will help lead to an elucidation of the processes involved in liquid combustion.

Experimental

Materials.—Two types of combustible liquids were investigated. One consisted of the homogeneous binary system 2-nitropropane-95% nitric acid in which the oxidizer and fuel were in different molecules. The other type consisted of ethyl nitrate, and an 82% metriol trinitrate (*i.e.*, methyltrimethylolmethane trinitrate)-18% triacetin (*i.e.*, glycerol triacetate) mixture in which the fuel and all the available oxygen were in the same molecule. These compounds were of varying degrees of purity. The 2-nitropropane was prepared by distillation of commercial grade material, and only the center fraction was used. This fraction had an index of refraction of 1.3950 at 20° using the sodium-D lines. The literature value is given as 1.3941 .³ Nitric acid was prepared by distillation of a 50-50 mixture of C.P. white

fuming nitric acid and concentrated sulfuric acid at a pressure of less than 2 millimeters of mercury. The resulting acid was analyzed and then diluted to 95% with distilled water. This acid contained less than 0.1% nitrogen dioxide. Eastman Kodak Co. white-label ethyl nitrate was used without further purification. The purity of the metriol trinitrate-triacetin mixture was about the same as that of the ethyl nitrate.

Apparatus.—The apparatus used in this study has been described previously.¹ In addition, several other types of recording instruments were used for temperature measurement where possible. A Sanborn recording oscillograph was used at low and intermediate burning rates, and a Leeds and Northrup Speedomax recorder was used at extremely low rates in order to check the cathode ray oscilloscope measurements. These two additional instruments did not have sufficient frequency response to reproduce faithfully the detailed shape of the temperature-time curve in most cases, but a comparison of some of the temperature levels was possible. A comparison of the results from the three different instruments gave excellent agreement with respect to surface temperature. All of these measurements were made with 7.5μ diameter platinum, platinum-10% rhodium thermocouples mounted in 3.7 mm. inside-diameter closed-end Pyrex tubes from which a temperature profile was obtained as the combustion wave passed over the thermocouple. The initial temperature of the liquid was 25° . The resulting temperature record is called the forward profile. A modified liquid holder was built later so that after the forward profile had been recorded as described above, the opening of a liquid filled reservoir connected to the combustion tube allowed the burning liquid to flow back up the tube, again passing over the thermocouple, to give what is called a reverse profile. This reverse profile gives the temperature record corresponding to starting the thermocouple in the gas phase above the liquid and ending in the liquid phase at room temperature.

Results and Discussion

At the outset it may be well to make a statement

(1) D. L. Hildenbrand, A. G. Whittaker and C. B. Euston, *THIS JOURNAL*, **58**, 1130 (1954).

(2) "Consumption rate" denotes the usual measured quantity, *i.e.*, the linear rate of regression of the surface uncorrected for deviation of the shape of the liquid-gas interface from a plane surface.

(3) "Handbook of Chemistry and Physics," Chemical Rubber Publishing Co., 33rd Edition, p. 1077.

regarding the validity of thermocouple measurements in the condensed phase since several investigators have challenged the usefulness of thermocouples on the basis of very steep calculated temperature gradients. In the cases of which the authors are aware, *e.g.*, the work of Olds and Shook,⁴ the gradients were calculated for substances burning at rates some 5 to 20 times higher than those investigated in this research and since the depth of the heated zone in the condensed phase decreases with increasing burning rate for a thermal model, it is not unreasonable to expect these steeper gradients at the higher rates. It is not intended to imply that all problems related to frequency response of thermocouples are necessarily eliminated by obtaining profiles at these lower rates, but rather that, because of the strong dependence of temperature gradient on rate and because of the physical dimensions of the smallest available thermocouple wire, the thermocouple method is mainly useful at relatively low rates of burning. Actually the experimental records showed that the temperature differences across the thermocouple was usually about 3 or 4 degrees in the steepest portion of the liquid phase rise and never exceeded 15 degrees at the highest rates studied. As will be pointed out, the experimental liquid phase profiles obtained are in good agreement with those calculated for a simple radiation and conduction model.

A representative forward and reverse temperature-time record obtained with the modified liquid holder is shown in Fig. 1. The reverse record does not show the plateau observed in the forward profile but does show the same smooth exponential variation of temperature with distance in the liquid phase, thus serving to show that the plateau is indeed caused by surface tension effects. Moreover, it is evident that because of these surface tension effects, the forward record misses a most interesting part of the profile, *i.e.*, the very rapid temperature rise in the gas phase adjacent to the surface shown in the reverse record and indicated by the arrow in Fig. 1. Because of the extremely large temperature gradient there (approximately 70,000 degrees per centimeter for the record in Fig. 1) a study of that part of the profile is exceedingly difficult. Indications are that important rapid gas phase reactions are taking place in this very narrow region close to the surface.

Variation of Surface Temperature with Pressure.

—The variation of surface temperature with bomb pressure for the system metriol trinitrate (82%)—triacetin was determined over the pressure range 34.9 to 100.3 atm. Results obtained from the experimental profiles are shown in Table I. It is clear that surface temperature was constant at $290 \pm 10^\circ$. A similar set of data was obtained for the system 2-nitropropane—95% nitric acid over the pressure range 14.5 to 62.2 atm. Surface temperature appeared to remain constant at about $190 \pm 15^\circ$ and showed no consistent trend. Because of a great deal of sub-surface random motion or turbulence, profiles obtained on this system were somewhat erratic, resulting in a larger spread of the

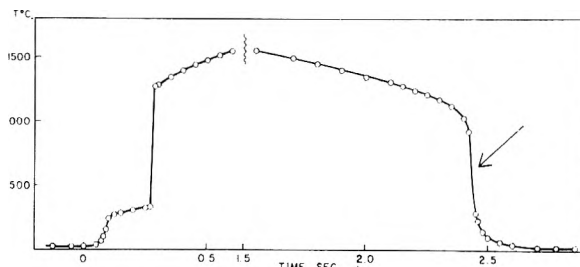


Fig. 1.—Forward and reverse profile for material trinitrate (82%)—triacetin, 54.4 atm.

data. For ethyl nitrate the variation of surface temperature with pressure was studied over the range from 1 to 62.2 atm. with the results shown in Table II. The uncertainty of the temperature measurements was less than $\pm 5^\circ$ in the low pressure range and increased to about $\pm 10^\circ$ at the higher pressures. The data show that surface temperature increases fairly rapidly with pressure up to about 14.5 atm. Above this pressure surface temperature increases much more slowly. It was of interest in this connection to compare surface temperature and boiling point as a function of pressure. Since no vapor pressure data on ethyl nitrate covering this pressure range were available in the literature, these measurements were carried out as a part of the study. The vapor pressure measurements were made in a special apparatus, with conditions similar to those under which the liquid was burned and were made rapidly enough to minimize the effects of thermal decomposition. Details of the measurements will be described in a separate article.

TABLE I

CONSUMPTION RATE, SURFACE TEMPERATURE AND MAXIMUM GAS TEMPERATURE FOR THE SYSTEM METRIOL TRINITRATE (82%)—TRIACETIN

Bomb pressure atm.	Consumption rate, cm./sec.	Surface temp., °C.	Max. gas temp., °C.
34.9	0.146	290	1530
48.6	.198	280	1510
62.2	.244	290	1520
75.8	.305	280	1530
89.4	.350	290	1310
100.3	.398	300	1310

TABLE II

CONSUMPTION RATE, SURFACE TEMPERATURE AND MAXIMUM GAS TEMPERATURE FOR ETHYL NITRATE

Bomb pressure atm.	Consumption rate, cm./sec.	Surface temp., °C.	Max. gas temp., °C.
0.92	...	70	...
2.0	...	83	...
3.0	0.020	94	940
4.3	.028	105	980
7.7	.052	120	1050
14.5	.122	140	1090
21.3	.178	145	1230
34.9	.279	149	1590
48.6	.378	155	1510
62.2	.429	165	1540

The vapor pressure and surface temperature data are plotted in Fig. 2 as log absolute pressure vs. reciprocal absolute temperature. It can be

(4) R. H. Olds and G. B. Shook, Presented at the 1952 Summer Meeting of the American Physical Society, Denver Colo. See also *Phys. Rev.*, **88**, 166 (1952).

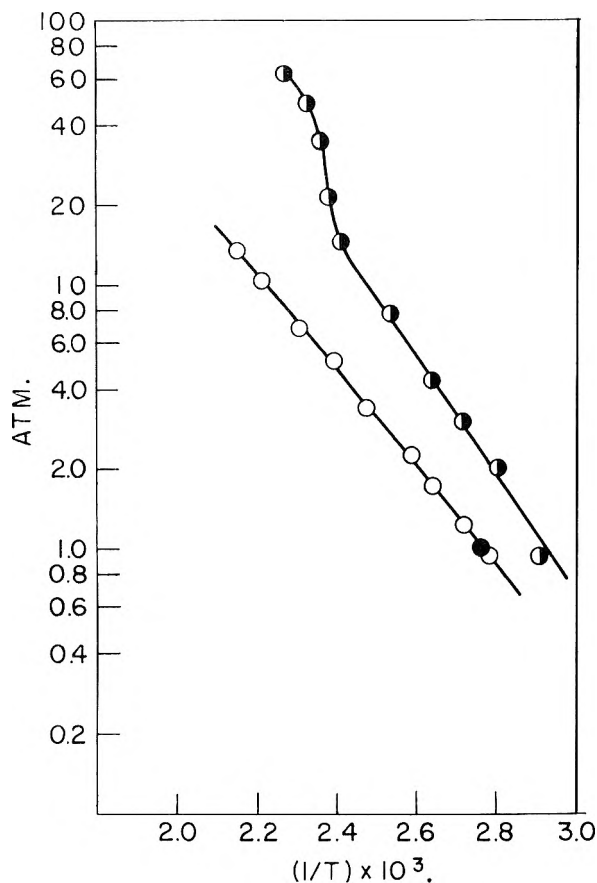
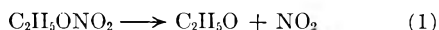


Fig. 2.—Comparison of burning surface temperature with boiling point of ethyl nitrate: O, boiling point; ●, surface temperature; ●, boiling point at 1 atm., literature value.

seen that in the region below 14.5 atm. the two curves are nearly parallel. Since the slope of the surface temperature curve in this region corresponds to a heat effect of approximately 10.5 kcal. per mole, it appears that surface temperature may be controlled by an evaporation process. However, from the data shown in Fig. 2, it is evident that the surface temperature is well below the thermodynamic boiling point at any given pressure as might be expected in a non-equilibrium type process in which the material is consumed as soon as it enters the gas phase. In the region above 14.5 atm. the situation appears to be different. At least up to 48.6 atm. surface temperature increased much more slowly with pressure than it did below 14.5 atm. If log consumption rate (data in Table II) is plotted against log of the reciprocal of the absolute surface temperature, a curve similar to the one shown in Fig. 2 results. The slope of this curve in the region covering the 14.5 to 48.6 atm. range was found to give an endothermic heat effect of about 30 kcal. per mole. It was observed during initial attempts to measure the vapor pressure of ethyl nitrate that thermal decomposition became easily detectable at about 140°, and since surface temperature just begins to exceed this value at pressures above 14.5 atm. it was possible that the reaction



came into play at this point. Because this mode of decomposition is endothermic reaction (1) would

tend to hold the surface temperature constant in spite of the fact that heat transfer to the liquid may increase as pressure rises. In order that this interpretation be valid, reaction (1) must occur in the liquid, and the reaction products must be immediately evaporated into the vapor phase where they can continue to react exothermically in accordance with mechanisms proposed by other investigators.⁵ Thus reaction (1) could be the primary factor controlling surface temperature in this region. Accepting the value of -8.0 kcal. per mole for the standard heat of formation of the ethoxy radical,⁶ 8.1 and -36.6 kcal. per mole as heats of formation of nitrogen dioxide⁷ and ethyl nitrate,⁸ respectively, reaction (1) is endothermic by 36.7 kcal. in the vapor phase. To convert this to liquid phase heat of reaction, values for the heat of vaporization of 9.1 and 9.2 kcal. were used for nitrogen dioxide⁹ and ethyl nitrate³ and 9.0 kcal. was assumed for the ethoxy radical. This gives a heat of reaction of 27.7 kcal. for reaction (1) in the liquid phase. From kinetic measurements, Levy^{5c} has obtained a heat of reaction of 41.2 kcal. for reaction (1) in the gas phase which leads to a liquid phase ΔH of 32.3 kcal. using the heats of vaporization given above. Since the reverse of reaction (1) is a reaction between radicals it is probable that its activation energy is small, hence the heat of reaction for equation 1 is approximately equal to the activation energy of this reaction. Consequently, the agreement of this energy value and the 30 kcal. obtained from the surface temperature data in the upper region of consumption rates may not be purely accidental. From the slope of the profile near the surface and surface temperature data it can be shown that reaction (1) would occur in a region about 20 μ below the liquid surface. This estimate was based on the assumption that reaction (1) was not appreciable below 140°.

If the above hypotheses are correct it appears that ethyl nitrate can undergo sustained combustion with a simple evaporation type mechanism, and it is unlikely that the suggested liquid phase reaction is essential. This does not mean that the evaporation process would be a slow step in the combustion mechanism. A simple kinetic theory calculation indicates that evaporation itself is several orders of magnitude more rapid than observed rates of burning, so that the speed of vaporization is most likely dependent on the rate of heat transfer to the liquid. In the case of the other two liquid systems studied, it was not possible to produce sustained combustion at pressures corresponding to the evaporation region of ethyl nitrate. Sustained combustion was obtained only in the region of constant or nearly constant surface temperature. Hence it was tentatively concluded that for these systems liquid phase reactions are essential to the combustion process. In addition to any changes in surface

(5) (a) G. K. Adams and C. E. H. Bawn, *Trans. Faraday Soc.*, **45**, 494 (1949); (b) L. Phillips, *Nature*, **165**, 564 (1950); (c) J. B. Levy, *J. Am. Chem. Soc.*, **76**, 3254 (1954); **76**, 3790 (1954).

(6) P. Gray, Fifth Symposium (International) on Combustion, Paper No. 39.

(7) Nat. Bur. Standards Circular No. 500, "Chemical Thermodynamic Properties," 1950.

(8) P. Gray and P. L. Smith, *J. Chem. Soc.*, 769 (1954).

(9) W. F. Giaque and J. D. Kemp, *J. Chem. Phys.*, **6**, 40 (1938).

temperature, all three systems showed a progressive decrease in the liquid preheat zone thickness with increasing pressure. For example, in the ethyl nitrate case the thickness varied from roughly 350 μ at the lower pressures to about 200 μ at the highest pressures studied. Although the data point out some interesting possibilities, the authors are reluctant to attach too much significance to surface temperatures *per se* and feel that in any comprehensive treatment of the combustion process, the entire temperature distribution must be examined in detail.

Variation of Maximum Gas Temperature with Pressure.—Table I gives the measured maximum gas temperatures for the metriol trinitrate system. Over the range studied, there is no apparent trend and the temperature is constant at about $1620 \pm 10^\circ$. An analysis of the data has shown, however, that the distance from liquid surface to maximum temperature varies smoothly and can be accurately represented by the relation

$$S = \frac{1.86 \times 10^3}{P^{1.51}}$$

where S is the distance in millimeters and P is the absolute pressure in atmospheres. It thus appears that the gas phase temperature gradients are strongly pressure dependent. This behavior is compatible with the observed increases in consumption rate at essentially constant maximum gas temperature, since the rate of heat transfer to the condensed phase is regulated by these changing gradients.

For ethyl nitrate, the measured maximum gas phase temperature (Table II) increases almost linearly from about 940° at 3.0 atm. to about 1280° at 24.7 atm., followed by a sharp rise to about 1600° at 35 atm. There is no further significant rise in maximum temperature above 35 atm. The measured gas temperatures are in good agreement with calculated temperatures based on the distribution of products observed in ethyl nitrate decomposition flames.¹⁰ Combustion in the low pressure region, where the nitrate ester burns without a luminous flame is characterized by the formation of relatively large amounts of nitric oxide and methane. The sharp rise to a maximum temperature of 1600° is accompanied by the appearance of a brightly luminous flame and the disappearance of CH_4 and NO in favor of CO and N_2 . In this case the distance from surface to maximum temperature can be expressed as

$$S = \frac{9.30 \times 10^3}{P^{2.12}}$$

No gas phase temperatures were obtained for the nitropropane-nitric acid system since the flame temperature far exceeded the melting point of the platinum thermocouples.

The concept that consumption rate is approximately linearly related to heat of explosion or maximum flame temperature is often encountered. This relation is probably true if a sufficiently narrow field of related substances is considered. However, it is not generally true, as is shown by the data in Tables I and II. Both the surface temperature and

the maximum flame temperature of the metriol trinitrate system are greater than the corresponding values for ethyl nitrate when compared at 34.9 atm. Yet the consumption rate of ethyl nitrate is greater by a factor of two. There are other instances of such behavior. The reason for this may be that surface temperature and maximum flame temperature are only two points on the profile and they alone do not uniquely define the temperature distribution. Consequently no valid general statement can be made concerning the effect of flame temperature on the consumption rate. A similar conclusion relating to solid powders has been reached by Crawford and co-workers.¹¹

The relatively weak influence of maximum gas temperature upon consumption rate may be further shown on examining the data of Table II giving the variation of these quantities with bomb pressure as measured for ethyl nitrate. The wide variations in gas temperature, especially near the point at which a luminous flame appears, are in no way reflected on consumption rate since the latter is a smooth function of pressure over this region with no inflection points. This relative indifference of consumption rate to the behavior of the final gas temperature is further evidence that the rate of burning is influenced much more strongly by reactions occurring very close to the liquid surface, particularly those responsible for the rapid initial gas phase temperature rise.

Theoretical Considerations.—Quite a number of theoretical treatments have been proposed to describe the combustion of solids or liquids and all could be examined in detail with respect to their compatibility with the results obtained in this study. By way of illustration only two such treatments will be considered briefly. Rice and Ginell¹² proposed that mass burning rate is controlled by the surface temperature according to the following Arrhenius type relation

$$M = A (\exp) - \Delta E/RT_s \quad (2)$$

where M is the mass burning rate, A a frequency factor, ΔE the activation energy of the rate controlling step at the surface, T_s surface temperature and R the gas constant. For the systems that show no change in surface temperature with consumption rate, equation 2 is obviously of no value. In the case of ethyl nitrate, equation 2 can be applied, but it must be carried out separately for the two regions of different activation energy, if it is assumed that the activation energies given above are the ones to be used in equation 2. In the region below 14.5 atm. the frequency factor A turns out to be of the order 10^{13} per sec. when the dimensions of concentration are removed. This value is not unreasonable but seems to indicate that each time a surface molecule undergoes collision it leaves the surface and enters the vapor phase. However, in the region above 14.5 atm. the frequency factor has a value of about 10^{22} which seems unreasonably high. As a result, equation 2 does not appear to be compatible with the data of any of the systems studied. On the other hand, the simple radiation-conduction

(10) G. K. Adams, W. G. Parker and H. G. Wolfhard, *Discs. Faraday Soc.*, No. 14, 97 (1953).

(11) B. L. Crawford, Jr., C. Huggett and J. J. McBrady, *This Journal*, **54**, 854 (1950).

(12) O. K. Rice and R. Ginell, *ibid.*, **54**, 885 (1950).

model treated by Reid¹³ appears to be more useful. In this treatment, an expression was developed for the temperature distribution in a burning liquid or solid resulting from heat conduction and radiation absorption. Consequently, a valid application of this treatment is necessarily restricted to a region below the burning surface where chemical reaction effects are negligible. An example was given in reference (1) in which this solution of the heat flow equation was fitted to three points on the temperature profile and values were obtained for some of the parameters of interest. This admittedly oversimplified procedure gave results that were extremely sensitive to the location of the three points chosen and so a more reasonable method was adopted whereby the entire temperature profile, or as much of it as desired, could be fitted. For the radiation-conduction model under consideration, solution of the heat flow equation gives a temperature distribution of the form

$$T = A \exp(-\alpha x) + B \exp(-\gamma x) + C$$

where A , B , C , α and γ are known or assumed to be constants, x is the distance variable, and T is the temperature. With the aid of the IBM Model 701 Electronic Data Processing Machine, a systematic searching procedure was carried out in which α and γ were varied in a predetermined fashion until a best fit to the data was obtained. In general, excellent fits could be obtained, depending on how much of the profile was included in the treatment. The details and results of the treatment will be described in a subsequent publication, but a few examples can be included here by way of explanation. For an ethyl nitrate profile obtained at a combustion pressure of 14.5 atm., the expression

$$T = 196.2 \exp(-164x) - 94.6 \exp(-339x) + 25.0 \quad (3)$$

where T is in degrees centigrade and x is in centimeters fits the liquid phase region with an average deviation for any one data point from the calcu-

(13) W. P. Reid, *THIS JOURNAL*, **57**, 242 (1953).

lated curve of less than one degree. By comparing equation 3 with equation 7 of reference (13), the unknown parameters may be evaluated. Because of an error in the derivation of equation 7 of reference (13), the value of A , the radiation intensity, calculated from equation 3 must be multiplied by the product of liquid density and specific heat in order to get its correct value. Calculated values obtained for the parameters A , α and h^2 are very reasonable and definitely the right order of magnitude. In applying the treatment to the metriol trinitrate system, it appears that for a profile obtained at a combustion pressure of 35 atm., only the portion of the profile below about 200° can be fitted with precision. As the treatment is extended to include points closer to the surface, the calculated best fit diverges rapidly from the data. Some rough stability measurements carried out at 35 atm. in a static system had previously shown that the metriol trinitrate mixture began to decompose vigorously at about 190°. It is thus possible that in addition to obtaining information about some important combustion parameters, one may be able to use this treatment for determining where and when chemical reaction begins to complicate the heat flow problem.

Note Added in Proof.—Work of a similar nature appeared¹⁴ at about the time this article was submitted. A difference in interpretation of the results exists between the two pieces of work and is based mainly upon locating the liquid surface on the experimental temperature profiles. However, the two sets of experiments have not been carried out on a comparable basis. Our work on defining the temperature structure of the combustion wave has been confined to the low pressure region in order to expand the preheat zone as much as possible, while that of S. and C. was done mainly at high pressures so as to improve the photography. It is believed that because of the marked variation of preheat zone thickness with mass burning rate for the thermal model, the bulk of the experiments of S. and C. were done at mass rates of burning too high to allow proper resolution of the structure of the temperature distribution in the condensed phase.

(14) R. Steinberger and K. E. Carder, *J. Phys. Chem.*, **59**, 255 (1955).

CORRELATION OF THE ACIDITY FUNCTION, H_0 , WITH ACTIVITIES OF ACID AND WATER

BY HENRY G. KUIVILA

Contribution from the Department of Chemistry, University of New Hampshire, Durham, N. H.

Received April 5, 1955

A linear correlation exists between h_0 and the ratio a_{HX}/a_{H_2O} for three acids. Perchloric and hydrochloric acids obey the equation $H_0 = 0.22 + 1.05 \log a_{HX}/a_{H_2O}$. Phosphoric acid obeys the equation $H_0 = -0.80 + 0.98 \log a_{HX}/a_{H_2O}$. Sulfuric acid gives a non-linear relationship. The possible thermodynamic and kinetic significance of the correlations are discussed.

An acidity function, H_0 , which measures the ability of a medium to transfer a proton to a neutral molecule has been defined by Hammett¹ as

$$-H_0 = \log a_{H^+} + \log \frac{f_B}{f_{BH^+}} \quad (1)$$

where a_{H^+} is the hydrogen ion activity and f_B and

f_{BH^+} are the activity coefficients of the neutral molecule and its conjugate acid, respectively. It has been shown by Brand² that H_0 can be expressed as a linear function of $\log (X_{H_2SO_4^-}/X_{H_2SO_4})$, where X refers to mole fraction, in the range 90–99.8% sulfuric acid. Deno and Taft³ have shown that eq.

(1) L. P. Hammett and A. J. Deyrup, *J. Am. Chem. Soc.*, **54**, 2721 (1932); L. P. Hammett, "Physical Organic Chemistry," McGraw-Hill Book Co., New York, N. Y., 1940, p. 267 ff.

(2) J. C. D. Brand, *J. Chem. Soc.*, 1002 (1950).

(3) N. C. Deno and R. W. Taft, *J. Am. Chem. Soc.*, **76**, 244 (1954).

TABLE I
 ACTIVITY AND H_0^a DATA FOR ACIDS, HX

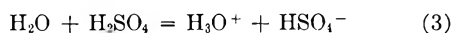
Acid ^b	M_{HX}	$\log a_{HX}$	$-\log a_{H_2O}$	$\log \frac{a_{HX}}{a_{H_2O}}$	$-H_0$	Δ^a
H ₃ PO ₄	0.537	-0.327	0.01	-0.327	-1.08	-0.75
	1.801	+ .2961	.0173	+ .313	- .48	.79
	3.402	.6902	.0352	.725	- .06	.78
	5.49	1.069	.0664	1.135	+ .37	.77
	8.35	1.496	.1187	1.616	.83	.79
	12.47	1.954	.210	2.164	1.32 ± 0.05	.84
	18.45	2.489	.350	2.839	2.00 ± .1	.84
	30.63	3.061	.604	3.665	2.86 ± .1	.79
	40.82	3.342	.785	4.127	3.34 ± .1	.79
	HClO ₄	0.200	-0.808	0.003	-0.802	-0.62
0.777		- .225	.012	- .214	- .07	.14
2.72		+ .56	.058	+ .62	+ .87	.25
4.60		1.09	.127	1.22	1.48	.26
8.31		2.06	.354	2.41	2.78	.37
10.83		2.71	.573	3.28	3.72	.46
12.32		3.07	.728	3.80	4.25	.45
12.78		3.17	.778	3.95	4.40	.45
14.09		3.48	.923	4.40	4.83	.43
15.64		3.83	1.109	4.94	5.30	.46
HCl	0.87	-0.15	0.013	-0.14	0	+0.14
	2.00	.31	.037	+ .35	0.60	.29
	3.26	.66	.070	.73	1.00	.27
	4.00	.85	.095	.95	1.20	.25
	6.00	1.29	.177	1.47	1.75	.28
	6.88	1.46	.214	1.67	2.00	.33
H ₂ SO ₄	0.5	-1.113	0.008	-1.121	-0.28	+0.84
	2	-0.602	.040	-0.56	+0.64	1.20
	4	- .173	.110	- .06	1.42	1.48
	7	+ .343	.260	+ .60	2.35	1.75
	10	.746	.444	1.19	3.18	1.99
	14	1.150	.697	1.85	4.09	2.25
	20.65	1.62	1.145	2.77	5.13	2.36
	30.6	2.08	1.75	3.83	6.20	2.37
	40.8	2.34	2.28	4.62	6.82	2.20
	57.8	2.53	2.97	5.50	7.58	2.08
	91.7	2.74	3.59	6.33	8.18	1.85

^a $-\log(a_{HX}/a_{H_2O}) - H_0$. ^b Sources of data. Phosphoric acid: activities, K. L. Elmore, C. M. Mason and J. H. Christensen, *J. Am. Chem. Soc.*, **68**, 2528 (1946). H_0 , E. Heilbronner and S. Weber, *Helv. Chim. Acta*, **32**, 1513 (1949). Perchloric acid: activities, R. A. Robinson and O. J. Baker, *Trans. Proc. Roy. Soc. New Zealand*, **76**, 250 (1946). H_0 , ref. 1, this paper. Hydrochloric acid: activities, M. Randall and L. E. Young, *J. Am. Chem. Soc.*, **50**, 989 (1928). H_0 , L. P. Hammett and M. A. Paul, *ibid.*, **56**, 827 (1934). Sulfuric acid: activities, to 20.65 m., S. Shankman and A. R. Gordon, *ibid.*, **61**, 2370 (1939); beyond 20.65 m., C. H. Greenewalt, *Ind. Eng. Chem.*, **17**, 522 (1925); water activity beyond 20.65 m., ref. 3, this paper.

2 is valid between 79 and 99.8% acid, f_{H_2O} being constant (-1.67) above 83% acid.

$$H_0 = -6.66 + \log \frac{X_{H_2O}}{X_{H_3O^+}} + 1.67 + \log f_{H_2O} \quad (2)$$

The values of the X 's can be evaluated using the value 50 for the equilibrium constant of reaction (3).



These relations lead to the conclusion that the values of $f_{H_3O^+}$, f_{H_2O} , $f_{HSO_4^-}$ and $f_{H_2SO_4}$ are probably all constant in the range 83-99.8% sulfuric acid.

In the course of investigations on acid catalysis in our laboratories correlation of H_0 with the activities of water and acid as indicated in eq. 4 have been revealed.

$$-H_0 = \alpha + \beta \log a_{HX}/a_{H_2O} \quad (4)$$

Data for phosphoric, perchloric, hydrochloric and

sulfuric acids⁴ have been examined and are listed in Figure 1 is a plot of the same data. The four acids give only three curves. Phosphoric acid yields one line of slope 0.98 and intercept -0.80. Hydrochloric and perchloric acids give a second line of slope 1.05 and intercept 0.22. Sulfuric acid on the other hand gives a non-linear plot with an initial slope of about 1.7 and a final slope of about 0.8.

If the validity of eq. 4 is real, and not merely fortuitous, certain thermodynamic conditions must obtain. Equations 1 and 4 may be combined with a_{H_2O} taken from eq. 5 to give eq. 6 in which a_1 is

$$K_{H_3O^+} = \frac{a_{H_2O} \times a_{H^+}}{a_{H_3O^+}} \quad (5)$$

replaced by $f_i C_i$. Now, if it is assumed that the acid

(4) These are the only acids for which adequate H_0 and activity data for testing eq. 4 appear to be available in the literature.

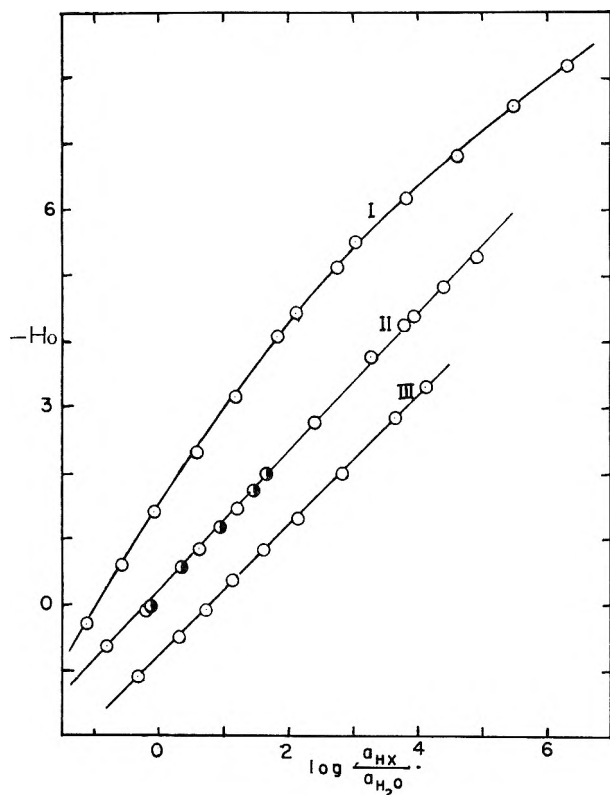


Fig. 1.—Correlation of H_0 with $\log a_{\text{HX}}/a_{\text{H}_2\text{O}}$: I, sulfuric acid; II, \bullet , hydrochloric acid, \circ , perchloric acid; III, phosphoric acid.

$$\text{const.} + \log \frac{f_{\text{HX}}C_{\text{HX}}}{f_{\text{H}_3\text{O}^+}C_{\text{H}_3\text{O}^+}} = \log \frac{f_{\text{B}}}{f_{\text{BH}^+}} \quad (6)$$

is essentially all dissociated then its stoichiometric concentration is equal to the hydronium ion concentration and eq. 7 must be satisfied. The assumption of complete dissociation is probably valid for per-

$$\log \frac{f_{\text{HX}}/f_{\text{H}_3\text{O}^+}}{f_{\text{B}}/f_{\text{BH}^+}} = \text{const.} \quad (7)$$

chloric and hydrochloric acids but it is certainly invalid for phosphoric acid ($K_a = 0.011$). Assuming constancy for the ratio $C_{\text{HX}}/C_{\text{H}_3\text{O}^+}$ also leads to eq. 7.

The case of phosphoric acid can be approached in two ways. First, we might assume that eq. 7 holds for it also. Then, since stoichiometric acid and hydronium ion concentrations cannot be equal they must exist in constant ratio in all solutions. Secondly, eq. 8 is valid for this acid since the second and third ionizations can be ignored in all but the

$$K_{\text{HX}} = \frac{a_{\text{H}_3\text{O}^+} \times a_{\text{X}^-}}{a_{\text{HX}} \times a_{\text{H}_2\text{O}}} = \frac{(a_{\text{H}_3\text{O}^+})^2}{a_{\text{HX}} \times a_{\text{H}_2\text{O}}} \quad (8)$$

most dilute solutions. Substituting a_{HX} from eq. 8 into eq. 6 leads to eq. 9. Although the latter is valid it demands constancy of the quotient of an activity ratio and an activity coefficient ratio and is therefore more complex than eq. 7.

$$\text{const.} + \log \frac{f_{\text{H}_3\text{O}^+} \times C_{\text{H}_3\text{O}^+}}{f_{\text{H}_2\text{O}} \times C_{\text{H}_2\text{O}}} = \log \frac{f_{\text{B}}}{f_{\text{BH}^+}} \quad (9)$$

Assuming constancy of the ratio $C_{\text{HX}}/C_{\text{H}_3\text{O}^+}$ is attractive from another point of view. For a weak acid the ratio will be greater than one. This can account for the fact that the line for phosphoric acid in Fig. 1 lies below the others if the two activity coefficient ratios in eq. 6 do not differ greatly from each other. Data for acids of intermediate strength, *e.g.*, trichloroacetic or trifluoroacetic, should produce lines lying between the lower two if these considerations are valid.

In terms of the activity ratio sulfuric acid is seen to be more acidic than perchloric acid and also to give a non-linear relationship. This may be attributable to the fact that no explicit account is taken of the role played by bisulfate. It is a twofold stronger acid than phosphoric and might well make a significant contribution to the acidity in the more dilute solutions. In the absence of activity data for bisulfate the curve for sulfuric acid cannot be interpreted reliably.

THE CRYSTAL GROWTH OF LEAD CHLORIDE FROM AQUEOUS SOLUTIONS¹

BY S. Z. LEWIN

Contribution from the Department of Chemistry, New York University, New York, N. Y.

Received April 18, 1955

The size, habit and transparency of lead chloride crystals obtained from aqueous solutions of NaCl, HCl and HClO, are correlated with the solubilities of PbCl₂ in these media, the time for crystallization to set in, and the rate of cooling and agitation during crystallization. The time for crystals to form and the particle weight are found to parallel the solubility, except for a pronounced inhibition of crystallization in concentrated chloride solutions. The unique effect of hydronium ions in promoting crystal growth, previously found for SrSO₄, is shown to be present.

A study of the crystal growth of strontium sulfate from solution² has disclosed a specific effect of hydronium ions in improving crystal size and perfection. This work made use of an experimental technique ("extractive crystallization") which produced relatively large crystals of that sparingly

soluble salt. In order to examine the hydronium ion effect under different experimental conditions, as well as to afford additional insight into crystal growth phenomena in general, the present study has been carried out. Lead chloride was chosen as particularly appropriate for these studies, for it has a solubility in water that is neither very large nor very small, and which can be altered conveniently over a wide range by the addition of vari-

(1) This work was supported in part by Contract No. AT(30-1)-1256 between the Atomic Energy Commission and New York University.

(2) S. Z. Lewin and J. E. Vance, *J. Am. Chem. Soc.*, **74**, 1433 (1952).

ous electrolytes. It also provides an opportunity to examine the effect of complex ion formation on crystal growth, since PbCl_3^- and PbCl_4^{--} exist in significant concentrations in solutions containing much chloride ion.

Experimental

The following solutions were saturated with PbCl_2 by placing a heated solution containing excess solid PbCl_2 in a thermostat kept at $25.00 \pm 0.05^\circ$ and stirring for 24 hours: water, HCl solutions ranging from 0.538 molal ($=m$) to 6.924 m ; NaCl solutions from 0.486 to 4.082 m ; HClO_4 solutions from 0.549 to 6.473 m . For each solution a number of 40.0-ml. portions were filtered into test-tubes containing amounts of solid PbCl_2 ranging from 0.0125 to 0.600 g., and the tubes were flame sealed.

Two types of experiment were performed: (A) those comprising a series of tubes in which the medium was kept constant and the amount of excess solid was varied; (B) series in which the amount of excess solid was constant, and the composition of the solution varied. In each experiment, the series of tubes was placed on a rotating rack in an oven and heated until the excess solid had completely dissolved. The tubes were then allowed to cool by either rapid immersion in a 25° thermostat, or by turning off the oven heater and allowing the temperature of the oven and its contents to fall gradually to room temperature. The oven was provided with a glass door through which the tubes were observed during the cooling process. In some runs, the tubes were rocked gently; in other runs, they were kept stationary. All tubes of a given series received identical pre-treatment, and were handled together at all times to provide the contents of the tubes with identical histories and ambient conditions. After the tubes had reached 25° and crystallization had taken place, they were opened, and the crystals were removed by suction filtration on a glass fritted disc, air-dried, placed on a microscope stage and photographed. In the case of the slow-cooling experiments, the time and temperature at which macroscopic crystallization first became evident in each tube were recorded, and the crystals or clusters finally obtained were counted and weighed. The crystals obtained from these solutions were shown by analysis to be pure PbCl_2 . No evidence was found for double salt formation between NaCl and PbCl_2 under the conditions of these experiments.³

Results

The individual measurements made in the course of this work showed a wide range of variation, and duplicate experiments often did not reproduce themselves, in terms of the parameters measured, within a factor of several hundred per cent. However, certain *phenomena, trends* and *relative relationships* invariably were found, and it is to these qualitative relationships that the results and conclusions reported here are limited.

A. Effect of Supersaturation.—Increase in the amount of excess PbCl_2 initially present in the medium resulted in a general decrease in the time elapsing before crystallization became visually apparent. In those media in which there was evidence of a tendency for crystallization to occur at the walls of the tube (see below), this tendency was diminished by increase in the initial supersaturation. The physical appearance of the crystals obtained from HCl and HClO_4 solutions did not change as the supersaturation was increased, but there was a marked effect on the crystals produced from water and NaCl solutions. At low supersaturations in the latter solutions, the crystal forms that predominate are long, slender needles which appear to be well-formed single crystals, together with irregular, opaque agglomerates having

a pebbled surface suggestive of the coalescence of many very small primary particles (Fig. 1a). As the supersaturation increases, both these forms disappear, and are replaced by bundles of rod-shaped masses lacking sharp edges or flat faces (Fig. 1b). These particles are fairly transparent and appear to be single crystal masses, the lack of characteristic crystal edges and faces suggesting that the growth took place under a large driving force. At still greater supersaturations, the crystal form improves considerably; sharp edges and plane faces come into evidence again (Fig. 1c), although all the particles are clusters of many individual crystals.

In the case of the HCl and HClO_4 solutions, there was no effect of the degree of supersaturation on the transparency, shapes or habits of the crystals.

B. Effect of Rate of Cooling.—For the water and NaCl solutions, the crystal growth becomes less regular and less unidirectional if the rate of precipitation is increased at a given condition of supersaturation. This can be seen by comparing Fig. 1d and 1e with Fig. 1a–1c. In the case of the HCl and HClO_4 solutions there was, apart from size, very little difference between the appearance of crystals obtained with rapid and with slow cooling. The crystal masses produced by rapid cooling were, in general, smaller than those produced by slow cooling, as shown in Figs. 1f and 1g.

C. Effect of the Medium.—There were marked differences in the sizes and appearance of crystals obtained at a given supersaturation from the various media employed. Table I shows data obtained in a typical run in which 0.05 g. of excess PbCl_2 was allowed to crystallize in stationary tubes by slow cooling in a variety of media. Although, as mentioned previously, little significance is attached to the absolute values of the last two columns in the table because of the general lack of reproducibility of the data, the trends shown in these measurements were shown in all other runs,

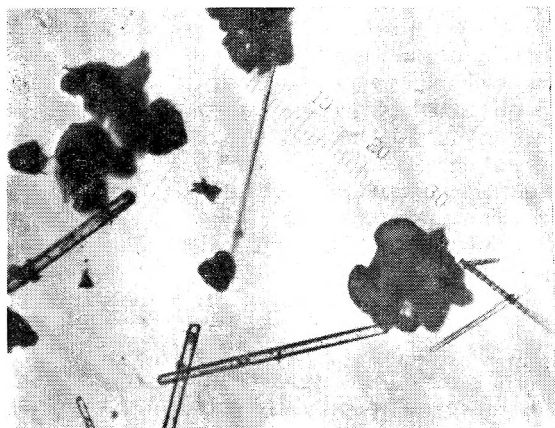
TABLE I
CRYSTALLIZATION OF PbCl_2 FROM AQUEOUS SOLUTIONS AT
CONSTANT INITIAL SUPERSATURATION; SLOW COOLING

Medium	Concn., m	Soly. of PbCl_2 per 1000 g. H_2O^a	Time for crystals to appear, hr.	Wt. per particle ($\text{mg.} \times 10^3$)
H_2O	...	10.59	4.0	8.5
HCl	0.538	1.561	2.0	5.5
HCl	1.002	0.9 ^b	1.3	5.0
HCl	2.155	1.3 ^b	1.4	3.0
HCl	3.261	2.1 ^b	2.5	3.0
HCl	4.884	2.8 ^b	2.5	6.0
HCl	6.924	5.4 ^b	4.7	13.5
NaCl	0.472	1.870	2.1	2.5
NaCl	1.013	1.784	4.8	2.0
NaCl	2.027	2.743	5	2.5
NaCl	4.022	8.367	5	5.5
HClO_4	0.549	10.88	4.1	8.5
HClO_4	1.037	10.56	2.5	9.0
HClO_4	2.324	7.421	2.3	4.0
HClO_4	3.457	5.183	1.7	3.0
HClO_4	4.212	4.3 ^b	1.2	3.0
HClO_4	6.473	1.781	0.4	3.0

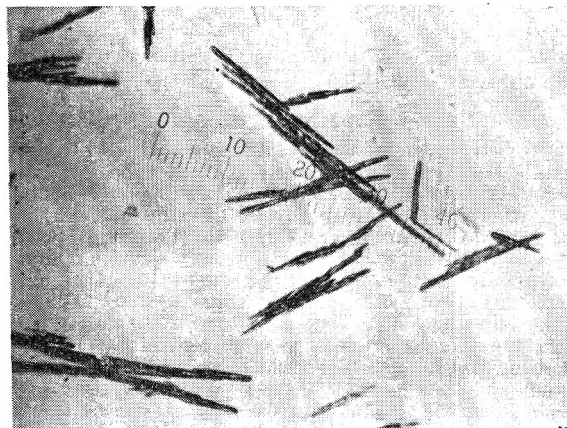
(3) Cf. S. Z. Lewin, J. E. Vance and L. B. Nelson, *J. Am. Chem. Soc.*, **75**, 2768 (1953).

^a Ref. 3. ^b Interpolated.

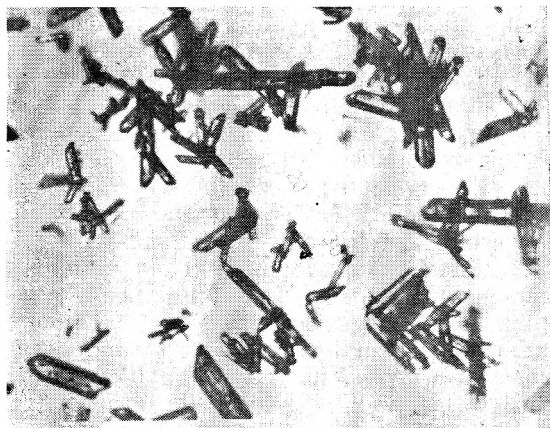
Fig. 1.—The relative sizes and shapes of PbCl_2 crystals obtained under otherwise comparable conditions as a function of the nature of the medium, and of the rate of crystallization; magnification $120\times$.



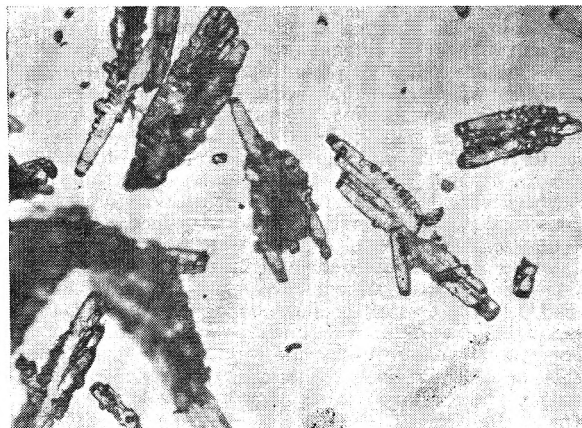
A.—0.1 g. of excess PbCl_2 crystallizing from water, slow cooling.



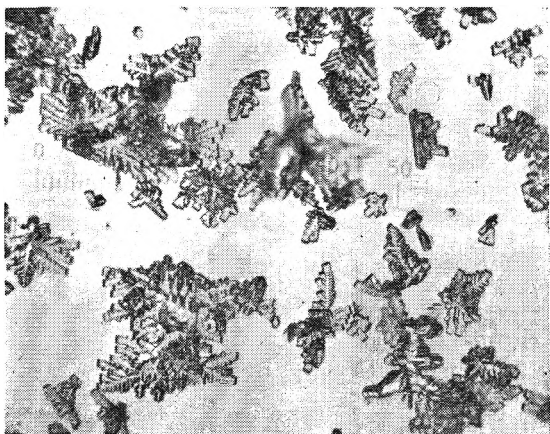
B.—0.4 g. of excess PbCl_2 crystallizing from water, slow cooling.



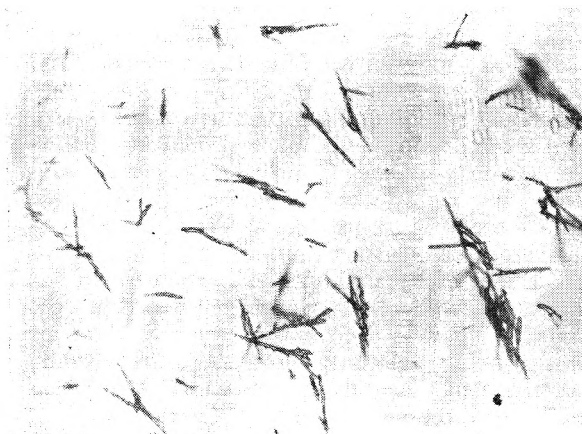
C.—0.6 g. of excess PbCl_2 crystallizing from water, slow cooling.



D.—0.2 g. of excess PbCl_2 crystallizing from water, rapid cooling.



E.—0.6 g. of excess PbCl_2 crystallizing from water, rapid cooling.



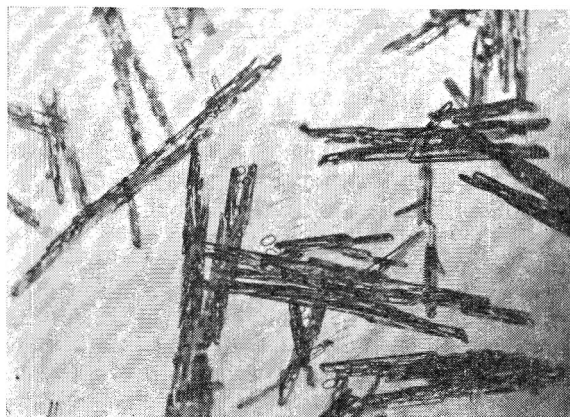
F.—0.6 g. of excess PbCl_2 crystallizing from $2m$ HCl , rapid cooling.

regardless of the amount of PbCl_2 crystallizing, of the rate of cooling, or of the agitation or lack thereof during the crystallization process. Therefore, these data are considered to provide a valid guide to the qualitative relationships involved.

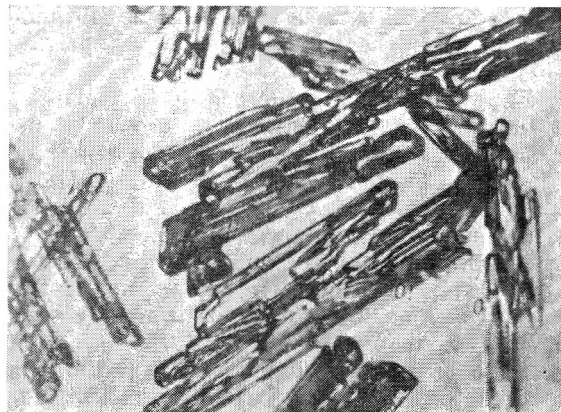
It will be noted that there is a direct relationship between the time for crystallization to become apparent, and the solubility: as the solubility in a given electrolyte solution increases, the time elapsing before crystallization occurs also increases.

However, for equal solubilities, solutions containing a high chloride ion concentration show much greater crystallization delays than the corresponding perchloric acid or water solutions. Also, the weight per particle tends to be highest from the solutions in which the solubility is highest, and the crystallization delay is greatest.

The crystals obtained from HCl and HClO_4 solutions were transparent, whereas those obtained from water and NaCl solutions tended to be



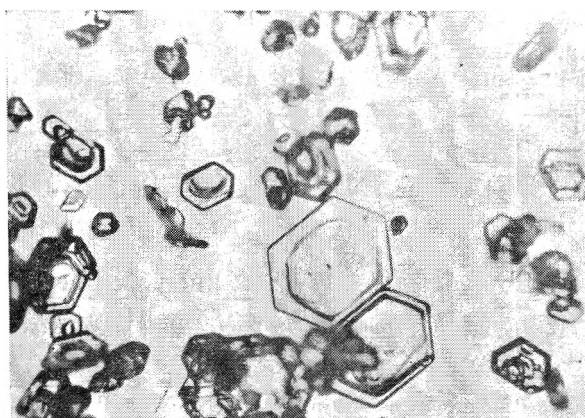
G.—0.1 g. of excess PbCl_2 crystallizing from 1*m* HCl; slow cooling.



H.—0.1 g. of excess PbCl_2 crystallizing from 4*m* HCl; slow cooling.



I.—0.1 g. of excess PbCl_2 crystallizing from 4*m* NaCl; slow cooling.



J.—0.1 g. of excess PbCl_2 crystallizing from 7*m* HCl; slow cooling.

opaque (*e.g.*, Fig. 1a and 1g to 1j). Increasing the concentration of the HClO_4 had, in general, no effect on the shape and appearance (as distinct from size) of the PbCl_2 crystals; but in the case of the HCl solutions, a change from long rods to regular hexagonal plates⁴ occurred between 4 and 6 *N* HCl (Fig. 1j), and in the NaCl solutions the higher concentrations gave crystals that were more squat (ratio of long to short dimensions closer to unity) than those obtained from lower NaCl concentrations (*e.g.*, Fig. 1i).

The crystals produced in the water solutions and the dilute (0.5 to 1.0 *m*) NaCl solutions were always found adhering to the walls of the glass tubes. At higher NaCl concentrations, and in all the acid solutions, the crystals were observed to form in the body of the liquid phase and showed no tendency to stick to the glass walls.

Discussion

In the case of a PbCl_2 crystal growing from a water solution in which the supersaturation is not great, the species that predominate in solution are probably Pb^{++} , PbCl^+ , PbCl_2 and Cl^- , and the crystal surface probably presents both Pb^{++} Cl^- sites to the solution. Since the crystal is anisotropic, one growth direction is favored over the others, and the production of long needle-like crys-

tals is possible if growth starts on a favorably situated single crystal seed. However, the strong adsorption of water molecules on the growing crystal surface introduces a propensity toward the formation of faults, fissures, overgrowths, etc., and makes it very probable that uninterrupted growth in a single direction will not occur, but that branching and inclusion of small pockets of mother liquor will be frequent. This would account for the preponderance of pebbled, opaque masses in the product obtained at low supersaturations from water solution (Fig. 1a). As the supersaturation increases, the ions in solution become better able to compete (due to their increased activity) with water molecules for positions at the crystal surface, and branching and opacity decrease (Fig. 1b and 1c).

In the HCl and HClO_4 solutions, the PbCl_2 crystals are transparent at all growth rates and supersaturations investigated. On the other hand, the crystals obtained from NaCl solutions are uniformly quite opaque. This suggests that the hydronium ions in the acid solutions participate in the crystal growth process in such a way as to decrease the probability of fault-production and mother liquor inclusion. It has been pointed out in connection with the previous studies on SrSO_4 crystal growth² that a high concentration of hydronium ions in solution might be expected to be uniquely effective in disrupting an adsorption layer of water molecules, thereby facilitating the addition of lattice

(4) This effect was previously observed by J. C. Bell, *J. Chem. Soc.*, **21**, 350 (1868).

ions to the crystal surface. This unique effect of hydrogen ions appears to play an important role also in the growth of PbCl_2 crystals.

At high chloride ion concentrations a marked inhibition of crystal formation and growth is observed. In these solutions the concentrations of Pb^{++} and PbCl^+ are low, and PbCl_3^- and PbCl_4^{--} are probably high. Also, the crystal surface probably has many adsorbed chloride ions, so that very few positive sites are offered to the solution. Since the addition of negative species such as the above complex ions to a negative surface site is for energetic reasons of low probability, the formation of macroscopic crystals under these conditions is greatly inhibited. It may be noted that in solutions of high chloride ion concentration, the specific effect of hydronium ions in producing fault-free crystal growth is still evident; PbCl_2 crystals obtained from concentrated NaCl solutions are opaque, whereas those obtained from concentrated HCl are transparent. It was also observed that

the marked disparity in ease of growth in different crystallographic directions that leads to the long, slender crystals tends to decrease in the presence of a high concentration of chloride ions (*cf.* Fig. 1i and 1j). Thus, the adsorption of chloride ions over the crystal surface not only introduces a barrier to growth, but also tends to wipe out the anisotropy of the surface.

The general parallelism observed for PbCl_2 in these experiments between solubility, crystallization time, and weight per particle indicates that where there is an inhibition to regular or rapid growth, as in water and the concentrated chloride solutions, there is also an inhibition of nucleation, so that the total growth occurs on a smaller number of centers, and the weight per particle increases.

Acknowledgment.—The author is indebted to Dr. John E. Vance for a number of helpful discussions. The photomicrographs were made by Mr. David K. Bulloch, and Mr. Harlow J. Fraden assisted in a number of the experiments.

THE KINETICS OF THE THERMAL DECOMPOSITION OF NITROCELLULOSE

BY R. W. PHILLIPS, C. A. ORLICK AND R. STEINBERGER

Contribution from the Allegany Ballistics Laboratory,¹ Hercules Powder Company, Cumberland, Maryland

Received April 15, 1955

The thermal decomposition of thin films of nitrocellulose has been studied by infrared spectroscopy and by a gravimetric technique. The kinetics are best approximated by a first-order curve with two or three branches. Typical values of the activation energy and Arrhenius frequency factor are 45.0 kcal./mole and 3.54×10^{18} sec.⁻¹, respectively.

Introduction

Nitrocellulose, as the major ingredient of smokeless powder, occupies a key position in the field of solid propellants. The kinetics and mechanism of its thermal breakdown are of considerable importance, inasmuch as they bear on the storage stability of these materials and may also be involved in the combustion process. An attempt has been made in the present study to determine the kinetic parameters of the reaction in the absence of secondary effects and to gain information as to possible mechanisms.

Only limited and somewhat contradictory data are available on the kinetics of decomposition of nitrocellulose.²⁻⁴ Estimated activation energies and Arrhenius frequency factors range from 28.5 to 56 kcal./mole, and from 10^{18} to 10^{24} sec.⁻¹, respectively.

In the previous studies, generally, the course of the reaction has been followed by the measurement of quantities only indirectly related to the composition of the residue. In this study, the progress

of the decomposition was followed by noting the changes in the infrared spectrum of a thin nitrocellulose film as a function of time. The infrared spectroscopic approach was chosen, since it enables one to measure directly the concentration of nitrate groups in the non-volatile residue and provides a description of structural changes associated with nitrate group removal. A correlative approach also was attempted, whereby the sample weight loss was measured as a function of time. Substantial agreement was noted between the kinetic parameters found by the two methods.

Experimental

Infrared Spectroscopic Study.—This work was performed with a Perkin-Elmer Model 21 Infrared Spectrometer fitted with NaCl optics. The spectra were recorded at the rate of about 1.5 minutes per micron with the slit control set at Program 4 with automatic suppression. Table I lists the

TABLE I

Group absorption	Frequency (cm. ⁻¹)		Slit width at ν_{\max} , μ
	ν_{\max}	ν_{\min}	
>C=O	1740	1852	37
-ONO ₂	1660	1852	45
-ONO ₂	1280	1220	66
"C-O-C"	1064	1220	93
-ONO ₂	840	770	156

groups whose absorptions were of special interest in this study; three nitrate group frequencies at 840, 1280, and 1660 cm.⁻¹, a carbonyl group frequency at 1740 cm.⁻¹, and a band at 1064 cm.⁻¹. The precise group assignment for this latter absorption band is unknown; however, it ap-

(1) An installation owned by the United States Government and operated for the U. S. Navy by the Hercules Powder Company under Contract NOrd 10431.

(2) S. Roginskii, *Physik. Z. Sowjetunion*, **1**, 640 (1932), as reported in N. Semenov, "Chemical Kinetics and Chain Reactions," Oxford at the Clarendon Press, 1935, p. 423.

(3) R. E. Wilfong, S. S. Penner and F. Daniels, *THIS JOURNAL*, **54**, 863 (1950).

(4) (a) J. F. Gizecki, *Chem. Ztg.*, **74**, 649 (1950); (b) R. D. Smith, *Nature*, **170**, 844 (1952).

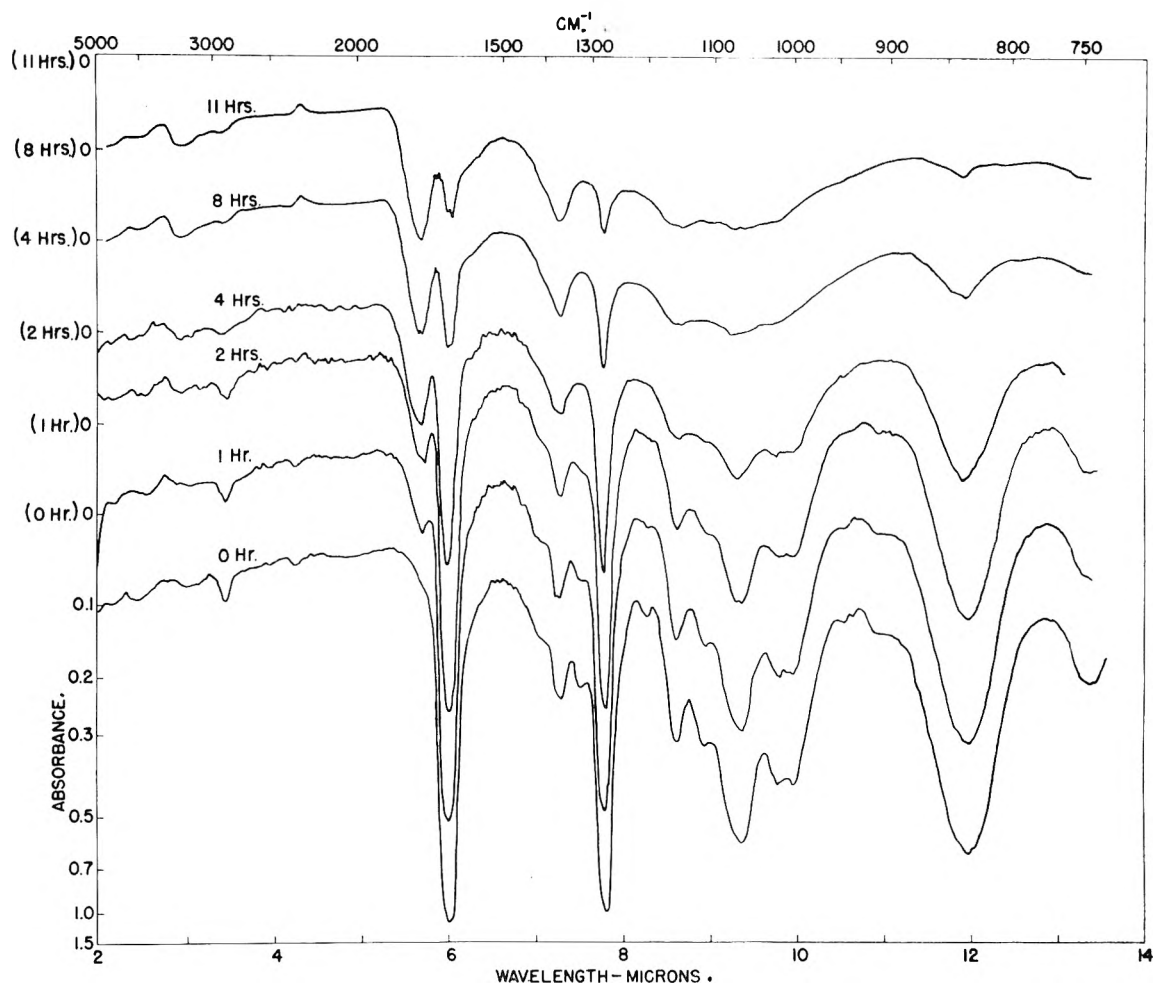


Fig. 1.—Infrared spectra of a 3μ film of 13.9% N nitrocellulose decomposed at 160° and 1 mm. pressure. The absorbance ($-\log$ transmittance) scale, shown for the 0 hour curve, has been shifted as indicated for the curves obtained at various heating times. The spectra were measured on a Perkin-Elmer Model 21 Infrared Spectrometer with NaCl optics.

pears to be associated with the basic cellulosic skeleton. For identification it is referred to as the "C-O-C" absorption band.

The intensity values of the various absorption bands were measured in absorbance units by a base line method. The group absorbance was the maximum absorbance value measured at the indicated frequency, less the base line absorbance, *i.e.*, the minimum absorbance. A Beer's law relationship was assumed between group absorbance and group concentration.

Films were cast on rock salt plates from acetone solution and dried overnight in a vacuum desiccator; this treatment was sufficient to remove the solvent to the point where it could not be detected in the spectrum. When additives were used, these were placed in the original solution and deposited with the nitrocellulose film. Film thickness was not allowed to exceed about 5μ except where the variation of film thickness was being studied; 3μ films were considered most desirable.

Decompositions were carried out in a sealed, thermostated infrared absorption cell, one window of which was easily removable to allow rapid introduction of the sample plate. The thermocouple sensing element was placed in a well as near as possible to the surface of the internal shoulder against which the sample was placed. The cell temperature was controlled to $\pm 0.15^\circ$ by means of a Gardsman thermoregulator.⁵ A switching arrangement made it possible to check the thermocouple output with a potentiometer for periodic calibration during a decomposition.

Films were decomposed at 140, 150, 160, 170, 180 and 190° under 1–2 mm. pressure unless other conditions are specified. Continuous evacuation was maintained during

the whole period of decomposition which ranged between 2 and 56 hours. The cell was brought to temperature before introduction of the sample plate, and a stable temperature was obtained within three minutes.

It seemed desirable to record at least three spectra per half life of the decomposing nitrate group. When decompositions were carried out at 160° or below, it was possible to obtain the requisite number of spectra for the wave length interval of 2 to 15μ (see Fig. 1). Above 160° it was impossible to record the complete spectrum due to the increased speed of decomposition. In these cases it was necessary to restrict spectral coverage, and only the nitrate absorption centered at 840 cm.^{-1} was recorded. Because of its isolation this was considered to be the most reliable of the three nitrate absorption bands.

During the course of a decomposition run it was found that the reaction rate changed slightly, although each part of the curve possessed first order characteristics, as indicated in Fig. 2. In an attempt to evaluate the relative importance of these rates, the following definitions were adopted. The *principal rate* is that whose duration, expressed in terms of its own half-life, has the greatest value; a reaction rate appearing before the principal rate is referred to as the *initial rate*, while a *final rate* is one following the principal rate.

Weight Loss Study.—The nitrocellulose films used in this study were cast on leveled glass discs by evaporation of the ethyl acetate solvent. The film was removed by water immersion and dried overnight in a vacuum desiccator. Unless otherwise stated, all films were 2– 3μ thick.

Changes in weight during the decomposition were measured with a quartz spiral balance⁶ which had a sensitivity of 0.302 mg./cm. A film of suitable weight was suspended

(5) Taco West Corp., Chicago, Illinois.

(6) Microchemical Specialties Company, Berkeley, Calif.

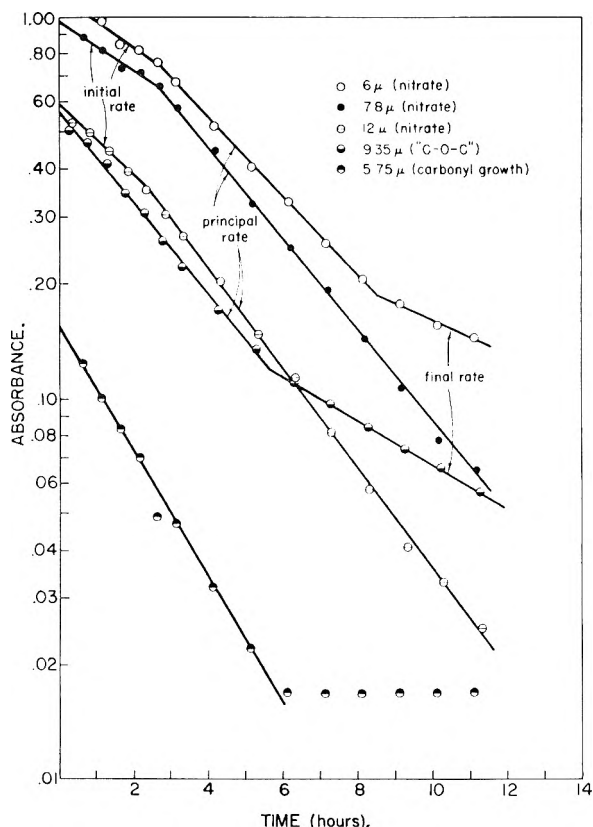


Fig. 2.—Log absorbance vs. time plots for 13.9% N nitrocellulose decomposed at 160° and 1 mm. pressure.

from the balance by means of a glass hook and the glass balance tube was evacuated. The lower end of the tube, containing the film, was immersed in a Wood's metal bath the temperature of which was controlled to $\pm 0.2^\circ$ by a Bristol controller.⁷ Inasmuch as the temperature of the bath varied somewhat over its length, the film weights were chosen so that the film was always within that region of the constant temperature bath complying to the stated temperature limits. The balance extension was measured with a cathetometer. As in the infrared study, continuous evacuation was maintained during the decomposition period.

At the beginning of an experiment, a five-minute preheating period was used in order to allow time for the film to approximate the bath temperature as well as for adjustment of the apparatus. An approximately 6% weight loss was encountered during this period; this weight loss was attributed to solvent removal even though various drying techniques failed to overcome the difficulty. The film weight at the end of the preheating period was used as the initial weight.

It was found that a constant film weight was never achieved regardless of the length of the decomposition period. In order to treat kinetically the weight loss data, a value for the final film weight was obtained by extrapolation of the final, nearly linear, and very gradual portion of the weight-time curve back to zero time. The plot of $\log(w_t - w_\infty)$ versus time, where w_t = film weight at any time, t , w_∞ = final film weight by extrapolation to zero time, could be represented by a series of straight lines, from which first-order reaction rate constants were derived.

Materials.—(1) Nitrocellulose: 13.9% N U. S. Naval Powder Factory Lot H-5 (13.91% N, Degree of substitution = 2.92) and Lot H-7 (13.96% N, D.S. = 2.93). (2) Nitrocellulose: 11.01% N (D.S. = 1.97), 12.6% N (D.S. = 2.45) and 13.38% N (D.S. = 2.72), commercial production lots from Hercules Powder Company. (3) Dextran nitrate⁸: native dextran kindly supplied by the Northern Regional Research Laboratory (Sample B-512, unhydrolyzed, Reference P.P. 55B was nitrated to 11.79% N (D.S.

= 2.2) with a nitric acid-sulfuric acid mixture. The fraction of 1,6-glucosidic linkages of the starting material has been estimated to be 95%.^{9,10} (4) Plasticizer: Flexol TOF (tri-2-ethylhexyl phosphate) Carbide and Carbon Chemical Company. The fraction boiling above 170° (1-2 mm.) was used. (5) Stabilizer, ethyl centralite (*sym*-diethyldiphenylurea), standard commercial grade, U.S. Naval Air Rocket Test Station, Lake Denmark, Dover, N. J.

Results

Nitrocellulose Decomposition.—A typical series of spectra recorded at various times during the decomposition of a nitrocellulose (13.9% N) film at 160° is shown in Fig. 1. From these spectra the changes in group absorbances were derived, as indicated in the log absorbance vs. time plots in Fig. 2. Except for changes in decomposition rate and therefore changes in time scale, this is considered typical for the decomposition of 13.9% N nitrocellulose over the whole temperature range studied.

Plots of $\log(w_t - w_\infty)$ vs. time from the weight loss study are very similar to the plots obtained in the infrared work for the nitrate group removal (see Fig. 2) and, for this reason, are not shown.

A summary of rate data for 13.9% N nitrocellulose from infrared studies is presented in Table II. It is noted that the carbonyl and "C-O-C" groups have rate constants equal, within the limits of experimental error, to the nitrate group rate constant. The results from the weight loss study are summarized in Table III. Arrhenius plots obtained from the results of the two studies are shown in Fig. 3.

TABLE II
PRINCIPAL DECOMPOSITION RATE CONSTANTS FOR 13.9% N NITROCELLULOSE AT 1-2 MM. PRESSURE

Temp., °C.	$k \times 10^5$ (sec. ⁻¹)				
	>C=O (1740 cm. ⁻¹)	-ONO ₂ (1660 cm. ⁻¹)	-ONO ₂ (1280 cm. ⁻¹)	"C-O-C" (1064 cm. ⁻¹)	-ONO ₂ (840 cm. ⁻¹)
142	1.19	1.03	1.02	0.889	1.14
152	4.67	2.33	3.06	3.19	3.64
160	11.4	7.86	8.67	8.72	9.03
172	49.4	35.6			36.7
180					88.6
190					273
$A \times 10^{-18}$ (sec. ⁻¹)	2.13	0.015	0.17	6.6	2.3
E (kcal./mole)	44.2	40.1	42.2	45.3	44.3

The accuracy of these results is best indicated by the 95% confidence limits on the activation energies, indicated in parentheses in Table III, and which average approximately 3 kcal./mole. On the basis of the precision of results, the weight loss data are considered more reliable than the infrared data and the values for 13.9% N nitrocellulose ($A = 9.0 \times 10^{18}$ sec.⁻¹, $E = 43.7$ kcal./mole) may be regarded as typical.

Effect of Pressure.—In order to ascertain how closely the reaction conditions needed to be controlled, the effects of pressure and film thickness were investigated.

(9) A. Jeanes and C. A. Wilham, *J. Am. Chem. Soc.*, **72**, 2655 (1950).

(10) J. W. Sloan, B. H. Alexander, R. L. Lohmar, I. A. Wolf and C. E. Rist, *ibid.*, **76**, 4429 (1954).

(7) The Bristol Company, Waterbury, Conn., Series 536 Controller.
(8) We are indebted to Dr. Nelson S. Marans for the preparation of this material.

TABLE III
EFFECT OF NITROGEN CONTENT ON NITROCELLULOSE DECOMPOSITION

	$k \times 10^5$ (sec. ⁻¹) ^a			A (sec. ⁻¹)		E (kcal./mole)	
	% N	Principal	Initial	Principal	Initial	Principal	Initial
Infrared study	13.96	9.03	4.36	2.3×10^{18}	2.9×10^{17}	44.3 (1.7)	43.2 (3.0)
	11.01	5.72		5.4×10^{18}		35.7 (2.6)	
Weight Loss Study	13.96	7.33	3.47	9.0×10^{18}	8.5×10^{15}	43.7 (2.1)	40.2 (6.3)
	13.38	6.72	4.06	1.1×10^{18}	3.7×10^{15}	44.0 (2.7)	41.4 (5.5)
	12.60	5.28	4.28	8.6×10^{18}	1.2×10^{19}	46.0 (1.7)	46.4 (2.9)
	11.01	3.97	3.72	4.5×10^{18}	2.8×10^{18}	45.4 (3.0)	45.4

^a Rate constants at 160°.

The pressure effect was studied by the infrared method using air as the pressurizing gas. The results are summarized in Table IV. Below 10 mm. pressure, the reaction rate and the course of the reaction are independent of the pressure. At 100 mm. and above the decomposition becomes more complicated, as evidenced by the appearance of absorptions at 2273 and 1587 cm.⁻¹. The 2273 cm.⁻¹ absorption has been attributed to the nitrile group. It first appeared in the 100 mm. decomposition run and was most intense in the decomposition at 400 mm. The 1587 cm.⁻¹ band has been attributed to the nitro group. It made its first appearance in the decompositions at 400 mm. and became most intense at 600 mm., which was the highest pressure employed. It was concluded from these data that pressure control was not critical, as long as the pressure did not exceed 10 mm.

TABLE IV
EFFECT OF PRESSURE ON THE DECOMPOSITION RATE OF 13.9% N NITROCELLULOSE AT 162° (PRINCIPAL RATE CONSTANTS)

Pressure (mm.)	Approx. thickness (μ)	>C=O (1740 cm. ⁻¹)	$k \times 10^5$ (sec. ⁻¹)			-C≡N (2273 cm. ⁻¹)
			-ONO ₂ (1660 cm. ⁻¹)	"C-O-C" (1064 cm. ⁻¹)	-ONO ₂ (840 cm. ⁻¹)	
2	2.3	18.3	11.7	11.7	11.7	None
10	1.9	14.3	10.4	10.4	12.0	None
100	1.9	13.8	11.7	10.7	11.3	Trace
200	1.5	16.8	2.97	8.94	8.6	^a
400	6.0	17.5	^b	^b	^b	^b
600	4.1	19.3	^b	^b	^b	11.7

^a The nitrile absorption appeared between 1/2 and 1 hour after decomposition was begun and remained constant during the balance of the decomposition period. ^b The rates of decomposition were very irregular. The decompositions did not seem to follow first-order kinetics.

Effect of Film Thickness.—The effect of film thickness was studied by both the infrared and weight loss methods. Table V summarizes the infrared data obtained at 162 and 190°. These data show a general tendency for the decomposition rate to decrease with increasing thickness. However, weight loss data with five films (2 to 13 μ thick) of 13.3% N nitrocellulose decomposed at 172° showed no significant changes in the weight-time relationships. The reason for this discrepancy is not clear. However, neither method showed an effect at the thickness level actually used, approximately 3 μ.

TABLE V
EFFECT OF FILM THICKNESS ON THE DECOMPOSITION RATE OF 13.9% N NITROCELLULOSE (PRINCIPAL RATE CONSTANTS)

Thickness (Ac-H) ^a (μ)	Thickness (μ)	$k \times 10^5$ (sec. ⁻¹)		
		>C=O (1740 cm. ⁻¹)	"C-O-C" (1064 cm. ⁻¹)	-ONO ₂ (840 cm. ⁻¹)
		160°		
0.024	1.2	21.4	15.4	16.8
.035	1.8	17.5	15.4	16.0
.049	2.5	15.4	13.3	15.4
.109	5.7	18.3	7.86	9.17
.179	9.4	20.2	5.36	10.1

190°		
0.029	1.5	308
.033	1.7	231
.037	1.9	308
.041	2.1	289
.060	3.1	243
.111	5.7	164
.137	7.0	149
.143	7.5	119
.170	8.8	136
.192	10.0	141

^a Absorbance of C-H band at 2900 cm.⁻¹.

Effect of Nitration Level.—Infrared studies were made on 11.01% N nitrocellulose at 140, 160 and 180°. Weight loss studies were made on 13.38, 12.6 and 11.01% N nitrocellulose samples, the temperature range of 152–190° being covered in approximately ten degree intervals. The kinetic data are summarized in Table III. Comparison of the results of these runs with those obtained with 13.9% N

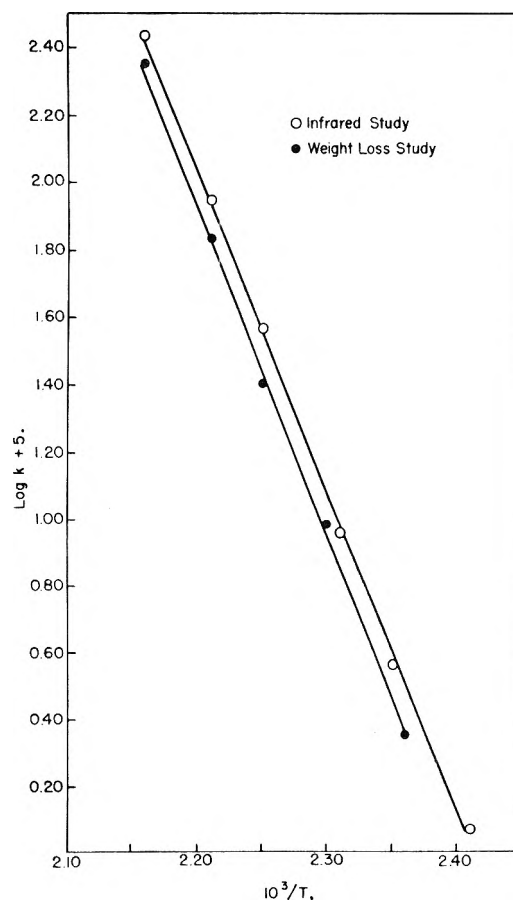


Fig. 3.—Arrhenius plots for decomposition of 13.9% N nitrocellulose.

nitrocellulose show that the initial rate constant remains the same, but that the principal rate constants decrease and approach the initial rate constant as the nitrogen content is decreased.

Effect of Additives.—Inasmuch as nitrocellulose is ordinarily used in the plasticized and stabilized condition, it was of interest to examine the effect of these additives on the decomposition kinetics. In Table VI are given the kinetic data obtained by the infrared method for films of nitrocellulose plasticized with various amounts of Flexol TOF, or stabilized with ethyl centralite. Flexol TOF was selected as the plasticizer because of its miscibility with nitrocellulose, high boiling point, and infrared transparency. At the 16.7 and 30% plasticizer levels, decompositions were carried out at 160° only, whereas a range of temperatures was covered at the 9.1% level. The infrared spectra of the 30% plasticizer experiment indicated that the plasticizer was evaporating down to the 15–20% level, so that a higher level of plasticization would be of little value. The presence of the plasticizer had no detectable effect on the course of the decomposition.

The decomposition of 13.9% N nitrocellulose in the presence of 4.76% ethyl centralite was performed at 160°, again no effect was noted. This experiment provided added assurance that no autocatalytic reaction was taking place under the conditions of this investigation.

TABLE VI

EFFECT OF PLASTICIZER AND STABILIZER ON DECOMPOSITION OF 13.9% N NITROCELLULOSE AT 160° (PRINCIPAL RATES)

% Additive	$k \times 10^5$ (sec. ⁻¹)				
	$>C=O$ (1740 cm. ⁻¹)	$-ONO_2$ (1660 cm. ⁻¹)	$-ONO_2$ (1280 cm. ⁻¹)	$"C-O-$ C" (1064 cm. ⁻¹)	$-ONO_2$ (840 cm. ⁻¹)
9.1% Flexol TOF	10.2	7.53	8.94	7.75	9.11
16.7% Flexol TOF	7.81	7.83	9.25	8.25	8.89
30% Flexol TOF	11.6	7.17	9.03	9.28	9.28
4.76% Ethyl Centralite	10.39	6.81	8.75	7.94	9.17

Dextran Nitrate.—Dextran nitrate seemed of considerable interest because of its great similarity to nitrocellulose, the principal difference being the lack of primary nitrate groups in dextran nitrate. Since any difference in decomposition rates between these two compounds could then be attributed to the primary nitrate group, the decomposition of dextran nitrate was studied by the same procedures used for nitrocellulose.

The rate constants determined from the 12 μ nitrate absorption and from the weight loss study are given in Table VII. It is observed that the rate constant at 160° is 1.5 to 2 times that for 13.9% N nitrocellulose, although the Arrhenius expressions do not differ materially. Initial rates were either absent or were only very slightly lower than the principal rate.

TABLE VII

RATE DATA FOR DEXTRAN NITRATE DECOMPOSITION	$k \times 10^5$ (sec. ⁻¹) ^a		E (kcal./mole)
	A	(sec. ⁻¹)	
Infrared study	19.25	3.2×10^{16}	40.1 ± 1.7
Weight loss study	11.05	1.1×10^{18}	43.6 ± 2.2

^a Rate constants at 160°.

Discussion

The study of the slow thermal decomposition of nitrocellulose is complicated by the fact that the gaseous products of the reaction are capable of reacting further with the solid residue. It is therefore of great importance to remove these gases, if it is desired to measure the rate of the primary decomposition. Several of the experiments described above point up the fact that, under the conditions of this investigation, only

the primary decomposition is occurring. First, if secondary reactions were occurring, pressure and thickness would be expected to have a profound effect on the reaction rates. Actually, no significant changes appear until drastic increases in pressure and thickness have been made. Second, a stabilizer would be expected to reduce secondary reactions if they were present. In actual fact, the presence of ethyl centralite had no effect on the reaction rate. Finally, the fact that essentially equal rates were obtained from all the frequencies employed in the infrared study and from the weight loss study suggests that the course of the reaction is straightforward and that secondary effects are not present.

Order of Reaction.—The data have been plotted as first-order curves. This represents a somewhat arbitrary choice, inasmuch as in condensed systems such as this, differences in reaction order may not be quite as apparent as they are in more dilute solutions. The division of the curves into two or three branches may actually mean that a more complex rate law should have been used. However, the method chosen has the advantage of simplicity and allows the data to be summarized in a straightforward manner. In this connection it is interesting to note the agreement between the activation energy obtained in the present work and that reported by Wilfong, Penner and Daniels³ who assumed zero-order kinetics.

Role of Physical State of Sample.—The present work shows that a plasticized nitrocellulose film decomposes at the same rate as an unplasticized film. The decomposition of nitrocellulose in solution also has been studied^{4b} and the reaction rate constant differs little from that observed in this investigation. It appears probable, therefore, that the decomposition process is independent of the physical nature of the sample.

Equivalence of Techniques.—The quantities measured by the two techniques used here are quite different, the changes in weight represent over-all changes in the molecule while the changes in the infrared spectra are very specific and apply only to the particular bond or group being measured. It is of interest to note, therefore, that the two techniques give quite comparable results.

Importance of Primary Nitrate Groups.—As previously mentioned the experiments with dextran nitrate were performed in order to observe the effect of replacing the primary nitrate group of nitrocellulose with a secondary one. A comparison of rate constants, Tables III and VII, shows that the rate constant for 11.89% N dextran nitrate at 160° is more than twice that for 12.6% N nitrocellulose. This is a greater difference than can be explained by the absence of primary nitrate groups and suggests that the three vicinal nitrate groups have a greater intrinsic decomposition rate than the two vicinal nitrate groups of nitrocellulose.

Carbonyl Growth.—Comparison of the rate constants (Table II) for the carbonyl and nitrate groups shows that the carbonyl growth equals the nitrate group loss. This is in accord with the commonly accepted mechanism of nitrate decomposition which involves the formation of alde-

hydes and ketones as a consequence of O-NO₂ bond fission.¹¹

Change of Rate during Decomposition.—The change in rate from the initial rate to a somewhat higher principal rate is difficult to explain. However, a clue is provided by the effect of nitrogen content. As the degree of nitration is lowered, the principal rate decreases and approaches the initial rate, which remains essentially constant. This change parallels an increase in the relative concentration of primary nitrate groups, as observed by Murray and Purves.¹²

A reasonable, though necessarily tentative, interpretation of this set of circumstances is that primary nitrate group decomposition is more important in the initial phases and that the principal rate involves the greater participation of secondary nitrate groups as the molecule is un-

(11) G. Gelernter, L. C. Browning and S. R. Harris, U. S. Department of Interior, Bureau of Mines, Summary Technical Report No. 3401 (1954).

(12) G. E. Murray and C. B. Purves, *J. Am. Chem. Soc.*, **62**, 3194 (1940).

stabilized by partial decomposition. According to this concept, the primary groups decompose somewhat more readily than the secondary ones; however, this is contrary to the evidence presented by Gelernter, Browning and Harris.¹¹

Mechanism of the Reaction.—It had been hoped at the inception of this study that the infrared spectra would provide valuable information regarding the course of the reaction. Unfortunately, it has not been found possible to be very specific about the assignment of the various absorption bands, other than the most obvious ones such as nitrate, carbonyl, etc., so that the details of the chemical changes remain obscure. The over-all features of the spectra suggest, however, that the basic structure of the carbon skeleton does not change drastically during the decomposition. Coupled with the fact that a substantial residue remains even after severe degradation, this indicates that denitration does not necessarily lead to chain-splitting and that the residue is still polymeric in structure.

SPECIFIC ADSORPTION OF ALKYL ORANGE DYES ON SILICA GEL

BY R. G. HALDEMAN¹ AND P. H. EMMETT

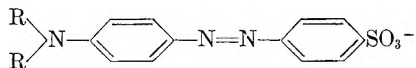
Contribution from the Multiple Fellowship of Gulf Research and Development Company, Mellon Institute, Pittsburgh, Pa.

Received April 25, 1955

A study has been made of the phenomenon of specific adsorption of the alkyl orange dyes on silica gels prepared in the presence of those dyes. The gels were prepared by F. H. Dickey² who first investigated this field. Dye and nitrogen adsorption isotherms were obtained on some of the gels. Batch dye adsorption experiments were made on the other gels. Residual dye content of the gels after preparation was measured. The results confirm the earlier work² in showing that silica gel samples have a specific adsorptive capacity for the particular alkyl orange present during the gel preparation. The specificity appears to disappear gradually when the gels are stored at room temperature.

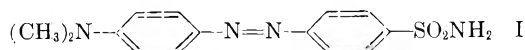
Introduction

The preparation of specific adsorbents was first demonstrated by Dickey.² He prepared silica gels³ in the presence of the alkyl oranges



(where R represents methyl, ethyl, *n*-propyl or *n*-butyl), and found that the gels preferentially adsorb the particular dyes or indicators used in their preparation.

Results on a second analogous series of gels⁴ prepared by Dickey were partially disclosed by Bernhard.⁵ Bernhard also confirmed the observations of Dickey by experiments on a new set of gels prepared in the presence of methyl orange, ethyl orange and *p*-dimethylamino-*p'*-sulfonamido-azobenzene (I).



He found that methyl orange and I were quite similar in adsorptive properties and that gels prepared

in the presence of either were about equally efficient in adsorbing both dyes. He concluded that in this case the specificity was independent of the negative charge on the *p'*-constituent.

Samples of each of Dickey's series of gels were examined in this Laboratory for dye adsorption about a year after their preparation; in addition, the A series was studied by nitrogen adsorption about six months after being prepared. The present report includes a summary of these and related measurements and a brief discussion of the possible origin of the selective properties of the gels.

Experimental

Dye solutions were prepared from samples of the alkyl oranges provided by Dickey. The spectra of the solutions agreed closely with the spectra of solutions prepared with alkyl orange dyes from other sources.

The nitrogen adsorption measurements at -195° were made in a conventional type apparatus.⁶ Surface areas were calculated by the BET procedure.⁷

Alkyl orange adsorption isotherms were obtained on the series A gels. A series of solutions of each dye was prepared ranging in concentration from 0.6×10^{-8} to 3.0×10^{-8} moles per cc. in 5% acetic acid. Thirty cc. of weak dye solution was added to 0.200 g. gel and shaken for six hours.

(6) W. E. Barr and V. J. Anhorn, "Scientific and Industrial Glass Blowing," Instruments Publishing Company, Pittsburgh, Pa., 1949, p. 257.

(7) S. Brunauer, P. H. Emmett and E. Teller, *J. Am. Chem. Soc.*, **60**, 309 (1938).

(1) American Cyanamid Company, Stamford, Conn.

(2) F. H. Dickey, *Proc. Natl. Acad. Sci.*, **35**, 227 (1949).

(3) These gels and their control ge. are designated Series "A" in our nomenclature.

(4) Called the "B" series in our nomenclature.

(5) S. A. Bernhard, *J. Am. Chem. Soc.*, **74**, 4946 (1952).

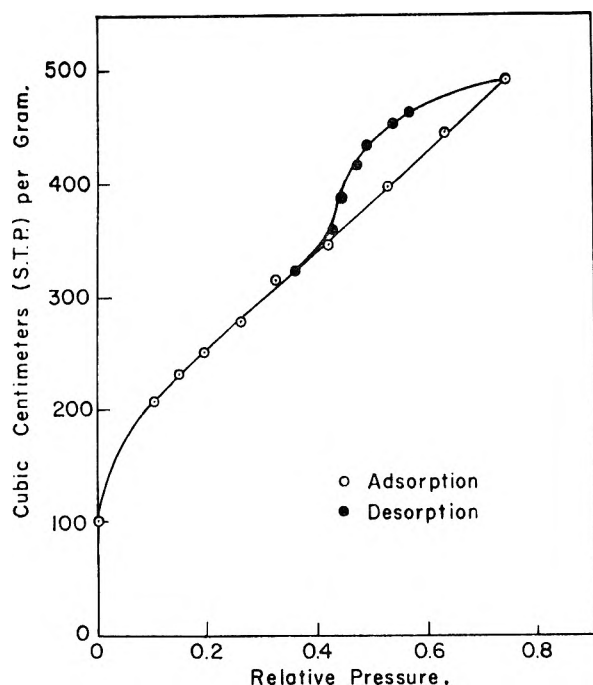


Fig. 1.—Nitrogen adsorption at -195° on control gel of series A.

The sample was then centrifuged for 15 minutes at 4000 r.p.m. in order to settle the fine gel particles. A 25-cc. sample of the solution was carefully withdrawn by pipet and analyzed for dye content by means of a Fisher electrophotometer. Now, 25 cc. of a more concentrated dye solution was added to the sample tube and the cycle repeated. The process was continued throughout the desired concentration range. The adsorbed dye could be desorbed by contacting the gel with 5% acetic acid in like fashion. The data for an adsorption isotherm were calculated by means of material balances for each treatment. The small portion of solution lost per cycle (about 1%) was assumed to have the same composition as the equilibrium solution of the treatment. The uncertainty in the calculated adsorption values is thought to be about 5%.

The dye adsorption measurements on series B gels were made by a batch procedure similar to that used by Dickey.² In each case dye solutions of concentration 3×10^{-8} mole per cc. were contacted with a gel in the weight ratio of 10 to 1. After several days equilibration the supernatant liquid was analyzed for dye concentration in the Carey recording spectrophotometer, due correction² being made for the background scatter of the small gel particles.

The residual dye content of each gel as received from Dickey was measured by dissolving a weighed sample in a measured, excess volume of 1 *N* sodium hydroxide solution. The dye, now present in solution as the yellow form, was estimated by means of the Carey spectrophotometer, calibrated with appropriate dye solutions in basic environment.

Estimation of the values of the basic dissociation constants of the alkyl oranges was made by spectrophotometric examination (in the region of 5000 Å.) of dye solutions of concentration 1.5×10^{-8} mole per cc. and pH values of 2.3, 3.38 and 12.6. The pH was regulated by the relative concentrations of acetic acid and sodium hydroxide. At pH 2.3 the solution was assumed to contain only the acidic form of the dye, at 12.6 only the basic form. The ratio of acid to basic form at pH 3.38 was estimated assuming a simple two-component dye system.

Results

Nitrogen Adsorption.—Nitrogen adsorption measurements at -195° were made on small portions of each of the various gels of series A about six months after their preparation. The isotherms were all very similar; a typical plot is indicated in Fig. 1. For each a hysteresis loop was observed in

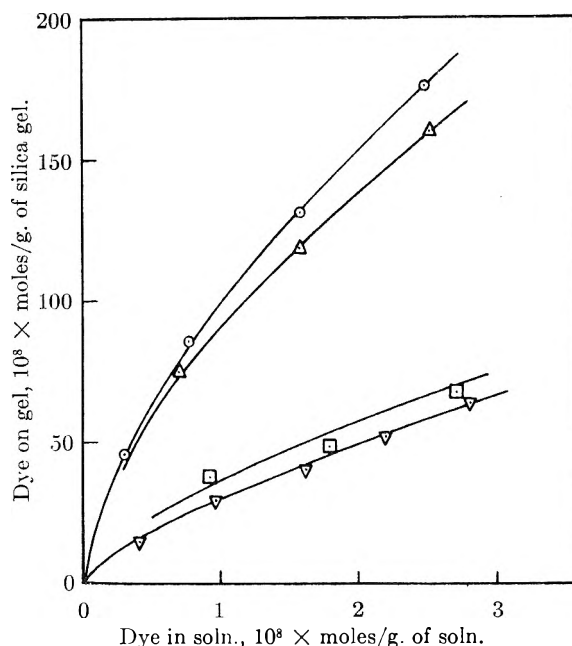


Fig. 2.—Adsorption of alkyl oranges on control gel of series A: ∇ , methyl orange; Δ , propyl orange; \square , ethyl orange; \circ , butyl orange.

the desorption curve, merging with the adsorption curve at a relative pressure of about 0.4. The point of closure represents a gel pore radius of 10–12 Å. as calculated by the Kelvin equation.⁸ The surface areas of the gels were very nearly the same, all being within one per cent. of the mean, 980 sq. m. per gram.

The close similarity in gross structure of the gels, as indicated by nitrogen adsorption, make it apparent that their specific adsorptive properties are not dependent on marked differences in gross physical structure. Unfortunately, the gel samples were evacuated for an hour at 200° before the adsorption runs with nitrogen. According to the results reported by Curti and Colombo⁹ this period of evacuation would be sufficient to destroy the specificity of the sample even though it is not high enough to appreciably sinter the silica gel. The surface area measurements reported here cannot, therefore, be used directly to obtain any detailed picture of the shape or size of the "foot prints" left by washing out the alkyl orange used in preparing the gel.

Dye Adsorption on Series A Gels.—An adsorption isotherm for each dye (in 5% acetic acid solution) on each gel of series A was determined. The dye adsorption isotherms on the control gel of series A are shown in Fig. 2. It will be noted that for each solution concentration, the adsorption of dye increases as the homologous series is ascended from methyl to butyl orange. The butyl adsorption is roughly three times the methyl adsorption, over the concentration range studied. The curve for ethyl orange is slightly above that of methyl, while the curve for propyl orange is slightly below that of butyl orange. Since this gel was prepared in the absence of any dye, no fading effect

(8) P. H. Emmett and T. W. DeWitt, *J. Am. Chem. Soc.*, **65**, 1253 (1943).

(9) R. Curti and U. Colombo, *Chimica e L'Industria*, **33**, 103 (1951).

is involved and it is expected that these isotherms are independent of the age of the gel.

The enhanced affinity of a particular gel for the dye in the presence of which the gel was prepared is illustrated in Fig. 3, in which the adsorption of methyl and propyl oranges on the various series A gels is presented. Although the specific effects are small, they are clearly discernible; methyl orange and propyl orange were definitely more strongly adsorbed on the gels prepared in the presence of these respective dyes than on the control gel. Similar specific effects were found for the adsorption of ethyl and butyl oranges on the various gels.

A direct comparison of the above results with Dickey's observation on the same gels cannot readily be made, because the latter measurements were made at very low equilibrium solution concentrations ($<0.2 \times 10^{-3}$ mole per gram), lower than any used in the present experiments. However, the specific effects reported above are much smaller than those found by Dickey. Inasmuch as our experiments were made on the samples about a year after their preparation, they are believed to indicate that the specific adsorptive properties tend to disappear with time. This concept is supported by the results on series B gels reported below and also by the findings of Curti and Colombo.⁹

It is worthy of note that the adsorption isotherms appear to be reversible as indicated by the isotherm in Fig. 3 for the adsorption of methyl orange on the gel prepared from methyl orange. Also, it was ascertained from examination of equilibrium solutions of methyl orange in contact with the butyl gel, and *vice versa*, that the dye remaining in the gel after the methanol extraction used in the preparation of the gel, is not displaced by dye from solution.

Dye Adsorption on Series B Gels.—A second series of gels prepared by F. H. Dickey were examined by us about a year after their preparation. Dickey's adsorption experiments on these gels have been partially reported by Bernhard.⁵ Our experiments were made by a batch technique under conditions analogous to those of Dickey. Our initial solution concentrations were about 3×10^{-5} molar, while those of Dickey varied from 1.5×10^{-5} molar for ethyl orange to 3×10^{-5} for propyl orange.

The values of relative adsorption power for the two series of experiments¹⁰ are indicated in Table I. It is evident that in both sets the relative adsorption is maximal for each dye on the gel prepared in its presence, although our results indicate much of the selectivity has vanished in the period between the preparation and testing of the samples.

Residual Dye Content.—The gels in both series A and B, as originally prepared, increase in red color intensity as the homologous series of preparative dyes is ascended from methyl to butyl orange. This dye remains in the gel even after the exhaustive methanol extraction used in preparing the gel. Further evidence that it is very strongly held by the gel is obtained from observations that it is practically inert to 5% acetic acid solution and 0.1 N sodium bicarbonate solution. In the latter solu-

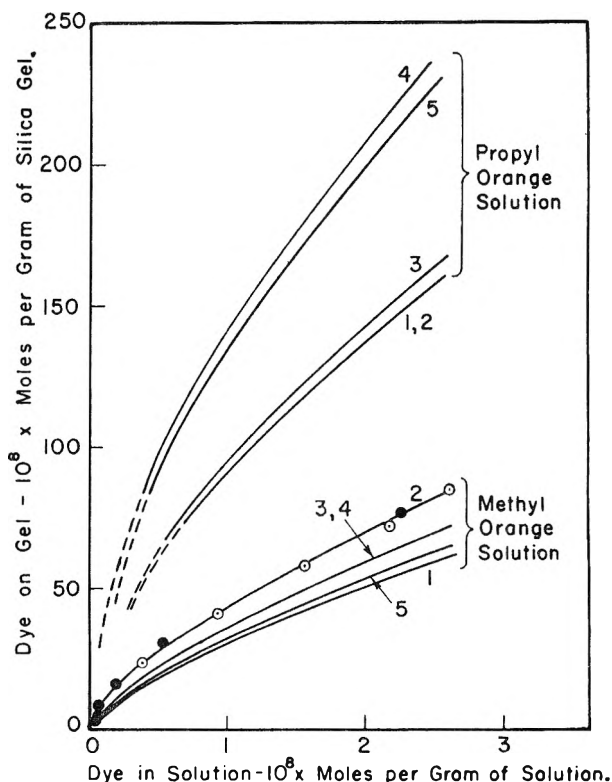
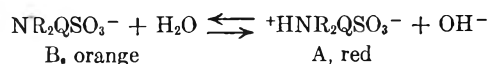


Fig. 3.—Adsorption of methyl and propyl orange on gels of series A: \circ , adsorption; \bullet , desorption. Gel 1 is a control. Gels 2, 3, 4 and 5 were prepared in the presence of methyl, ethyl, propyl and butyl oranges, respectively.

tion there is little color change of the dye in 12 hours. In contrast an alkyl orange adsorbed on a control gel from a solution at pH 6 produces a red coloration which disappears instantly when the pH is changed to about 8 by addition of sodium bicarbonate. This seems to indicate that the residual dye is not readily accessible to the aqueous phase, and is perhaps bound within the gel structure.

The residual dye content of the gels of both series was determined spectrophotometrically after the gels were dissolved in sodium hydroxide. The results are given in Table II. The dye contents are seen to increase regularly as the homologous series is ascended, and the concentration on each member of the B series is several times greater than that on its counterpart in the A series. The actual concentrations of residual dye in the original samples are quite small, the largest being 60×10^{-8} mole per gram. If this material were entirely on the surface of the gel it would cover less than 0.1% of the surface.

Basic Dissociation Constants of the Indicators.—To see whether correlation exists between the basic dissociation constants, K_b , of the respective dyes and some of their adsorption properties, the values of K_b were roughly determined. We used dye solutions of concentration 1.5×10^{-3} mole per cc. at pH 3.38, where forms B and A in the equilibrium¹¹



(10) Dickey's complete results on the B series were obtained by private communication.

(11) I. M. Kolthoff and C. Rosenblum, "Acid-Base Indicators," The Macmillan Co., New York, N. Y., 1937, p. 145.

TABLE I
RELATIVE ADSORPTION POWER^a OF SERIES B GELS^b
Relative adsorption power for

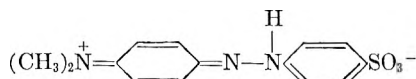
Gel prepared with	Methyl orange		Ethyl orange		Propyl orange		Butyl orange	
	Dickey	H & E	Dickey	H & E	Dickey	H & E	Dickey	H & E
Methyl orange	9.4	2.0	5.8	1.4	2.1	1.2	1.9	1.2
Ethyl orange	4.9	1.4	39	1.9	7.4	1.8	4.2	1.4
Propyl orange	4.2	1.4	23	1.8	37	3.2	26	2.9
Butyl orange	3.1	1.2	12	1.5	37	3.4	44	5.3

^a The "Adsorption power" is defined as the ratio of dye concentration on the gel to the dye concentration in solution. The "relative adsorption power" is then the ratio of the "adsorption power" of a particular gel to the "adsorption power" of the control for the same dye. ^b Conditions: wt. solution, wt. gel, 10:1; solution concentrations, H & E, 3×10^{-8} mole/cc.; Dickey, 2.26, 1.55, 2.94, 2.08×10^{-8} mole/gram for methyl to butyl orange, respectively.

TABLE II
RESIDUAL DYE CONTENT OF GELS

Gel prepared with	Series	Residual dye, 10^{-8} mole/g.
Methyl orange	A	1
Ethyl orange	A	3
Propyl orange	A	15
Butyl orange	A	18
Methyl orange	B	7
Ethyl orange	B	12
Propyl orange	B	50
Butyl orange	B	60

are present in appreciable concentrations. Usually, in the acid form, the proton is considered to be bound to an azo nitrogen atom,¹² thus



The ratio of A to B was determined spectrophotometrically. The values of K_b were calculated according to the equation

$$\bar{K}_b = \frac{(\text{A})(\text{OH}^-)}{(\text{B})} = \frac{(\text{A})K_w}{(\text{B})(\text{H}^+)}$$

neglecting any correction for salt effect or the possibility of tautomeric dye structures other than A and B.

The values of K_b at 25°, given in second column of Table III, are seen to increase regularly as the

TABLE III
RELATION BETWEEN K_b AND ADSORPTION DATA

Dye	$10^{11} \times K_b$ (25°)	Series A gels		
		Dye adsorption on control gel at soln. conc., 1×10^{-5} molar ^a	Residual dye in gel prepared with dye ^a	Relative ^b adsorption power of gel for preparative dye
Methyl orange	2 ± 1	30	1	3.5
Ethyl orange	4 ± 2	36	3	9
Propyl orange	9 ± 3	90	15	20
Butyl orange	11 ± 3	100	18	15

^a Units: 10^{-8} mole/gram. ^b These data are taken from the original paper of Dickey.²

homologous series of dyes is ascended. The mean of literature values of K_b for methyl orange¹³ is about 3×10^{-11} at 25°. Data for the other alkyl oranges have not been reported. From the fact that the pH range of color change of ethyl orange seems to be higher than methyl by about 0.4 unit,¹⁴ a value

of K_b of about 7×10^{-11} is calculated for ethyl orange. Our values for methyl and ethyl oranges are somewhat lower than these but in about the same ratio.

Discussion

The correlation between the basic dissociation constant for the alkyl oranges and the adsorptive properties of these dyes on the various gels is demonstrated for series A gels in Table III. Thus, adsorption on the control gel from solutions of concentration 1×10^{-8} mole per cc., the residual dye content of the specific adsorbents, and the relative adsorption power of each gel for its preparative dye all increase nearly in proportion to K_b . These relationships seem to furnish information about the mechanism of formation of the specific adsorbents and the adsorption processes thereon. (A correlation also exists with molecular size of the dye, but the variation in van der Waals forces as the result of changes in length of the alkyl groups, should not be critical. The azobenzene part of the molecule should determine the van der Waals forces, mainly.)

Since the adsorption of the alkyl oranges from solution at pH 5 or 6 (where the basic dye structure exists) on a control gel produces the red coloration of the acid form of the dye, it seems reasonable to assume that the adsorption occurs through hydrogen bonding between a surface silanol group and a nitrogen atom of the dye (probably an azo nitrogen, but this is not important to the argument). The strength of such a hydrogen bond would be expected to increase with the electron donating ability, or basicity, of the adsorbate. As K_b is a measure of basicity, it is calculated that the strength of the hydrogen bond formed in this way may increase by about one kilocalorie as the adsorbate is changed from methyl to butyl orange. This variation should be sufficient to account for the relative adsorbabilities of the dyes on the control gel.

Iler¹⁵ has studied the association between polysilicic acid and polar organic molecules. The compounds which he found to interact with polysilicic acid invariably contained electron donor atoms. He inferred from his data that hydrogen bonds between the electron donor atoms and the silanol groups were formed. For example, in his study of the secondary amines, he found the interaction increased markedly as the homologous series was ascended from methyl to *n*-amyl. The basicity of these amines increases as the series is ascended, with the exception of di-*n*-propylamine.¹⁶ The inter-

(12) Ref. 11, p. 228.

(13) Ref. 11, p. 290.

(14) Ref. 11, p. 143.

(15) R. K. Iler, *This Journal*, **56**, 673 (1952).

(16) N. F. Hall, and M. R. Sprinkle, *J. Am. Chem. Soc.*, **54**, 3469 (1932).

action of the orange dyes with silicic acid may be considered to be analogous, *i.e.*, the amount of dye which reacts with the structure increases with the basicity of the dye.

When a gel is formed in the presence of a dye, it seems likely that most of the combined dye will be situated on or near the surface, since such interaction should generate defects in the gel structure. However, part of the dye may be trapped within the gel and become inaccessible to aqueous and alcoholic extraction. If the extent of gel-dye interaction depends on dye basicity, the amount of residual dye in a gel would be expected to increase, as observed, with the basicity of the dye, other conditions being held constant.

It seems reasonable to suppose that in the process of methanol extraction, which follows gel formation and drying, dye molecules on or near the surface are removed leaving micropores ("footprints") of geometry and properties characteristic of the dye. The number of such pores should increase with the basicity of the dyes.

If the specific adsorption sites are considered to be micropores created at gelation time, and to persist after drying and methanol extraction of the dye, the geometry of the pore could have considerable influence on the relative adsorption of dye molecules differing principally in gross dimensions. Thus, for sites originating from methyl orange, larger homologs would tend to be excluded, resulting in a screening effect. On the other hand, a pore originating from butyl orange would be expected to hold less securely homologs of smaller size because of poorer fit and therefore weaker van der Waals forces. The latter observation though qualitatively in the right direction does not seem to be entirely adequate to explain the fifteen-fold differences (as observed by Dickey) in relative adsorption of butyl and methyl oranges on the butyl gel of series B. However, this geometric or shape factor originally suggested by Pauling¹⁷ and Dickey² still seems to be the only one that can reasonably account for the observed results.

It should be noted that in the comparison of relative adsorption power among the gels, the variable of basicity of adsorbate is largely eliminated because the adsorption is expressed relative to the adsorption of the same dye on the control. This seems to be supported also by the observation of Bern-

hard,⁵ that I which has about the same molecular size as methyl orange (but probably a different K_b) has about the same relative adsorptive properties.

The question naturally arises as to the relative sorption capacity per unit area of the gel covered with dye "imprints" or "footprints" compared to the part of the surface containing no such imprints. From the relative amount of dye and water glass used in the gel preparation ("0.5 g. of dye with 30 ml. of aqueous sodium silicate (d^{20} 1.401)")² one can calculate that no more than 10% of the total surface of the gel could be covered by imprints of dye molecules assuming that each dye molecule covers about 100 Å.² of the surface. It follows that if the "relative adsorption power" is 1.5 for a given dye, and if 10% of the surface consists of imprints, then the sorptive capacity per unit area is about 6 times as great for the "footprints" as for the rest of the gel. If the relative adsorptive power is taken as 15, as found by Dickey² for butyl orange adsorption on a gel prepared with butyl orange, the sorptive capacity of the footprints calculates out to be 140 times that of the rest of the surface. Furthermore, if the per cent. of the surface consisting of "footprints" is less than the 10% upper limit, the relative sorption capacity per unit area of the footprints becomes even greater than the factors of 6 or 140 calculated above. Accordingly, it can be safely concluded that the surface capacity per unit area of imprints from a given dye is many fold greater than that of the remainder of the gel surface.

In conclusion, it should be noted that the principle of preparing specific adsorbents by a procedure that creates "footprints" of some desired component that one wishes to purify has already been applied by Curti and Colombo¹⁸ to the separation of the optical isomers of camphosulfonic acid. They¹⁹ have also suggested a number of other specific separations that probably can be accomplished by chromatographic techniques employing this type of specific adsorbent.

Acknowledgment.—The authors wish to thank F. H. Dickey for supplying the gel samples and dye samples used in this investigation, and for permission to disclose some unpublished data. We also thank the Chemical Physics Department of Mellon Institute for aid with some of the analytical work.

(18) R. Curti and U. Colombo, *J. Am. Chem. Soc.*, **74**, 3961 (1952).

(19) R. Curti, U. Colombo and F. Clerice, *Gazz. chim. ital.*, **82**, 491 (1952).

(17) L. Pauling, *Chem. Eng. News*, **27**, 913 (1949).

ASSOCIATION OF N-H COMPOUNDS.^{1,2} I. IN BENZENEBY NORMAN E. WHITE³ AND MARTIN KILPATRICK*Contribution from the Departments of Chemistry of the University of Pennsylvania, Philadelphia, Pa., and Illinois Institute of Technology, Chicago, Illinois*

Received April 27, 1955

The association by H-bonding of a number of nitrogen-containing organic compounds, each of a different type, has been measured cryoscopically in benzene in the concentration range 0.005 to 0.1 molal. From the association factor it has been found possible to describe each case in terms of one or more equilibrium constants. Of the eight cases considered, four indicate continuous association with polymers of all orders, the other four show limited association, two indicating cyclic dimers and the other two dimers and trimers.

The problem of the interaction of molecules of the same species to form associates in the vapor phase and in solution has been the subject of numerous investigations. In the vapor phase, in solution, and in the solid phase it is often necessary to consider stable associates beyond dimers but the data do not seem to justify any special assumptions as to stability of particular associates such as tetramers or hexamers.^{4,5}

In solution the problem is complicated by the interaction of the solute with the solvent, as well as with itself, and deviations from ideality due to interactions other than association seriously limit the range of study by methods such as freezing-point lowering. Hunter and his co-workers⁶ in their study of "mesohydric tautomerism" have reported cryoscopic data for a great many nitrogen com-

by Davison.⁷ The concentration of the solute was determined by measuring the relative densities of the solutions with a newly designed, magnetically operated metal float of about 10 ml. volume, which could detect a change of three density units in the seventh place. The details of the density method will be given elsewhere.

Purification of Materials.—Benzene—J. T. Baker C.P. thiophene-free benzene was treated successively with concentrated sulfuric acid, water, concentrated sodium hydroxide and water. After drying with calcium chloride it was fractionally crystallized and fractionally distilled. All of the benzene so treated was mixed together to ensure homogeneity before storage. Before use, a portion was refluxed for an hour over potassium metal and then distilled directly into the freezing point cells. The freezing point of different portions as measured by a calibrated thermohm under actual experimental conditions varied from 5.501 to 5.481°, with an average value of 5.492 ± 0.004° for twenty-six samples. This value is in general agreement with that reported by Davison,⁷ and Kraus and co-workers,⁸ but somewhat lower than more recently reported values.⁹

TABLE I
MELTING POINTS OF SOLUTES

Name	Abbr.	M.p., °C.	M.p., °C., lit.	Ref.
Triphenylmethane	TPM	93.2–93.4	92.3–92.5	7, 10
Azobenzene	AZB ^a	68.0–68.1	69.1, 66, 68	11
2- <i>n</i> -Butylbenzimidazole	BB ^b	154.5–155.0	155.0–155.5	12
Benzotriazole	BZT	96.0–96.2	98–99, 96–97	13, 14
N,N'-Diphenylguanidine	DPG	147.5–147.7	147.5–147.8	15
N,N'-Diphenylformamidine	DPFAD	140.2–140.6	137–138 139.0–140.1	16, 17
3,5-Dimethylpyrazole	DMP	106.5–107.0	107	18
Diazoaminobenzene	DAAB ^d	98.0–98.5	98	19, 20
Benzaldehyde phenylhydrazine	BZPH	156.5–157.0	155, 149–50	21, 22
N-Phenyl-N'- <i>p</i> -tolylacetamidine	PTA ^c	93.2–93.6	90, 93	23, 24

^a Orange crystals. ^b Laboratory preparation from Dr. A. R. Day. ^c Obtained from the Biochemical Manufacturing Co., Defiance, Ohio. ^d Golden yellow crystals.

pounds and interpret their data in terms of cyclic and linear associates. All of the data are at high concentrations of the solute where the cryoscopic method is not too reliable for accurate calculations.

After an analysis of Hunter's data, a few compounds were selected for study in benzene by the freezing point method in the range 0.005 to 0.1 molal.

Experimental

Apparatus.—The apparatus and experimental method for the temperature measurements were the same as used

(1) Taken in part from the dissertation based upon experimental work concluded in 1946, presented by Norman E. White to the Faculty of the Graduate School of the University of Pennsylvania in 1954 in partial fulfillment of the requirements for the degree of Doctor of Philosophy.

(2) Presented before the Division of Physical and Inorganic Chemistry, 127th Meeting of the American Chemical Society, Cincinnati, Ohio, March 27–April 7, 1955.

(3) Drexel Institute of Technology, Philadelphia, Pa.

(4) E. W. Johnson and L. K. Nash, *J. Am. Chem. Soc.*, **72**, 547 (1950).

(5) G. Allen and E. F. Caldin, *Quart. Rev.*, **7**, 255 (1953).

(6) For references see L. Hunter, *J. Chem. Soc.*, 806 (1945).

(7) J. A. Davison, *J. Am. Chem. Soc.*, **67**, 228 (1945).

(8) B. C. Barton, D. A. Rothrock and C. A. Kraus, *ibid.*, **74**, 786 (1952).

(9) For literature, see F. W. Thompson and A. R. Ubbelohde, *Trans. Faraday Soc.*, **46**, 349 (1950).

(10) R. E. Richards and H. W. Thompson, *Proc. Roy. Soc. (London)*, **A195**, 1 (1948).

(11) G. S. Hartley, *J. Chem. Soc.*, 634 (1938).

(12) W. O. Pool, H. J. Harwood and A. W. Ralston, *J. Am. Chem. Soc.*, **59**, 178 (1937).

(13) J. E. Fagel and G. W. Ewing, *ibid.*, **73**, 4360 (1951).

(14) R. Damschroder and W. Peterson, *Org. Syntheses*, **20**, 16 (1940).

(15) M. M. Davis and P. S. Schuhmann, *J. Research Natl. Bur. Standards*, **39**, 221 (1947).

(16) D. N. Shigorin and Ya. K. Syrkin, *J. Phys. Chem. (USSR)*, **23**, 241 (1949).

(17) R. M. Roberts, *J. Am. Chem. Soc.*, **72**, 3608 (1950).

(18) R. H. Henry and W. M. Dehn, *ibid.*, **71**, 2297 (1949).

(19) C. M. Knowles and G. W. Watt, *ibid.*, **64**, 935 (1942).

(20) L. Hunter, *J. Chem. Soc.*, 320 (1937).

(21) H. Stobbe and R. Nowak, *Ber.*, **46**, 2887 (1913).

(22) D. Jerchel and R. Kuhn, *Ann.*, **568**, 185 (1950).

(23) M. Sen and J. N. Ray, *J. Chem. Soc.*, 646 (1926).

(24) L. Hunter and J. A. Marriott, *ibid.*, 777 (1941).

The solutes unless otherwise stated were Eastman Kodak White Label products purified by repeated crystallization using, whenever practicable, two different solvents of which the last was usually benzene. In each case the purified product was dried several hours under vacuum at 10 to 20° below its melting point in an Abderhalden drier using phosphorus pentoxide as a desiccating agent. The criterion of purity was taken to be not so much the actual melting point as its sharpness, and especially its constancy after further recrystallization. All the crystals were pure white unless otherwise stated. Table I lists the melting points with comparisons with the literature.

All compounds except benzaldehyde phenylhydrazone appeared to be stable as solids and in benzene solution. This compound rapidly underwent air oxidation in benzene, giving yellow solutions, due to a partial conversion to dibenzaldehyde phenylhydrotetrazone. Although precautions to exclude oxygen and light were taken, the density determinations showed a slow but measurable increase in density.

The Cryoscopic Constant for Benzene.—A calculation of the constant K_f° for a one molal, ideal solution at infinite dilution using a value for the latent heat of fusion of benzene of 2351 cal./mole²⁵ at $T_0 = 278.66^\circ$ yields $5.127 \pm 0.009^\circ$ for the cryoscopic constant. Using 1.82 cal./mole for the difference in heat capacities of liquid and solid benzene at T_0 , the dependence on temperature is given by the equation

$$K_f = 5.127^\circ - 0.054\Delta T_f \quad (1)$$

where ΔT_f is the freezing point depression. Davison⁷ used the equation

$$K_f = 5.088^\circ - 0.055\Delta T_f \quad (1a)$$

and Kraus⁸ has recently reported 5.088 as an average value using hexaethylbenzene as solute. In the present investigation triphenylmethane and azobenzene were used as standard substances and sufficient data were obtained over the range 0.005 to 0.1 molal to evaluate both the slope and intercept for equation 1. The data are presented graphically in Figs. 1 and 2. The equation for triphenylmethane by least squares is

$$K_f = 5.144^\circ - 0.221\Delta T_f \quad (1b)$$

and for azobenzene

$$K_f = 5.144^\circ - 0.171\Delta T_f \quad (1c)$$

The greater slope than 0.055 may indicate a slight deviation from ideality due to interaction but an experimentally determined equation is preferred to the one calculated from the value of the latent heat of fusion and the difference in heat capacities. The equation actually used was the least squares equation for both solutes

$$K_f = 5.144^\circ - 0.204\Delta T_f \quad (1d)$$

where the average deviation is 0.022 K_f unit and the probable error 0.002. Since the molalities of the solutions studied were in the range 0.005 to 0.1 the value of K_f used was from 5.10 to 5.02.

Determination of Molecular Weights.—The molalities determined by density, together with the freezing point depressions, the average molecular weight and the association ratio are given in Tables II through IX.

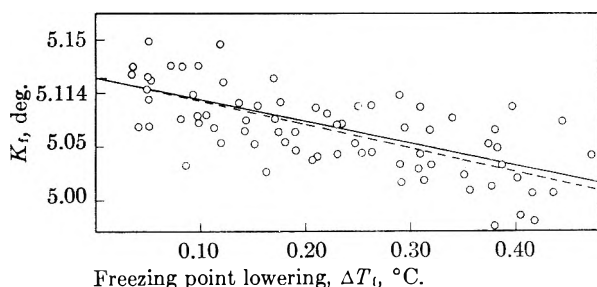


Fig. 1.—Triphenylmethane, change of cryoscopic constant with temperature: dotted line, TPM only—75 points; solid line TPM & AZB—120 points.

(25) American Petroleum Research Project 44 at the National Bureau of Standards: Selected Values of Properties of Hydrocarbons, Table 5a. Alkylbenzenes, Jan. 31–Aug. 31, 1945.

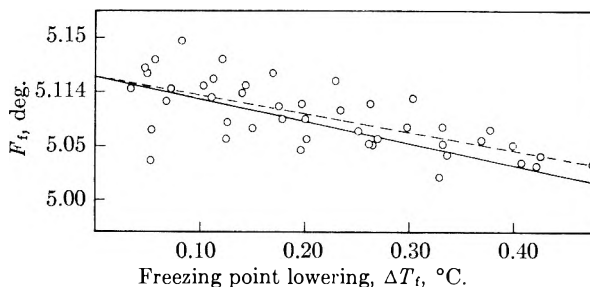


Fig. 2.—Azobenzene, change of cryoscopic constant with temperature: dotted line, AZB only—45 points; solid line, TPM & AZB—120 points.

TABLE II

THE CRYOSCOPIC DATA FOR SOLUTIONS OF 2-*n*-BUTYL-BENZAMIDAZOLE

Formula weight = $M_0 = 174.24$.

Q Molality $\times 10^3$	ΔT_f $^\circ\text{K.} \times 10^2$	M mol. wt.	M/M_0 association factor
5.83	2.691	192.9	1.107
10.70	4.367	218.0	1.251
14.08	5.188	241.3	1.385
15.86	5.627	250.6	1.438
21.19	6.524	288.7	1.657
26.35 ^a	6.963	336.3	1.930

^a Approximate limit of solubility in benzene at 5.5°.

TABLE III

THE CRYOSCOPIC DATA FOR SOLUTIONS OF BENZOTRIAZOLE

Formula weight = $M_0 = 119.12$.

Q molality $\times 10^3$	ΔT_f $^\circ\text{K.} \times 10^2$	M mol. wt.	M/M_0 association factor
11.30	5.172	132.8	1.115
11.36	5.241	131.7	1.106
16.37	7.055	140.9	1.183
16.53	7.151	140.4	1.179
20.77	8.552	147.5	1.238
24.98	9.780	155.0	1.301
25.18	9.882	154.6	1.298
29.75	11.109	162.4	1.363
30.36	11.205	164.3	1.379

TABLE IV

CRYOSCOPIC DATA FOR SOLUTIONS OF N_2N' -DIPHENYLGUANIDINE

Formula weight = $M_0 = 211.26$.

Q molality $\times 10^3$	ΔT_f $^\circ\text{K.} \times 10^2$	M mol. wt.	M/M_0 association factor
7.24	3.097	252.2	1.194
8.54	3.493	263.9	1.249
14.25	5.590	274.8	1.301
20.01	7.405	291.1	1.378
20.76	7.800	286.7	1.357
26.71	9.687	296.6	1.404
29.08	10.281	304.4	1.441
36.16	12.518	310.6	1.470
39.74	13.520	315.8	1.495
45.84	15.440	318.8	1.509
51.57	17.030	324.9	1.538
54.08	17.822	325.6	1.541
55.24	18.132	326.8	1.547
71.88	22.692	339.1	1.605

TABLE V
CRYOSCOPIC DATA FOR SOLUTIONS OF
N,N'-DIPHENYLFORMAMIDINE
Formula weight = $M_0 = 196.24$.

Q , molality $\times 10^3$	ΔT , $^{\circ}\text{K.} \times 10^2$	M , mol. wt.	M/M_0 , association factor
8.42	3.384	249.42	1.271
11.77	4.555	258.8	1.319
20.23	7.478	270.8	1.380
25.52	9.081	281.0	1.432
34.28	11.968	286.1	1.458
41.17	13.983	294.0	1.498
52.64	17.611	297.9	1.518
62.79	20.444	305.7	1.558
76.19	24.473	309.5	1.577
84.19	26.565	314.8	1.604
92.48	29.165	314.4	1.602

TABLE VI
CRYOSCOPIC DATA FOR SOLUTIONS OF
3,5-DIMETHYLPYRAZOLE
Formula weight = $M_0 = 96.13$.

Q , molality $\times 10^3$	ΔT , $^{\circ}\text{K.} \times 10^2$	M , mol. wt.	M/M_0 , association factor
8.03	3.249	121.3	1.262
21.13	7.272	142.4	1.481
26.02	8.642	147.5	1.534
34.38	10.624	158.4	1.648
37.89	11.713	158.3	1.647
47.52	13.547	171.5	1.784
53.89	15.265	172.5	1.794
66.75	17.680	184.3	1.917
72.52	19.178	184.5	1.919
83.10	21.313	190.0	1.977
94.96	23.322	198.3	2.063
110.10	26.625	201.2	2.093
124.49	29.915	209.2	2.176

TABLE VII
CRYOSCOPIC DATA FOR SOLUTIONS OF
DIAZOAMINO BENZENE
Formula weight = 197.23.

Q , molality $\times 10^3$	ΔT , $^{\circ}\text{K.} \times 10^2$	M , mol. wt.	M/M_0 , association factor
8.24	4.169	199.0	1.009
8.91	4.499	199.4	1.011
17.16	8.589	200.8	1.018
19.14	9.596	200.4	1.016
27.90	13.831	202.4	1.026
32.21	15.969	202.2	1.025
36.08	17.808	202.9	1.029
45.46	22.322	203.5	1.032
45.69	22.432	203.5	1.032
61.70	30.008	204.9	1.039
63.00	30.905	203.1	1.030
80.93	39.270	204.6	1.038

Precision of Measurements.—Determinate errors have been eliminated where possible, or allowance made for them, and the residual errors have been estimated from the A.D.'s the deviation of the mean for all quantities which are a mean of several similar measurements.

For the temperature measurements the constancy was 0.1 $\mu\text{v.}$, equivalent to 0.00007 $^{\circ}$, and since two temperatures are measured for each ΔT , the maximum uncertainty was taken as 0.2 $\mu\text{v.}$ which gives a resultant error of less than 0.5% at Q , the stoichiometric molality = 0.01; 0.2% at $Q = 0.05$ and 0.1% at $Q = 0.1$. The resultant error in es-

TABLE VIII
CRYOSCOPIC DATA FOR SOLUTIONS OF
BENZALDEHYDEPHENYLHYDRAZONE
Formula weight = $M_0 = 196.24$.

Q , molality $\times 10^3$	ΔT , $^{\circ}\text{K.} \times 10^2$	M , mol. wt.	M/M_0 , association factor
7.91	3.978	199.2	1.015
15.87	8.000	198.4	1.011
25.24	12.656	199.2	1.015
37.36	18.869	199.2	1.015
48.76	24.233	200.0	1.019
63.10	31.281	200.0	1.019
73.87	36.324	201.1	1.025

TABLE IX
CRYOSCOPIC DATA FOR SOLUTIONS OF
N-PHENYL-N'-p-TOLYLACETAMIDINE
Formula weight = $M_0 = 224.29$.

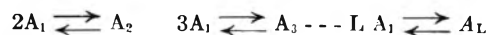
Q , molality $\times 10^3$	ΔT , $^{\circ}\text{K.} \times 10^2$	M , mol. wt.	M/M_0 , association factor
7.26	3.672	226.5	1.010
10.25	5.255	222.9	0.994
13.53	6.868	225.4	1.005
19.26	9.856	223.4	0.996
20.81	10.497	226.5	1.010
29.40	14.851	225.6	1.006
29.65	14.851	227.6	1.015
41.20	20.553	228.1	1.017
42.29	21.172	227.2	1.013
54.44	25.945	229.2	1.022
57.73	28.595	229.0	1.021
70.65	34.654	230.6	1.028
74.62	33.616	230.3	1.027

timating the concentration of the solute varied somewhat more for different solutes but was less than 0.8% at $Q = 0.01$, 0.4% at $Q = 0.05$ and 0.1% at $Q = 0.1$. The corresponding probable error in the association factor $f = M/M_0$ was calculated to be 1% at $Q = 0.01$, 0.4% at $Q = 0.05$ and approximately 0.1% at $Q = 0.1$. The effect of these errors on the reliability of the equilibrium constants will be discussed in the analysis of the data.

Figure 3 shows that the association factor changes quite differently with concentration for the various solutes.

Analysis of the Data

Consider the following association reactions



with the equilibrium constants

$$K_{12} = \frac{n_2}{(n_1)^2} \quad K_{13} = \frac{n_3}{(n_1)^3} \quad K_{1L} = \frac{n_L}{(n_1)^L} \quad (2)$$

where L is the polymer order, n_L represents the concentration in moles per 1000 g. of solvent species A_L . The total concentration or the stoichiometric concentration of single molecules, Q , is given by

$$Q = \sum_{L=1}^{L=k} Ln_L = \sum_{L=1}^{L=k} LK_{1L}(n_1)^L \quad (3)$$

where k = the highest order polymer and $K_{11} = 1$. Similarly the apparent concentration N is the sum of the concentrations of the various associates present including the remaining monomers

$$N = \sum_{L=1}^{L=k} n_L = \sum_{L=1}^{L=k} K_{1L}(n_1)^L \quad (4)$$

If equation 4 be differentiated with respect to n_1

$$\frac{dN}{dn_1} = \sum_{L=1}^{L=k} LK_{1L}(n_1)^{L-1} \quad (5)$$

and multiplying through by n_1

$$n_1 \frac{dN}{dn_1} = \sum_{L=1}^{L=k} LK_{1L}(n_1)^L = Q \text{ from eq. 3} \quad (6)$$

Letting f represent the association factor

$$f = \frac{Q}{N} \quad (7)$$

$$\frac{n_1}{N} \frac{dN}{dn_1} = \frac{d \ln N}{d \ln n_1} = f \quad (8)$$

To continue further, n_1 must be evaluated, or a relationship between f and N or Q established.

Method of Lassette.—Lassette,^{26,27} in a review of association, noted that three simple cases were encountered

$$(i) \quad f = 1 + \alpha Q \quad (9)$$

$$(ii) \quad f = 1 + \beta N \quad (10)$$

$$(iii) \quad f = 1 + \alpha Q + \beta N \quad (11)$$

where α and β are constants independent of f , N and Q . Putting these values of f into (8), integrating the differential equation, expressing N in powers of n_1 by the method of Lagrange, and comparing with equation 4

$$K_{1L} = \frac{(\alpha L)^{L-1}}{L!} \text{ where } \beta = 0 \quad (12)$$

$$K_{1L} = \beta^{L-1} \text{ where } \alpha = 0 \quad (13)$$

$$K_{1L} = \frac{1}{L!} \prod_{q=0}^{L-2} [\alpha L + \beta(L-q)] \quad (14)$$

The Lassette treatment is applicable to continuous association, and equations 9, 10 and 11 enable one to distinguish readily between limited and continuous association. Lassette gave examples of the use of the above equations and their applicability to the data of the present work will be illustrated.

Method of Dunken.—Dunken^{28,29} considers three situations: (1) only one polymer is formed, and

$$K_{1L} = \left[\frac{(L-1)f}{Q} \right]^{L-1} \times \frac{f-1}{(L-f)^L} \quad (15)$$

(2) continuous association occurs with polymers of all orders formed with equal ease, and

$$K_{12} = \frac{f(f-1)}{Q} = K_{23} = K_{34} = \dots K_{(L-1)L} \quad (16)$$

(3) continuous association occurs with polymers of all orders present simultaneously, though in this case the tendency to associate is not independent of the order of the polymers involved. Two different situations can be imagined here: one in which the higher polymers are favored and the association factor increases rapidly, apparently without limit, and one in which the lower polymers are favored so that the association factor does level off to a limit as the concentration increases. From equations 3 and 4

$$f = \frac{Q}{N} = \frac{n_1 + 2K_{12}(n_1)^2 + 3K_{13}(n_1)^3 \dots LK_{1L}(n_1)^L}{n_1 + K_{12}(n_1)^2 + K_{13}(n_1)^3 \dots K_{1L}(n_1)^L} \quad (17)$$

(26) E. N. Lassette, *Chem. Revs.*, **23**, 259 (1937).

(27) E. N. Lassette, *J. Am. Chem. Soc.*, **59**, 1383 (1937).

(28) H. Dunken, *Z. physik. Chem.*, **45B**, 201 (1940).

(29) K. L. Wolf, H. Dunken and K. Merkel, *ibid.*, **46B**, 287 (1940).

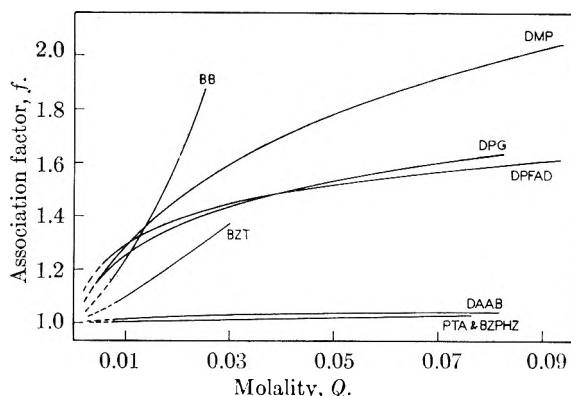


Fig. 3.—Composite plot of the association curves.

Dunken uses equation 15 to evaluate K_{12} at values of f near unity, and extrapolates to infinite dilution. The extrapolated value of K_{12} can then be introduced into equation 17, thereby reducing the number of unknowns by one. The next step is to assume values for n_1 and K_{13} , and K_{13} is found by trial and error. Illustrations of the application of the above equations are given in the papers of Dunken²⁸ and in a more recent review article.³⁰ If the calculation from equation 17 involves only K_{12} and K_{13} the method of successive approximations is not too laborious. A similar extrapolation method has been used recently for the vapor phase association of butyric acid³¹ in which dimers and trimers are formed, and by Coggeshall and Saier.³²

Method of Bjerrum.—Bjerrum³³ has calculated n_1 (which corresponds to the ligand in the complexing of ions) from f , N and Q by solving equation 8 for $d \ln n_1$ and integrating

$$\ln n_1 = \int_{N=n_1}^N \frac{1}{Q} dN = \int_{f=1}^f \frac{1}{Q} d\left(\frac{Q}{f}\right) \quad (18)$$

In the limit $Q = N$ as $f \rightarrow 1$ an integration can be carried out graphically or numerically using Simpson's formula. For a precise calculation it is necessary to know f at values not much greater than unity. With n_1 known for various values of f and Q , the association constants can be calculated by equation 17. The general applicability of this method has been shown. The weakest link in this method is the determination of a value of n_1 to use as the initial point, but we get approximate values of K and adjust the value for n_1 by successive approximations. Once n_1 is known the K 's can be determined by the method of Fronaeus³⁴ from the relationship

$$F(n_1) = \frac{N/n_1 - 1}{n_1} = K_{12} + K_{13}(n_1) + \dots \quad (19)$$

and if $F(n_1)$ be plotted *vs.* n_1 the intercept will be K_{12} and the slope of the curve where $n_1 \rightarrow 0$ will be K_{13} . When K_{12} is known K_{14} can be evaluated, etc.

Calculation of Equilibrium Constants

2-*n*-Butylbenzimidazole.—For all three methods of calculation the data must be consistent and ac-

(30) K. L. Wolf and R. Wolff, *Angew. Chem.*, **61**, 191 (1949).

(31) R. E. Lundin, F. E. Harris and L. K. Nash, *J. Am. Chem. Soc.*, **74**, 743 (1952).

(32) N. D. Coggeshall and E. L. Saier, *ibid.*, **73**, 5414 (1951).

(33) J. Bjerrum, *Kem. Maanedssblad*, **24**, 21 (1943).

(34) S. Fronaeus, Dissertation, "Komplexsystem hos Koppar," Lund, 1948.

TABLE X
ASSOCIATION CONSTANTS FOR 2-*n*-BUTYLBENZIMIDAZOLE IN BENZENE

Constant	Lassette series ($\alpha = 57.1 \pm 0.4$ ($\beta = -42.4 \pm 0.4$)	Dunken series (Succ. Approx.)	Bjerrum-Fronaues series
K_{12}	14.8 ± 0.6	16.0 ± 0.5	15 ± 1
K_{13}	640	770 ± 80	800 ± 100
K_{14}	36,000	$33,000 \pm 7,000$	$40,000 \pm 20,000$
K_{15}	2.3×10^6	$2.5 \pm 0.5 \times 10^6$	5×10^6 to 50%
K_{16}	1.5×10^8	$1.7 \pm 0.5 \times 10^8$	2×10^8 to 50%
K_{17}	1.1×10^{10}	$1.3 \pm 0.2 \times 10^{10}$	1.5×10^{10} to 50%
K_{18}	8.1×10^{11}	$8 \pm 1.5 \times 10^{11}$	12×10^{11} to 50%
K_{19}	6.2×10^{13}	$6 \pm 1 \times 10^{13}$	Limit of method

curate in the dilute range. Since the experimental data are not reliable below 0.005 *M* it is necessary to fit the association curve with an algebraic equation whenever possible and extrapolate to a more dilute range. For the data of Table II for 2-*n*-butylbenzimidazole, this took the form $f = 1 + aQ + bQ^2$. For the Lassette treatment, equation 11 is applicable as shown by the linearity of a plot of $f(f - 1)/Q$ versus f in Fig. 4 since

$$\frac{f(f - 1)}{Q} = \beta + \alpha f \text{ from eq. 11}$$

With α and β known the equilibrium constants for what must be a continuous type of association are evaluated from equation 14 and given in Table X. Equation 17 of the Dunken procedure is applicable and K_{12} is evaluated by equation 15 and plotted against Q as shown in Fig. 5. With K_{12} evaluated, K_{13} , etc., were found by successive approximations and are given in Table X. The values of n_1 were also determined by graphical integration of equation 18 and the equilibrium constants evaluated by equation 19 and the results tabulated in Table X.

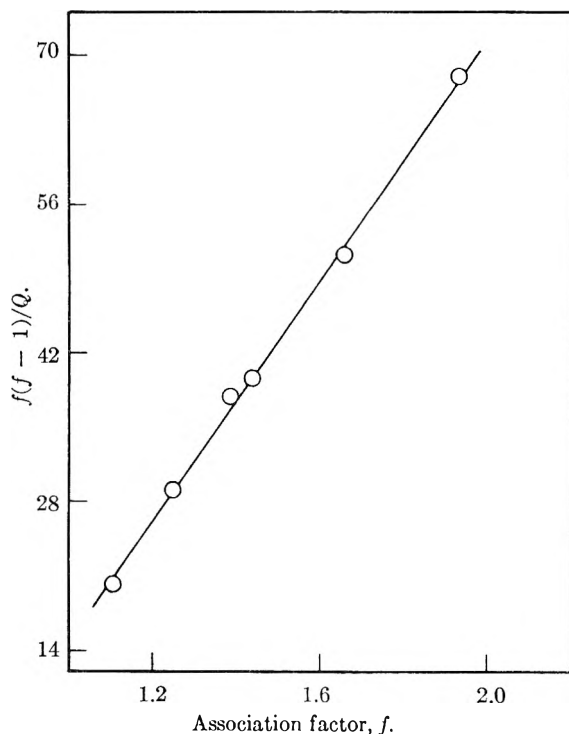


Fig. 4.—Lassette plot of the experimental points for BB.

All three methods give essentially the same values and the agreement is shown by the graph (Fig. 6) of f vs. $\log n_1$ where the smoother curve from the calculation by the Bjerrum method is compared with the experimental points for f with n_1 calculated from the K 's found by the Lassette or Dunken procedure.

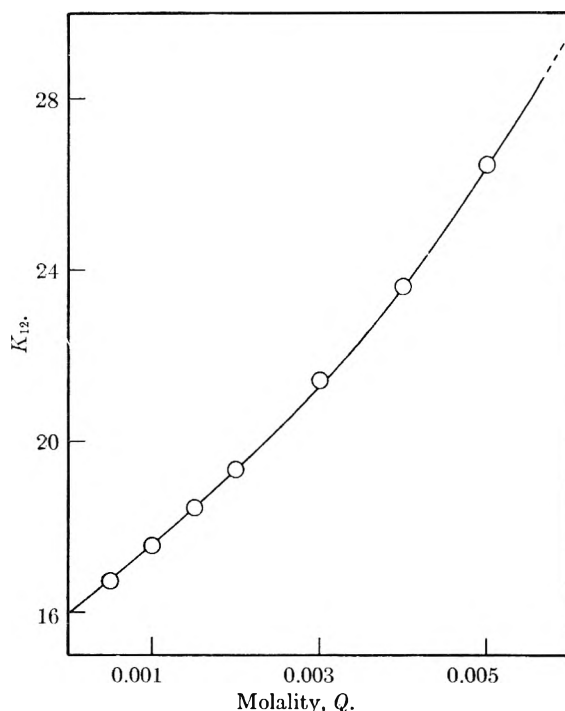


Fig. 5.—Dunken plot of derived points for BB to evaluate K_{12} by extrapolation to $Q = 0$.

The number of association constants which are significant and can properly be quoted at any concentration is determined by the concentration of the corresponding associates in comparison with the uncertainty of the over-all concentration at that point. For example, if we take the A.D. of the least square smoothed curve through the original data as representing the probable error of f , and N calculated from it, then at 0.02 molal the uncertainty of f is 0.003 unit in 1.611. Since $N = Q/f$ the uncertainty of N is also 0.18% or 0.000023 unit. In the Dunken method of calculation the concentration of undecamers is 0.000024 which is larger than the uncertainty of N while the concentration of dodecamers is 0.000018 which is less than the uncertainty of N . Hence it appears that all constants up to K_{111} are meaningful at $Q = 0.02$. Simi-

TABLE XI
ASSOCIATION CONSTANTS FOR BENZOTRIAZOLE IN BENZENE

Constant	Lassette procedure		Dunken procedure (Succ. Approx.)	Bjerrum-Fronaeus procedure
	($\alpha = 13.9 \pm 0.8$ ($\beta = 3$))	($\alpha = 20.4 \pm 0.2$ ($\beta = -11.1 \pm 0.2$))		
K_{12}	13.9 ± 0.8	9.3 ± 0.3	7.0 ± 0.5	8.5 ± 0.5
K_{13}	300	180	220 ± 20	195 ± 15
K_{14}	7000	4400	7000 ± 3000	$2400 \pm 50\%$
K_{15}	2×10^5	1.2×10^5	$9 \pm 4 \times 10^4$	$3 \times 10^5 \pm 50\%$

larly at 0.01 molal constants through K_{16} are significant.

However, in the use of successive approximations, especially if they are made graphically, the errors are obviously magnified and numerical values given for the higher order constants cannot be taken too seriously. All values for the equilibrium constants for the lower orders have been reduced to two significant figures after calculation, as this represents the order of precision.

Benzotriazole.—Table XI gives the comparison of the equilibrium constants calculated in similar fashion. In this case the analysis was somewhat more troublesome which may be due to experimental difficulties in obtaining the data. Here again we appear to be dealing with continuous association with the tendency to associate increasing as the degree of association increases.

N,N'-Diphenylguanidine.—The inapplicability of equations 9, 10 and 11 indicates that we are not dealing with a continuous type of association and this case is a good illustration of the use of the Lassette procedure, which enables one to distinguish between a limited and a continuous type of association. The Dunken and Bjerrum-Fronaeus procedures both indicate that the data can be satisfactorily represented with only dimers and trimers. Table XII gives the equilibrium constants evaluated by the two methods.

TABLE XII
THE EQUILIBRIUM CONSTANTS FOR
N,N'-DIPHENYLGUANIDINE

Constant	Dunken	Bjerrum-Fronaeus
K_{12}	52.5 ± 1	53.7
K_{13}	290 ± 20	350

N,N'-Diphenylformamidine.—Here again the Lassette procedure is not applicable and we are dealing with limited association. The analysis shows that the data can be represented within the accuracy of the measurements on the basis of $K_{12} = 69.1$ or 68.7 by the other two methods. Roberts¹⁷ has determined the molecular weight of DPFAD in benzene by the freezing point method, using the usual Beckmann technique, and an analysis of his data also indicates dimers, but with a lower value of K_{12} of 19.

3,5-Dimethylpyrazole.—This is also a case of limited association and the Dunken procedure indicates that the data can be reasonably well fitted on the basis of trimers alone with $K_{13} = 2280$ while the Bjerrum-Fronaeus procedure indicates dimers and trimers with $K_{12} = 2.45$ and $K_{13} = 2500$.

Diazoaminobenzene.—This compound proved to be but slightly associated, the increase in f at the

highest concentration used (0.08 m) being only 4%. However, the data yield a value of K_{12} between 0.52 and 0.54 and this is not in disagreement with the experimental data of Hunter²⁰ in the same solvent.

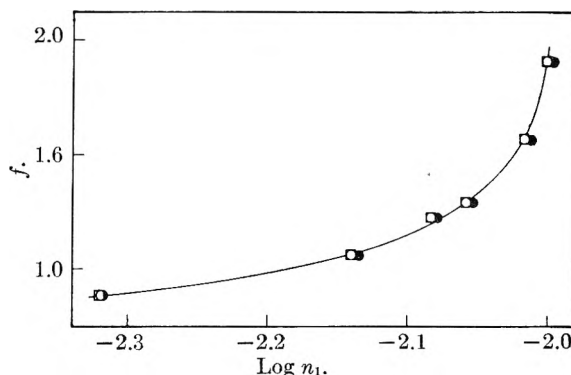


Fig. 6.—BB in benzene, showing agreement for n_1 from each of the three methods at the experimental points. Curve drawn from Bjerrum's n_1 's: O, Bjerrum (graphical integration); ●, Lassette (from α & β); □, Dunken (succ. approx.).

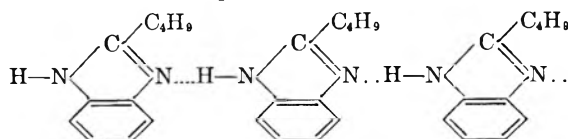
Benzaldehyde Phenylhydrazone.—The slight association in this case also makes the analysis impractical but the Lassette treatment favors continuous association if the results can be interpreted as reliable in view of the experimental difficulties due to oxidation. Runs in which oxidation was evident yielded higher association factors than the one reported in Table VIII where oxidation was at a minimum.

N-Phenyl-N'-p-tolylacetamidine.—The small association of this compound limits drastically the reliability of any conclusions, but the Lassette treatment (using equation 9) seems to indicate continuous association with K_{12} about 0.4 and smaller constants for the higher orders.

The results of the analyses are summarized in Table XIII.

Discussion of Results

BB.—For 2-*n*-butylbenzimidazole a possible linear association complex can be formulated as



BZT.—Benzotriazole is believed to be a resonance hybrid of three tautomeric structures.

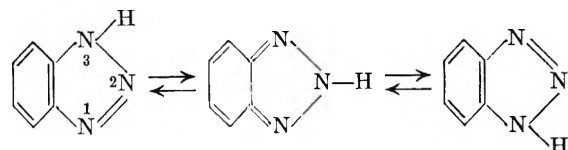
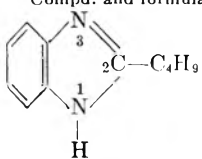
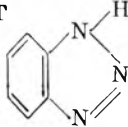
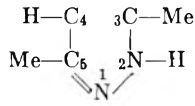
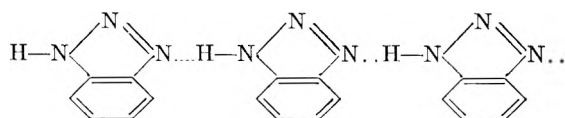


TABLE XIII
SUMMARY OF THE EQUILIBRIUM CONSTANT ANALYSIS OF THE ASSOCIATION OF EIGHT COMPOUNDS IN BENZENE

Compd. and formula	Degree of assn.	Lassette treatment	Dunken treatment	Bjerrum-Fronaeus treatment	Type of assn. and order of polymers	Type of polymer indicated
BB 	High	K 's from α and β ; $\frac{f(f-1)}{Q}$ vs. f Plot	K 's by successive approx.	First 3 K 's by extrapoln.; rest from simultaneous eq. or by difference	Continuous; all orders	Linear
BZT 	High	K 's from α and β ; $\frac{f(f-1)}{Q}$ vs. f Plot	K 's by successive approx.	As for BB above	Continuous; all orders	Linear
DPG PhHN—C(NH ₂)=NPh	High	Non-applicable	Only K_{12} and K_{13} involved	Fronaeus plot of $F(n_1)$ vs. n_1 indicates only K_{12} and K_{13}	Limited; 2 orders only	Linear dimers and cyclic trimers
DPFAD PhN=CH=NPh	High	Non-applicable	K_{12} is constant	Fronaeus function $F(n_1) = \text{constant} = K_{12}$	Limited; 1 order only	Cyclic dimers
DMP 	High	Non-applicable	K_{13} is very nearly constant	Fronaeus plot of $F(n_1)$ vs. n_1 shows K_{12} and K_{13}	Limited; 2 orders only	Linear (?) dimers and cyclic trimers
DAAB PhN=N—NPh	Slight	Non-applicable	K_{12} levels off to a constant	Seems to give only K_{12} , but of doubtful reliability	Limited; 1 order only	Cyclic dimers
PTA PhN=C(CH ₃)NHC ₆ H ₄ CH ₃	Slight	K 's from α ; f vs. Q plot	Not carried out—impracticable	Seems to give only K_{12} , but of doubtful reliability	Continuous; all orders	Linear
BZPHZ PhCH=N—NPh	Slight	K 's from α ; f vs. Q plot	Not carried out—impracticable	Seems to give only K_{12} , but of doubtful reliability	Continuous; all orders	Linear

The first and third structures shown are equivalent, of course, and as a result the characteristics of this structure probably predominate. Accordingly, linear polymers from 1,3-association seem most likely as

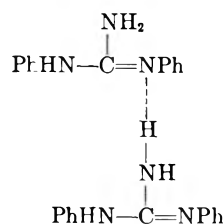


A 1,2-linear association cannot be entirely excluded, however.

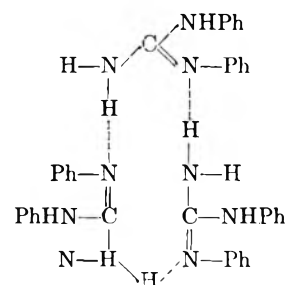
Hunter³⁵ states that almost strainless models can be made for cyclic dimers from 1,2-association, and cyclic trimers from 1,3-association. The association data and its analysis appear to rule out the possibility that these two polymers are formed exclusively, either separately or in combination, but whether they may be formed at first, then unfold to form a larger linear polymer as the concentration increases, a study of equilibrium constants cannot say.

DPG.—The evidence indicates that the association complexes are a mixture of dimers and trimers

only, so we have the problem of explaining how and why these are the only two formed. Reasonable structures can be formulated for both linear and cyclic polymers and in this case it seems likely that we have both: a linear dimer and a cyclic trimer. At least this assumption affords the simplest explanation of the presence of the polymers; a linear dimer is formed at first but as soon as it adds another unit molecule with increasing concentration, becoming a trimer, it closes ends to form the more stable cyclic structure so that the association would be effectively stopped. Possible structural formulas for each of these polymers are



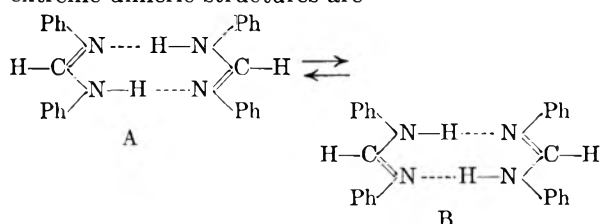
Linear dimer



Cyclic trimer

It should be noted, however, that a cyclic dimer would have an 8-membered ring of which two would be hydrogen atoms. Since the H-bond is believed to have a 180° valence angle, the ring would in effect be reduced to six members which should be a more stable structure. Ordinarily it would be expected that a dimer containing a 6-membered ring structure would be formed in preference to a linear dimer, so our assumption above of a linear dimer must be considered tentative.

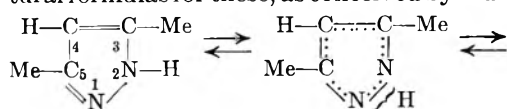
DPFAD.—Since our analysis indicates that only dimers are formed in both solvents, they have in all probability a cyclic structure. Either of the two extreme tautomeric structures of DPFAD could lead to a cyclic dimer presumably and, in fact, a resonance hybrid of both would be the expected state of affairs in the solution. The two extreme dimeric structures are



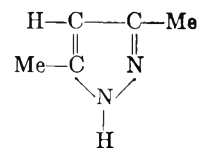
This should be an especially stable dimer since it has an 8-membered ring structure of which the two hydrogens with presumably 180° valence bonds reduce it in effect to a 6-membered ring. DPFAD is, of course, the ammonia analog of formic acid which is known to form a very stable dimeric polymer; the above structures exactly parallel those usually written for the latter.

The foregoing structures for the polymers of this compound afford an especially clear example of Hunter's mesohydric tautomerism and its relationship to H-bond association. If the dimer A breaks up into monomers (and we must for purposes of discussion talk as though each extreme structure is actually present) we obtain one tautomer, while if it is the B dimer which breaks apart we obtain the other tautomer. The necessary transfer of a proton from one nitrogen to the other within the molecule to effect the tautomerization is seen to result directly from H-bond association which Hunter suggests is always the case, and is in fact the mechanism of the tautomerization. Obviously, if the substituted groups on the two nitrogens are alike, the two nitrogen atoms and the two tautomers become exactly equivalent as in this example. If the substituted groups differ, then no such equivalence is possible. It is also clear that if all of the hydrogens of the amino- and imino-groups are substituted away, then no H-bond association and no tautomerization can take place; the two are found to disappear together.

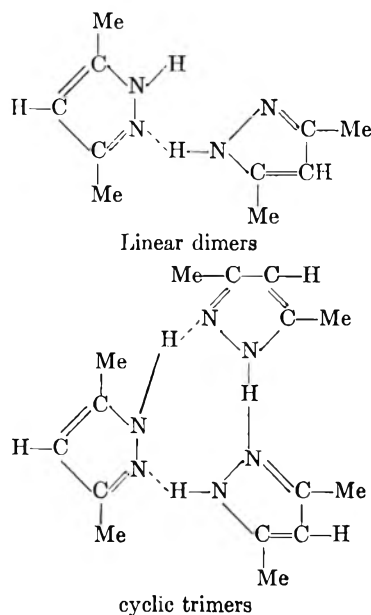
DMP.—The tautomerism of DMP can be represented by two extreme structures, the resonance hybrid of which partakes of the structure of both. Structural formulas for these, as conceived by Hunter³⁶ are



(36) L. Hunter and H. T. Hayes, *J. Chem. Soc.*, 1 (1941).



From either of the above extreme structures, plausible structures for both dimers and trimers can be formulated. The trimers are almost certainly cyclic while the dimers, which are present in such small concentrations as to suggest that they are of only temporary existence—on their way to becoming trimers, are probably linear. Possible structures for each are



It is seen that cyclic trimers are held together by a 9-membered ring which includes three hydrogen atoms. With 180° H-bonds, the ring is, in effect, hexagonal—which would seem to be a stable and therefore preferred structure. Consequently a cyclic trimer appears very likely. This, of course, accords with our conclusions from the equilibrium constant analysis.

A cyclic dimer would have only a 6-membered ring which, since two are hydrogen atoms, would be in effect a 4-membered, and therefore less stable, ring.

If one regards the solvent as inert, the association reaction may be considered analogous to the autoprotolysis of an acid in a medium of low dielectric constant where the resulting addition compound does not dissociate and the proton is not completely transferred. As higher associates are formed, the acidity of one associate taking part in the reaction is decreased or increased, while the acidity of the monomer remains the same. Since the protons are not actually transferred one should not expect to find a simple quantitative relationship between acidity and polymerization. However the effect of the formation of associates should not have much effect after three or four additions of a monomer and we might find that all polymers beyond a certain order would be formed with equal ease from the next lower one by the simple addition of a monomer, *i.e.*, $A_{L-1} + A \rightleftharpoons A_L$ with only one $K =$

TABLE XIV

AGREEMENT OF EXPERIMENTAL AND CALCULATED f 's USING ONLY K_{12} , K_{13} , K_{14} AND K FOR 2-*n*-BUTYLBENZIMIDAZOLE IN BENZENE

Molality Q	Exptl. f (incl. est. error)	$K = 49.5$	Caled. f , with Lassettre K 's		Dunken K 's
			$K_{12} = 14.8$	$K_{13} = 640$	
0.00583	1.107 ± 0.021	1.120	1.108	1.116	1.116
.01070	1.251 ± .012	1.288	1.244	1.253	1.253
.01408	1.385 ± .010	1.411	1.349	1.364	1.364
.01586	1.438 ± .010	1.487	1.427	1.438	1.438
.02119	1.657 ± .010	1.655	1.647	1.664	1.664
.02635	1.930 ± .010	1.738	1.87	1.83	1.83
	Av. difference = 3.3%		1.3%	1.4%	1.4%

$K_{(L-1)L}$ rather than directly from monomers, *i.e.*, $LA \rightleftharpoons A_L$ each with a separate K_{1L} .

To test this alternative approach to the association equilibria, we make use of an equation for f first set down by Bjerrum and used by him in his discussion of the association of the alcohols.³³

$$f = \frac{\left(\frac{1}{1 - Kn_1}\right) + 2(K_{12} - K)n_1 + 3(K_{13} - K^2)(n_1)^2 + \dots}{\left(\frac{1}{1 - Kn_1}\right) + (K_{12} - K)n_1 + (K_{13} - K^2)(n_1)^2 + \dots}$$

in which K is the desired over-all association constant, and K_{12} , K_{13} , etc., have their usual meaning.

It may be remarked that the proposed alternative treatment of the association equilibria of BB which is embodied in Bjerrum's equation above has also been used in its essence in several instances in the past by other investigators. For example, Coggeshall and Saier³² found a K_{12} for dimers and an over-all K for the remaining higher polymers satisfactory for several phenols and higher alcohols in CCl_4 ; Kreuzer and Mecke^{37,38} found that an over-all K represents the association of several of the lower alcohols (except MeOH), also in CCl_4 , provided $K_{12} = 0$,—an unusual situation but one also encountered by Bjerrum³³ in reviewing similar data in cyclohexane; and Briegleb³⁹ used individual K_{1L} 's for the first few polymers in HF vapor and an over-all K for the higher orders. The assumption that the stepwise growth and degradation of all polymers larger than those of the first few orders by the addition or loss of another monomer can all be represented by a single equilibrium constant is also basic to Flory's⁴⁰ treatment of the polymerization equilibria of the higher polymers.

The only question remaining now is just how large the polymers must be before it can be assumed that each subsequent addition of another monomer takes place with equal ease, *i.e.*, that a single K applies to each reaction equally well. In other words, how many individual K_{1L} 's must be kept for the low-ordered polymers before an over-all K can be determined for all the higher orders. In the examples above, the over-all K applied from trimers up in the case of the phenols and alcohols, but not until pentamers were reached in the case of HF. One possible source of assistance in making the decision in our case is the knowledge that cer-

tain of the properties—those which do not depend on molecular weight—of successive members of a homologous series of organic compounds undergo little change upon the addition of another CH_2 group once the chain has grown to a 3 or 4 carbon length, *e.g.*, the ionization constants of the normal straight-chain carboxylic acids are practically constant from propionic acid on up, and in this case it has been shown there is a rough parallelism between the ionization constant of the acid and its association constant for dimers.⁵

In accordance with the Lassettre treatment both the consecutive constant and the average constant increase with increasing order L since $L! > (L-1)!$ If we take the $(L-1)$ th root of the association constants in column two of Table X, the average K increases from 39 for pentamers 53 for nonamers and if we extend the calculation to the limit of significant constants the 14th root of K_{115} is 63. The corresponding consecutive constants $K_{1L}/K_{1(L-1)}$ go from 64 to 76 and begin leveling off at 82. Calculations show that the best agreement with the experimental data is given by an average constant of $K = 49.5$ beyond tetramers but the average difference is twice as great as that given by the Lassettre or Dunken treatments using 15 constants. Table XIV presents the comparison.

It is to be noted that these combinations of K 's and the Bjerrum equation give high results at low concentrations and low results at high concentrations.

This treatment of the data to reduce the number of K 's involved is not nearly so satisfactory as the Lassettre, or the Dunken, treatment from the standpoint of reproducing the experimental data. On the whole, the authors favor the original Lassettre and Dunken treatments of the association data, especially the former, because of the better agreement with experiment for these two series of K 's. Whatever the order of the polymers, an association constant for them does exist and fortunately the Lassettre treatment makes its calculation a simple matter. Moreover, for this case of BB in benzene, the Lassettre treatment of the data clearly shows that the various $K_{(L-1)L}$ equilibrium constants are not quite independent of the order of the polymers, *i.e.*, independent of L , at least not until the polymers contain some 12 or 14 units molecules, so that finding a value for this K which will apply equally well to all polymers larger than tetramers, is at best a compromise and cannot possibly describe the equilibria as well as the individual K 's will do.

(37) J. Kreuzer and R. Mecke, *Z. physik. Chem.*, **49B**, 309 (1941).(38) R. Mecke, *Disc. Faraday Soc.*, **9**, 161 (1950).(39) G. Briegleb, *Z. physik. Chem.*, **51B**, 9 (1941); **52B**, 368 (1942); **53B**, 225 (1943).(40) P. J. Flory, *J. Chem. Phys.*, **12**, 425 (1944); **14**, 49 (1946).

In the above discussion we have assumed along with others that benzene is an inert solvent in spite of the gradual accumulation of evidence to the contrary.^{41,42}

To the extent that H-bonding with the solvent occurs, not only will the degree of association of the solute be less but, more importantly, both solvation and orientation of the solvent molecules about the solute will affect the entropy of the system in a more complicated manner.

The low solubility of benzimidazole in benzene is probably due to its high degree of association in the solid state but few structures of crystals involving N—H—N bonding have been reported.⁴³

(41) L. A. K. Staveley, I. H. E. Jeffes and J. A. E. Moy, *Trans. Faraday Soc.*, **39**, 5 (1943).

(42) M. Vipatrick and F. E. Luborsky, *J. Am. Chem. Soc.*, **75**, 577 (1953).

(43) J. Donohue, *ibid.*, **56**, 502 (1952).

It is of interest that *syn-p*-chlorobenzaldoxime forms dimers⁴⁴ while *anti-p*-chlorobenzaldoxime shows continuous polymerization in the solid state.⁴⁵

Acknowledgments.—The authors wish to thank the Allied Chemical and Dye Corporation for the award of a fellowship to the junior author (N.E.W.) in 1945–1946. Thanks are also due to Prof. Jannik Bjerrum of the University of Copenhagen and Dr. Kristian Højendahl of the Royal Veterinary and Agricultural College, Copenhagen, Denmark, for the benefit of critical discussions. The senior author would also like to express his appreciation of the kindness of Prof. Axel Tovborg-Jensen of the latter institution in providing facilities during his visit as Fulbright research scholar in 1953.

(44) B. Jerslev, *Nature*, **166**, 741 (1950).

(45) B. Jerslev, private communication.

TESTS OF A SIMPLIFIED GENERAL MODEL FOR ADSORPTION OF RARE GASES ON SOLIDS¹

By J. G. ASTON, R. J. TYKODI AND W. A. STEELE

Contribution from the College of Chemistry and Physics of The Pennsylvania State University, University Park, Pa.

Received April 28, 1955

A model of a heterogeneous surface with five types of sites is considered. On the basis of this model the thermodynamic properties, including the isotherms, have been deduced for helium, neon and argon adsorbed on titanium dioxide. The results are compared with the experimental data.

Introduction

In the study of the adsorption of gases on solids, the trend has been to give more and more attention to the energetic heterogeneity of the adsorbent surface.^{2–5} Numerous attempts have been made to interpret experimental results in terms of site distribution functions which were arbitrarily picked so as to give best agreement with experiment.^{2a,6} These attempts have been complicated by the presence of lateral interaction at moderate coverages. In this paper, a simple site distribution was assumed in order to explain the results of some experiments on the adsorption of helium on titanium dioxide at various temperatures. In this case, the magnitudes of the heats involved (600–200 cal. per mole for the heat of adsorption compared to 20 cal. per mole for the heat of vaporization) make it reasonable to assume that lateral interaction is negligible for coverages less than the B.E.T. monolayer; thus one can safely apply the simple theory developed here. In addition, the adsorption of neon and argon on similar samples of titanium dioxide is interpreted in terms of the theory, and the deviations from it are discussed.

(1) This research was carried out under Contract N6 ONR-269 Task Order X of the Office of Naval Research and Contract DA-36-061-ORD-403 of the Office of Ordnance Research.

(2) (a) G. D. Halsey and H. S. Taylor, *J. Chem. Phys.*, **15**, 624 (1947); (b) G. D. Halsey, *ibid.*, **16**, 931 (1948).

(3) T. L. Hill, *ibid.*, **17**, 762 (1949).

(4) F. C. Tompkins, *Trans. Faraday Soc.*, **46**, 569 (1950).

(5) G. D. Halsey, *J. Am. Chem. Soc.*, **73**, 2693 (1951).

(6) L. E. Drain and J. A. Morrison, *Trans. Faraday Soc.*, **48**, 316 (1952).

Theory

1. Isotherms.—By straightforward statistical mechanical considerations it can be shown^{3,7} that for localized adsorption of N molecules on Z sites, of which Z_i have energy (more strictly a free energy) of adsorption $-\epsilon_i$ relative to the gas state at infinite dilution,⁸ the isotherm equation for monolayer adsorption is

$$\theta = \sum_i F_i / [1 + \lambda^{-1} \exp(-\epsilon_i/kT)] \quad (1.1)$$

where $\theta = N/Z$, $F_i = Z_i/Z$, and

$$\lambda = ph^3/kT(2\pi mkT)^{3/2}j(T) = p/f(T)$$

$j(T)$ being the internal partition function for a gas molecule.

For multilayer adsorption, subject to the B.E.T. postulates,⁷ the appropriate expression is

$$\theta = \sum_i c_i X F_i / (1 + c_i X - X)(1 - X) = \sum_i F_i \theta_i \quad (1.2)$$

where $X = p/p_0$, p_0 is the vapor pressure of the liquid, $c_i = \exp(\epsilon_i - \epsilon_0)/kT$, and $-\epsilon_0$ is the energy (or more strictly free energy) per molecule of the bulk liquid.

2. Distribution Function.—Honig and Rosenbloom⁹ have shown that a real site distribution

(7) N. L. Balazs, *Physica*, **17**, 865 (1951).

(8) Since the vibrational energy of the adsorbed molecule is not specifically considered, the site energies are really site free energies. See Appendix.

(9) J. M. Honig and P. C. Rosenbloom, Symposium on "Problems Relating to the Adsorption of Gases on Solids," Kingston, Ont., Sept. 10–11, 1954 (to be published in *Can. J. Chem.*).

function (which should be nearly continuous) can be decomposed into a finite number of sets of sites in such a way that, for adsorption limited to the monolayer, the discontinuous distribution will yield isotherms which bound the isotherm based on the actual nearly continuous distribution. Thus a quite simple distribution was chosen: namely, that the surface of the adsorbent could be characterized by five discrete sets of sites,¹⁰ with energy determined by topographic location. The energy of adsorption on a site in the i 'th set was taken to be $-i\epsilon$ (one would guess that helium occupying the place of an atom missing from the surface would have an energy of adsorption close to five times that of an atom adsorbed on the flat surface.)

The distribution function was assumed to have the form

$$Z_i = aw_i \exp(-iy) \quad (2.1)$$

where $w_i = 1, 4, 6, 4, 1$ for $i = 1, 2, 3, 4, 5$ and $y = \epsilon/kT$. We hasten to add that any or all of the integers could equally well be irrational. The relative values of w_i are perhaps to a small extent dictated by physical intuition. The energy of adsorption on this surface is thus assumed to have finite upper and lower limits, in contrast to other treatments of this problem.^{2a,11}

Equations 1.1 and 1.2 now become

Monolayer

$$\theta = \sum_{i=1}^5 F_i / [1 + p^{-i} f(T) \exp(-i\epsilon/kT)] \quad (2.2)$$

Multilayer

$$\theta = \sum_{i=1}^5 F_i c_i X / (1 + c_i X - X)(1 - X) \quad (2.3)$$

3. Molar Thermodynamic Quantities.—In transforming from extensive quantity per molecule to extensive quantity per mole the following relations were used:

$$-\epsilon/k = (\bar{E}_n - \bar{E}_{gas})/R = \Delta E/R \quad (3.1)$$

$$\bar{H}_n \cong \bar{E}_n \quad (3.2)$$

$$\bar{H}_{gas} \cong \bar{E}_{gas} + RT \quad (3.3)$$

$$\Delta \bar{H} \cong \Delta \bar{E} - RT \quad (3.4)$$

where the wavy bars refer to molar properties.

For localized adsorption without lateral interaction, the integral heat of adsorption \bar{Q} (cal./mole) is given by

Monolayer

$$\bar{Q} = -N^{-1} \sum_{i=1}^5 iN_i \Delta \bar{H} \quad (3.5)$$

Multilayer

$$\bar{Q} = -N^{-1} (N_0 \Delta \bar{H}_0 + \sum_{i=1}^5 iN_i \Delta \bar{H}) \quad (3.6)$$

where $\Delta \bar{H}_0$ is the molar heat of liquefaction of the bulk liquid, N_0 is the number of molecules with energy $-\epsilon_0$ and N_i is the number with energy $-\epsilon_i$.

Similarly, the isosteric heat of adsorption q_{st} is given by

(10) It was later discovered that the contribution of the two sets of sites of largest energy was quite small; thus, a simpler distribution function having only the lower three sets of sites in it will give almost as good an approximation as the more complicated one used here.

(11) R. Sips, *J. Chem. Phys.*, **16**, 490 (1948).

$$q_{st} = \left(\frac{\partial \bar{Q}}{\partial N} \right)_T = \bar{Q} + N \left(\frac{\partial \bar{Q}}{\partial N} \right)_T \quad (3.7)$$

Application

The five-site model was used to correlate data obtained for the adsorption of helium, neon and argon on titanium dioxide. There are two adjustable parameters remaining in the model: ϵ and V_m . However, the V_m 's for each of the systems considered should be the same, if the number of sites per unit area remains the same for each gas and sample of solid. Furthermore, if the adsorption, in these cases, is due only to van der Waals interaction between gas and solid, ϵ should be roughly equal to the van der Waals interaction of a single gas atom with the planar surface. This quantity can be estimated by a number of alternate methods which will be further discussed below. The occurrence of high energy sites is thus tacitly assumed to be due to the presence of cracks and surface roughness where the adsorbed molecule has more adsorbent nearest neighbors than on a flat surface.

In each case, the area of the sample was determined by the B.E.T. nitrogen method, and the amount of gas adsorbed was expressed in units of cubic centimeters of gas adsorbed, at standard conditions of temperature and pressure, per square meter of adsorbent surface (cc./m.²—STP). Then $\theta = V_a/V_m$, where V_m is the monolayer capacity and V_a is the amount adsorbed.

Helium-Titanium Dioxide.—The adsorption of helium on titanium dioxide had been studied by Mastrangelo and Aston¹² and also by Aston, Mastrangelo and Tykodi.¹³ The model was fitted to isotherms taken at 4.17, 13.96 and 20.28°K., and also to a heat of adsorption curve measured at 17.1°K. The fit of the model to the data is shown in Figs. 1 and 2. The following values were chosen for the parameters: $\Delta E = -180$ cal./mole, $V_m = 0.38$ cc./m.²—STP. Above the helium critical temperature, the monolayer form was used (eq. 2.2). For the 4.17° isotherm, it was found necessary to introduce two layers of sites with energies greater than ΔE_0 (energy of liquefaction) due to the large value of ΔE relative to ΔE_0 . If we assume that the site energies decay according to the cube of the distance from the surface,¹⁴ the site energies in the second layer will have practically the same distribution, but with ΔE reduced by a factor of eight. For the 4.17° isotherm, at pressures greater than 0.10 mm., the first layer was found to be full and the second and higher layers were calculated from eq. 2.3, using $\Delta E = 22$ cal./mole. In Fig. 1, the isotherm predicted by this calculation is shown by curve b. Curve a is the isotherm predicted by the B.E.T. equation, with V_m (B.E.T.) = 0.56 cc./m.²—STP. At high coverages, the experimental curve falls considerably below the curve predicted by the model (a fairly common failing of the B.E.T. theory).

(12) S. V. R. Mastrangelo and J. G. Aston, *ibid.*, **19**, 1067 (1951).

(13) J. G. Aston, S. V. R. Mastrangelo and R. J. Tykodi, *ibid.*, in press.

(14) (a) W. M. Champion and G. D. Halsey, *THIS JOURNAL*, **57**, 646 (1953); (b) L. Meyer, *Phys. Rev.*, **97**, 22 (1955).

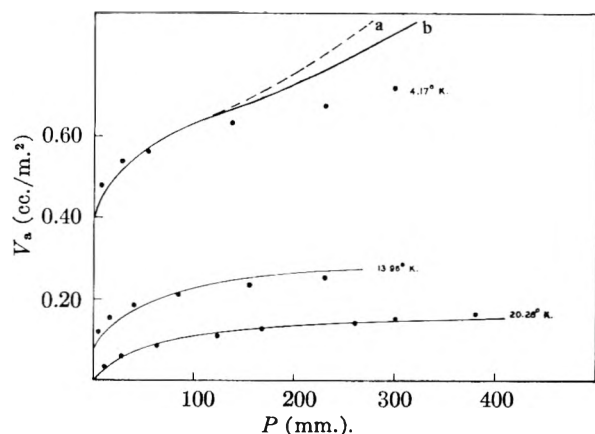


Fig. 1.—Isotherms of helium on titanium dioxide. Circles are experimental points, curves are constructed from the model. Curve a is given by the ordinary B.E.T. equation, and curve b, by the multilayer equation (eq. 2.3) with an extra layer of helium preadsorbed (see text).

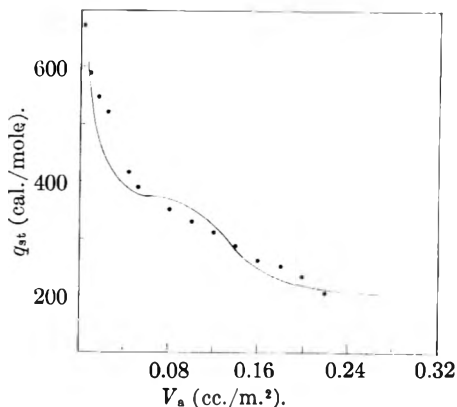


Fig. 2.—Heats of adsorption of helium on titanium dioxide. The curve is calculated from the model. The experimental points (partly calorimetric heats and partly isosteric) were determined at 17.1°K.

Neon-Titanium Dioxide.—The neon system has been studied by Tykodi, Aston and Schreiner.¹⁵ The model was compared to isotherms taken at 30.00°K. and 45.93°K., and to the heats of adsorption at 30.0°K. The fit is shown in Figs. 3 and 4. The parameters chosen to fit the model to experiment were $\Delta E = -600$ cal./mole, $V_m = 0.46$ cc./m.² STP. For the calculations at 30.00°, the multilayer equation was used; for those at 45.93°, the monolayer form was used (the critical temperature of neon is 44.54°K.).

Argon-Titanium Dioxide.—This system has been studied by Morrison, *et al.*¹⁶ The model was compared to isotherms measured at 85 and 120°K. and to heats of adsorption determined at 85°K. The multilayer form of the equation was used in both cases here. The results are shown in Figs. 5 and 6. The parameters chosen to obtain the fit are as follows: $\Delta E = -2000$ cal./mole, $V_m = 0.24$ cc./m.²—STP.

Discussion

In Table I (col. 3) the ΔE 's obtained from the fitting of the model to experiment are listed. Also

(15) R. J. Tykodi, J. G. Aston and G. D. L. Schreiner, *J. Am. Chem. Soc.*, in press.

(16) (a) L. E. Drain and J. A. Morrison, *Trans. Faraday Soc.*, **48**, 316 (1952); (b) J. A. Morrison, J. M. Los and L. E. Drain, *ibid.*, **47**, 1023 (1951).

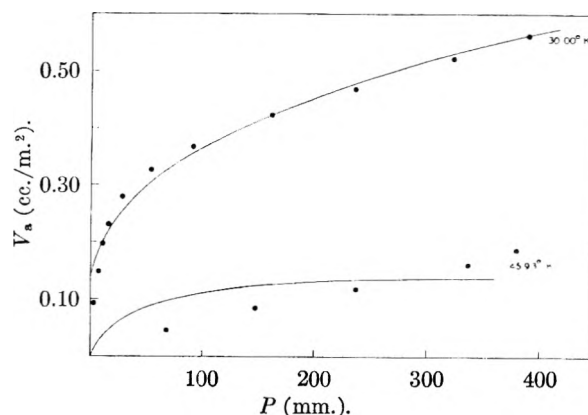


Fig. 3.—Isotherms of neon on titanium dioxide. Circles are experimental points, and the curves are constructed from the model.

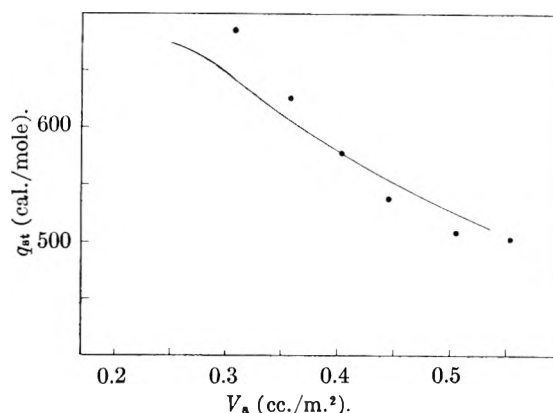


Fig. 4.—Heats of adsorption of neon on titanium dioxide (measured at 30°K.). Curve is calculated from the model, and the circles are experimental points.

given are theoretical estimates of the van der Waals energy of interaction of a single adsorbate molecule with the planar adsorbent surface. These were calculated by two alternate methods.

If it is assumed that the adsorbent acts as if it were a planar array of argon atoms, then the energy of interaction of an adsorbate molecule sitting on a square of argon atoms arranged at the optimum distance can be calculated. If the potential energy for the interaction between two molecules of the same species is written as $p_{x,x}$, and the potential between unlike molecules as $p_{x,z}$, then, for any fixed condition, the rule that $|p_{x,z}| = \sqrt{|p_{x,x}||p_{z,z}|}$ is approximately valid.^{17,18} Using the maximum value of $|p_{x,x}|$ as calculated on the basis of an exp-six Buckingham potential function,^{17,18} $\Delta E_{x,A}$ is given by $|\Delta E_{x,A}| = 4|p_{x,A}|_{\max}$. The values thus calculated are given in col. 4.

TABLE I

MOLAR ENERGIES OF INTERACTION (GIVEN IN CAL./MOLE)

Gas	ΔH_{vap}	ΔE	$\Delta F_{x,A}$	$\Delta E_{x,\text{TiO}_2}$
Argon	1330	2000	985	2000
Neon	360	600	545	800
Helium	12	180	270	370

(17) E. A. Mason and W. E. Rice, *J. Chem. Phys.*, **22**, 522 (1954).

(18) E. A. Mason and W. E. Rice, *ibid.*, **22**, 843 (1954).

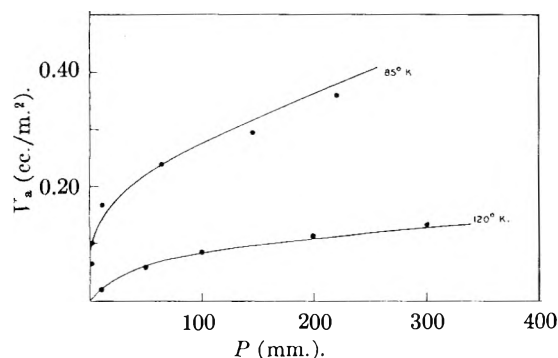


Fig. 5.—Isotherms of argon on titanium dioxide. Circles give experimental points and the curves are constructed from the model.

In the alternate method, ΔE is obtained by utilizing the Kirkwood-Müller formula to give the interaction between unlike atoms. This equation, as modified by Steele and Halsey¹⁹ for a planar adsorbent surface and a twelve-six (Lennard-Jones) potential function, gives an expression for $\epsilon(r)$, the energy of interaction as a function of distance from the surface. If we set $\Delta E = \epsilon(r)_{\max.}$, we obtain

$$\Delta E_{x, \text{TiO}_2} = \pi N_0 C / 8r^{*3}$$

where N_0 is the number of TiO_2 molecules per cc., C is the Kirkwood-Müller constant (see eq. 2.5 of ref. 19), and r^* is the distance at which the adsorbate molecule-adsorbent interaction is a maximum. The atomic polarizabilities and susceptibilities for TiO_2 (used to evaluate the Kirkwood-Müller constant) were those given by Roberts²⁰ and Van Vleck,²¹ respectively. r^* was estimated by taking a weighted average of the ionic radii of the oxygen ion and the titanium ion as given by Pauling²² (the value used was 1.2 Å.) and adding to it the radii of the rare gas atoms listed by Hirschfelder, Bird and Spotz.²³ All other parameters were taken from Steele and Halsey.²⁴ The values thus calculated (col. 5) agree fairly well with the ΔE 's calculated from experimental data with the aid of the model. As a matter of fact, the agreement is better than it appears to be, for reasons discussed in the Appendix.

In column two of Table I, the heats of vaporization are given for neon, argon and helium. When these figures are compared to the heats of adsorption shown in Figs. 2, 4 and 6, it is plain that one is not justified in neglecting lateral interaction when considering the results for neon and argon. However, some qualitative conclusions can be drawn about the effect of lateral interaction on the predictions of the crude theory. At coverages near the monolayer (the region of the isotherm where the model was fitted), the $-\Delta E$ of the model will be somewhat larger than that predicted on the basis of the interaction of a molecule with the flat

(19) W. A. Steele and G. D. Halsey, *THIS JOURNAL*, **59**, 57 (1955).

(20) S. Roberts, *Phys. Rev.*, **76**, 1215 (1949).

(21) J. H. Van Vleck, "The Theory of Electric and Magnetic Susceptibilities," Oxford University Press, Clarendon, 1932, p. 225.

(22) L. Pauling, "The Nature of the Chemical Bond," Cornell University Press, Ithaca, N. Y., 1948, p. 346.

(23) J. O. Hirschfelder, R. B. Bird and E. L. Spotz, *Chem. Revs.*, **44**, 205 (1949).

(24) W. A. Steele and G. D. Halsey, *J. Chem. Phys.*, **22**, 979 (1954).

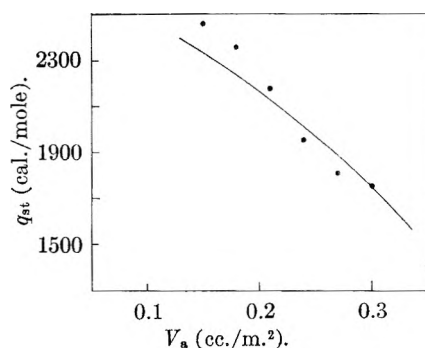


Fig. 6.—Heats of adsorption of argon on titanium dioxide (measured at 85°K.). Curve is calculated from the model, and circles give experimental points.

surface, due to added energy of interaction with neighboring adsorbate molecules. When one goes to lower coverages, the adsorbate molecules will no longer have this energy; therefore, the energy of adsorption predicted by the model will be too large and, also, the amount of adsorption at low coverages predicted by the model will be larger than that observed experimentally. In Figs. 3 and 5, it can be seen that below $V_a \sim 0.1$ cc./m.² g., the model predicts too much adsorption, as would be expected for attractive lateral interaction.

In Table II, monolayer capacities are given for the systems considered. The true area of the

TABLE II
MONOLAYER CAPACITIES (GIVEN IN CC./M.²-STP)

Gas	V_m (liq.)	V_m (B.E.T.)	V_m (model)
Argon (85°K.)	0.27	0.23	0.24
Neon (30°K.)	.36	.46	.46
Helium (4.2°K.)	.23	.54 ^a	.38

^a This is actually a double layer. The true monolayer capacity is given by the modified B.E.T. theory of Aston and Mastrangelo²⁵ as 0.28.

sample was assumed to be that given by the B.E.T. plot of the nitrogen adsorption, using 0.25 cc./m.² g.—STP as the nitrogen monolayer capacity. Column 3 gives the monolayer capacities obtained by plotting the isotherms for various gases according to the B.E.T. form. If the 4.17° helium isotherm is plotted according to the modified (two layer) B.E.T. equation proposed by Aston and Mastrangelo²⁵ for helium adsorption below its critical temperature, 0.28 cc./m.² g. is obtained for the monolayer capacity of the true monolayer (the apparent monolayer comes at nearly twice this value.) Also, an excellent fit of model to experiment is obtained for that isotherm. However, as expected, the heats predicted by the modified B.E.T. theory deviate considerably from experiment.

If the adsorbate is taken up as a liquid, with liquid packing, then the monolayer capacities given by the B.E.T. V_m 's should be equal to those in column 3; however, if the adsorption is site-wise, as assumed in the model, the V_m (model) listed in column 4 should all be equal to 0.25 cc./m.² g.

It is clear that the agreement of the V_m 's with theory is not too good. The V_m (model) values

(25) J. G. Aston and S. V. R. Mastrangelo, *ibid.*, **19**, 1067 (1951).

listed fall into two groups: argon and nitrogen ($V_m \sim 0.25$) and helium and neon ($V_m \sim 0.40$). It is probable that the discrepancy between the groups is due to molecular size: in a finely powdered material like the titanium dioxide used in these studies, an appreciable per cent. of the sites occur in cracks and inner voids. In such a case, there will be more area available to the smaller atoms which can penetrate more deeply into the cracks. Also, helium and neon, which interact less strongly with the surface, should diffuse into inner voids more easily than argon or nitrogen. Steele and Halsey,²⁴ using a different approach to the problem, have come to the same conclusions concerning a number of high area powders.

Conclusions

The five site model of adsorption without lateral interaction has several attractive features. It predicts the type of heat of adsorption curves most often observed experimentally in that it allows, in a very simple way, the high heats of adsorption (several times the energy of vaporization of the liquid) often observed. Also, it offers a possible solution to the apparently anomalous adsorption characteristics of helium. On the other hand, it suffers from the neglect of lateral interaction which limits it, in most cases, to coverages lower than those encountered in practice.

The chief function of the model is to set physically reasonable upper and lower bounds to the energies of adsorption relative to a given surface. The completely *a priori* deduction of a distribution function from the laws of crystal growth has proven too formidable; however, this model shows that such an approach is at least qualitatively correct, and yields the bounding values mentioned above. For convenience, we have assumed a discrete energy spectrum for intermediate energies of adsorption; a continuous distribution of adsorption energies intermediate between the bounding values is also compatible with the physical model (topographic heterogeneity) on which this model is based. Honig and Rosenbloom⁹ have shown that there is very little distinction between the two types of distribution, in so far as heats and isotherms are concerned. However, from the measured configurational entropies of neon¹⁵ and argon,¹⁵ it is clear that the discrete energy spectrum used here does not allow for sufficient heterogeneity of the surface; a more realistic model, using a more nearly continuous energy distribution might be

expected to effect a considerable improvement in the calculated entropies.

Finally, if the effect of lateral interaction could be adequately included in the crude picture presented here, a general method for the treatment of adsorption at low coverages might be developed.

Acknowledgments.—The discussions with Dr. S. V. R. Mastrangelo and Dr. G. D. Halsey (mostly critical) during the early stages of this work were invaluable. Likewise were the discussions with Dr. E. A. Mason during the later stages. Thanks are due to J. A. Morrison for supplying us with the data on argon in advance of publication.

Appendix

As mentioned in the text, the symbol ϵ_i as used in this paper is actually a free energy.³ Actually, for monolayer adsorption, ϵ_i is the sum of the energy of interaction of the particle with the adsorbate and $-kT$ times the log of the molecular partition function of the adsorbed particle. Similarly, for multilayer adsorption, ϵ_i is the sum of the energy of interaction and $-kT$ times the log of the molecular partition function of the particle in the adsorbed state divided by the molecular partition function of the particle in the liquid. It follows that, in using the same ϵ_i for monolayer and multilayer adsorption, one must implicitly set $j_{liq.} \simeq 1$, where $j_{liq.}$ is the molecular partition function for the liquid. Furthermore, when the van der Waals energy of interaction is compared with ϵ_i , as is done in this work, it is necessary to assume the $j_i \simeq 1$, where j_i is the vibrational (or hindered translational) partition function for the adsorbed particles on the i 'th site.

The assumption that $j_i/j_{liq.} \simeq 1$ is a fairly common one²⁶; however, it is not so easy to say that the vibrational part of the internal partition function of an adsorbed molecule can be neglected. Orr²⁷ has calculated that the vibrational contribution to the total energy of adsorption of argon on potassium chloride is about 3% at 80°K. This energy will be somewhat larger for neon, and is possibly quite appreciable for helium at 15°K. It would be quite difficult to make a quantitative estimate for this quantity, but it is undoubtedly the cause of at least a part of the difference between ΔE (model) and ΔE (van der Waals).

(26) S. Brunauer, "Adsorption of Gases and Vapors," Princeton University Press, Princeton, N. J., 1943, p. 154.

(27) W. J. C. Orr, *Trans. Faraday Soc.*, **35**, 1247 (1939).

THE SORPTION OF GASES BY VACANT CLATHRATE COMPOUNDS

BY J. R. DACEY, J. F. SMELKO AND D. M. YOUNG

*The Royal Military College of Canada, Kingston, Ontario**Received April 28, 1955*

The diffusion of nitrogen and hydrogen into the lattice of $[(\text{CH}_3)_3\text{As}\cdot\text{PdCl}_2]_2$ has been studied and sorption isotherms measured for nitrogen at -78 and 0° and for hydrogen at -183° in the pressure range 2–80 cm. The sorption of nitrogen at -78° is exceptionally slow, more than nine days being required for the establishment of equilibrium of the first admission of gas. The results are discussed in terms of the crystal structure of the sorbent.

Interest in this Laboratory has recently been focussed on the sorption of gases in very fine capillaries. The pores of Saran charcoal, prepared by the pyrolysis of polyvinylidene chloride, have been shown to be small (10 to 20 Å. across) and slot-like in cross-section.¹ It has since been demonstrated² that if vinylidene chloride monomer be sorbed, polymerized and pyrolyzed within the charcoal, even smaller pores result. Repetition of this treatment ultimately yields pores too small to admit nitrogen molecules.

Solids capable of forming gas inclusion (clathrate³) compounds are also possible sources of sorbents with ultrafine pores. Some of these compounds can be prepared so that the lattice is gas-free; they thus possess a considerable internal void composed of a number of cells. Sorption could occur in these cells if the sorbate molecules were small enough to pass the narrow constrictions between them. Three such "vacant" clathrates have been examined. Vacant β -quinol, prepared by crystallization from ethanol,⁴ should sorb water vapor and ammonia and, if the temperature is low enough, hydrogen and helium. The clathrate $\text{Ni}(\text{CN})_2\cdot\text{NH}_3\cdot(\text{C}_6\text{H}_6)_x$,⁵ from which the benzene can be removed by evacuation at room temperature,⁶ should be capable of sorbing benzene and molecules similar to or smaller than benzene. The complex $[(\text{CH}_3)_3\text{As}\cdot\text{PdCl}_2]_2$, whose crystal lattice contains a number of cylindrical tunnels,⁷ may be regarded as a vacant clathrate compound because crystallization from dioxane yields a dioxane inclusion compound.

Preliminary experiments, using a sensitive quartz spiral technique, have confirmed that these materials are all capable of sorbing measurable amounts of certain gases and vapors. β -Quinol, however, is unsuitable for quantitative study because of its high vapor pressure; $\text{Ni}(\text{CN})_2\cdot\text{NH}_3$, prepared by evacuation of the benzene clathrate, has been shown by X-ray methods to undergo a slow collapse of the lattice, resulting in a compact structure with no internal void.⁶ The compound $[(\text{CH}_3)_3\text{As}\cdot\text{PdCl}_2]_2$, on the other hand, is chemically and crystallographically stable, has a negligible vapor pressure at room temperature and a high melting (decomposition) temperature. This paper presents a

preliminary survey of the sorptive properties of this unusual material.

Experimental and Results

Materials.— $[(\text{CH}_3)_3\text{As}\cdot\text{PdCl}_2]_2$ was prepared by the general method given by Mann and Purdie.⁸ The final product was recrystallized from ethanol with very slow cooling, yielding large deep red needles. The recrystallized material was analyzed gravimetrically by the dimethylglyoxime method (found: Pd, 35.2; calcd. Pd, 35.8). It decomposed without melting at 235° and the density was found by flotation to be 2.19 (cp. the value of 2.14 calculated from the dimensions of the unit cell⁷).

Spectroscopically pure nitrogen, hydrogen and helium were supplied by the Air Reduction Company.

Apparatus.—The apparatus was similar to that described by Tompkins and Young,⁹ except that a mercury manometer (10 mm. bore with an internal glass pointer) was used in place of the oil manometer. 1.94 g. of sorbent was contained in a 3.6 cm.³ bulb; the total volume of the dead space was 9.42 cm.³. Crushed ice, solid carbon dioxide and acetone, and liquid oxygen stirred by a continuous stream of oxygen gas were used to maintain temperatures of 0, -78 and -183° , respectively. Initially and between each experiment, the sorbent was outgassed for several days at room temperature in a vacuum of 5×10^{-6} mm., higher temperatures being avoided for fear of decomposition or loss by evaporation. The criterion for freedom from occluded gas was that no measurable pressure (*i.e.*, >0.002 cm.) should develop on isolating the constant volume system for one hour.

Results.—The amount of nitrogen sorbed by the whole needles at -183° was measurable, but extremely small. It was found, however, that the pulverized material was capable of occluding much greater amounts of gas. Accordingly a portion of the crystals was finely pulverized in an agate mortar and used for the quantitative measurements described below.

Isotherms were measured for nitrogen at 0, -78 and -183° and for hydrogen at -183° . The results are shown in Fig. 1. Generally the sorption was so slow that only in some cases was it possible to establish equilibrium. The slowest sorption was that of nitrogen at -183° ; the curve given in Fig. 1 does not represent the equilibrium isotherm, which lies somewhere between the curve shown and the vertical axis. It was not feasible to follow this process to equilibrium. The sorption of nitrogen at 0° was much faster, equilibrium being reached at each point within three or four days, but the amount sorbed was too small to permit accurate measurement. As a compromise, a detailed study was made of the sorption of nitrogen at -78° , at which temperature the sorption is appreciable and not prohibitively slow (seven to ten days for each dose of gas to come to equilibrium). The amount of nitro-

(1) J. R. Dacey and D. G. Thomas, *Trans. Faraday Soc.*, **50**, 740 (1954).

(2) J. R. Dacey and D. G. Thomas, *Can. J. Chem.*, **33**, 344 (1955).

(3) H. M. Powell, *J. Chem. Soc.*, 68, 571, 815 (1948); 298, 300, 468 (1950).

(4) D. F. Evans and R. E. Richards, *ibid.*, 3932 (1952).

(5) D. F. Evans, O. Ormrod, B. B. Goalby and L. A. K. Staveley, *ibid.*, 3346 (1950); H. M. Powell and J. H. Raynor, *Nature*, **163**, 566 (1949); J. H. Raynor and H. M. Powell, *J. Chem. Soc.*, 319 (1952).

(6) Preliminary experiments.

(7) A. F. Wells, *Proc. Roy. Soc. (London)*, **167A**, 169 (1938).

(8) F. G. Mann and E. Purdie, *J. Chem. Soc.*, 873 (1936); see also F. G. Mann and A. F. Wells, *ibid.*, 702 (1938).

(9) F. C. Tompkins and D. M. Young, *Trans. Faraday Soc.*, **47**, 77 (1951).

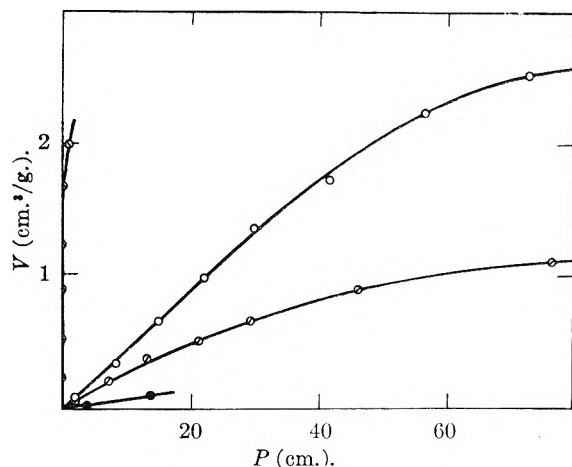


Fig. 1.—Sorption isotherms: \odot , \circ , \bullet , N₂ at -183, -78 and 0°, respectively; \ominus , H₂ at -183°.

gen sorbed is plotted as a function of time from the moment of admission, for the first and second doses of nitrogen, in Fig. 2. The fluctuations in the curve for the second dose are due to variations in the pressure of nitrogen caused by changes in room temperature. The first dose did not reach equilibrium even after nine days, but it is reasonable to assume that the amount sorbed after nine days differs but little from the true equilibrium value. Subsequent doses all came to a steady equilibrium value in about seven days.

Hydrogen was both appreciably and rapidly sorbed at -183°, equilibrium being attained within 24 hours from the moment of admission of each dose. The isotherm is given in Fig. 1 and the amount sorbed as a function of time, for the second dose, in Fig. 2.

Discussion

According to Wells,⁷ the tunnels in [(CH₃)₃As·PdCl₂]₂ run along the length of the needles, as does the cleavage plane. In the whole needles, therefore, the number of "entrances" per unit length of tunnel is very small, so that the sorption even of small molecules may be expected to be slow. Grinding probably results in preferential cleavage along the length of the needles, splitting open some of the tunnels, but some cleavage may occur in other directions.¹⁰ Such random cleavage would cause an increase in the number of entrances per unit length of tunnel and a corresponding reduction in the average tunnel length; the velocity of sorption may thus be increased by grinding. The lower sorptive capacity of the whole needles was probably only apparent, due to the extreme slowness of the process.

The crystal structure diagrams given by Wells⁷ suggest that the narrowest diameter of the tunnels (*i.e.*, the constrictions between adjacent "cells") is determined by the positions of the methyl groups and is approximately 4.3 Å. When this substance is crystallized from dioxane, the resulting clathrate compound has lattice dimensions 1.5% greater than those of the "empty" crystals. This suggests that the dioxane molecule, which Wells assumes to be an oblate spheroid (radius 3.54 Å,

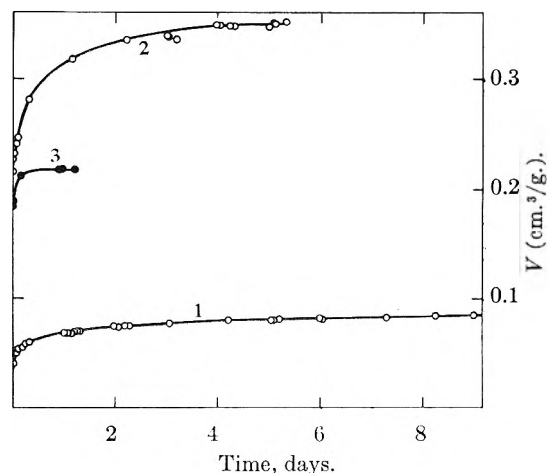


Fig. 2.—Sorption as a function of time: 1, N₂ at -78° (first dose); 2, N₂ at -78° (second dose); 3, H₂ at -183° (second dose).

effective thickness 3.7 Å.), fits tightly into a vacant lattice cell, and thus provides a convenient, if approximate, measure of the volume of the latter.

Barrer¹¹ has classified molecular sieves into three groups on the basis of the diameters of the molecules which they sorb or exclude. The smallest pores, those of calcium- and barium-rich mordenites (Class 3) have estimated minimum diameters between 3.84 and 4.00 Å. These materials are capable of occluding small molecules (He, Ne, H₂, O₂, N₂ and H₂O) rapidly, larger molecules (A, HCl and NH₃) moderately rapidly. Noting that the present material has an estimated minimum diameter of 4.3 Å., it is perhaps surprising that nitrogen and hydrogen are so slowly occluded. Clearly, whether or not a particular porous solid can sorb molecules of a given size depends only on geometrical considerations, but additional factors control the sorption velocity. The molecules may have to surmount a potential energy barrier and probably there are in the present sorbent exceptionally high barriers at the narrow constrictions separating adjacent cells. Nitrogen and hydrogen may therefore have less mobility in the pores of the present sorbent than they would have in the smaller pores of Class 3 molecular sieves. It may be noted in passing that, on purely geometrical grounds, A, CH₄ and C₂H₆ should also be sorbed.

The crystallographic data indicate that there is one "cell" per [(CH₃)₃As·PdCl₂]₂ molecule,⁷ so that if it be assumed that at saturation there is one sorbed gas molecule per cell, the amount of gas sorbed at saturation should be about 40 cm.³ at S.T.P. per gram of sorbent. In the case of hydrogen there may even be two molecules per cell. The observed maximum amounts of gas occluded (see Fig. 1) are much lower than 40 cm.³/g., for which discrepancy there are a number of possible reasons. First, the arbitrary outgassing criterion (*vide infra*) does not provide any guarantee that the sorbent is free from occluded gas at the start of each experiment. Although the analysis indicates quite high purity, it would require only a few occluded solvent molecules effectively to close off a large part

(10) D. M. Young, *Trans. Faraday Soc.*, **50**, 838 (1954).

(11) R. M. Barrer, *Quart. Rev.*, **3**, 293 (1949).

of the labyrinth system. Secondly, imperfections in the lattice structure may also cause some tunnels to be shut off from the exterior. Thirdly, the above value of 40 cm.³/g. refers to an infinite crystal; grinding has the effect of converting internal into external surface, on which the sorption of nitrogen at -78° or of hydrogen at -183° would be entirely

negligible at the pressures used in the present experiments. Finally, under the conditions used it is unlikely that saturation even of the pore system was ever achieved.

The authors wish to express their thanks to the Defence Research Board of Canada for generous financial support (Grant No. 356).

HOMOGENEOUS CATALYTIC HYDROGENATION. III. ACTIVATION OF HYDROGEN BY CUPROUS AND SILVER ACETATES IN PYRIDINE AND DODECYLAMINE

BY LEON WRIGHT, SOL WELLER AND G. A. MILLS

Contribution from the Houdry Process Corporation, Linwood, Pennsylvania

Received May 2, 1955

Molecular hydrogen is activated by cuprous and silver acetate dissolved in pyridine or dodecylamine. Kinetic measurements were made at 78 and 100° for the hydrogenation of silver and cupric acetate in these solvents. The rate of hydrogenation is expressed by $-dH/dt = k_{PH_2} [M^I]$, where $[M^I]$ represents the concentration of silver or cuprous acetate. The rate of hydrogenation of cupric acetate is approximately independent of the concentration of cupric acetate. Molecular weight studies of pyridine solutions of silver and cuprous acetates at 115°, considered in relation to the first order kinetics, demonstrate that the rate-determining step involves the reaction of hydrogen with a metal ion monomer. Possible structures for the metal-hydrogen complex and modes of hydrogen-hydrogen bond scission are discussed. Deuterium exchanges with a hydrogen donor in the cuprous acetate-pyridine system in a manner analogous to that previously found in quinoline. No exchange is observed during the reduction of silver acetate in pyridine by deuterium. The reduction of silver acetate by deuterium is 30% slower than that by hydrogen.

Introduction

The activation of molecular hydrogen in homogeneous solutions offers an opportunity to define the molecular structure of the catalyst and of the catalyst-hydrogen complex. A solution of cuprous acetate in quinoline is capable of activating molecular hydrogen for the reduction of *p*-benzoquinone and cupric acetate.^{1a,1b} Some work also has been reported on the change in catalytic activity as effected by variations in catalyst solvent for this system.^{1b} The present paper includes a kinetic study of the catalyzed hydrogenation of cupric acetate by pyridine and dodecylamine solutions of cuprous acetate. Since Wilmarth² reported that quinoline solutions of silver acetate absorbed hydrogen rapidly at 100°, with the formation of silver metal, a kinetic study also was made of the activation of hydrogen by pyridine solutions of silver acetate. These experiments were carried out at 78 or 100°, a hydrogen pressure of 515 mm. and cuprous or silver acetate concentrations from 0.01 to 0.18 molar. Molecular weight determinations, by the method of boiling point elevation, were made for silver and cuprous acetates in pyridine at 115°. Finally, a few isotopic rate and exchange experiments were made with deuterium as a tracer.

Apparatus and Materials

The general experimental procedure has been previously described.^{1b} The cuprous acetate^{1b} contained 51.7% Cu (theor. = 51.6%). C.P. cupric acetate monohydrate was obtained from the J. T. Baker Co. Silver acetate was obtained from the General Chemical Division, Allied Chemical and Dye Corp., as an anhydrous white salt containing 62.4%

Ag (theor. = 64.6%). These chemicals were used without further purification.

Pyridine, reagent grade, was obtained from the Allied Chemical and Dye Corp. and distilled in a still of 22 theoretical plates at a reflux ratio of 15:1. The fraction boiling at 115–116° was collected and stored over activated alumina. Pyridine, white label grade, was obtained from the Eastman Kodak Co. as a water-white liquid and used as received. This material was used only in the experiments listed in Table I.

TABLE I

SILVER ACETATE REDUCTION IN PYRIDINE,^a 78°, 515 MM. H₂

Run no.	(AgOAc) mole/l.	First-order rate constant ^b × 10 ²	Remarks
1	0.025	2.28	
2	.050	2.37	Duplicate runs were made
3		2.30	
4	.100	2.49	
5	.150	2.40	
6	.050	2.47	Solvent dried over activated Al ₂ O ₃ ; duplicate runs made
7		2.47	

^a Forty ml. of pyridine, E. K. Co. White Label charged in each run plus the required millimole quantities of silver acetate. ^b Specific rate constant including the effect of hydrogen pressure; units, min.⁻¹ at 515 mm. hydrogen.

Dodecylamine (90%) was obtained from Armour and Co. and distilled in a 22-plate still under reduced pressure. A fraction boiling at 154° and 40 mm. pressure was collected and stored over activated alumina.

Cylinder hydrogen was purified by passage over platinum-containing Houdry Type 3 reforming catalyst at 450° and over dried silica-alumina (Houdry S-45) at -195° .

Deuterium was obtained from the Stuart Oxygen Co. and used as received.

The molecular weights of cuprous and silver acetates were determined ebullioscopically in pyridine at atmospheric pressure. The apparatus used for the boiling point determinations was a modified Cottrell apparatus fitted with a Beckmann thermometer and heated with a recessed electrical heater.

(1) (a) M. Calvin, *J. Am. Chem. Soc.*, **61**, 2230 (1939). (b) S. Weller and G. A. Mills, *ibid.*, **76**, 769 (1953); L. W. Wright and S. Weller, *ibid.*, **76**, 3345 (1954), papers I and II in this series.

(2) W. K. Wilmarth, Ph.D. Thesis, University of California, 1942.

Experimental Results

Silver Acetate Hydrogenation.—The course of a typical hydrogenation of silver acetate in pyridine is shown in Fig. 1. The quantity of hydrogen absorbed increases, at a rate decreasing with time, until the amount of hydrogen absorbed is approximately that calculated for reduction of silver acetate to silver metal. In most cases, at the end of each run, the solutions were filtered through a fine sintered glass filter. The amount of silver recovered was usually equivalent to the amount of hydrogen absorbed.

A study was made of the effect of hydrogen pressure and silver acetate concentration on the rate of silver acetate reduction. Within the limits of experimental error, the rate of reduction at 78° is linearly dependent on hydrogen pressure over the range 94 to 415 mm. It is necessary to correct for the pyridine partial pressure in order to obtain the effect of hydrogen pressure.

The rate of silver acetate reduction is directly proportional, at constant hydrogen pressure and 78°, to the concentration of silver acetate. This is demonstrated in Table I by the constancy of the values of k , the "first-order" specific rate constant, over a sixfold increase in silver acetate concentration (0.025 to 0.15 molar). As illustrated by the experiment in Fig. 1, the reaction is satisfactorily first order over at least two-thirds of the reduction, but it becomes greater than first order over the last one-third.

The rate of gas-liquid equilibration is believed not to be limiting in these experiments, since increasing the shaking rate of the reactor assembly by 50% did not affect the rate constant of a typical (0.05 molar AgOAc) reduction experiment.

The absolute values of the specific rate constant, k , were found to differ by a factor of two when pyridine of different sources was used, pyridine obtained from Allied Chemical supporting a faster rate than Eastman pyridine; however, all experiments involving comparisons of rate constants were carried out with the same batch of solvent. No attempts were made to determine the cause of this rate difference other than to demonstrate that the small amount of water, 0.2–0.4 wt. %, usually present in pyridine did not affect the rate of silver acetate reduction (runs 2 and 6, Table I).

The apparent activation energy for silver acetate reduction by gaseous hydrogen was determined to be 14.4 kcal./mole in the temperature range 64.7–78.4°. When correction is made for the temperature dependence of hydrogen solubility in pyridine, the activation energy for reaction between silver acetate and dissolved hydrogen is increased to about 16 kcal./mole. (It is assumed that the heat of solution of hydrogen in pyridine approximately equals that in quinoline.^{1a}) It was also necessary in these experiments to take into account the variation of the pyridine vapor pressure with temperature. This was done by changing the total pressure so that at each temperature the same partial pressure of hydrogen existed.

The fact that the apparent energies of activation of hydrogen by the cuprous acetate-quinoline system^{1b} and the silver acetate-pyridine system

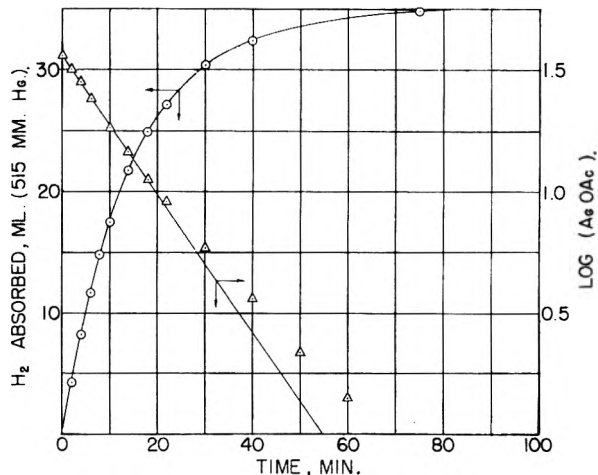


Fig. 1.—Reduction of silver acetate in pyridine at 78°; 2.0 mmoles AgOAc; 40 ml. pyridine.

are experimentally of the same order of magnitude suggests that the entropies of activation for these two systems are similar.

A few miscellaneous experiments were carried out to determine the effect of different solvents on the reduction of silver acetate by hydrogen. Dodecylamine appears to be a satisfactory solvent for the reduction reaction at 78°; the specific rate constant is within 10–20% of that obtained with pyridine under similar conditions. An aqueous 0.05 molar solution of silver acetate is *not* measurably reduced by hydrogen at 100°, although the color of the solution does change from water white to cloudy gray on charging the evacuated reactor with hydrogen. A saturated solution in glacial acetic acid is also not reduced by hydrogen over a one-hour period at 78°.

If a solvated silver ion alone is responsible for the observed activation of hydrogen, any soluble monovalent silver salt should, in principle, be capable of activating hydrogen. Although silver chloride is soluble in pyridine, it was found that a 0.05 molar solution does not measurably absorb hydrogen over a two-hour period at 100°. This indicates that the activation of hydrogen by silver acetate is, in some way, related to the nature of the bonding between the silver and acetate ions.

The observation that the rate of silver acetate reduction decreases with increasing reaction time, Fig. 1, implies that silver metal is not a catalyst for the reduction of silver acetate. This point was further demonstrated by reducing, consecutively, two millimole charges of silver acetate in the same pyridine solution. Within 5–10%, the reduction rates were identical. This also demonstrates that the small amount of acetic acid produced (2 mmoles) during the first reduction does not seriously affect the reduction of the second charge of silver acetate.

Hydrogenation of Cupric Acetate.—Typical curves for the hydrogenation of cupric acetate monohydrate, catalyzed by cuprous acetate in pyridine, are shown in Fig. 2. Similar results are obtained in dodecylamine solution. The reaction is autocatalytic, the induction period almost disappearing when sufficient cuprous acetate is added

initially. In all cases the quantity of hydrogen absorbed is close to the theoretical value for the reduction of cupric acetate to cuprous acetate. After reduction to the cuprous state is complete, further reduction to metallic copper seems to occur very slowly, if at all; this is shown by the flatness of the final portions of the hydrogen absorption curves and by the absence of metallic copper on filtration of the solution at the end of an experiment.

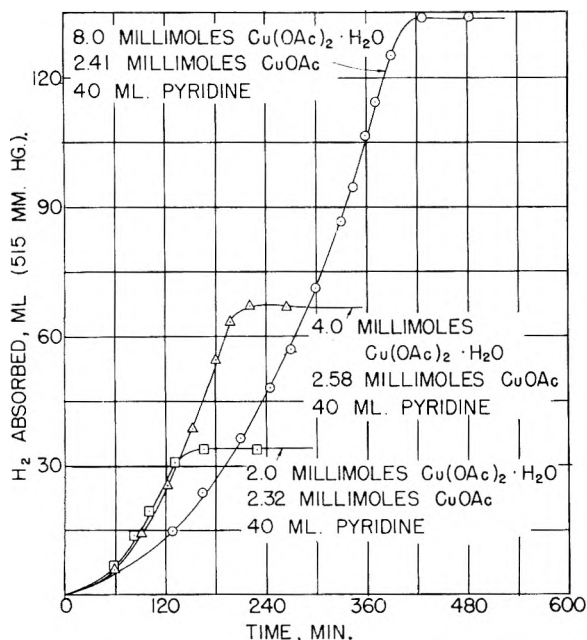


Fig. 2.—Reduction of cupric acetate in pyridine at 100°; effect of cupric acetate concentration.

A study was made of the effect of hydrogen pressure and cupric acetate concentration on the rate of reduction at 100°. Within the limits of experimental error, the initial rate of reduction, expressed as ml. (STP) hydrogen absorbed per unit time, was linearly dependent on hydrogen pressure over the range 37–282 mm. for pyridine solutions, and over the range 290–750 mm. for dodecylamine solutions. The reduction is, therefore, first order in hydrogen pressure.

As Fig. 2 shows, at fixed cuprous acetate concentration, the same initial rate was observed for 0.05 and 0.10 *M* cupric acetate in pyridine. (The rate was actually lower for the highest cupric acetate concentration, 0.20 *M*; this may result from an inhibition by water, added indirectly as part of the cupric acetate monohydrate.) Three similar experiments in dodecylamine solution, at cupric acetate concentrations of 0.025, 0.050 and 0.075 *M*, showed the same independence of rate on cupric acetate concentration. This result is qualitatively different from that of Dakers and Halpern, who found the rate of reduction of aqueous cupric acetate solutions, at 100° and 190 p.s.i. hydrogen pressure, to be proportional to the cupric concentration.³

The curves in Fig. 2 show that the instantaneous rate of hydrogenation, which depends on the instantaneous concentration of cuprous acetate,

increases with increasing time almost up to the point of complete reduction of cupric acetate to cuprous acetate. The individual points in Fig. 3 represent instantaneous rates, calculated from the curves for five experiments in pyridine solution, as a function of the total cuprous acetate present at the corresponding time. (Five experiments in dodecylamine solution, covering a range of cuprous acetate concentration up to 0.14 *M*, showed the same linear dependence of rate on cuprous acetate concentration.) The total cuprous acetate was taken as the sum of the cuprous acetate initially added and that produced by reduction of the cupric salt. Inspection of Figs. 1 and 3 shows that the rate of reduction of both silver and cupric acetates by hydrogen in these studies is expressible in the form

$$\text{Rate} = k p_{H_2} [M^I]$$

where $[M^I]$ represents the total concentration of silver or cuprous acetate.

Molecular Weight Studies.—The first-order dependence of the hydrogenation rate on the total concentration of silver or cuprous acetate can be interpreted on the basis either that the catalytically active species is a monomer, or that it is a dimer, provided, in the latter case, that the dimerization constant is so high that substantially all of the catalyst molecules are present as dimers. In order to resolve this problem, the extent of dimerization in pyridine was studied by determining the apparent molecular weights of cuprous acetate and of silver acetate in pyridine at 115° by the boiling point elevation method. The results of this study are given in Fig. 4, in which the apparent molecular weights are plotted as a function of the salt concentration. Extrapolation of these data yields an apparent molecular weight at infinite dilution of 122 for cuprous acetate and 162 for silver acetate, in reasonable agreement with the monomer formula weights of 123 and 168, respectively. The increase in apparent molecular weight with increasing concentration (Fig. 4) may be interpreted as resulting from formation of a dimer or more highly associated complex.⁴ The computed dimerization constant is quite small, however, and it varies systematically with concentration; for cuprous acetate it increases from a value of 0.5 mole⁻¹ l. at 0.1 *M* to 1.2 mole⁻¹ l. at 0.6 *M*. This drift in the dimerization constant may be attributed to the increasing formation of *n*-mers (*n* > 2) at higher concentrations.⁴

It is clear from Fig. 4 that over the concentration range in which kinetic studies were made (up to 0.18 *M*), the extent of dimerization of cuprous acetate does not exceed 15%, and that of silver acetate does not exceed 25%. Taken in conjunction with the results of the kinetic studies, this means that the catalytic species for both salts in pyridine is the monomer.

It was found impractical to study molecular weights in dodecylamine at temperatures near 100° because of the low vapor pressure of this solvent. As a result, although the kinetic behavior for cupric acetate reduction was similar for solutions in dodecylamine and in pyridine, it was not possible

(3) R. G. Dakers and J. Halpern, *Can. J. Chem.*, **32**, 969 (1954).

(4) Cf. F. M. Batson and C. A. Kraus, *J. Am. Chem. Soc.*, **56**, 2017 (1934).

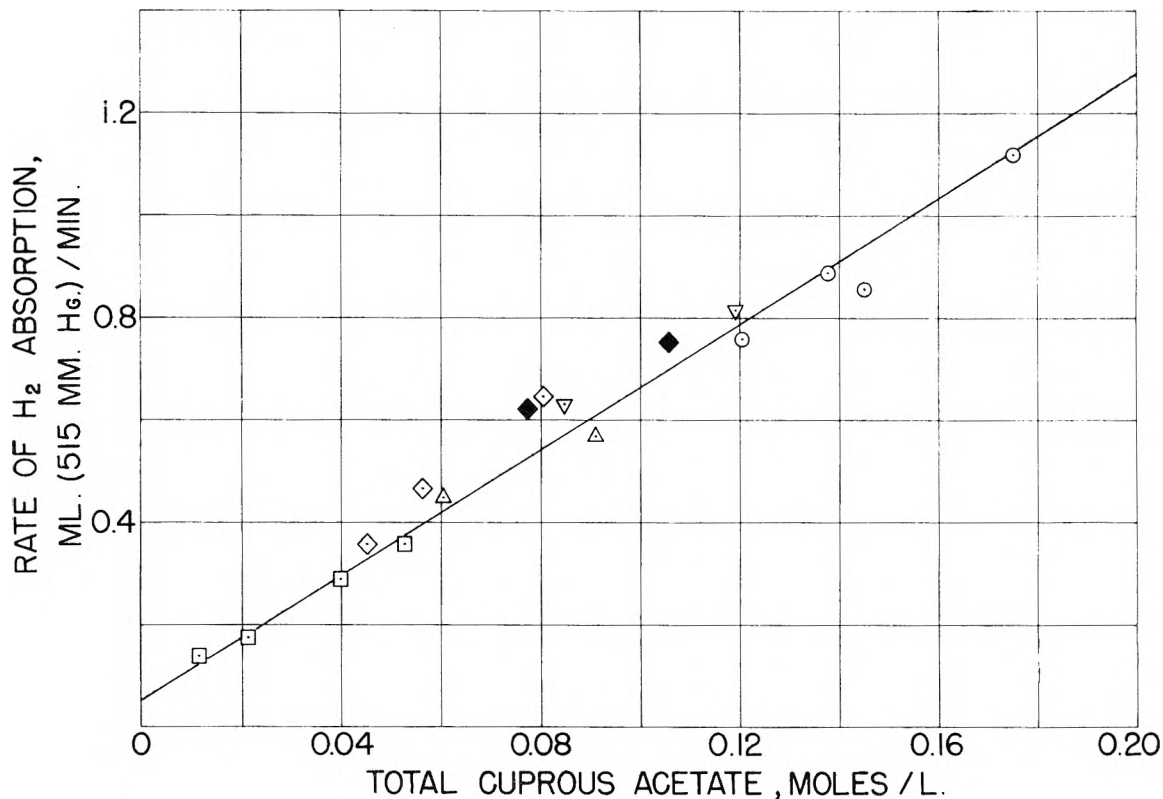


Fig. 3.—Reduction of cupric acetate; instantaneous rate *vs.* total cuprous acetate concentration pyridine, 100°.

to rule out the possibility that in dodecylamine most of the cuprous acetate is dimerized and that the dimer is the catalytically active species.

Exchange and Isotopic Rate Studies.—When deuterium is activated by the cuprous acetate–quinoline system, isotopic exchange occurs with a hydrogen donor in solution.^{1b} A similar exchange reaction is observed when solutions of cuprous acetate in either pyridine or dodecylamine are treated with deuterium at 100°. The “half-time” for exchange in pyridine solution is approximately one-half hour. By contrast, *no* exchange occurs either during or after the reduction of silver acetate in pyridine by either pure deuterium or a hydrogen–deuterium mixture at 78°. The failure of exchange to occur in the presence of metallic silver is consistent with the inability of the metal to catalyze the reduction of silver acetate (see above). The non-occurrence of exchange during the reduction, when hydrogen is certainly being dissociated, results from the fact that the hydrogen, once activated, is rapidly removed by the irreversible reaction with silver acetate before it can return to the gas phase (see ref. 1b).

The silver acetate–pyridine system also differs from the cuprous acetate–quinoline system in that the reduction of silver acetate at 78° by deuterium proceeds at a rate that is 30% slower than the reduction by hydrogen. It had previously been found that the rate of quinone reduction, catalyzed by cuprous acetate in quinoline, is the same within 5–10% with deuterium as with hydrogen.^{1b}

Discussion

The combined results of the kinetic and molecular weight studies reported here demonstrate that,

at least over the concentration range studied, the molecule responsible for the activation of hydrogen is *not* a dimer of silver or cuprous acetate in pyridine solution. This conclusion is contrary to that

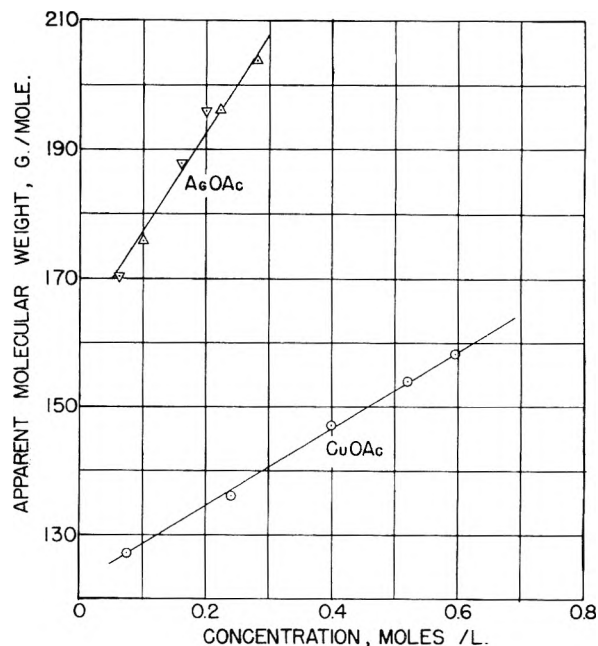


Fig. 4.—Apparent molecular weight *vs.* concentration of silver acetate and cuprous acetate.

previously obtained for cuprous acetate in quinoline.^{1a, 1b} There is no question about the validity of the earlier results; a non-first-order rate law for the activation of hydrogen by cuprous acetate in quinoline has been independently established both

by Weller and Mills^{1b} and by Wilmarth and Barsh.⁵ One can only speculate on the reason for the difference between the quinoline and the pyridine systems. It seems probable that the difference is related to the different size of the solvent molecules. Construction of scale models shows that for cuprous acetate in pyridine solution, for example, there is no steric hindrance to the formation of a tetrahedral, four-coordinated monomer of formula CuPy_3OAc , Py representing a pyridine molecule; sp^3 hybrid orbitals would be involved in the formation of this complex. In quinoline, however, a solvated, monomeric molecule of formula CuQ_3OAc is sterically much less favorable, as is shown by the interference between the coordinated quinoline molecules in a scale model. As a result, a three-coordinated dimeric molecule may be preferentially formed in quinoline solution.^{1b} Certainly the apparent dimerization constant for cuprous acetate in quinoline ($\sim 11 \text{ mole}^{-1} \text{ l. at } 100^\circ$) is 10–20 times greater than it is in pyridine.

It has become clear during the past two years that the homogeneous activation of hydrogen does not require the intervention of a dimeric (or higher) metal species. Wilmarth and his co-workers^{6,7} have described base-catalyzed exchanges in which no metal at all is involved. In other cases, such as the systems described in this paper, apparently only a monomeric metal species participates. In this group also fall the solutions of cupric acetate³ and mercuric acetate^{8,9} in water, which Halpern and his co-workers have shown to react homogeneously with hydrogen at elevated pressures. In view of Halpern's results, it also seems likely that much of Ipatieff's early work on the reduction of aqueous solutions of metal salts by hydrogen under pressure will also fall in this class.¹⁰

(5) W. K. Wilmarth and M. K. Barsh, *J. Am. Chem. Soc.*, **75**, 2237 (1953).

(6) W. K. Wilmarth, J. C. Dayton and J. M. Flournoy, *ibid.*, **75**, 4549 (1953).

(7) W. K. Wilmarth and J. C. Dayton, *ibid.*, **75**, 3553 (1953).

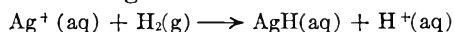
(8) J. Halpern, G. Kounek and E. Peters, *Research*, **I**, S61 (1954).

(9) E. Peters and J. Halpern, personal communication.

(10) For a summary, see V. N. Ipatieff, "Earlier Work on Hydrogenation at High Temperatures and Pressures," in Dunstan, "The Science of Petroleum," Vol. III, Oxford, England, 1938, p. 2133.

It then becomes pertinent to examine the energetics for, and the detailed nature of, the splitting of the hydrogen molecules in such systems. Even when the catalyst for hydrogen activation is a monomeric species, it is necessary, for reasons of energetics, that both fragments of the hydrogen molecule be able to simultaneously form bonds (or the equivalent) of considerable stability. For example, Wilmarth's postulated mechanism of the hydroxyl ion-catalyzed exchange,⁶ which involves the transitory formation of a hydride ion, is conceivable only for a solvent of high dielectric constant, since only in this case will the solvation energy of the hydride ion be large enough to make the energetics reasonable.

In the case of cuprous and silver acetates in pyridine, both a heterolytic split of hydrogen (into a proton and a hydride ion) and a homolytic split (into two hydrogen atoms) should be considered as possible rate-determining steps. If two atoms are formed, both may become attached to the metal ion; although no metal salt of this nature is known to exist, there is some evidence that this may be the case for iron hydrocarbonyl, $\text{H}_2\text{Fe}(\text{CO})_4$. Alternately, one hydrogen atom may go to the metal ion and one to a pyridine molecule with the formation of a radical. If a split into a hydride ion and a proton occurs, the hydride ion might react with, for example, the silver ion to form a solvated silver hydride molecule, and the proton might react with pyridine to form pyridinium ion. It is worth noting that for the reaction



ΔH° is in the neighborhood of +30–35 kcal. (The heat of hydration of gaseous silver hydride is estimated to be about –10 kcal./mole.) Since the over-all activation energy must at least equal the (endothermic) heat of the rate-determining step, this high ΔH° value is consistent with the failure of aqueous silver acetate to be reduced by hydrogen. The corresponding ΔH° value for pyridine solutions cannot be computed because of inadequate data, but qualitative considerations of the difference in heats of solvation of silver and hydrogen ion indicate that the value might be 5–10 kcal. lower than in water.

CORRESPONDING STATES IN MULTILAYER STEP ADSORPTION

BY TERRELL L. HILL

*Naval Medical Research Institute, Bethesda, Maryland**Received May 4, 1955*

The successive steps found recently in the physical adsorption isotherms for argon and krypton on a relatively uniform surface (a graphitized carbon black) are interpreted from the point of view of corresponding states in the different layers. It is found that the second and third layers for krypton and the third and higher layers for argon are "normal," in this sense. It is pointed out that the Ising model for a two-dimensional hexagonal lattice, some of whose exact properties are known, should be applicable to this problem.

Several striking physical adsorption isotherms have been published recently¹⁻³ which show steps associated with the adsorption of successive layers of gas molecules on the adsorbent surface. These isotherms have been observed at low temperatures and on very uniform surfaces. This possibility has been discussed theoretically for some time,⁴⁻⁸ especially by Halsey.

The object of the present note is to point out that a principle of corresponding states can be used to furnish "unperturbed" or "reference" behavior with which the actual location of successive steps may be compared with profit. The argument is independent of any particular model of an adsorbed layer, but is more nearly applicable the sharper the steps (low temperature, uniform surface).

This note should be considered as supplementary to the earlier discussions of Halsey and co-workers.^{7,8}

Corresponding States.—We now give the argument for the idealized or "reference" case. Actual systems with step isotherms will deviate from this in varying degrees. Let θ_i be the fraction of the i th layer filled in a system with a perfectly uniform adsorbent surface and at a sufficiently low temperature so that steps (Fig. 1) or quasi-steps occur. We wish to compare "corresponding states" in successive layers. The best choice of θ_i for this purpose is $1/2$ since for θ_i near zero or unity, molecules will be going into the $(i - 1)$ th or $(i + 1)$ th layer, respectively, as well as into the i th. Ideally, the filling in of each successive layer follows the same pattern (and hence the term "corresponding state") in the neighborhood of the appropriate $\theta_i = 1/2$, because the intermolecular forces *within* each successive layer are the same. In effect, in successive layers, we have monolayer adsorption in an external field which is constant in the neighborhood of $\theta_i = 1/2$ but which differs for each value of i . This external field is provided by the layers of gas already adsorbed (1, 2, . . . $i - 1$) and by the adsorbent (see Fig. 2). Because the external field depends on i , the chemical potential (and hence the relative

pressure) at which successive steps take place will vary with i .

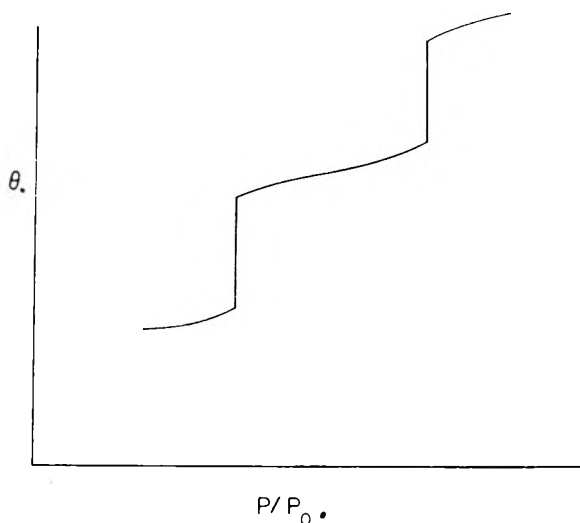


Fig. 1.

First, we calculate the external potential field, U_i , for a molecule being adsorbed in the i th layer at $\theta_i = 1/2$ (or $\theta = i - 1/2$, where θ is the total number of adsorbed layers). It is clearly appropriate to recognize the layer-like structure of the adsorbate in this calculation, and we also treat the adsorbent as having a layered structure, since the surface is assumed uniform (crystalline). We consider van der Waals attractive interactions only, and sum over layers but integrate within each layer to obtain the total interaction.⁹ Let $-\alpha_s/r^6$ be the intermolecular potential for a pair of gas molecules and $-\alpha_a/r^6$ the potential for a gas and a solid molecule. Let n_a and n_s be the surface densities (number of molecules/cm.²) in each layer of adsorbate and adsorbent, respectively. Then for a gas molecule at a distance z from an adsorbate layer, the total interaction potential between the gas molecule and the adsorbate layer is $-\pi n_a \alpha_a / 2z^4$. Similarly, for a gas molecule and an adsorbent layer, the potential is $-\pi n_s \alpha_s / 2z^4$. From Fig. 2, we see that the required total external potential field, including all layers, is

$$U_i = -\frac{\pi n_a \alpha_a}{2} \sum_{j=1}^{i-1} (jh_a)^{-4} - \frac{\pi n_s \alpha_s}{2} \sum_{j=0}^{\infty} [(i-1)h_a + h + jh_s]^{-4} \quad (1)$$

(9) T. L. Hill in "Structure and Properties of Solid Surfaces," University of Chicago Press, Chicago, Illinois, 1953, edited by R. Gomer and C. S. Smith, p. 394.

(1) M. H. Polley, W. D. Schaeffer and W. R. Smith, *THIS JOURNAL*, **57**, 469 (1953).

(2) J. H. Singleton and G. D. Halsey, *ibid.*, **58**, 330, 1011 (1954).

(3) C. H. Amberg, W. B. Spencer and R. A. Beebe, *Can. J. Chem.*, **33**, 305 (1955); R. A. Beebe, C. H. Amberg and W. B. Spencer, O.N.R. Technical Report No. 6, Research Contract N8-onr-66902, Feb. 1955.

(4) T. L. Hill, *J. Chem. Phys.*, **15**, 767 (1947).

(5) G. D. Halsey, *ibid.*, **16**, 931 (1948).

(6) T. L. Hill, *Advances in Catalysis*, **4**, 211 (1952).

(7) W. M. Champion and G. D. Halsey, *THIS JOURNAL*, **57**, 646 (1953).

(8) J. H. Singleton and G. D. Halsey, *Can. J. Chem.*, **33**, 184 (1955).

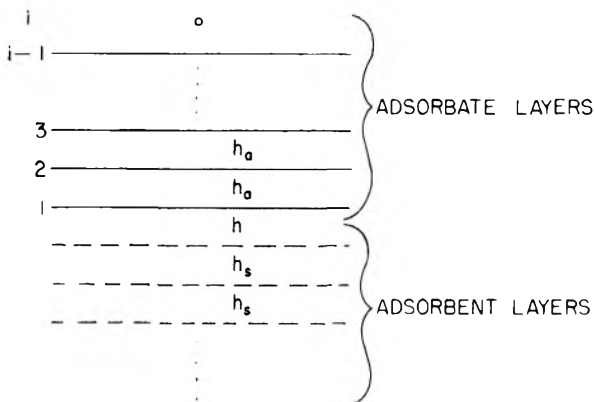


Fig. 2.

In the limit of bulk condensation of gas molecules on the adsorbent ($i = \infty$)

$$U_\infty = -\frac{\pi n_a \alpha_a}{2} \sum_{j=1}^{\infty} (j h_a)^{-4} \quad (2)$$

For the temperature T of interest, let $\mu^*(T)$ be the "intrinsic" chemical potential at which the phase transition would occur ($\theta_i = 1/2$) if a monolayer could exist by itself, omitting from μ^* the contribution from the three-dimensional partition function for vibration of a molecule in the neighborhood of its equilibrium point.¹⁰ Let j_i be this vibrational partition function for a molecule at $\theta_i = 1/2$. If we assume j_i is determined only by its environment of nearest neighbors (which are in layers $i - 1$ and i), then we have $j_2 = j_3 = \dots = j_\infty$; but j_1 would be different in general. Thus the chemical potential μ_i at which the phase transition occurs ($\theta_i = 1/2$) in the i th layer is

$$\begin{aligned} \mu_i &= \mu^* - kT \ln j_\infty + U_i = \mu_{\text{gas}}^\circ \\ &= \mu^\circ(T) + kT \ln p_i \quad (3) \\ & \quad i = 2, 3, \dots \end{aligned}$$

where p_i is the equilibrium gas pressure (or fugacity, for an imperfect gas) and μ° is a "standard free energy". For the first layer

$$\mu_1 = \mu^* - kT \ln j_1 + U_1 = \mu^\circ(T) + kT \ln p_1 \quad (4)$$

Because $j_1 \neq j_\infty$ (and for other reasons), the first layer is exceptional. In the following we confine ourselves primarily to $i = 2, 3, \dots$

In the limit $i \rightarrow \infty$

$$\mu_\infty = \mu^* - kT \ln j_\infty + U_\infty = \mu^\circ(T) + kT \ln p_\infty \quad (5)$$

where p_∞ is the vapor pressure of bulk adsorbate at T . Combining eqs. 3 and 5

$$\begin{aligned} \ln \frac{p_i}{p_\infty} &= \frac{U_i - U_\infty}{kT} = \frac{\alpha \pi n_a \alpha_a}{2kTh_a^4} \sum_{j=1}^{\infty} j^{-4} - \\ & \quad \frac{\pi n_a \alpha_a}{2kTh_a^4} \sum_{j=0}^{\infty} \left(i - 1 + \frac{h}{h_a} + j \frac{h_a}{h_a} \right)^{-4} \quad (6) \end{aligned}$$

This equation relates the "corresponding" equilibrium gas pressures for the i th layer and the limiting layer $i \rightarrow \infty$.

Although eq. 6 itself can be used in applications, a much simpler relation is obtained if we introduce the further approximation of setting h and h_s equal

(10) The Ising model for a two-dimensional hexagonal lattice should be able to furnish μ^* to a very good degree of approximation in most cases. But the absolute value of μ^* from a particular model is not needed for present purposes.

to h_a . This approximation would in general be serious for $i = 1$ but much (and progressively) less so for higher layers. Equation 6 simplifies to

$$\ln \frac{p_i}{p_\infty} = -\beta f_i \quad (7)$$

where

$$\beta = \frac{\pi}{2kTh_a^4} (n_s \alpha_a - n_a \alpha_a) \quad (8)$$

$$f_i = \sum_{j=i}^{\infty} j^{-4} = \frac{\pi^4}{90} - \sum_{j=1}^{i-1} j^{-4} \quad (9)$$

Table I gives the first few values of f_i . Equation 7 is the analog of the Frenkel-Halsey-Hill equation⁶ for a hypothetical homogenous adsorbate.

TABLE I

i	f_i	i	f_i
1	1.08232	4	0.007478
2	0.08232	5	.003571
3	.01982	6	.001971

We adopt eq. 7 as our "ideal" or "reference" equation; the approximation made in passing from eq. 6 to eq. 7 will then be included in the possible causes for deviation of experimental data from eq. 7. As already indicated, the first adsorbed layer should in any case be expected to be anomalous.

Application to Argon and Krypton.—We use the published curves^{2,3} for argon and krypton on a graphitized carbon black which presumably has a nearly uniform surface.¹ In order to relate θ to the amount of adsorption, it is assumed that inflection points and the centers of steps occur at $\theta = 1.5, 2.5$, etc. On this basis we find the correspondences

$$\begin{aligned} \theta = 1 &\leftrightarrow \theta \text{ (argon, ref. 2) } = 1.09 \text{ (av. of 1.10, 1.06 and 1.11 for } i = 2, 3, 4) \\ &\leftrightarrow \theta \text{ (krypton, ref. 2) } = 1.02_3 \text{ (av. of 1.02}_7 \text{ and 1.02 for } i = 2, 3) \\ &\leftrightarrow v \text{ (krypton, ref. 3) } = 3.11 \text{ (av. of 3.06 and 3.14 for } i = 2, 3) \end{aligned}$$

The average for the last case is actually 3.10 but we use 3.11, since this is the location of the minimum in the integral molar entropy curve,³ which is available in this case only.

Table II gives calculated values of β from eq. 7 and Table I for argon² and krypton² at 77°K. and krypton³ at 90°K.

TABLE II

i	θ	Argon ² at 77°K.		Krypton ² at 77°K.		Krypton ³ at 90°K.	
		p/p_∞	β	p/p_∞	β	p/p_∞	β
1	0.5	0.00173	5.9	0.00170	5.9
2	1.5	.350	12.8	.411	10.8	0.449	9.7
3	2.5	.639	22.6	.810	10.6	.831	9.3
4	3.5	.837	23.8	.945	7.6	.963	5.0
5	4.5	.913	25.5	.9933	1.9
6	5.5	.952	25.0

For argon, the third and higher layers give essentially the same β and hence illustrate the concept of corresponding states discussed above. But the

(11) A new effective n_s should be used for n_s in the following equations in order to preserve the true volume density of the adsorbent

$$n_{s(\text{eff.})} = h_a n_{s(\text{true})} / h_{s(\text{true})}$$

second layer (and the first as expected) is anomalous. For krypton, the second and third layers are "normal" (or "corresponding") but the higher layers are anomalous. This is obvious qualitatively, of course, since the steps unexpectedly disappear completely¹² beginning with the fourth layer. This aspect of the krypton isotherm is discussed in detail by Singleton and Halsey.³

Discussion. (1).—The distance h_a between layers¹³ in solid argon is 3.16 Å. and in solid krypton 3.36 Å. The interlayer distance h_s in graphite is 3.35 Å. In the absence of direct experimental information, as good an assumption as any is that, in Fig. 2, $h = (h_a + h_s)/2$. Thus one possible reason why the second adsorbed layer of krypton is normal, while the second layer of argon is not, is that the simplification made in passing from eq. 6 to eq. 7 introduces an appreciable error for argon but not for krypton. Other contributions to this difference in behavior could arise, for example, from the detailed nature of the packing of argon and krypton atoms on a graphite surface.

(2).—The steps in the argon isotherm are less pronounced than in the krypton isotherms. One reason for this is that the corresponding temperature of argon is higher, though again the details of the packing of the argon and krypton atoms could be important or even dominant. Argon at 77°K. has a corresponding temperature of $T/T_t = 0.92$, while krypton has 0.66 at 77°K. and 0.78 at 90°K., where the reference temperature T_t is the triple point temperature.

One would expect that the critical temperature T_{2c} for the condensation of a new crystalline layer should be provided fairly accurately (in any layer but the first) by the two-dimensional hexagonal (honeycomb) Ising model.^{10,14} If the nearest neighbor interaction energy is $-w$ (only nearest neighbor interactions are taken into account in the theory), the critical temperature is given by $w/kT_{2c} = 2.634$. If $-\epsilon$ is the potential energy at the minimum (corresponding to a distance r^*) in the interaction curve for a pair of gas molecules, and if we take r^* as the nearest neighbor distance in the hexagonal lattice, then it is easy to calculate by summation that higher neighbor attractive interactions lower the potential energy of the lattice further by 11.5%. Thus the effective w (if we take care of higher neighbors in this way) is 1.115 ϵ , or $\epsilon/kT_{2c} = 2.36$.

Now, from the usual three-dimensional law of corresponding states,^{15,16} $T_t/T_{3c} = 0.555$, $\epsilon/kT_{3c} =$

(12) In general, steps are expected to die out gradually owing to an accumulation of imperfections in the building of the lattice.

(13) Calculated from the density at the triple point.

(14) See, for example, G. H. Wannier, *Rev. Modern Phys.*, **17**, 50 (1945).

(15) See, for example, E. A. Guggenheim, "Thermodynamics," North-Holland Publishing Co., Amsterdam, 1949.

(16) T. L. Hill, *J. Chem. Phys.*, **16**, 399 (1948).

0.783 and hence $\epsilon/kT_t = 1.411$, where T_{3c} is the usual gas-liquid three dimensional critical temperature. Thus $T_{2c}/T_t = 0.60$, which should be compared with the values above of 0.92 (argon) and 0.66 and 0.78 (krypton). According to this estimate, the experimental temperature in all of these cases is above T_{2c} . This could account for the fact that the steps are not vertical (especially in the argon isotherm), though again other possible contributions must be considered: adsorbent not perfectly uniform; and imperfect packing of adsorbed molecules on the adsorbent and on each other. Measurement of isotherms with steps over a wide temperature range would be of considerable interest in this connection.¹⁷

Incidentally, the value $T_{2c}/T_{3c} = 0.783/2.36 = 0.33$ refers here to *localized* adsorption in a hexagonal lattice (with an optimal nearest neighbor distance); this is to be compared with the ratio⁶ $T_{2c}/T_{3c} \cong 0.53$ for mobile adsorption.

(3).—Let us test the simple assumption that the discrepancy between $\beta = 5.9$ (first layer) and $\beta = 10.7$ (second and third layers) for krypton in Table II is due entirely to the difference between j_1 and j_∞ , referred to above. Instead of eq. 7 we have

$$\ln \frac{p_1}{p_\infty} = -\beta f_1 + \ln \frac{j_\infty}{j_1} \quad (10)$$

Using $\beta = 10.7$, the experimental value of p_1/p_∞ in Table II, and classical vibrational partition functions for order of magnitude purposes, we find

$$\ln \frac{j_\infty}{j_1} = 5.2 = \ln \left(\frac{kT}{h\nu_\infty} \right)^3 \left(\frac{h\nu_1}{kT} \right)^3$$

or

$$\nu_1/\nu_\infty = 5.7$$

One expects $\nu_1/\nu_\infty > 1$, but $\nu_1/\nu_\infty = 5.7$ seems too high to be reasonable.

(4).—The decrease in β from 10.7 (77°K.) to 9.5 (90°K.) for krypton in Table II is in good agreement with the $\beta \sim 1/T$ dependence predicted by eq. 8 (neglecting the effect of temperature on n_s , n_a and h_a in first approximation).

(17) NOTE Added May 17, 1955.—The author is indebted to Dr. Hadden Clark for making available before publication (*THIS JOURNAL*, **59**, 1068(1955)) a manuscript describing the measurement of the krypton adsorption isotherm on the same surface as above^{2,3} at 70.2°K. Vertical steps are obtained at this temperature in the first and second layers, but the third layer step is not vertical.

We have here $T/T_t = 0.605$. Thus the experimental value of T_{2c}/T_t (for the second layer) appears to be between 0.605 and 0.66 (see above), say at 0.62. This is in good agreement with the theoretical value of 0.60 deduced above.

The third layer step is presumably not vertical at 70.2°K. because of lattice building imperfections.

Whereas one might expect different critical temperatures in first and second layers because of somewhat different horizontal nearest neighbor distances and slight heterogeneities in the surface, in the present system the experimental value of T_{2c}/T_t for the first layer also appears to be in the range 0.605 to 0.66 (the first layer step is vertical at 70.2°K. but not at 77°K.).

VERTICAL DISCONTINUITIES IN THE ADSORPTION ISOTHERM OF KRYPTON ON GRAPHITIZED CARBON BLACK

BY HADDEN CLARK

Research Service Department, American Cyanamid Co., Stamford, Conn.

Received May 7, 1955

Adsorption isotherms of krypton on graphitized carbon black have been measured at 70.2°K., with attainment of equilibrium checked by desorption measurements wherever experimentally feasible. The risers of the stepwise isotherm were found to be vertical discontinuities in both the first and second layer adsorption. The pressures at which these discontinuities occur have been calculated using an equation for stepwise isotherms developed by Singleton and Halsey. Good agreement is found between experiment and theory. The calculated isosteric heats of adsorption are found to agree with the heats measured calorimetrically by Amberg, *et al.* These calculations support the validity of the observed vertical discontinuities as representing true equilibrium conditions.

There has been some difference of opinion as to the validity of observed vertical discontinuities in adsorption isotherms. In reviewing this controversy, recent publications^{1,2} have emphasized the need for careful experimental technique, since an observed discontinuity may be due to lack of equilibrium. An indisputable check is the determination of both adsorption and desorption isotherms. If the two coincide, equilibrium has been reached. This precaution was observed in previous work on two-dimensional critical temperatures of gases adsorbed on sodium chloride.³

A primary requirement for adsorption at constant pressure is that a large fraction of the solid surface be energetically homogeneous.⁴ An exceptionally uniform surface has been found in a graphitized carbon black (P-33, 2700°) produced by Godfrey L. Cabot, Inc.⁵ Clear stepwise isotherms of rare gases

adsorbed at 77°K. on this surface have been reported.⁶ These steps, however, are not vertical. To determine whether a vertical discontinuity results when the temperature is lowered, isotherms of krypton adsorbed on graphitized carbon black were measured at 70.2°K.

Experimental Apparatus and Procedure

A Wooten and Brown⁷ adsorption apparatus was used with two McLeod gages to cover the pressure range up to 1 mm. A Pirani gage was also employed to follow pressure changes in the system. At a pressure of 0.1 mm., sensitivity of the gage was such that a change of 1 mm. on the galvanometer scale equalled a pressure change of 0.0003 mm. The temperature was maintained by use of a cryostat⁸ containing liquid nitrogen at a constant pressure. The graphitized carbon black (P-33, 2700°) was obtained from Dr. W. R. Smith of Godfrey L. Cabot, Inc., Cambridge, Mass. A very small sample (0.087 g.) spread on the bottom of a flattened glass bulb allowed rapid attainment of equilibrium. The solid was evacuated for five days at 300° to the "stick" vacuum of a 10⁻⁶ mm. McLeod gage. The sample was then alternately saturated with krypton at 77°K. and evacuated at 300° several times. Between experiments, overnight evacuation was deemed sufficient.

To ensure that true equilibrium was reached, both adsorption and desorption measurements were made for second and third layer adsorption. Unfortunately, desorption measurements were not feasible for checking the first layer adsorption. At such low pressures only a minute increment of gas would be desorbed at each point, making the determination of the full step a very lengthy procedure.

Results and Discussion

Experimental data are shown in Fig. 1. Vertical discontinuities are found both in the first layer adsorption on the carbon surface, and during the subsequent adsorption of krypton in the second layer. The step was no longer vertical when the third layer of krypton was being adsorbed.

Although only adsorption points were used to determine the amount of krypton adsorbed at the lowest pressures, duplicate experiments indicated that approximately 0.9 cc. was adsorbed at constant pressure. As the carbon surface itself is known to be very uniform, these data indicate that the first layer of adsorbed krypton atoms presents an extremely compatible surface for further adsorption. However, because of the lower adsorption energies involved in the second layer, it is expected that the critical temperature at which the riser of the second layer becomes vertical will be lower than the temperature at which the riser of

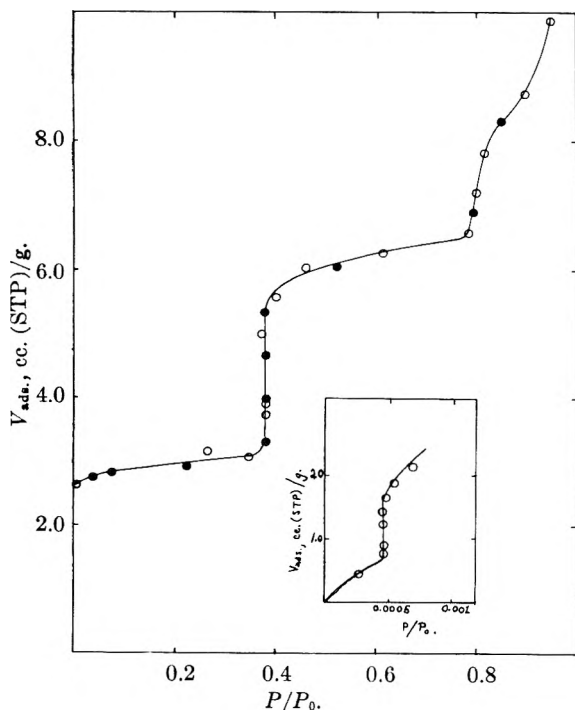


Fig. 1.

- (1) E. V. Ballou, *J. Am. Chem. Soc.*, **76**, 1199 (1954).
- (2) M. L. Corrin and C. P. Rutkowski, *THIS JOURNAL*, **58**, 1089 (1954).
- (3) S. Ross and H. Clark, *J. Am. Chem. Soc.*, **76**, 4291 (1954).
- (4) S. Ross and W. Winkler, *ibid.*, **76**, 2637 (1954).
- (5) M. H. Polley, W. D. Schaeffer and W. R. Smith, *THIS JOURNAL*, **57**, 469 (1953).

- (6) J. H. Singleton and G. D. Halsey, Jr., *ibid.*, **58**, 1011 (1954).
- (7) L. A. Wooten and J. R. C. Brown, *J. Am. Chem. Soc.*, **65**, 113 (1943).
- (8) W. J. C. Orr, *Proc. Roy. Soc. (London)*, **A173**, 349 (1939).

the first step is vertical. It is of interest to note that the stepwise adsorption of the third layer does not take place at constant pressure.

The position of the risers in the isotherm can be calculated theoretically using an equation developed by Singleton and Halsey.⁹ They have modified Hill's equations¹⁰ for stepwise isotherms, and, with appropriate assumptions, obtained an equation giving the position of the riser of the n th step in terms of p/p_0

$$\ln(p/p_0)_n = -E_1/n^3kt + (w/kt)(1 - g) \quad (1)$$

E_1 is an energy of adsorption, w the lateral interaction energy, and g a lattice compatibility factor. Using data for krypton adsorption on P-33 at 77°K., Singleton and Halsey calculated E_1/kt and $(w/kt)(1 - g)$ to be 7.9 and 0.09, respectively. These numerical values, corrected for the change in temperature, were used to apply their equation to the adsorption isotherm at 70.2°K.

The partial pressure at which the first riser occurs was corrected for thermal transpiration, using the equation¹¹

$$P_1/P_2 = (T_1/T_2)^{1/2} \quad (2)$$

This equation is valid where the mean free path of the gas is very large compared to the diameter of the tubing. Results of the comparison are shown in Table I and it can be seen that agreement is very good for all three steps.

(9) J. H. Singleton and G. D. Halsey, *Can. J. Chem.*, **33**, 184 (1955).

(10) T. L. Hill, *J. Chem. Phys.*, **15**, 767 (1947).

(11) S. C. Liang, *Can. J. Chem.*, **33**, 279 (1955).

TABLE I
POSITION OF THE RISERS IN TERMS OF p/p_0

	Step I	Step II	Step III
p/p_0 { Calcd.	1.9×10^{-4}	0.37	0.79
{ Exptl.	2.2×10^{-4}	0.38	0.80

TABLE II
HEATS OF ADSORPTION (CAL. /MOLE)

	Step I	Step II	Step III
Calcd. (isosteric)	4,300	2,700	2,600
Calorimetric (Amberg, <i>et al.</i>)	4,400	2,800	2,700

Approximate isosteric heats of adsorption were calculated f from isotherms at 70 and 77°K., and compared with heats of adsorption measured experimentally by Amberg, *et al.*¹² The values are in good agreement with those measured calorimetrically. Agreement of the heat of adsorption in the first layer, however, is probably fortuitous since the higher pressure was not corrected for thermal transpiration. Thermal transpiration data for this pressure range are not available, and the pressure is too high for equation 2 to apply.

The preceding data and discussion are felt to provide definite evidence for the existence of vertical discontinuities in adsorption isotherms.

Acknowledgment.—The author wishes to thank Dr. G. D. Halsey, Jr., for the suggested use of his theoretical isotherm equation.

(12) C. H. Amberg, W. B. Spencer and R. A. Beebe, *ibid.*, **33**, 305 (1955).

DIFFERENTIAL THERMAL ANALYSIS OF SOME HETEROPOLY ACIDS OF MOLYBDENUM AND TUNGSTEN

BY SHERWOOD F. WEST^{1,2} AND L. F. AUDRIETH

Department of Chemistry, University of Illinois, Urbana, Illinois

Received May 9, 1955

The method of differential thermal analysis together with X-ray diffraction and dehydration studies has been employed to investigate the thermal behavior of some 12-heteropoly molybdic and tungstic acids. Heating curves for the hydrated acids reveal the same pattern type in all cases. The gradual, low temperature endotherm observed is ascribed to the removal of water. Such water is considered to be zeolitic in nature, since its removal does not alter the crystal lattice. The vigorous, high temperature exotherm recorded in each case marks the decomposition of the cage-like structure of the heteropoly compound to give a more compact crystalline product consisting largely of the oxides of Mo(VI) and W(VI), respectively. X-Ray powder diffraction patterns of acid samples heated to constant weight at successive temperatures covering the complete heating range have established these structural changes.

Introduction

Even before the structures of the hydrated, 12-heteropoly acids of molybdenum and tungsten had definitely been established, Scroggie and Clark³ found that samples of 12-silicotungstic acid, air-dried, dried at 100°, and dried at 220° gave powder diffraction patterns having the same d-spacings. When dried at 100°, this substance contains 8H₂O. Six molecules of water can be removed by fur-

ther dehydration without altering the structure to give the product SiO₂·12WO₃·2H₂O, which is regarded as the anhydrous acid. Ferrari and Nanni⁴ later studied the ammonium, potassium and thallium salts of the 12-acids of molybdenum and tungsten and from X-ray studies of the anhydrous materials prepared by prolonged heating at 140° concluded that the water content of the highly hydrated salts is zeolitic in nature. Practically no other data are to be found relating to the thermal stability of these acids or their salts, yet they are used widely at elevated temperatures where they function as highly active catalysts.

(1) Abstracted in part from the doctoral dissertation presented to the Graduate College of the University of Illinois, 1955.

(2) Victor Chemical Works Research Fellow in Chemistry, University of Illinois, 1954-1955.

(3) A. G. Scroggie and G. L. Clark, *Proc. Nat. Acad. Sci.*, **15**, 1 (1929); A. G. Scroggie, Thesis, University of Illinois, 1928.

(4) A. Ferrari and O. Nanni, *Gazz. chim. ital.*, **69**, 301 (1939).

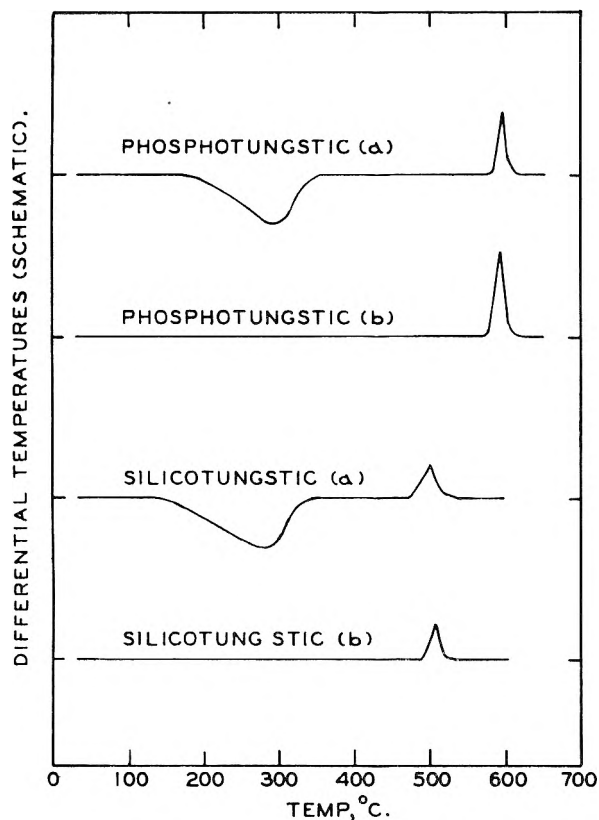


Fig. 1.—Differential thermal analysis of some heterotungstic acids.

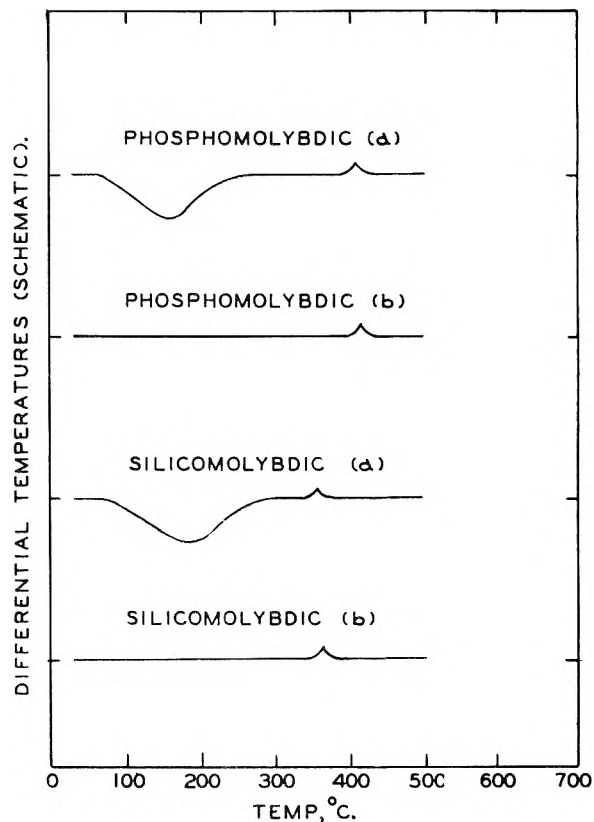


Fig. 2.—Differential thermal analysis of some heteromolybdic acids.

The present investigation was undertaken to study the thermal stability of some hydrated 12-heteropoly molybdic and tungstic acids by the method of differential thermal analysis (D.T.A.). This technique is particularly suitable for detecting reactions that occur in the solid state. Weight loss studies coupled with X-ray diffraction data have served to define the indicated structural changes with some degree of certainty.

Experimental

Preparation of Materials.—The hydrated hetero acids of Mo(VI) and W(VI) with the formulas $H_4[SiMo_{12}O_{40}] \cdot xH_2O$, $H_4[SiW_{12}O_{40}] \cdot xH_2O$, and $H_3[PW_{12}O_{40}] \cdot xH_2O$ were prepared by acidification of the sodium salts of the component acids and subsequent extraction with ether as directed by North.⁵ The preparation of 12-phosphomolybdic acid⁶ differs in that the isolation of the free acid does not involve an ether extraction step. An aqueous solution (1.5 l.) of molybdic oxide (1 mole) and phosphoric acid ($1/12$ mole) is first boiled for three hours with rapid stirring. The unreacted MoO_3 is removed by filtration and the solution concentrated to a volume of 100 ml. Cooling of the concentrate followed by crystallization and filtration yields 120 g. of wet crystals. The product is dried *in vacuo* over concentrated sulfuric acid without being washed to give 101 g. of the desired product in the form of deep yellow crystals.

Experimental Procedure.—Ten-gram samples of the various hetero acids were heated at the rate of 8–10° per minute employing a D.T.A. apparatus described previously.⁷ The resulting heating curves are depicted schematically in Figs. 1 and 2. Since all thermograms revealed a single broad, low temperature endotherm for each of the hydrated samples (curves labeled (a)), repeat runs were made (curves

labeled (b)) on specimens dried to constant weight above the endothermic peak temperatures. The dehydrated materials were employed in order to establish with greater certainty the temperatures at which the exothermic breaks occur. The thermal data are summarized in Table I. It is to be noted that the hetero-tungstic acids are more stable thermally than the hetero-molybdic acids. In each case, compounds containing a central phosphorus atom are more stable thermally than those containing silicor.

X-Ray powder diffraction patterns of the heteropoly acids heated to temperatures above the exotherm were found in all cases to be characteristic of the heavy metal oxide. The powder patterns were recorded on film employing a camera of 7 cm. radius and nickel filtered $Cu K\alpha$ radiation. The d-spacings are plotted as functions of the goniometer angle and compared with the patterns of pure MoO_3 and WO_3 in Fig. 3. The patterns of the pure oxides were obtained from the A. S. T. M. Card Index file.

Examination of Fig. 3 reveals certain dissimilarities between the heteropoly acid residues and the corresponding heavy metal oxides. The discrepancies are particularly noticeable in the hetero-tungstic acid series. The absence of some of the lines in the corresponding acid residues may be due in part to the low degree of crystallinity in these residues. For comparison purposes, X-ray spectrometer patterns of the acid residues as well as of the pure metal oxides listed in Fig. 3 were recorded with the aid of a General Electric XRD-3 spectrometer. These patterns emphasize the noticeably higher background in the acid residues, indicating the presence of an amorphous phase. The resultant scattering is thus probably responsible for obscuring some of the weaker lines. A general line broadening is also apparent in the ignited acids, which may be attributed to reduced particle size.

In order to trace the decomposition of these compounds, heteropoly acid specimens were next heated to constant weight at successive temperatures covering the complete heating range. Intermediate temperatures were chosen to bracket the reactions indicated by the heating curves. Samples were then withdrawn for X-ray analysis when weight losses were no longer apparent.

In the case of the hetero-tungstic acids, the structure of

(5) H. S. Booth, "Inorganic Syntheses," Vol. I, McGraw-Hill Book Co., Inc., New York, N. Y., 1939.

(6) A. Linz, *Ind. Eng. Chem., Anal. Ed.*, **15**, 459 (1942).

(7) R. K. Osterheld and L. F. Audrieth, *THIS JOURNAL*, **56**, 38 (1952).

TABLE I
 THERMAL BEHAVIOR OF SOME HETEROPOLY ACIDS

	Drying temp., °C.	Endothermic, ^a °C.	Exothermic, ^a °C.
Phosphotungstic	(a) 25, vac.-H ₂ SO ₄	175-296	580-595
	(b) 300		573-592
Silicotungstic	(a) 25, vac.-H ₂ SO ₄	140-278	470-500
	(b) 300		487-508
Phosphomolybdic	(a) 25, vac.-H ₂ SO ₄	63-159	390-408
	(b) 200		397-412
Silicomolybdic	(a) 25, vac.-H ₂ SO ₄	64-180	336-355
	(b) 200		340-362

^a The recorded temperatures are considered accurate to $\pm 5^\circ$.

the free acid was maintained up to the exothermic decomposition point. A phosphotungstic acid specimen heated at 100, 200, 300 and 400° gave powder diffraction patterns having the same d-spacings. This material remained colorless until heated to 500°. At this point, the acid turned yellow and yielded a diffraction pattern characterized by high background and in which the lines were blurred. Further heating of the sample to constant weight at 575° yielded an olive green product whose diffraction pattern was identified as that of tungstic oxide.

A silicotungstic acid specimen heated at 100, 250 and 300° remained colorless and yielded powder diffraction patterns having the same d-spacings. When heated to 450°, the acid turned yellow; complete decomposition had occurred. A diffraction pattern characteristic of WO₃ was obtained.

Both silico- and phosphomolybdic acids showed visible evidence of decomposition when heated for longer periods of time, even at 100°. Changes in color from yellow to green to pale blue were observed on progressive heating. Samples of these materials heated at 100 and 200° yielded diffraction patterns characterized by high background, indicating the presence of an amorphous phase. However, the presence of a few sharp lines in these patterns confirms the existence of a definite structure in this temperature range. When heated at 450°, the same samples yielded diffraction patterns clearly characteristic of molybdenum trioxide. Complete decomposition had thus been brought about at this temperature.

Discussion

An examination of the heating curves reveals the same pattern in all four cases. The gradual, low temperature endotherm may be ascribed to the removal of water. Water in excess of the composition of the anhydrous acid is apparently zeolitic in nature, since its removal does not alter the crystal lattice. The high temperature exotherm recorded in each case marks the decomposition of the complex heteropoly anionic structure, yielding essentially a mixture of oxides. Although evidence has been advanced for the existence of small amounts of other compounds in some of these residues,⁸ diffraction patterns of the ignited acids reveal only lines characteristic of the heavy metal oxide. This is not surprising if the low percentage content of SiO₂ or P₂O₅ in the hetero-molybdic acid residues is taken into consideration (3.48% SiO₂ in SiO₂·12MoO₃; 3.95% P₂O₅ in P₂O₅·24MoO₃).

The relative instability of the hetero-molybdic acids compared with the corresponding tungsten compounds undoubtedly is due to the instability of MoO₃, itself. Decomposed hetero-molybdic acids are always tinted blue, indicating the presence of oxidation states of molybdenum lower than VI. Impurities such as dust apparently bring about this reduction. The volatility of MoO₃ may also

be a contributing factor. This oxide melts at 795°, but it has an appreciable vapor pressure well below its melting point (0.30 mm. at 700°). Thus MoO₃ may be sublimed freely from hetero-molybdic acid residues at 700°. Tungstic oxide, by contrast, melts at 1,473° and boils above 1,750°.

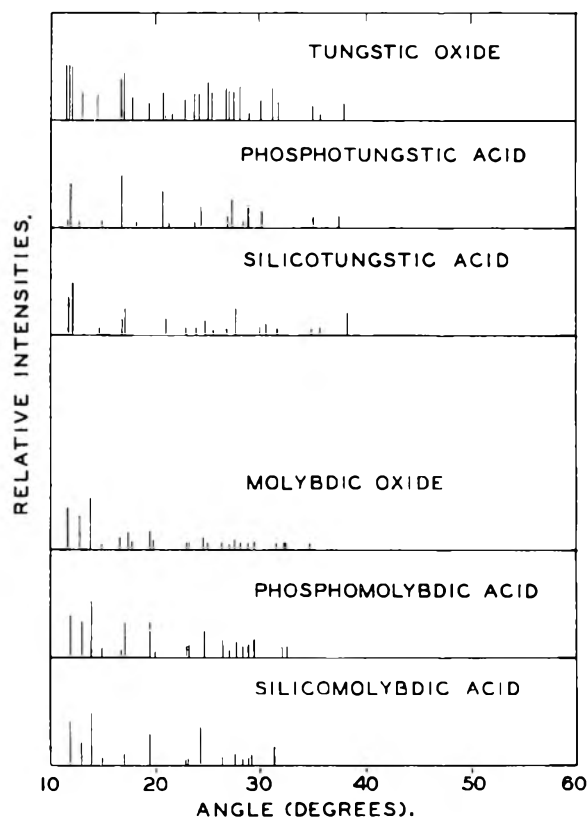


Fig. 3.—Comparison of X-ray diffraction patterns of WO₃, MoO₃ and products obtained by thermal treatment of some hetero-tungstic and hetero-molybdic acids.

The enhanced thermal stability of the phospho acids would indicate that the higher positive charge of the P(V) is more effective in binding the anion together. Metatungstic acid, H₃[W₁₂O₄₀] \cdot xH₂O, is said to decompose at 50°.⁹ When the void in the center of the [W₁₂O₄₀]⁻⁶ anion is filled with a Si⁺ ion, the decomposition temperature is raised by approximately 400°, and still higher when a P⁺ ion is substituted. Apparently, the presence of a central,

(8) M. Nardelli and O. Seaglioni, *Gazz. chim. ital.*, **81**, 464 (1951).

(9) M. Sobolew, *Z. anorg. Chem.*, **12**, 30 (1896); A. Rosenheim and F. Kohn, *ibid.*, **69**, 254 (1941).

positively charged species stabilizes the complex against thermal vibrations and resultant decomposition.

The same factors are also operative in the molybdenic acids, but in this series no meta acid has been prepared. This fact lends further emphasis to the lesser stability of this series. In the light of the previous discussion of relative stabilities, one would be forced to predict that 12-acids containing boron, for example, should be even less stable thermally than those containing silicon. As 12-boromolybdenic acid has not as yet been prepared, this line of reasoning does not seem to be inconsistent.

The differential thermal method is a dynamic rather than a static one, and this must be borne in mind when interpreting such heating curve data. The thermal reactions are not instantaneous, and they are recorded as functions of the sample temperature, which is continuously increasing as the reaction takes place. It is thus not surprising that some of the reactions under study may be brought about by prolonged heating at temperatures well below those indicated by the thermograms.

The technique of differential thermal analysis has recently been used to good advantage in the investigation of certain catalyst powders.¹⁰ That the heteropoly acids and their salts are useful as catalysts is quite apparent from the volume of patent literature¹¹ covering this particular application. Most of these patents specify pre-ignition of the catalyst at several hundred degrees. This treatment precludes the existence of the heteropoly acids, as such, in many instances. Past work has served to emphasize the desirability of a large surface area in a highly active catalyst. The anhydrous heteropoly acids may be prepared simply by drying at the proper temperature. In this condition, they should offer a very porous surface of high area, by virtue of the holes left in the lattice due to the removal of water. Such a surface might be expected to be far more reactive than that encountered in the ignited acid residues.

(10) V. S. Ramachandran and S. K. Bhattacharyya, *J. Sci. Ind. Res. (India)*, **13A**, 365 (1954).

(11) D. H. Killeffer and A. Linz, "Molybdenum Compounds," Interscience Publishers, Inc., New York, N. Y., 1952.

SOLVOLYSIS OF HAFNIUM AND ZIRCONIUM TETRACHLORIDES IN METHYL AND ETHYL ALCOHOLS^{1,2}

BY CLYDE R. SIMMONS AND ROBERT S. HANSEN³

Contribution No. 390 from the Ames Laboratory, Iowa State College, Ames, Iowa

Received May 9, 1955

Equilibrium constants \bar{K}_n for the reactions $MCl_4 + nROH \rightleftharpoons MCl_{4-n}(OR)_n + nHCl$, where M is Zr^{IV} or Hf^{IV}, ROH is methanol or ethanol, and $n = 1, 2, 3, 4$, were obtained at 25° by potentiometric dilution measurements and, independently, by conductimetric dilution measurements. Results obtained by the two different methods were found to be in good agreement. Solvolysis of both tetrachlorides was more extensive in methanol than in ethanol. Solvolysis of HfCl₄ was more extensive than that of ZrCl₄ in both solvents, the difference being greater in methanol than in ethanol.

Introduction

Previously reported work from this Laboratory has shown that zirconium spectrographically free of hafnium can be prepared by passing a solution of zirconium and hafnium tetrachlorides in methanol through a silica gel column if the original hafnium-to-zirconium ratio is about 0.02 (this is the common ratio in naturally occurring zirconium sources). By differential stripping of the silica gel following the absorption purification, fractions with hafnium-to-zirconium ratios of about 2 were obtained.⁴ Several alcohols were investigated as solvents; efficiency of separation was in the order methanol > ethanol > propanol-1 > propanol-2. The present investigation was undertaken to clarify the solvent effect in this separation.

Theoretical

In the reaction

(1) Work was performed in the Ames Laboratory of the Atomic Energy Commission.

(2) Based in part on a dissertation submitted by Clyde Robert Simmons in partial fulfillment of the requirements for the degree of Master of Science, Iowa State College, Ames, Iowa, December, 1954.

(3) Institute for Atomic Research and Department of Chemistry, Iowa State College, Ames, Iowa.

(4) (a) R. S. Hansen and K. Gunnar, *J. Am. Chem. Soc.*, **71**, 4158 (1949); (b) R. S. Hansen, K. Gunnar, A. Jacobs and C. R. Simmons, *ibid.*, **72**, 5043 (1950).



we shall assume activities of MCl_4 and $MCl_{4-n}(OR)_n$ equal to their concentrations and the activity of the solvent (ROH) equal to unity. Let $\beta = (a_{HCl})^{-1} = (\gamma_{\pm} C_{HCl})^{-2}$, where C_{HCl} is the free HCl concentration, let m_0 be the molarity of undissociated MCl_4 , and M_T the total concentration of M^{IV} in all forms. Then

$$C_{HCl} = m_0 \sum_{n=1}^4 n \bar{K}_n \beta^n \quad (2)$$

$$M_T = m_0 \left\{ 1 + \sum_{n=1}^4 \bar{K}_n \beta^n \right\} \quad (3)$$

whence

$$\bar{n} = \frac{C_{HCl}}{M_T} = \frac{\sum_{n=1}^4 n \bar{K}_n \beta^n}{1 + \sum_{n=1}^4 \bar{K}_n \beta^n} \quad (4)$$

If \bar{n} is obtained as a function of β experimentally, the constants \bar{K}_n can be obtained which represent this function as well as possible according to eq. 4. Approximate values of \bar{K}_1 and \bar{K}_2 can be obtained from intercept and limiting slope of a plot of (β/\bar{n})

against β ; approximate values of $K_n = \bar{K}_n/\bar{K}_n - 1$ can be obtained from the value of β at which $\bar{n} = n - 1/2$.⁵ The constants can then be refined by trial and error.

Experimental determination of the function $\bar{n}(\beta)$ involves determination of the quantities M_T , C_{HCl} and a_{HCl} . M_T can be established by preparation or by quantitative precipitation with ammonia and ignition to MO_2 . a_{HCl} can be inferred as a function of C_{HCl} from e.m.f. measurements on solutions of anhydrous HCl in alcohol using a cell containing hydrogen and silver-silver chloride electrodes, following the discussion given by Harned and Owen.⁶ The mean ionic activity coefficient γ_{\pm} for HCl can be established as a function of HCl concentration from these measurements. a_{HCl} can then be measured potentiometrically in the MCl_4 solution and C_{HCl} calculated, assuming that the dependence of a_{HCl} on C_{HCl} is unaffected by the presence of compounds such as $\text{M}(\text{OR})_n\text{Cl}_4 - n$. Alternately, the specific conductance of anhydrous HCl-alcohol solutions can be established as a function of C_{HCl} . The specific conductance of the MCl_4 -alcohol solution can then be measured, the C_{HCl} calculated, assuming the dependence of specific conductance on C_{HCl} is unaffected by the presence of compounds such as $\text{M}(\text{OR})_n\text{Cl}_4 - n$. a_{HCl} can then be calculated from C_{HCl} , the same assumption being involved.

Both methods were used in the present research.

Experimental

Commercial grade ZrCl_4 was freed from hafnium according to the procedures developed in this Laboratory,³ converted to the oxychloride, and the oxychloride further purified by recrystallization from 1:1 aqueous HCl solution. Hafnium oxide obtained from Union Carbide and Carbon Co., Oak Ridge, Tennessee, was converted to the tetrachloride, then to the oxychloride, and the oxychloride purified by recrystallization. The oxychlorides were then ignited to oxides in both cases, and the oxides converted to tetrachlorides by heating the oxides in a stream of helium and carbon tetrachloride to approximately 450° , the tetrachlorides subliming into a collector as formed. On completion of chlorination the CCl_4 supply was turned off, and the apparatus was swept out with a helium stream.

Methanol and ethanol were purified by the method of Lund and Bjerrum,⁷ followed by distillation through a 30-plate Oldershaw column at reflux ratio of 10:1.

Anhydrous hydrogen chloride was prepared by the action of concentrated reagent grade sulfuric acid on reagent grade sodium chloride, and was not further purified.

In preparation of solutions, considerable care was taken to avoid introduction of water, formation of water by reaction of HCl and alcohol, and loss of HCl in dissolution of the tetrachlorides. Solutions of anhydrous HCl in alcohols were prepared by bubbling anhydrous HCl through alcohols whose temperatures were maintained at 0° , the exit tube containing a bulb filled with drierite. Solutions of MCl_4 in alcohol were prepared as follows. The collector tube containing the MCl_4 sublimate was removed from the chlorinator train and immediately capped. The MCl_4 was then transferred to a clean, dry, 300-ml. flask. This flask was then connected to a second similar flask containing the alcohol. Connections were such that the assembly could be chilled to 0° , evacuated, closed, and mixture accomplished by inverting the assembly.

(5) J. Bjerrum, "Metal Ammine Formation in Aqueous Solutions," P. Haase and Son, Copenhagen, 1941.

(6) H. S. Harned and B. B. Owen, "The Physical Chemistry of Electrolytic Solutions," Chapter 11, Reinhold Publ. Corp., New York, N. Y., 1950.

(7) H. Lund and J. Bjerrum, *Ber.*, **64B**, 210 (1931).

Conductance measurements were made by means of an Industrial Instrument Co. Model RC-16 bridge, modified to permit null point determination by means of a Heathkit Model 08 oscilloscope. External capacitors were used as necessary to secure balance. Three conductance cells were constructed with cell constants 31.05, 5.52 and 0.78 reproducible to 1% determined from conductances of 0.1, 0.01 and 0.001 *M* aqueous KCl solutions, respectively.

Potentiometric measurements were made by means of a Leeds and Northrup Model 7552 potentiometer and Rubicon galvanometer. Palladized platinum-hydrogen electrodes were prepared according to the method of Hamer and Acree⁸ and silver-silver chloride electrodes according to the method of Noyes and Ellis⁹ as modified by Owen.¹⁰ Solutions once prepared and placed in the electrolytic cell were freed from oxygen by bubbling nitrogen presaturated with solvent alcohol through the solution for 30 minutes. Periods of from 1 to 4 hours were allowed for attainment of electrochemical equilibria, and results obtained were reproducible to 0.2 millivolt.

All measurements were made in cells immersed in a water-bath at a temperature of $25.00 \pm 0.05^\circ$.

Results

Results are presented graphically in Fig. 1. In this figure the ordinate is \bar{n} , the ratio of hydrochloro-

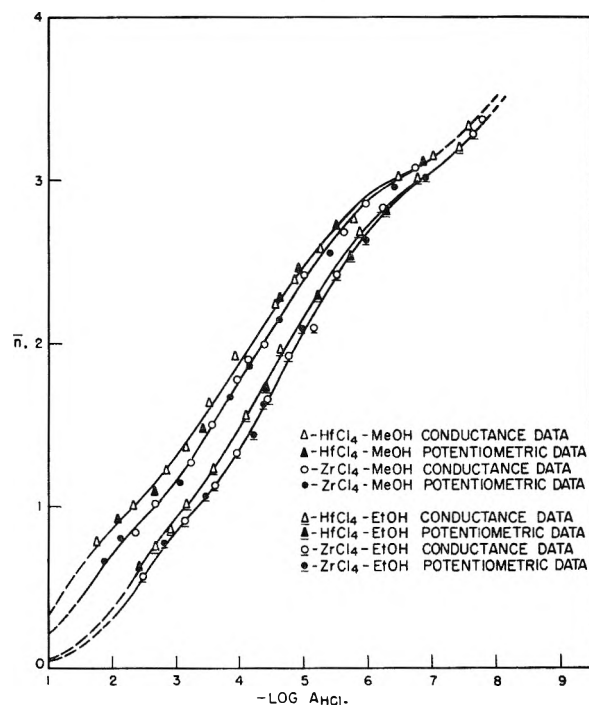


Fig. 1.—Solvolysis of ZrCl_4 and HfCl_4 in methanol and ethanol at 25° . Ordinate is the ratio of moles HCl formed by solvolysis to total moles M^{IV} . Abscissa is the negative logarithm (to base 10) of HCl activity. Curves are calculated from the listed constants; points are experimental.

ric acid concentration to total metal concentration. The abscissa is $-\log_{10} a_{\text{HCl}}$. Points are experimental and curves were calculated from eq. 4, using the following constants: ($p\bar{K}_n = -\log_{10} \bar{K}_n$).

System	$p\bar{K}_1$	$p\bar{K}_2$	$p\bar{K}_3$	$p\bar{K}_4$
$\text{ZrCl}_4\text{-CH}_3\text{OH}$	1.62	5.18	10.41	18.25
$\text{HfCl}_4\text{-CH}_3\text{OH}$	1.29	4.64	9.74	17.57
$\text{ZrCl}_4\text{-C}_2\text{H}_5\text{OH}$	2.40	6.68	12.20	20.09
$\text{HfCl}_4\text{-C}_2\text{H}_5\text{OH}$	2.30	6.35	11.81	19.68

(8) W. J. Hamer and S. F. Acree, *J. Research Natl. Bur. Standards*, **33**, 87 (1944).

(9) A. A. Noyes and J. H. Ellis, *J. Am. Chem. Soc.*, **39**, 2532 (1917).

(10) B. B. Owen, *ibid.*, **60**, 2229 (1938).

SOME PHYSICAL CHEMICAL STUDIES WITH HETEROPOLY ACIDS¹BY MELVIN C. BAKER,² PHILIP A. LYONS AND S. J. SINGER*Contribution No. 1302 from the Sterling Chemistry Laboratory, Yale University, New Haven, Connecticut**Received May 10, 1955*

The Svedberg equation for velocity ultracentrifugation has been tested with sedimentation, diffusion and density measurements of solutions of some heteropoly acids. The assignment of the formula $PW_{12}O_{42}^{-7}$ to the phosphotungstate ion at pH 4.5 can be justified, and the molecular weight calculated by the Svedberg equation is in good agreement with the formula weight. For phosphomolybdic acid at pH 4.5, however, the state of the solute is not certain. The calculated molecular weight is consistent with the formula $PMO_{11}O_{39}^{-7}$ for the major solute species.

With a view toward critically testing the fundamental equations of velocity ultracentrifugation, an investigation has been made of the sedimentation and diffusion properties of some heteropoly acids. These substances are apparently well-suited to these tests, because, although their molecular weights are in the range 1000-3000, they are dense and have relatively large and accurately determinable sedimentation coefficients; furthermore, some of them are well-defined pure compounds whose molecular weights are accurately known. Such studies with silico-12 tungstic acid (STA) $H_4SiW_{12}O_{40} \cdot xH_2O$, have been reported,³ for which the correct molecular weight (within about 1%) was obtained by use of the Svedberg equation for velocity ultracentrifugation,⁴ $M = RTs/(1 - \bar{V}_p)D$. In this paper, similar tests of the equation have been made with the analogous phosphotungstic and phosphomolybdic acids, which are somewhat complicated by the different chemical behavior of these substances compared to STA. These studies have also provided some new information concerning this behavior.

Materials and Methods.—C.P. phosphotungstic acid (PTA) was obtained in the hydrated form from the Fischer Scientific Co. It was stored over anhydrous $CaCl_2$ until it attained constant weight, and was then analyzed for residual water of hydration.³ The dried acid has the average composition $H_3PW_{12}O_{40} \cdot 5H_2O$ (expressed in a formula corresponding to silicotungstic acid) or $H_7PW_{12}O_{42} \cdot 3H_2O$ (expressed as a heptabasic acid, for reasons to be given).

Two samples of C.P. phosphomolybdic acid (PMA) were obtained from the Mallinckrodt Chemical Co., labeled $P_2O_5 \cdot 20MoO_3 \cdot xH_2O$ and $P_2O_5 \cdot 24MoO_3 \cdot xH_2O$. These are referred to as PMA-1 and PMA-2, respectively. In solution at pH 4.5, the sedimentation and diffusion properties of these samples are indistinguishable (see below). Most of the studies have been performed with PMA-1. Since it appears that no species of 10:1 Mo/P ratio exists⁵ and for other reasons to be developed, we consider PMA-1 to be $H_7PMO_{11}O_{39} \cdot xH_2O$.⁶ After PMA-1 was dried over $CaCl_2$, the residual hydration was determined by two independent methods. (a) An aliquot was precipitated with benzoin α -oxime,⁷ heated to constant weight at 500-525°, and weighed as MoO_3 . (b) An aliquot was heated to constant weight at 400° and weighed as $P_2O_5 \cdot 22MoO_3$. The results

indicated an average composition $H_7PMO_{11}O_{39} \cdot 5H_2O$ for PMA-1. PMA-2, after drying, was analyzed for residual water by the second method, being weighed as $P_2O_5 \cdot 24MoO_3$. Its average composition was $H_3PMO_{12}O_{40} \cdot 13H_2O$.

The ultracentrifuge, diffusion and density measurements were all performed in sodium acetate-acetic acid buffer, pH 4.58, ionic strength 0.2, by methods previously reported.³ In this buffer, the anions of the heteropoly acids sediment and diffuse without significant interference from electric potentials.

Experimental Results

The results of the sedimentation experiments (performed in the synthetic-boundary cell⁸) at various values of C , the weight per cent. heteropoly acid in solution, are given in Table I. The least-squares straight line through the PTA data satisfies the relation $S_{25}^w = 3.66 - 0.16C$ svedbergs, and for PMA-1, $S_{25}^w = 2.04 - 0.14C$. The results for PMA-2 fall on the same line. The estimated precision of S is $\pm 3\%$.

TABLE I
SEDIMENTATION CONSTANTS OF HETEROPOLY ACIDS^a

PTA		PMA	
Concn., ^b wt. %	S_{25}^w , svedbergs	Concn., ^b wt. %	S_{25}^w , svedbergs
1.103	3.49	1.056	1.90
1.473	3.50	1.056	1.86
2.881	3.13	2.087	1.79
2.881	3.25	2.087	1.73
2.881	3.12	2.087	1.68
3.469	3.18	3.144	1.71
4.808	2.74	3.840	1.54
7.178	2.60	3.840	1.51
7.178	2.64	5.569	1.23
9.201	2.13	5.569	1.24

^a In acetate buffer, pH 4.58, I/2 0.2. ^b % by weight of heteropoly acid in the buffer solution.

In order to make certain that the heteropoly acid anions sediment and diffuse without the interference of electric potentials in the acetate buffer, several sedimentation experiments were performed in buffers of the same pH and different ionic strength. The results of Table II indicate that at ionic strength 0.2 the electric potentials are negligible.³

The differential diffusion coefficients determined by the Gouy interferometric technique are given in Table III. For PTA, the drift in C_t over 85% of the gradient curve was less than 0.2%. This is a very important criterion for solute homogeneity. For PMA-1, however, a noticeable drift in C_t indicated that more than one solute species was present, and the diffusion coefficients are therefore less well-

(8) E. G. Pickels, W. F. Harrington and H. K. Schachman, *Proc. Nat. Acad. Sci.*, **38**, 943 (1952).

(1) Taken from the thesis submitted by M. C. Baker in partial fulfillment of the requirements for the Ph.D. degree at Yale University, June, 1955. This investigation was supported in part by grants from the Rockefeller Foundation, and from the Atomic Energy Commission under Contract AT-(30-1)-1375.

(2) Du Pont Predoctoral Fellow, 1954-1955.

(3) M. C. Baker, P. A. Lyons and S. J. Singer, *J. Am. Chem. Soc.*, **77**, 2011 (1955).

(4) T. Svedberg and K. O. Pedersen, "The Ultracentrifuge," Oxford Univ. Press, London, 1940.

(5) P. Souchay and J. Faucherre, *Bull. soc. chim., France*, **18**, 355 (1951).

(6) L. Malaprada, *Ann. chim.*, [10] **11**, 172 (1929).

(7) I. M. Kolthoff and E. B. Sandell, "Textbook of Quantitative Inorganic Analysis," Revised Ed., The Macmillan Co., New York, N. Y., 1943, p. 727.

TABLE II

EFFECT OF IONIC STRENGTH ON SEDIMENTATION OF HETEROPOLY ACIDS^a

Acid	Concn., wt. %	Ionic strength	S_{25}^w svedbergs	
			Obsd.	Calcd. ^b
PTA	4.32	0.3	3.01	2.96
	3.64	.1	3.05	2.93
PMA	3.64	.3	1.61	1.55
	3.63	.1	1.25	1.60

^a In acetate buffers, pH 4.58. ^b Interpolated in data of Table I.

defined. The data follow the relations: for PTA, $D_C = (3.701 + 0.176C) \times 10^{-6}$ cm.²/sec.; and for PMA-1, $D_C = (3.95 + 0.30C) \times 10^{-6}$, corrected to water at 25°.

TABLE III

DIFFUSION COEFFICIENTS OF HETEROPOLY ACIDS^a

PTA		PMA	
Concn., ^b wt. %	$D_{15}^w \times 10^6$, cm. ² /sec.	Concn., ^b Wt. %	$D_{15}^w \times 10^6$, cm. ² /sec.
1.015	3.905	0.434	4.08
3.065	4.266	.463	4.05
6.329	4.911	.481	4.15
		.945	4.32
		2.081	4.58
		2.785	4.87

^a In acetate buffer, pH 4.58, $\Gamma/2$ 0.2. ^b % by weight of heteropoly acid in the buffer solution.

Partial specific volumes for the anhydrous acids³ were calculated from density measurements at 25°. For $H_7PW_{12}O_{42}$, $\bar{V} = 0.142$; $H_7PMO_{11}O_{39}$ (PMA-1), $\bar{V} = 0.244$; and $H_3PMO_{12}O_{40}$ (PMA-2), $\bar{V} = 0.218$. The last value has no significance, since the species in solution (see below) is clearly not $PMO_{12}O_{40}^{-3}$.

Discussion

It is to be noted that the extrapolated values of S and D for PTA are considerably smaller than those for silicotungstic acid³ (which are 4.56 svedbergs and 4.515×10^{-6} cm.²/sec., respectively). Since the partial specific volumes and molecular weights of PTA and STA are very similar, these results indicate that the structures of the acid anions in solution at pH 4.5 must be quite different. (Under these conditions,³ STA exists as $SiW_{12}O_{40}^{-4}$). Additionally, the relative heterogeneity of solutions of PMA, as observed in diffusion, suggests that its behavior is different from STA.

The stability of the heteropoly acids has been the subject of a voluminous literature which cannot be reviewed here. In sufficiently acid solutions, the ions $SiW_{12}O_{40}^{-4}$, $PW_{12}O_{40}^{-3}$ and $PMO_{12}O_{40}^{-3}$ are stable. As the solutions are made more alkaline, however, the acids generally decompose stepwise into smaller ions. In our studies, the nature of the species at pH 4.5 only need be considered, and several observations bearing on this question will be discussed. Solutions of heteropoly acids in the acetate-acetic acid buffer, pH 4.58, ionic strength 0.2, generally exhibit a pH more acid than the buffer itself. If this pH change is attributed to the liberation of H ions from the heteropoly acids, a simple calculation, neglecting activity coefficient corrections, gives the number, n , of H ions liberated per molecule. This number is close to 7 (Table IV)

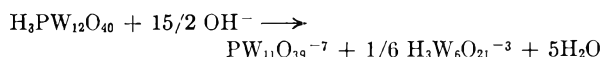
for both PTA and PMA, whereas it is 4 for STA.³ The higher basicity of these acids has been observed by others.⁹

TABLE IV

Acid	Concn., wt. %	pH of buffered soln. ^a	n^b
PTA	1.31	4.47	7
	3.24	4.28	7
	3.62	4.21	7
	6.62	3.83	7
	2.77	4.10	7
PMA-1	1.16	4.40	7
	2.77	4.10	7
	4.37	3.75	7
PMA-2	0.804	4.49	6
	1.74	4.30	6
	2.70	4.17	7
	3.48	4.01	7

^a In acetate buffer, pH 4.58, $\Gamma/2$ 0.2. ^b Number of protons liberated per molecule of heteropoly acid, see text.

There are several possible ways, however, in which this higher basicity may be achieved. PTA, for example, (a) might be represented as heptabasic, $H_7PW_{12}O_{42} \cdot (x - 2)H_2O$, as well as tribasic, $H_3PW_{12}O_{40} \cdot xH_2O$; or (b) might undergo a decomposition reaction¹⁰ such as



In the former case, only the single solute species $PW_{12}O_{42}^{-7}$ would exist in solution, whereas in the latter case, the solute would be heterogeneous. The strictly Gaussian diffusion boundaries of PTA at pH 4.5, as observed by the Gouy technique, are entirely incompatible with the latter possibility. The homogeneity of PTA and its heptabasicity therefore strongly indicate that the species in solution is $PW_{12}O_{42}^{-7}$. This is further confirmed by the molecular weight calculated from the Svedberg relation (Table V), which is in good agreement with the expected value.¹¹

TABLE V

PHYSICAL CONSTANTS OF HETEROPOLY ACIDS^a

Acid	S_0 , svedbergs	$D_0 \times 10^6$, cm. ² /sec.	\bar{V}^b , cc./g.	Mol. wt. ^c formula
PTA	3.66	3.701	0.142	2.86×10^3 2909 ^d
PMA-1	2.04	3.95	.244 ^e	1.69×10^3 1706 ^f

^a In acetate buffer, pH 4.58, $\Gamma/2$ 0.2. ^b For anhydrous acids, of formula corresponding to anion.^{d,f} ^c For anhydrous anion.^{d,f} ^d For anion $PW_{12}O_{42}^{-7}$. ^e Calculated ignoring dissociation occurring in solution. Only an approximate value. ^f For anion $PMO_{11}O_{39}^{-7}$.

From these data we may calculate the friction ratio,⁴ f/f_0 , where f is the observed friction coefficient, and f_0 that for the equivalent sphere. For the $PW_{12}O_{42}^{-7}$ ion, $f/f_0 = 1.2$, whereas for $SiW_{12}O_{40}^{-4}$, $f/f_0 = 1.0$.¹² The departure of f/f_0 from unity,

(9) H. Barnes and R. A. Peters, *Biochem. J.*, **26**, 2203 (1932); G. Toennes and M. S. Elliot, *J. Biol. Chem.*, **111**, 61 (1935); M. Jean, *Compt. rend.*, **223**, 155 (1946); J. Ripan and J. Liteanu, *ibid.*, **224**, 196 (1947).(10) P. Souhay, *Ann. Chim.*, [11] **20**, 70 (1945); [12] **2**, 203 (1947).(11) Within current experimental error, interaction effects¹² among the species in this multicomponent system may be neglected.(12) M. Wales and J. W. Williams, *J. Polymer Sci.*, **8**, 449 (1952).

while significant, cannot be interpreted unambiguously. It may be due to the binding of water by the ion (the extra charge on the PTA ion compared to the STA ion may be a factor) or to an asymmetry in the molecular shape, or to both. If the $PW_{12}O_{42}^{-7}$ ion is asymmetric, a profound change in structure from that of the essentially spherical¹³ $H_3PW_{12}O_{40} \cdot 5H_2O$ acid is suggested.

For PMA, it is not possible to define the nature of the species in solution with certainty. The facts that, in diffusion, the solute is clearly heterogeneous; the solutions exhibit a basicity near 7; and PMA-1 and PMA-2 are indistinguishable in sedimentation or diffusion, suggest that at pH 4.5 the

(13) J. F. Keggin, *Proc. Roy. Soc. (London)*, **144A**, 75 (1934); R. Signer and H. Gross, *Helv. Chim. Acta*, **17**, 1076 (1934).

principal species is $PW_{11}O_{39}^{-7}$, along with some decomposition products. If, as a first approximation, \bar{V} for PMA-1 is utilized in conjunction with the extrapolated sedimentation and diffusion constants for PMA, the calculated molecular weight agrees with the expected value (Table V) within experimental error.

In the previous paper, data obtained with STA were shown to conform closely with the Svedberg equation. With the assignment of the formula $PW_{12}O_{42}^{-7}$ to the PTA anion at pH 4.5, the PTA data also provide a critical test of the Svedberg equation. These experiments demonstrate further that sedimentation and diffusion experiments may be useful in the elucidation of the structures of related compounds.

ON THE MELTING POINT OF GERMANIUM

BY F. X. HASSION, C. D. THURMOND AND F. A. TRUMBORE

Bell Telephone Laboratories, Inc., Murray Hill, New Jersey

Received May 12, 1955

Conflicting values for the melting point of germanium can be found in the literature. The present experiments indicate the true value to be $937.2 \pm 0.5^\circ$ as obtained by Greiner and Breidt. Freezing points were obtained from cooling curve measurements on germanium melts under high vacuum, in contact with GeO_2 or under atmospheres of H_2 , He, N_2 or Ar. Melting points were determined by a visual method for germanium samples which had been melted previously in contact with GeO_2 at 1000° , or under vacuum or hydrogen. The freezing and melting points in all cases were the same within experimental error.

1. Introduction

At least thirteen independent determinations of the melting point of germanium ranging from 925 – 975° appear in the literature.^{1–13} The most widely quoted value of the melting point of germanium is 958 – 959° .^{14–17} Recent reference works apparently refer to the survey of Kelley¹⁸ who accepted the experimental results of Dennis, Tressler and Hance.² This melting point is in

(1) W. Biltz, *Z. anorg. allgem. Chem.*, **72**, 313 (1911); *C. A.*, **6**, 176 (1912).

(2) L. M. Dennis, K. M. Tressler and F. E. Hance, *J. Am. Chem. Soc.*, **45**, 2033 (1923).

(3) J. H. Müller, E. F. Pike and A. K. Graham, *Am. Phil. Soc. Proc.*, **65**, 15 (1926).

(4) T. R. Briggs, R. O. McDuffie and L. H. Willisford, *This Journal*, **33**, 1080 (1929).

(5) F. H. Roninger, *ibid.*, **33**, 1085 (1929).

(6) R. Schwarz and G. Elstner, *Z. anorg. allgem. Chem.*, **217**, 289 (1934).

(7) H. Maucher, *Forschungsarbeiten über Metallkunde und Röntgen Metallographie*, **20**, 32 (1936).

(8) H. Stöhr and W. Klemm, *Z. anorg. allgem. Chem.*, **241**, 305 (1939).

(9) K. Ruttewit and G. Masing, *Z. Metallkunde*, **32**, 52 (1940).

(10) R. C. Sangster and J. N. Carman, *J. Chem. Phys.*, **23**, 206 (1955).

(11) E. S. Greiner and P. Breidt, Jr., *J. Metals*, **7**, 187 (1955).

(12) E. S. Candidus and D. Tuomi, *J. Chem. Phys.*, **23**, 588 (1955).

(13) M. Hoch and H. L. Johnston, *ibid.*, **22**, 1376 (1954).

(14) "Handbook of Chemistry and Physics," Chemical Rubber Publishing Co., Cleveland, Ohio, 36th Edition, 1954–55.

(15) C. J. Smithells, "Metals Reference Book," Interscience Publishers, Inc., New York, N. Y., 1949.

(16) O. Kubaschewski and E. Evans, "Metallurgical Thermochemistry," Butterworth-Steiner Ltd., 1951.

(17) L. L. Quill, "The Chemistry and Metallurgy of Miscellaneous Materials: Thermodynamics National Nuclear Energy Series IV-19B," McGraw-Hill Book Co., New York, N. Y., 1950.

(18) K. K. Kelley, *U. S. Bureau of Mines Bul.*, 393 (1936).

surprisingly poor agreement with more recent measurements, as can be seen in Table I. Since 1929 the reported germanium melting points have all been between 934 and 943° , when determined by standard methods.¹⁹

TABLE I

SUMMARY OF Ge MELTING POINT DETERMINATIONS		
M.p., °C.	Method ^a	Ref.
916 ± 5	V—saturated with GeO_2	1
958 ± 5	V— H_2 atm.	1
958.5	TA— H_2 atm.; repeated fusions under H_2	2
959 ± 5	V— H_2 atm.	3
975 ± 5	V—vacuum	3
925	TA— H_2 atm.; before fusions under H_2	4
943	TA— H_2 atm.; after 42 fusions under H_2	4
949	TA— H_2 atm.; after 132 fusions under H_2	4
955 ± 5	TA— H_2 atm.; many fusions under H_2	5
940	TA— H_2 atm.	6
940	TA—vacuum	7
940–941	TA— H_2 atm.	8
943	TA— H_2 atm.	9
934.5	?	10
937.2 ± 0.5	TA—He atm.	11
940 ± 1.5	TA—vacuum, Ar, N_2 atm.; in contact with GeO_2 ; from H_2 fusion	12
965–970	?	13

^a V—visual; TA—thermal analysis, i.e., cooling and/or heating curves.

The commonly accepted explanation of this discrepancy is that the germanium melting point is lowered by the presence of small amounts of

(19) NOTE ADDED IN PROOF.—The authors are now aware of the value of 957° obtained by J. H. Downing and D. Cubicciotti [*J. Am. Chem. Soc.*, **73**, 4025 (1951)] using thermal analysis.

oxygen which can only be removed by repeated fusions under hydrogen.⁴ None of the melting points reported since 1929 was obtained with germanium treated in this manner.

In this paper experiments are described which show that the best value for the melting point of germanium is $937.2 \pm 0.5^\circ$, given by the work of Greiner and Breidt.¹¹ Both the melting point and freezing point have been determined under a variety of conditions. The freezing point was determined from cooling curves on germanium melts under vacuum, in contact with GeO_2 , or exposed to H_2 , He, A and N_2 atmospheres. The melting points of samples previously melted under vacuum, under hydrogen and under air were determined visually under vacuum, helium and air. A visual melting point also was obtained on two specially prepared germanium samples. One was remelted under hydrogen many times, and the other was recovered from a melt of Ge and GeO_2 . In all cases the melting and freezing points were in the range $937.5 \pm 2^\circ$.

2. Experiments and Results

2.1 Source and Purity of Materials.—The germanium obtained from the Western Electric Company was prepared by the hydrogen reduction of GeO_2 in graphite. This material was zone refined under a nitrogen atmosphere. Single crystals, which were subsequently grown from material similar to that used for melting point determinations, had resistivities greater than 20 ohm-cm. Spectrographic and mass spectrometer analyses disclosed no impurity at a concentration greater than 1 part in 10^4 . Vacuum fusion gas analysis indicated the presence of hydrogen, oxygen and unidentified inert gases all at concentrations less than 1 part in 10^4 .

2.2 Freezing Point Determinations.—Cooling curves were obtained on 70 to 80 g. melts of germanium in graphite crucibles of $\frac{3}{4}$ inch inside diameter. The crucibles were placed in a mullite tube which was 16 inches long and $1\frac{1}{8}$ inches in inside diameter. The mullite tube was fitted with a water-cooled brass head through which passed a vitreous silica thermocouple protection tube and a stirrer. The silica rod stirrer with a loop on the end could be manually raised and lowered through a tight fitting rubber tube on the brass head. A stream of gas could be led into and out of the mullite tube through the head. The thermocouple junction was located in the melt about $\frac{1}{2}$ inch above the bottom of the crucible. The assembly was heated in a Globar furnace.

In a typical run the mullite tube, containing a germanium-filled graphite crucible, was flushed with H_2 , He, A or N_2 while the temperature was raised to 1000° and held for 1 hour. In one case the temperature reached 1400° . The thermocouple protection tube and stirrer were lowered into position after the germanium had melted. In cooling, the voltage drop across the furnace was decreased to such a value that the cooling rate just above the freezing point was from 2 to 6 deg./min. The thermal arrests lasted 5 to 10 minutes. Supercooling often occurred but seldom persisted for more than 2 minutes. Thermocouple e.m.f.'s were read at 30-second intervals with a Leeds and Northrup Portable Precision Potentiometer. Stirring was maintained as long as possible.

The thermocouples were made of 0.030 inch diameter Pt and Pt, 10% Rh wires which were annealed in air between 1300 and 1400° for 1 hour. These were then calibrated under an argon atmosphere against the freezing points of C.P. silver and a copper sample certified by the National Bureau of Standards. Periodic calibrations, using the same assembly as for the germanium cooling curves, gave no indication of thermocouple changes. A linear deviation of corrected thermocouple readings from standard tables was assumed between calibration points and extrapolated to the freezing point of germanium.

Freezing points were obtained under atmospheres of H_2 , He, A and N_2 . No detectable change in freezing point

could be associated with these different ambients. A value of $937.7 \pm 1.0^\circ$ was obtained.

In one experiment GeO_2 powder (18.1 g., hexagonal modification) was added to 71.6 g. of germanium which had a freezing point of $937.4 \pm 1^\circ$. This mixture of GeO_2 and Ge was heated for 16 hours under argon at about 950° . During the heating the thermocouple protection tube was above the melt. The melt was occasionally stirred with the silica stirrer which was also above the melt when not in use. After 16 hours of heating, the freezing point was $936.9 \pm 1.0^\circ$. Some weight had been lost by the crucible and contents during the heating. This could be attributed to the diffusion of GeO to the cool upper walls of the tube and to reaction between GeO_2 and graphite to give CO , CO_2 and Ge. Inspection of the cooled melt revealed a black glassy layer on the surface of the solidified germanium. The black glassy layer on the surface was taken as evidence that excess oxygen was present during the cooling curve measurements.¹²

The freezing point of pure germanium was also obtained under a vacuum in a silica tube. This tube, 1 inch in diameter with a re-entrant thermocouple well at the bottom, was heated in the same Globar furnace used for other cooling curves. The tube was connected to a pumping station through a graded seal and ground glass joint. With 178 g. of germanium in the tube, the system was evacuated to better than 10^{-6} mm. and then slowly heated. A thin dark ring formed on the cool wall of the silica tube just above the furnace which probably was condensed GeO vapor coming from a small amount of adsorbed or dissolved oxygen. After the germanium had melted, pumping was continued until 10^{-7} mm. was read with an ion gage. The cooling curve which was then obtained gave an arrest at $937.7 \pm 1.0^\circ$ which was 10 minutes long.

2.3 Melting Point Determinations.—Visual melting points were obtained by sealing small samples of germanium (5 to 50 mg.) into vitreous silica tubes. Each tube was placed inside another silica tube in which was sealed a cylindrical block of copper under an argon atmosphere. The tubes containing the germanium samples were butted against a Pt and Pt, 10% Rh thermocouple, and the entire assembly heated in a 1 by 12 inch tubular furnace. The copper block reduced the thermal gradient to about 0.1–0.3° per cm. near the middle of the furnace. The furnace temperature was manually controlled by means of a Powerstat supplied with constant voltage from a Sola transformer. The thermocouple e.m.f.'s were measured with a Leeds and Northrup type K2 potentiometer. The thermocouples were calibrated periodically, using this same visual technique, against the melting points of C.P. silver and samples of aluminum certified by the National Bureau of Standards.

In a typical run the temperature was raised to a value near the expected melting point and held constant for at least 3 to 5 minutes to permit thermal equilibrium. The sample was then removed, and the presence or absence of melting, *i.e.*, the rounding off of the edges of the sample, was noted. By this procedure the melting point uncertainty could be limited to $0.3\text{--}1.0^\circ$ for a given sample.

Melting points were obtained for germanium samples which had previously been melted under high vacuum, hydrogen or air. The silica tubes containing the samples were filled with a partial pressure of He or air, or were evacuated to pressures of 10^{-5} to 10^{-6} mm. before sealing. All the melting points were the same within experimental error and were found to be $938.1 \pm 1.5^\circ$.

Two additional melting points were obtained on germanium samples which had been prepared under special conditions. The first sample of germanium came from a melt which was prepared by the usual hydrogen reduction of GeO_2 in graphite, and then cycled many times under H_2 . A high purity graphite boat filled with enough GeO_2 to make a 370-g. ingot of Ge was placed in a quartz tube furnace, and reduction to germanium sponge was accomplished by heating in a flow of hydrogen at atmospheric pressure for 3 hours at 675° . The sponge was fused by raising the temperature to 1020° . Cyclic freezing and melting under hydrogen was then begun. The temperature was held at 1020° for 1.5 hours, lowered to 800° in 1 hour, held at 800° for 0.5 hour, and then raised to 1020° in 1.5 hours. This treatment corresponded to one cycle. After 42 cycles, the boat was drawn into a cooling chamber and removed a few hours later. The hydrogen was taken from house lines serviced by tank hydrogen. The process-

ing was done in a reduction system which had been used solely for the preparation of germanium.

A portion of the germanium ingot prepared in the above manner was sealed in a small silica tube under He and the melting point determined. It was found to be $937.4 \pm 1.5^\circ$ in good agreement with the other melting and freezing experiments.

The second germanium sample was recovered from a black glass-like phase which was obtained from a 1:1 mixture (mole ratio) of powdered GeO_2 and Ge which had been heated to about 1000° for five minutes in a silica tube sealed under vacuum. The germanium button, which was recovered by etching away the surrounding phase in concentrated aqueous HF, was sealed into a small silica tube under He, and the melting point was determined. The melting point was the same, to within $\pm 1^\circ$, as that for untreated Ge.

3. Discussion and Conclusions

The possibility that the melting point of germanium is sensitive to the presence of small amounts of oxygen which can be removed by remelting many times under hydrogen, seems to be ruled out by the experiments which have just been described. We were unable to alter the melting point significantly by either intentionally adding excess oxygen in the form of GeO_2 , or by trying to remove oxygen by many remelts under hydrogen. Recently, Candidus and Tuomi¹² have suggested a Ge- GeO_2 phase diagram which is consistent in a qualitative way with the experimental results of Hoch and Johnston.¹³ No lowering of the freezing point of germanium due to the presence of oxygen was observed until the concentration of oxygen in the melt was approximately 60 atom per cent. Candidus and Tuomi also report that the melting point of germanium which had been zone refined under H_2 or N_2 was not significantly altered by running cooling curves under vacuum or under H_2 or A atmospheres.

The possibility that the germanium we have used contains an unidentified impurity which lowers the true melting point of germanium approximately 20 degrees seems to be precluded by the following considerations. The germanium was analyzed by a number of different methods, and these revealed no impurities at concentrations greater than 1 part in 10^4 . Since the heat of

fusion of germanium is about 8.1 kcal.,²⁰ the freezing point lowering constant is around 3 or 4 degrees per atom per cent. impurity. That is, an impurity concentration of 5 or 6 atom per cent. would be required to lower the melting point 20 degrees and thus to account for the observations reported in the early literature. This concentration of liquid phase impurity would be required if the liquid phase were an ideal solution and if the solubility of the impurity in solid germanium were very small. If the solid solubility, or rather the distribution coefficient, were not negligible, the freezing point lowering constant would be a smaller number,²¹ and even larger impurity concentrations would be required to depress the melting point 20 degrees.

Since our melting and freezing point determinations are in agreement with the results obtained by Greiner and Breidt on similar high purity material, and since they have a smaller probable error assigned, we conclude that the melting point of germanium is $937.2 \pm 0.5^\circ$. This value is in disagreement with that of 940° reported by Candidus and Tuomi. However, it appears that their experiments were mainly designed for the measurement of melting point differences rather than absolute values. Specifically, their thermocouple was not surrounded by the melt but was inserted in the bottom of a long graphite boat containing the melt.²² Inasmuch as the cooling curve experiments of this study and that of Greiner and Breidt conformed more closely to the conventional methods for accurate freezing point determinations, it is believed that the figure of 937.2 is the correct value.

Acknowledgments.—We wish to thank K. M. Olsen for the special germanium preparations, G. W. Guldner and A. L. Beach for the vacuum analysis and N. B. Hannay for mass spectrometer data. The technical assistance of M. Kowalchik, Mrs. L. Eary and C. R. Isenberg is gratefully acknowledged.

(20) E. S. Greiner, *J. Metals*, **4**, 1044 (1952).

(21) L. S. Darken and R. W. Gurry, "Physical Chemistry of Metals," McGraw-Hill Book Co., New York, N. Y., 1953, p. 324.

(22) D. Tuomi and E. A. Candidus, private communication.

MECHANISMS OF PERMEATION OF SILVER, COPPER, AND MERCURY GASES OF SOLID GRAPHITE WALLS¹

BY RUSSELL K. EDWARDS AND JAMES H. DOWNING

*Contribution from the Department of Chemistry, Illinois Institute of Technology, Chicago, Illinois**Received May 14, 1955*

Volatilization measurements conducted with mercury, silver and copper liquids from National Carbon graphite containers of grade AGX show that mercury and silver may pass through the walls by the mechanism of capillary flow whereas copper passes through the walls by activated diffusion. The activation energy found in the latter case was 20.7 kcal. for the containers used.

Introduction

During an investigation of the thermodynamics of the liquid Cu-Ag system by volatilization measurements from graphite effusion containers into vacuum, it became necessary to understand the mechanism of extraneous volatilization which appeared to take place through the graphite container walls.² Experiments show that there is an important difference in the mechanism by which copper permeates solid graphite as compared with the mechanism by which silver and mercury pass through the material.

Vaporization of Mercury from Graphite Effusion Crucibles of Variable Orifice Dimensions

Mercury was vaporized into vacuum from graphite effusion crucibles having cylindrical "short tube" effusion orifices whose effective areas varied over a range as high as a factor of 25. The immediate objective was to obtain, for later use in the study of the Cu-Ag liquid system, calibrated "effective" effusion orifice sizes from measurements of the rate of vaporization of some similar metallic liquid whose vapor pressure as a function of temperature was known accurately and quite independently of any effusion vapor pressure determinations. However, the results furnish insight as to the mechanism by which mercury may pass through a graphite wall.

Experimental

Effusion crucibles were fabricated in two pieces and are shown in cross-sectional view in Fig. 1. Graphite, grade AGX from the National Carbon Division of Union Carbide and Carbon Corporation, was used. The caps were carefully machined and polished to precision step-fits with the main crucibles so removal, as required in the work with copper and silver, was possible. Shown also is a portion of a graphite rod, hollowed at the end to minimize heat conduction, which was used in the latter measurements to support the crucible. Shown in Fig. 2 is the essential portion of the apparatus used in the effusion vaporization measurements of mercury in the temperature range 25–100°. The apparatus was immersed to within a few inches of the cold finger level in an oil thermostat whose temperature could be controlled to within less than 0.1°. On one end of the vacuum chamber a ground glass taper was sealed, and this fitted to a cold finger which was refrigerated with liquid nitrogen. The other end of the vacuum chamber was reduced to form a small tube which served as an inlet for a thermocouple. The chromel-alumel thermocouple left the tube through a vacuum-tight wax seal in a region re-

moved from the oil-bath. The thermocouple junction was positioned so it would rest in the recess at the base of the graphite crucible. The graphite effusion crucibles were seated in a heavy-walled, machined aluminum can which aided in eliminating thermal gradients along the effusion crucibles. The thermocouple was calibrated against a standard platinum resistance thermometer. A side tube from the vacuum chamber was connected with a pumping system consisting of a mercury diffusion pump backed by a Welch Duo-Seal mechanical pump, and vacuum pressures were measured with a McLeod gage. Both the mercury pump and the McLeod gage were isolated from the rest of the vacuum system with liquid nitrogen-cooled traps which prevented mercury vapor from entering the remaining vacuum system. Argon gas could be admitted to the system through a suitable stopcock, and a mercury bubbler was provided to limit the maximum argon pressures to slightly over an atmosphere.

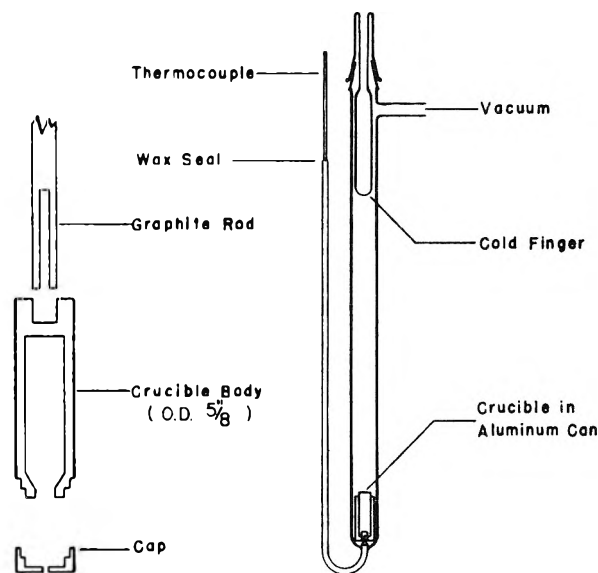


Fig. 1.—Graphite effusion crucible.

Fig. 2.—Mercury calibration apparatus.

The procedure in carrying out a run was to lower the effusion crucible, containing the mercury and housed in the aluminum can, to the bottom of the vacuum chamber. The vacuum chamber was then closed, and the system pumped down to a good vacuum, which usually required about one minute. Argon was introduced at a pressure of an atmosphere to eliminate vaporization loss during the period of 10 to 15 minutes required to attain temperature equilibrium between the crucible and the oil-bath. The system was then rapidly evacuated and timing was begun as soon as the vacuum pressure was reduced to 10^{-4} mm. of mercury. Liquid nitrogen was poured into the cold finger to trap the vaporized mercury and aid in maintaining a good vacuum in the vicinity of the effusion crucible. Vacuum pressures were read periodically on the McLeod gage. A run was terminated by introducing argon gas once more and raising the crucible to a cool position. The mass of effusion was determined by weight loss, and weighings were performed on an Ainsworth Semimicro balance.

(1) (a) Based on part of a thesis by J. H. Downing, submitted to the Illinois Institute of Technology in partial fulfillment of the requirements for the Ph.D. degree, May, 1954. (b) This work was supported by the U. S. Office of Naval Research, U. S. Navy, through Contract N7-onr-329, Task Order II, and through Contract NONR 1406, Task Order II.

(2) R. K. Edwards and J. H. Downing, to be published.

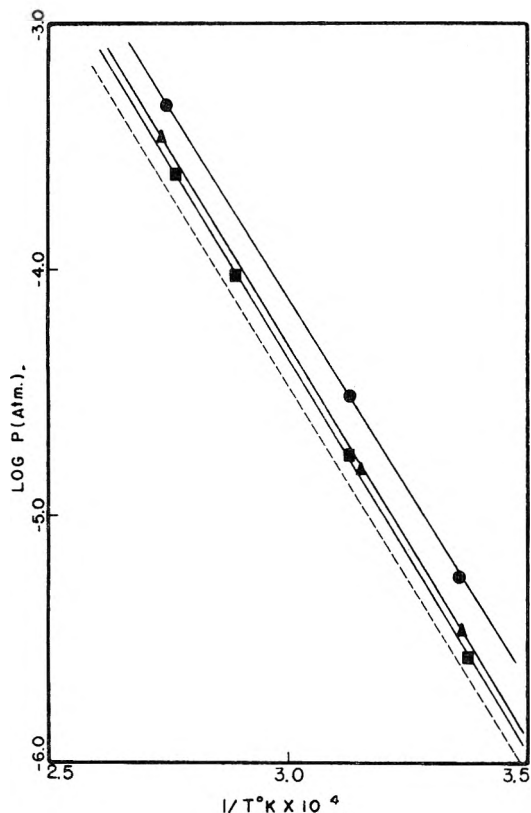


Fig. 3.—Mercury vaporization data (results of present study calculated with Clausius corrected area compared with data of Giaque and Busey): ●, S_c ; ▲, M_c ; ■, L_c ; — — —, Giaque and Busey.

Preliminary measurements had shown that a period of over 30 minutes was required to reach temperature equilibrium in an evacuated system, and this was prohibitively long. Also, to allow equilibration in the presence of air was entirely unsatisfactory for thin films of oxide formed over the surfaces of the liquids and this resulted in seriously reduced apparent vapor pressures.

Because of the tendency of mercury to form an oxide film, high purity, triple-distilled mercury was carefully redistilled *in vacuo* and a center cut of the distillate taken each time for calibration work.

Results and Discussion

Three effusion crucibles were used and they will hereinafter be designated L, M and S to correspond, respectively, with whether their effusion orifices are "large," "medium" or "small." Their effusion orifice areas or "effective" areas will hereinafter be designated by the above symbols with the additional subscript symbols, "a," "c" and "g" to identify, respectively, "measured area," "effective area—area corrected by use of the Clausius³ short-tube correction factors," or "effective area as obtained by these calibration experiments using liquid Hg and the vapor pressure values of Giaque and Busey,⁴ and the Knudsen⁵ effusion equation." A tabulation of effusion crucible orifice dimensions is given below in Table I in which "s" refers to the length of the orifice tube.

The results of the measurements of the volatilization of liquid mercury are given in Fig. 3 wherein

(3) P. Clausius, *Ann. Physik*, **12**, ser. 5, 961 (1932).

(4) W. Giaque and R. Busey, *J. Am. Chem. Soc.*, **75**, 1529 (1953).

(5) M. Knudsen, "The Kinetic Theory of Gases," Methuen and Co., London, 1934.

TABLE I
EFFUSION CRUCIBLE ORIFICE DIMENSIONS

Crucible	a , cm. ²	s , mm.	c , cm. ²	g , cm. ²
L	0.0182	1.22	0.0103	0.0134
M	.0099	1.52	.0043	.00620
S	.0018	1.80	.00043	.00104

apparent vapor pressures have been calculated through the Knudsen effusion equation using orifice areas L_c , M_c and S_c . Also given there is the line representing the true vapor pressure of mercury from the work of Giaque and Busey.

The data show that the percentage error in the apparent vapor pressures is systematic with orifice areas in a manner to be expected if mercury vapor were escaping through the graphite walls in addition to normal effusion through the orifices. The slopes of all the apparent vapor pressure curves given in Fig. 3 are identical within 400 cal. with those of the true vapor pressure curves. Since this is true in spite of the fact that up to twice as much extraneous as normal vaporization is encountered, it follows that the mechanism of extraneous escape is in clear accord with that of capillary flow. Barrer⁶ has discussed molecular flow of gases in solid capillary systems. At low gaseous pressures, the capillary flow mechanism shows normal effusion pressure dependency for permeation into a vacuum. The applicable equation is identical to the Knudsen effusion equation except that a simple parameter, usually assumed to be negligibly temperature dependent, appears in the former in place of the effective orifice area in the latter.

It is well to note that the apparent vapor pressures could conceivably be brought into accord with the true values if a significantly low accommodation coefficient were assumed to contribute simultaneously to error in the Clausius corrections and to non-saturation of the vapor phase within the effusion crucibles. Such an alternate explanation seems improbable in view of the work to be discussed later in this paper.

Vaporization of Silver from Graphite Effusion Crucibles of Variable Orifice Dimensions

Liquid silver was vaporized into vacuum from the three crucibles, which had been calibrated as noted above, and additionally from one of the crucibles without an effusion orifice.

Experimental

The high temperature vacuum apparatus used is described elsewhere.² In this apparatus the crucibles were supported in a horizontal position during effusion because of advantages offered in minimizing temperature gradients at the high temperatures involved. The pure silver was placed in the crucible in an amount such that when melted, the liquid level was at a point about midway along the bevel of the inner wall at the forward end.

For a given measurement the weighed crucible with its charge was subjected to evacuation for degassing and then brought rapidly to the desired temperature by sudden introduction to the hot zone of the vacuum apparatus. The vacuum was maintained at less than 10^{-4} mm. throughout the duration of the volatilization which was of the order of 100 minutes. At the end of a run rapid cooling *in vacuo* was achieved by withdrawal of the crucible from the hot zone of the apparatus. The temperature of the crucible

(6) R. M. Barrer, "Diffusion in and through Solids," Cambridge University Press, Cambridge, England, 1941.

during the runs was obtained in terms of a proximate Pt, Pt-Rh (10%) thermocouple which had been calibrated to read true crucible temperatures. Weight differences for the crucible between successive runs were obtained and rates of loss for various temperatures were calculated. First runs were discarded as being less reliable than subsequent runs. The materials and apparatus used, the procedures in temperature measurement and calibration, and the handling and cleaning of the crucible are described in detail elsewhere.²

In addition to the measurements made using the three crucibles of different orifice sizes, verifying experiments were carried out in a crucible without an orifice. For this purpose a replica cap without orifice was fitted to the main body of the crucible formerly having the smallest orifice. It is well to note that all crucibles were identical in material and dimensions except for the variations in the caps with their effusion orifices.

Results and Discussion

The results of the measurements are shown graphically in Fig. 4 in which logarithms of calculated vapor pressures are plotted *versus* reciprocal absolute temperatures. The situation is quite comparable with that encountered for the vaporization of mercury in these crucibles. The magnitude of the calculated pressures, based on measured orifice areas corrected by the Clausius short-tube factors, varies systematically with orifice area in a manner to be expected, assuming extraneous volatilization in addition to orifice volatilization. Again, from the observation that the slopes of the curves are the same within 700 cal. in spite of the fact that up to more than twice as much extraneous as orifice vaporization is encountered, it follows once more that the mechanism of extraneous vaporization is in accord with that of capillary flow as discussed above. Also shown in Fig. 4 are the results from confirming measurements in which rates of vaporization from a crucible without effusion orifice were determined. Since rates of vaporization should be directly proportional to the gas pressure for either effusion or capillary flow, a plot of the logarithm of the rate of vaporization *versus* the reciprocal absolute temperature yielding the same slope as the other curves verifies that the mechanism of extraneous vaporization is in accord with that of capillary flow. Actually the precise term to plot is the logarithm of (the rate of vaporization multiplied by the square root of the absolute temperature), but the alteration so produced in the slope is negligible.

Plots, shown also in Fig. 4, of the calculated pressures based on the mercury-calibrated effective effusion orifice areas (all orifices corrected for the thermal expansion of graphite) indicate that some additional effective area is available to silver over that available to mercury gas.

It is possible to treat the data to arrive at the true vapor pressure of silver. The equation which has been used to obtain the calculated silver pressures is

$$P_c = \frac{Q_t(2\pi RT/M)^{1/2}}{a_g} \quad (1)$$

in which P_c is the silver pressure, Q_t is the total rate of vaporization, a_g is the mercury-calibrated effective effusion orifice area, and the other terms are those normally appearing in the Knudsen effusion equation. If, however, some additional effective extraneous area, a_{ex} , is available for silver

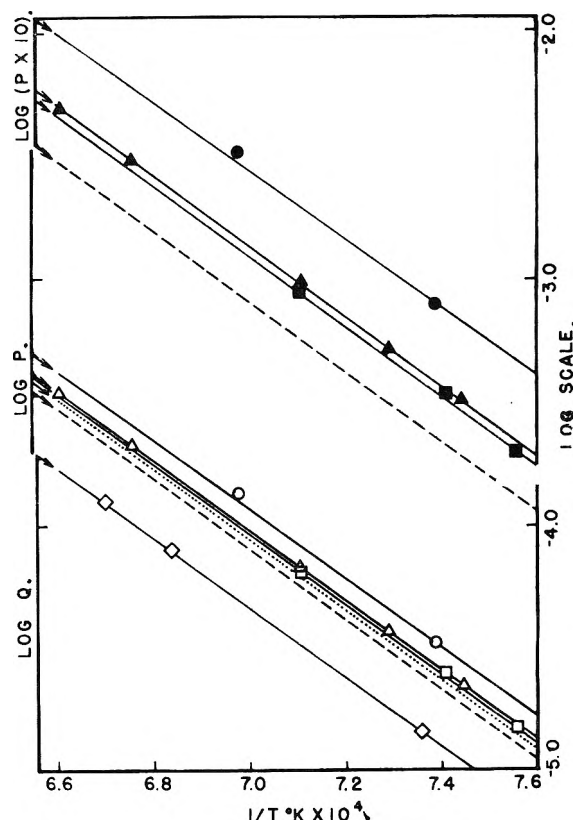


Fig. 4.—Silver vaporization data: Pressures are in atmospheres. Q is rate of no-orifice vaporization in grams per minute. A factor of 10 has been used in one case to adjust the vertical ordinate. Lines are from least squares treatment of the data. Some data beyond the range of the graph were considered for crucible S. ●, S_c , Claus. cor. area; ○, S_g , Hg calib. area; ▲, M_c , Claus. cor. area; △, M_g , Hg calib. area; ■, L_c , Claus. cor. area; □, L_g , Hg calib. area; ◇, small crucible, S, used without orifice; — — —, data from Kelley; ·····, extrapolation of data of this study.

vaporization, the true silver pressure, P_0 , would be given by

$$P_0 = \frac{(Q_g + Q_{ex})(2\pi RTM)^{1/2}}{(a_g + a_{ex})} \quad (2)$$

in which Q_g refers to the rate of vaporization through the effective mercury-calibrated area and Q_{ex} refers to the rate of vaporization through the additional extraneous area, a_{ex} . Thus the calculated pressure would be related to the true pressure by

$$P_c = P_0 \left(1 + \frac{a_{ex}}{a_g} \right) \quad (3)$$

Assuming that a_{ex} is the same for all three of the crucibles, one can expect a linear plot of P_c *versus* $1/a_g$ and can obtain P_0 from the intercept when $1/a_g$ approaches zero. An example of such an extrapolation for silver is shown in Fig. 5 and the derived data for the true vapor pressure of silver obtained through the extrapolation procedure are shown in Fig. 4. These data have been evaluated through the $(\Delta F^0 - \Delta H_0^0)/T$ functions calculated from the data listed by Kelley^{7,8} to obtain an average value of $\Delta H_0^0 = 68,690$ cal. for the molar heat of sublimation of silver at the absolute zero

(7) K. K. Kelley, *U. S. Bur. Mines Bull.*, **476**, 158 (1949).

(8) K. K. Kelley, *ibid.*, **477**, 82 (1948).

of temperature. The result is in substantial agreement with the recent work of McCabe and Birchenall⁹ who obtained $68,070 \pm 290$ cal. from evaluation of their own measurements and some of the previous work. Kelley¹⁰ obtained a value of 69,004 cal. based on the data of Harteck, and it is seen that our results lie between these two evaluations. A line based on the evaluation of Kelley is shown in Fig. 4 for comparison. Heats of vaporization as determined from least squares treatment of any of the curves in Fig. 4 are the same value to within ± 1.7 kcal. and the activation energy for the diffusion of silver through the graphite walls is therefore zero within this uncertainty.

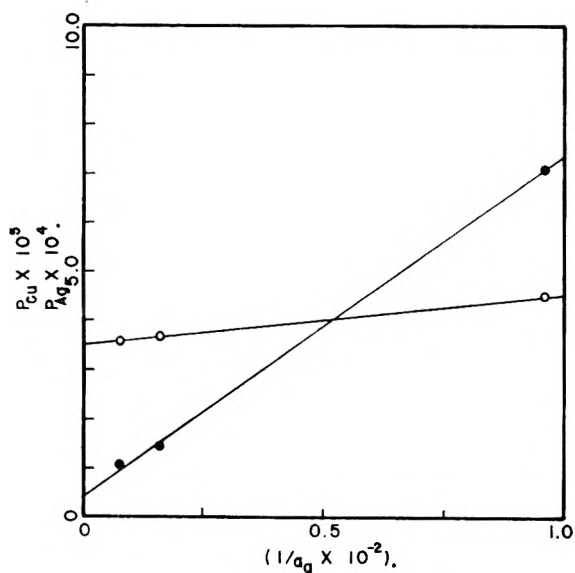


Fig. 5.—Extrapolation of silver and copper vaporization; data at 1470°K. (pressures are in atmospheres; a_g is the Hg calib. orifice area in cm.²; O, Ag; ●, Cu.)

In Knudsen effusion work it is always desirable to establish that molecular flow conditions exist in the pressure region of the experimental measurements. This may usually be done by varying the orifice dimensions to smaller and smaller sizes until calculated pressures show no variation with hole size. Such a procedure also verifies that effects due to possible low accommodation coefficients are eliminated. The extraneous vaporization through the crucible walls encountered in the present work renders such a test impossible. However, an alternate test was made. Consideration of the equation for the combined effects of molecular effusion and viscous flow exodus of gas through an orifice will show that as gas pressures increase to the point of rendering viscous flow important, calculated pressures derived from use of the simple Knudsen effusion equation will become increasingly too high. Therefore measurements for silver were made at increasingly higher vapor pressures until the anticipated systematic deviation from a straight line of the logarithm of the calculated vapor pressure as a function of reciprocal absolute temperature became obvious. It was thus possible to ascertain that viscous flow was insignificant in

crucible L below 1410°K. and in crucible M below 1520°K. The results are in good agreement with an estimation which was made, based on the Knudsen rule-of-thumb criterion that the mean free path of the molecule should be at least ten times the orifice diameter in order that effusive flow prevail. One may calculate that effusion conditions should obtain up to about 1540°K. for crucible L and to higher temperatures for the other crucibles. For copper the calculations indicate that effusion conditions should obtain up to 1810°K. in crucible L and to higher temperatures in the other crucibles.

Vaporization of Copper from Graphite Effusion Crucibles of Variable Orifice Dimensions

Liquid copper was vaporized into vacuum from the three crucibles with orifices, and additionally from one of the crucibles without an effusion orifice, in the same manner as the measurements described above for liquid silver.

Results and Discussion

The results of the measurements are shown graphically in Fig. 6. Once more the magnitude of the calculated pressures, based on measured orifice areas corrected by the Clausing short-tube factors, varies systematically with orifice area in a manner indicating considerable extraneous volatilization in addition to orifice volatilization; the measurements made in crucible S without an effusion orifice verify this as a fact. However, contrasted with the analogous measurements for mercury and for silver, the slopes of the plots also vary systematically with orifice sizes. Consequently, the mechanism of extraneous volatilization is predominantly other than that of capillary flow as discussed in those cases.

We may consider the diffusion of copper gas through solid graphite into vacuum in the manner of Jost's¹¹ general treatment. For a given temperature

$$Q_d = bDhP_0 \quad (4)$$

in which Q_d is the rate of loss of material from the crucible into vacuum by the diffusion process, b is a constant of the geometry, D is the diffusion coefficient, h may be taken as a Henry's law constant, and P_0 is the true pressure of copper gas prevailing within the crucible. As one might also expect some loss by the capillary flow mechanism, the equation for calculated pressures at any given temperature would be

$$P_c = \frac{(Q_g + Q_{ex} + Q_d)(2\pi RT/M)^{1/2}}{a_g} \quad (5)$$

Relating equations 2, 4 and 5 one may obtain

$$P_c = P_0 \left[1 + \frac{a_{ex} + bDh(2\pi RT/M)^{1/2}}{a_g} \right] \quad (6)$$

Thus here also a plot of P_c versus $1/a_g$ at a given temperature should extrapolate linearly to P_0 as $1/a_g$ approaches zero. An example of such a plot for copper is included in Fig. 5. The values for the vapor pressure of liquid copper obtained through the extrapolation procedure lead to the line shown in Fig. 6 in which they are compared

(9) C. L. McCabe and C. E. Birchenall. *J. Metals*, **5**, *AIIME Trans.*, **197**, 707 (1953).

(10) K. K. Kelley, *U. S. Bur. Mines Bull.*, **383**, 94 (1935).

(11) W. Jost, "Diffusion in Solids, Liquids, Gases," Academic Press, Inc., New York, N. Y., 1952.

with the recent work of Hersh.¹² More recent values obtained in this Laboratory¹³ are in closer agreement with the extrapolation values than with those of Hersh. The value of $\Delta H_0^0 = 80,400$ cal. for the molar heat of sublimation of copper at the absolute zero of temperature results from evaluation of the extrapolation data as compared to 81,080 cal. obtained by Hersh. A line based on this latter value is given in Fig. 6.

From a least squares evaluation of the slope of the logarithm of the rate of vaporization from the crucible without orifice *versus* the reciprocal absolute temperature and taking the heat of vaporization of liquid copper in this temperature range as 75.0 kcal.,¹³ one can calculate an activation energy of 20.7 kcal. for the permeation by copper of the graphite crucibles used. The correction for the term involving the capillary flow mechanism was found to be relatively negligible. This could be ascertained by assuming that approximately the same effective area for capillary flow was available for copper as for silver; so that the effective area was calculable from the no-orifice measurements conducted with the liquid silver, for which only capillary flow was of importance. Only about 0.6% of the loss is calculated for the capillary mechanism.

It is clear, of course, that the activation energy given above involves components due to both the diffusion coefficient and the Henry's law coefficient. The activation energy found is quite comparable to values¹¹ usually found for the diffusion of gases through metals and solids.

The activated diffusion encountered in the copper measurements implies¹¹ that copper is to some extent soluble in the graphite. Some nuclear reactor graphites¹⁴ have been found to pick up Cu, Si and Fe as a result of distillation of these impurities into the graphite during manufacture. The interaction between copper and graphite may perhaps be related to the interaction known to exist between the alkali metals and graphite in the interlamellar compounds of graphite.^{15,16}

(12) H. N. Hersh, *J. Am. Chem. Soc.*, **75**, 1529 (1953).

(13) R. K. Edwards and M. B. Brodsky, to be published.

(14) W. L. de Keyser and R. Cypres, *Bull. centre phys. nucleaire univ. Bruxelles*, No. 35, 28 (1952); *C. A.*, **47**, 4064a (1953).

(15) H. L. Riley, *Fuel in Sci. and Practice*, **24**, 8 (1944).

(16) H. L. Riley, *ibid.*, **24**, 43 (1944).

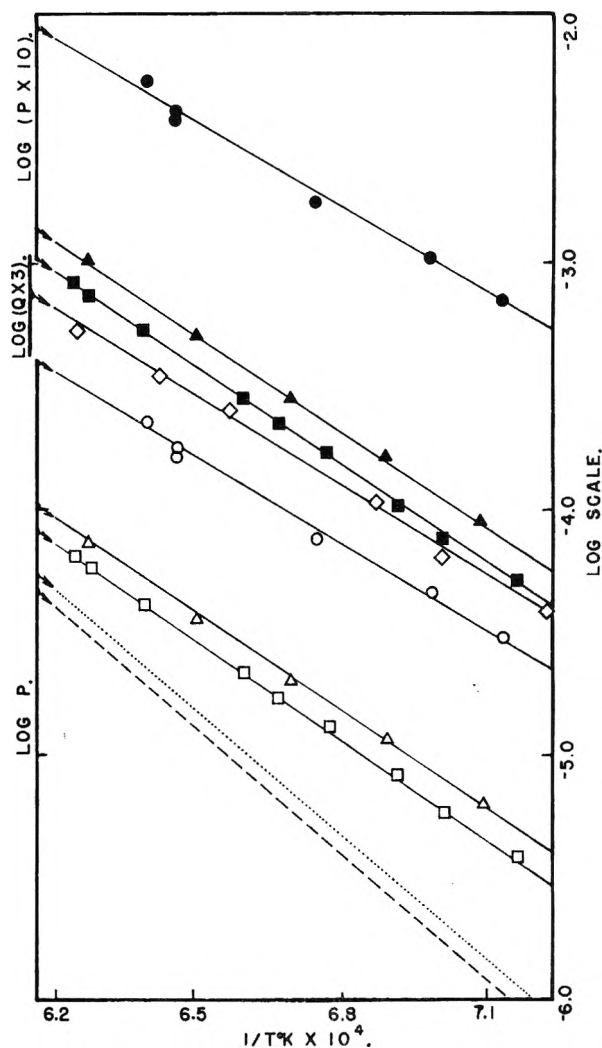


Fig. 6.—Copper vaporization data, pressures are in atm.; Q is rate of no-orifice vaporization in grams per minute. Numerical factors are included to adjust vertical ordinates. Lines are from least squares treatment of the data: \bullet S_c , Claus cor. area; \circ , S_g , calib. area; \blacktriangle , M_c , Claus cor. area; \triangle , M_g , calib. area; \blacksquare , L_c , Claus cor. area; \square , L_g , calib. area; \diamond , small crucible, S, used without orifice; ———, data from Hersh; , extrapolation of data of this study.

However, it does seem surprising that silver should be so markedly different in behavior from copper.

THE THERMAL DECOMPOSITION OF STIBINE

BY KENZI TAMARU

Frick Chemical Laboratory, Princeton University, Princeton, N. J.

Received May 20, 1955

The decomposition of stibine has been studied by a static method. The decomposition was dependent only upon the partial pressure of stibine, being independent of the partial pressure of hydrogen. The order of the reaction was 0.75 at 10° and increased as the reaction temperature became higher, until it became unity at 45°. The activation energy of the reaction was 8.8 kcal./mole at 40 cm. stibine pressure decreasing as the pressure became lower. The Langmuir expression is applicable to the results, but the calculated constants in the expression have no meaning, as in the case of Stock's results. Stibine decomposition in deuterium at 25° did not produce any hydrogen deuteride, which showed that no exchange reaction between hydrogen and deuterium took place on the antimony surface, while the decomposition of the stibine and deuterostibine mixture produced a large amount of hydrogen deuteride. The possibility of capillary condensation of stibine on the antimony film has been examined and shown to be possible under the experimental conditions. The rate-determining step of the over-all reaction has been briefly discussed.

As reported in a series of papers,¹ the decomposition of arsine on arsenic surfaces is a first-order reaction in respect to arsine, while the germane decomposition on germanium surface is zero order. It was suggested that the rate-determining step is the chemisorption of arsine in the former case, while in the latter case, it is the desorption of chemisorbed hydrogen from the germanium surface.

As an example of another hydride decomposition, the decomposition of stibine has been studied. This decomposition was already studied by Stock and his collaborators.² They found that the order of the reaction at 25° was 0.6 in respect to stibine, and that hydrogen had no effect upon the reaction rate. Those who have analyzed their data³⁻⁶ explained these facts on the basis of the unimolecular decomposition of stibine in the adsorbed state. Recently, however, it was found⁶ that the data could not be explained on the basis of the Langmuir concept, as the calculated constants of the Langmuir expression have no physical meaning.

Experimental

Preparation of Stibine.—Stibine was prepared by adding antimony trichloride powder to a solution of lithium aluminum hydride in ethylene glycol dimethyl ether in dry nitrogen. As this reaction was fairly violent, the solution of lithium aluminum hydride was cooled with liquid nitrogen when the antimony trichloride was added, and after the chloride addition the liquid nitrogen was removed to allow the solution to warm up gradually. The stibine was evolved before the reaction vessel reached room temperature and was condensed in a liquid nitrogen trap. After purification by distilling several times using liquid nitrogen and solid carbon dioxide, the stibine was stored in a liquid nitrogen trap.

For the preparation of deuterostibine, lithium aluminum deuteride was used instead of hydride.

Apparatus and Procedure.—The experiment was carried out in a static system. Three pear-shaped Pyrex reaction vessels (A, B and C) attached to mercury manometers by means of capillary tubing were used. Each of the vessels was about 67 cc. in volume. Before the stibine was intro-

duced into the reaction vessel a vacuum of less than 10⁻⁴ mm. was obtained by means of a mercury diffusion pump backed by a Cenco Hy-Vac oil pump.

Since hydrogen is the only gaseous constituent resulting from the decomposition, the rate of the reaction was followed by observing the total pressure of the system.

As the usual grease was reported^{2b} to be attacked by stibine, silicone grease was used, but this also was attacked by the gas.

Experimental Results

The stibine decomposed very slowly on the glass surface but, as antimony covered surface, the decomposition rate became faster and after 200 cm. stibine had been decomposed in a vessel at 25° the reaction rate became reproducible. In many runs a retardation was observed during the first few per cent. of decomposition. This retardation was omitted from consideration in the following treatment.

When the stibine was decomposed, the pressure increased to about three halves of the original. To have exact data the measured pressure had to be corrected, taking the van der Waals attraction of stibine into consideration and, secondly, as a small fraction of stibine sometimes decomposed when it evaporated, leaving black antimony powder behind. Thus, the initial observed pressure of stibine did not always show its exact partial pressure. The initial pressure of stibine was, consequently, obtained from the end-point of the decomposition.

According to the van der Waals equation

$$P = \frac{nRT}{v - nb} - \frac{n^2a}{v^2}$$

where n is the number of moles of the gas. In the case of stibine decomposition, n moles of stibine becomes $3n/2$ moles of hydrogen after the decomposition. The pressure difference (ΔP_0) between the hydrogen pressure after the decomposition and three halves of the initial stibine pressure can be calculated as follows, where the subscripts S and H show stibine and hydrogen, respectively

$$\Delta P_0 = P_H - \frac{3}{2} P_{S_0} = \left(\frac{n_H RT}{v - n_H b_H} - \frac{n_H^2 a_H}{v^2} \right) - \frac{3}{2} \left(\frac{n_S RT}{v - n_S b_S} - \frac{n_S^2 a_S}{v^2} \right)$$

where $n_H = 3/2 n_S$, $v = 67$ cc., $T = 273 + 25$, $a_H = 0.24 \times 10^6$ atm. cc.², $b_H = 26.6$ cc./mole, while a_S and b_S can be guessed from the constants

(1) (a) K. Tamaru, M. Boudart and H. Taylor, *THIS JOURNAL*, **59**, 801 (1955); (b) P. Fensham, K. Tamaru, M. Boudart and H. Taylor, *ibid.*, **59**, 806 (1955); (c) K. Tamaru, *ibid.*, **59**, 777 (1955).

(2) (a) A. Stock and O. Guttman, *Ber.*, **37**, 901 (1904); (b) A. Stock, F. Gomolka and H. Heynemann, *ibid.*, **40**, 532 (1907); (c) A. Stock, E. Echeandia and P. R. Voigt, *ibid.*, **41**, 1309 (1908).

(3) A. Stock and M. Bodenstein, *ibid.*, **40**, 570 (1907).

(4) C. N. Hinshelwood, "Kinetics of Chemical Change," Oxford Univ. Press, New York, N. Y.

(5) K. J. Laidler, "Catalysis," Vol. 1, edited by P. H. Emmett, Reinhold Pub. Corp., New York, N. Y., 1954, p. 146.

(6) M. Boudart, "Structure and Properties of Solid Surfaces," edited by G. R. Gomer and C. S. Smith, Univ. of Chicago Press, Chicago, Illinois, 1953, p. 400.

for such gases as PH₃, NH₃, H₂S and SeH₂⁷ as 6.1 × 10⁶ atm. cc.² and 69.0 cc./mole, respectively. Hence

$$\Delta P_c = \frac{3}{2} n_s R T \left(\frac{1}{v - n_H b_H} - \frac{1}{v - n_s b_s} \right) - \frac{3}{2} \frac{n_s^2}{v^2} \left(\frac{3}{2} a_H - a_s \right)$$

The first term of the right side of the equation, which contains *b*, can be ignored in comparison with the second term. When the initial pressure of stibine is 2/3 atm.

$$\Delta P_0 = \frac{3}{2} \frac{n_s^2}{v^2} \left(a_s - \frac{3}{2} a_H \right) = 0.5 \text{ cm.}$$

In other words, when 2/3 atm. stibine is decomposed at 25°, the pressure of the reaction vessel will become 765 mm. after the decomposition.

In the course of the decomposition, when a fraction *x* of the stibine has been decomposed, the pressure increase (*A*) should be

$$A = (P_H + P_S) - P_{S_0} = \left[\frac{n_s(1-x)RT}{v - n_s(1-x)b_s} - \frac{n_s^2 a_s(1-x)^2}{v^2} + \frac{3/2 n_s x R T}{v - 3/2 v_s x b_H} - \frac{(3/2 n_s x)^2 a_H}{v^2} \right] - \left\{ \frac{n_s R T}{v - n_s b_s} - \frac{n_s^2 a_s}{v^2} \right\}$$

where the total observed pressure at *x* fraction decomposition, (*P_H* + *P_S*), is shown in the square brackets, and the initial observed pressure, (*P_{S0}*), in the parentheses. Thus the correction term should be

$$- \frac{n_s^2}{v^2} \left[(1-x)^2 a_s + \left(\frac{3}{2} x \right)^2 a_H - a_s \right]$$

or

$$\frac{n_s^2}{v^2} \left[(2-x)x a_s - \left(\frac{3}{2} x \right)^2 a_H \right]$$

as the correction terms containing *b* are negligibly small. Usually the (3/2*x*)² *a_H* term can be ignored, as *a_H* is much smaller than *a_S*. As *x* in the correction term can be considered as approximately equal to 2*A*/*P_{S0}*, we can correct the observed pressure increase in this way.

Thus correcting the partial pressure of stibine, the pressure changes of stibine during the decomposition at various temperatures and pressures are shown in Figs. 1, 2, 3.

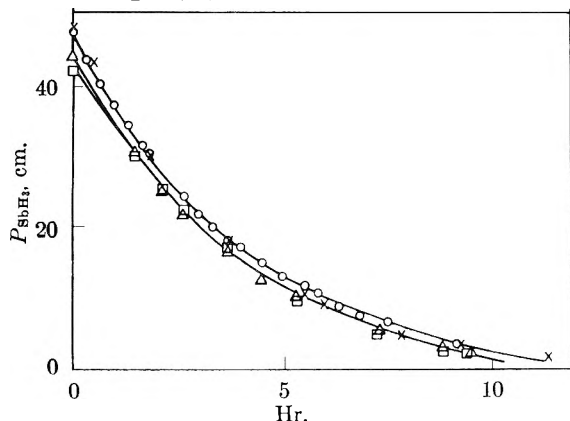


Fig. 1.—Decomposition of stibine at 25°.

(7)	H ₂ S	H ₂ Se	NH ₃	PH ₃
a	4.35	5.18	4.10	4.56 × 10 ⁶ atm. cc. ²
b	42.9	46.4	37.1	51.6 cc./mole.

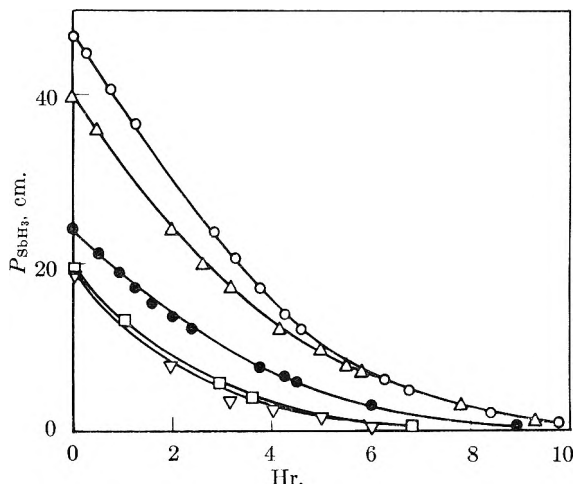


Fig. 2.—Influence of pressure on stibine decomposition at 25° (●, SbD₃; ○, with 0.5 cc. air).

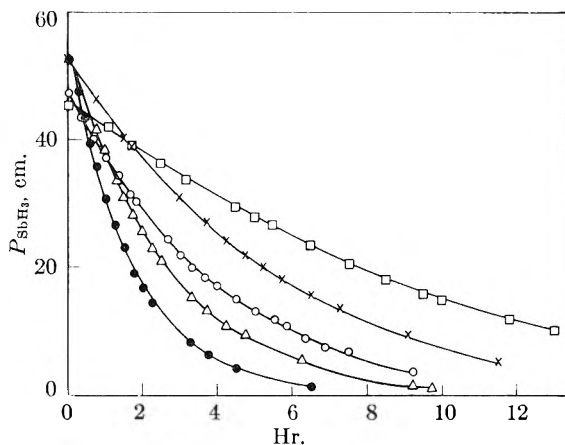


Fig. 3.—Influence of temperature on stibine decomposition: □, 10°; ×, 20°; ○, 25°; △, 35°; ●, 45°.

The order of the reaction was calculated for each experiment applying the expression

$$-dP/dt = k_1 P^n \tag{1}$$

or

$$P^{1-n}/1 - n = C - k_1 t$$

which can fit satisfactorily as shown in Figs. 4 and 5. Table I shows the values of *k₁* and *n* for each experiment, where the suffixes *a*, *b* and *c* show the reaction vessels in which the experiment was carried out.

TABLE I
VALUES OF *k₁* AND *n* IN EQUATION 1

Exp. No.	Temp., °C.	<i>k₁</i> , hr. ⁻¹ cm. ¹⁻ⁿ	<i>n</i>
28c	25	0.63	0.85
34c	25	.57	.86
38c	25	.53	.80
22c ^a	25	.68	.75
47c ^b	25	.58	.76
36a	25	.56	.74
56b	10	.26	.75
51b	20	.36	.80
40b	25	.43	.85
49b	25	.45	.82
37b	25	.50	.80
53b	35	.40	.97
52b	45	.58	1.00

^a 0.5 cm. oxygen was mixed with the reactant. ^b SbD₃ decomposition.

TABLE II
APPARENT ACTIVATION ENERGIES OF THE REACTION AT VARIOUS PARTIAL PRESSURES OF STIBINE

Pressure cm.	10°	20°	log V 25°	35°	45°	Apparent activation energy, kcal./mole
10	0.158	0.356	0.479	0.576	0.760	6.9
20	.384	.597	.725	0.868	1.061	7.9
30	.515	.737	.870	1.039	1.238	8.4
40	.608	.836	.972	1.159	1.362	8.8

From Fig. 2 and Table I it can be seen that the decomposition rate is only dependent upon the partial pressure of stibine, being independent of that of hydrogen; and the order of the reaction in-

creases as the reaction temperature becomes higher, until it gets to first order at 45°.

The dependence of the reaction rate upon the reaction temperature is shown in Table II and Fig. 6, where $\log v$ from Table I is plotted against $1/T$ and the apparent activation energies of the reaction at different pressures are obtained as shown in Table II. The activation energy decreases at lower pressures.

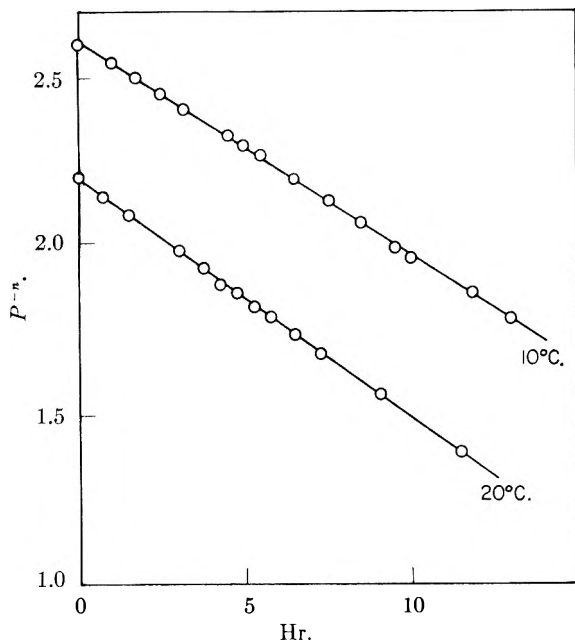


Fig. 4.—Decomposition of stibine, $-dP/dt = kP^n$, $n = 0.75$ at 10°, $n = 0.80$ at 20°.

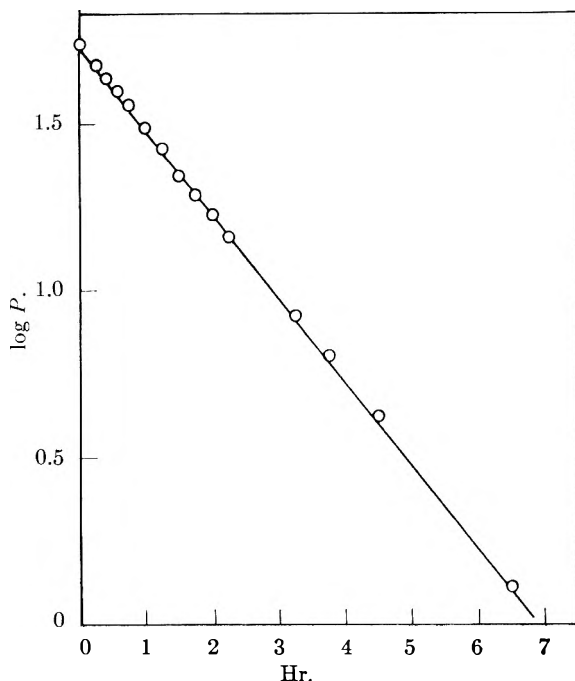


Fig. 5.—Decomposition of stibine at 45°.

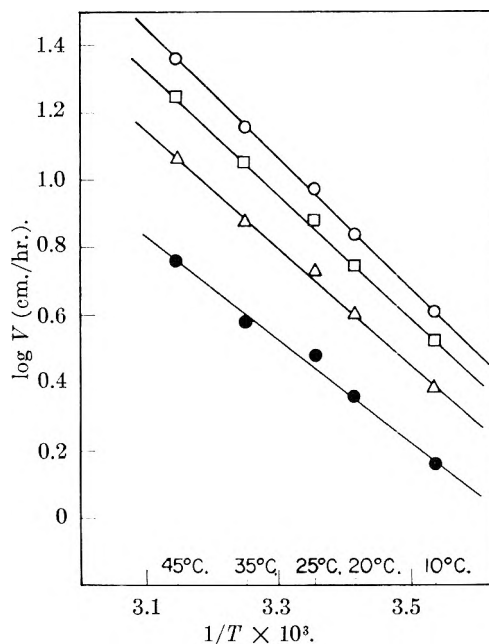


Fig. 6.—Dependence of stibine decomposition rate upon temperature at various pressures: O, 40 cm.; □, 30 cm.; △, 20 cm.; ●, 10 cm.

All these data are qualitatively the same as the experimental results obtained by Stock and co-workers,² but the order of the reaction was a little higher, though the initial pressures were different, and the reaction rates were faster than the data of Stock.

When a small amount of oxygen was mixed with the stibine, the reaction rate was not so remarkably affected as in the case of germane decomposition as shown in Table I. The decomposition curve for deuterostibine lies at the lower boundary of the curves obtained for the decomposition of stibine under similar conditions as shown in Fig. 2 and Table I.

When the Langmuir expression

$$-\frac{dP}{dt} = \frac{k_2 b P}{1 + b P} \quad (2)$$

was applied instead of equation 1, it was found that the experimental results could also be expressed by the equation, as shown in Fig. 7 in the integrated

form. The values of b and k_2 in the equation 2 are shown in Table III.

TABLE III
VALUES OF b AND k_2 IN EQUATION 2

Temp., °C.	b , cm. ⁻¹	k_2 , cm./hr.
10	0.0162	10.3
20	.0121	21.0
25	.0105	31.8
35	.0015	252
45	.000	∞

The theoretical expression for b is $b_0 e^{q/RT}$, where b_0 depends only slightly upon temperature according to the assumption⁸ made concerning the modes of motion of the molecules in the adsorbed state. If q is constant, its value becomes 4.8 kcal./mole from the results at 10, 20 and 25°, which is a little less than the molar heat of liquefaction of stibine, *viz.*, 5.1 kcal./mole and, similarly, the activation energy from the temperature coefficient of k_2 was 12.3 kcal./mole.

After the decomposition of deuterostibine, stibine was decomposed in deuterium at 25°, and the reaction product was analyzed with a mass-spectrometer. On the other hand, deuterostibine and stibine were decomposed separately and a deuterium-hydrogen (1:1) mixture was thus introduced into a reaction vessel, being kept standing for one week at 25°. The gas mixtures before and after being introduced into the reaction vessel were analyzed in the same way. All of these three samples contained only a few per cent. of hydrogen deuteride, respectively, showing that no exchange reaction between hydrogen and deuterium took place on the antimony surface. However, when the mixture of stibine and deuterostibine was decomposed in the reaction vessel, a large amount of hydrogen deuteride was found in the reaction product.

Discussion

As the boiling point of stibine is fairly high, *viz.*, -17° at one atm., and the antimony film itself is fairly porous, having a roughness of 50 from the measurement of the surface area,^{1c} the possibility of capillary condensation of stibine on the film should be examined.

The surface tension (σ) of the liquid stibine can be obtained from the equation

$$\sigma = \left[\frac{D - d}{M} (\text{Parachor}) \right]^4$$

where D and d are the densities of liquid and gas states, respectively, and M the molecular weight. The parachor of stibine is 117.3 and D and d are 2.3 and 0.012 (10°, 2.24 atm.), respectively.⁹ Consequently $\sigma = 19.9$ dyne/cm. at 10°.

According to Kelvin's equation

$$RT \ln \frac{P_C}{P_D} = - \frac{2\sigma v}{r}$$

where v is the molar volume of the liquid, which is 55 cc. for stibine and P_C and P_D are the vapor pressure of the condensed liquid and the saturated va-

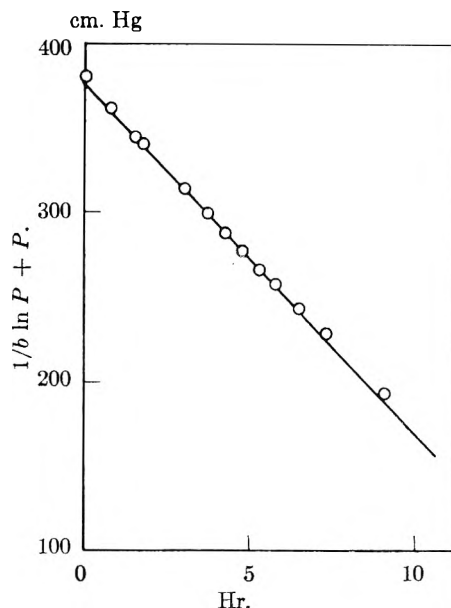


Fig. 7.—Decomposition of stibine at 20°, $-dP/dt = kbP/1 + bP$.

por pressure, respectively, and r is the radius of the capillary tubing. If we assume r is 10^{-8} cm., as a minimum radius of the capillary, P_C/P_D becomes 9.1×10^{-5} , which shows that capillary condensation can take place above 0.16 mm. stibine pressure. If P_C is 0.66 atm., r becomes 0.8×10^{-7} cm., which means that in all the capillaries which are finer than this, capillary condensation occurs when the pressure of stibine is above 0.66 atm.

Thus, in treating the experimental data of stibine decomposition on the porous antimony surface we must take the possibility of capillary condensation of stibine into consideration.

Boudart⁶ tried to analyze Stock's results and got the following values for k_1 , k_2 , b and n in equations 1 and 2.

TABLE IV

Temp. °C.	ANALYSIS OF DATA OF STOCK			
	b , mm. ⁻¹ $\times 10$	k_2 , mm./hr.	n	k_1
0	2.5	12	0.55	0.22
25	2.92	60.6	.56	1.11
50	2.2	330	.63	3.5
75	1.5	1600	.65	12

He found that the rate equation 2, which corresponds to a Langmuir surface, has the practical advantage of simplicity, but its excellent fit has no physical meaning, having too large a value of b_0 ,⁶ that is, of the order of 10^{-4} mm.⁻¹, and a too small q , which is less than 2 kcal./mole. The rate equation 1, on the other hand, derived from the concept of a heterogeneous surface is more satisfactory theoretically, although it, too, must be considered as an approximation to the real situation.

In our experiments, as mentioned above, the Langmuir rate equation 2, though it fits excellently, has the same difficulty, having large b_0 and a small value of q .

The statistical mechanical calculation of the rates of the elementary steps of the decomposition suggests, as will be shown in detail in a later re-

(8) G. Damköhler and R. Edse, *Z. physik. Chem.*, **B53**, 117 (1943).

(9) Landolt-Boörnstein, "Tabellen."

port, that, at higher temperature, the rate-determining step of the over-all reaction is the chemisorption of stibine on the antimony surface, which is first order, but, as the temperature becomes lower, or at room temperature, the desorption rate of the chemisorbed hydrogen from the antimony surface, having larger activation energy than the chemisorption, becomes slow enough to be comparable with the chemisorption rate, and the order of the reaction begins to decrease from unity. If the reaction temperature is extremely low, the desorption rate will become rate-determining, and the over-all process should be zero order. The experimental region studied corresponds consequently to the transition between the two kinds of rate-determining steps.

If this is the case, stibine adsorption on the an-

timony surface is not in equilibrium at room temperature during the decomposition as was assumed in expression (2), and it is quite natural, therefore, that the Langmuir expression has no physical meaning in this case.

Acknowledgments.—The author wishes to express his thanks to Professor Johr. Turkevich who was kind enough to analyze the samples with his mass-spectrometer.

The preceding work was carried out with the assistance of a post-doctoral fellowship kindly provided by the Shell Fellowship Committee of the Shell Companies Foundation, Inc. It also forms part of a program on Solid State Properties and Catalytic Activity supported by the Office of Naval Research N6 onr-27018. For this support we wish to express our appreciation and thanks.

MICROWAVE ADSORPTION AND MOLECULAR STRUCTURE IN LIQUIDS. X. THE RELAXATION TIMES OF NINE HETEROCYCLIC MOLECULES^{1,2}

BY RUSSELL S. HOLLAND³ AND CHARLES P. SMYTH

Contribution from the Frick Chemical Laboratory, Princeton University, Princeton, N. J.

Received May 20, 1955

Measurements of dielectric constant and loss at wave lengths of 1.24, 3.22, 10.7 and 33.3 cm. and 577 m. have been carried out at temperatures from 1 to 60° upon pyridine, γ -picoline, pyrrole, pyrrolidine, quinoline, isoquinoline, thiophene, tetrahydrofuran and furan in the pure liquid state and upon dilute solutions of pyridine in heptane. The critical wave lengths and molecular relaxation times calculated from these results, together with the results in the literature for toluene, are shown, with one exception, to be consistent with the molecular sizes and shapes and the viscosities of the liquids. The Debye relationship between molecular relaxation time, molecular radius and liquid viscosity is shown to apply satisfactorily to the closely related molecules of pyridine, γ -picoline and toluene, in contrast to its failure for dilute solutions when measured viscosities are used. The relation of the molecular relaxation times calculated for these three liquids to the molecular sizes and shapes indicates that the effect of internal field upon the molecular relaxation time obtained by Powles and by O'Dwyer and Sack as a first order approximation is more nearly correct than the Debye relationship or the supposedly more exact second order approximation of O'Dwyer and Sack.

The program of investigation carried out in this Laboratory upon the relation between dielectric relaxation and molecular structure has encompassed a variety of comparatively simple polar organic molecules,⁴⁻¹⁰ most of which are more or less flexible or nearly spherical. Nine heterocyclic compounds, all but two of which are aromatic in character, have been selected in the present work to demonstrate the behavior of rigid molecules. Five of the compounds have five-membered rings, two have six-membered rings,

and two are a fused ring system of two six-membered rings. All have been measured as pure liquids, and, in addition, pyridine has been investigated as a polar solute in heptane solution.

Purification of Materials.—*n*-Heptane from the Phillips Petroleum Co. was used as solvent without purification. The pyridine used was "spectro grade" from the Eastman Kodak Company and the γ -picoline and tetrahydrofuran were from Brothers Chemical Company, while the other six compounds were from Matheson, Coleman and Bell, Inc. The pyridine was refluxed for 48 hours over barium oxide and fractionated. The quinoline and isoquinoline were refluxed for 48 hours over barium oxide and fractionated at reduced pressure. The pyrrole, thiophene, γ -picoline, tetrahydrofuran, pyrrolidine and furan were fractionally distilled, the two latter substances immediately before use. Boiling points or melting points and refractive indices found for the sodium-D line are tabulated below for comparison with the literature values.

(1) This research has been supported in part by the Office of Naval Research. Reproduction, translation, publication, use or disposal in whole or in part by or for the United States Government is permitted.

(2) This paper represents a part of the work submitted by Mr. R. S. Holland to the Graduate School of Princeton University in partial fulfillment of the requirements for the degree of Doctor of Philosophy.

(3) Procter and Gamble Fellow in Chemistry, 1953-1954.

(4) W. M. Heston, Jr., E. J. Hennelly and C. P. Smyth, *J. Am. Chem. Soc.*, **70**, 4093 (1948).

(5) H. L. Laquer and C. P. Smyth, *ibid.*, **70**, 4097 (1948).

(6) E. J. Hennelly, W. M. Heston, Jr., and C. P. Smyth, *ibid.*, **70**, 4102 (1948).

(7) W. M. Heston, Jr., A. D. Franklin, E. J. Hennelly and C. P. Smyth, *ibid.*, **72**, 3443 (1950).

(8) A. D. Franklin, W. M. Heston, Jr., E. J. Hennelly and C. P. Smyth, *ibid.*, **72**, 3447 (1950).

(9) A. J. Curtis, P. L. McGeer, G. B. Rathmann and C. P. Smyth, *ibid.*, **74**, 644 (1952).

(10) F. H. Branin, Jr., and C. P. Smyth, *J. Chem. Phys.*, **20**, 1121 (1952).

Substance	B.p., °C.	Lit. b.p., °C.	n_D^{20}	Lit. n_D^{20}
<i>n</i> -Heptane			1.3881	1.3878
Pyridine	114.4-114.7	115.3	1.5096	1.5096
Pyrrole		129.7	1.5097	1.5035
Pyrrolidine	84.3 (756 mm.)	88.5	1.4385	1.4431
Furan	31	31-32	1.4222	1.4216
Thiophene	83.5-83.8	84.1	1.5281	1.5285
Quinoline	M.p. -19-20	M.p. -19.5	1.6202	1.6245
			(24.9°)	(24.9°)
γ -Ficoline	143.8 (752 mm.)	143.1	1.5029	1.5029
Tetrahydrofuran	64.5-65	65-66		

TABLE I
 DIELECTRIC CONSTANTS AND LOSSES OF HETEROCYCLIC COMPOUNDS

t , °C.	n_D^2	ϵ'	ϵ''	ϵ'	ϵ''	ϵ'	ϵ''	ϵ'	ϵ''	ϵ_0
		1.24		3.22		10.7		33.3 cm.		
Pyridine										
1	...	6.740	5.46	11.49 ^a	4.79 ^a	14.65 ^b
20	2.279	7.386	5.24	11.62 ^a	3.74 ^a	13.25	1.42	13.55
40	...	7.969	5.10	11.32 ^a	3.53 ^a	12.32	1.00	12.45
60	...	8.333	4.31	10.63 ^a	2.22 ^a	11.36	0.78	11.44
γ -Picoline										
1	2.299	4.166	3.03	7.267	4.64	12.49	2.89	12.86	1.00	(13.1)
20	2.267	4.355	3.72	8.165	4.14	11.59	2.16	12.06	0.71	(12.2)
40	2.235	4.715	4.05	8.726	3.68	10.93	1.67	11.30	0.55	(11.3)
60	2.206	5.432	4.36	8.893	3.04	10.29	1.21	10.57	0.40	(10.5)
Pyrrole										
1	(2.311)	4.482	2.22	6.575	2.33	8.370	1.11	8.42 ^b
20	2.279	4.829	2.40	7.003	2.00	8.046	0.87	8.10
40	2.250	5.251	2.53	7.055	1.59	7.670	0.64	7.76
60	(2.216)	5.569	2.35	6.978	1.24	7.362	0.47	7.45
Pyrrolidine										
1	(2.101)	3.777	1.94	5.095	2.57	9.29 ^b
20	2.069	4.131	2.15	5.781	2.42	7.57 ^b	1.40 ^b	8.257	(0.57)	8.30
40	2.046	4.425	2.08	6.118	1.91	7.24	0.71	7.282	(0.26)	7.36
60	2.025	4.511	1.86	6.020	1.35	6.57	0.51	6.627	(0.16)	6.60
Quinoline										
1	2.654	3.227	0.75	3.532	1.42	9.325	2.19	9.70
20	2.631	3.226	1.04	3.904	1.93	8.896	1.27	9.03
40	2.605	3.276	1.29	4.398	2.27	8.473	0.86	8.40
60	2.582	3.441	1.63	4.898	2.32	8.082	0.64	7.81
Isoquinoline										
25	...	3.242	1.00	3.821	1.85	9.834	2.16	10.43
40	...	3.267	1.20	4.038	2.20	9.714	1.65	9.88
60	...	3.339	1.55	4.563	2.53	9.307	1.10	9.22
Thiophene										
1	2.357	2.370	0.176	2.816	0.082	2.823	0.011	2.837
20	2.334	2.697	.154	2.752	.064	2.764	.013	2.769
40	2.299	2.650	.124	2.697	.051	2.700	.006	2.701
60	2.266	2.582	.090	2.603	.038	2.634	.007	2.635
Furan										
1	(2.060)	3.009	0.318	3.088	0.129	3.067	0.021	3.095
20	2.023	2.920	0.245	2.958	0.092	2.964	0.014	2.954
Tetrahydrofuran ^{b,c}										
1	2.00	6.92	2.95	8.38	1.44	8.90
20	1.98	6.91	2.14	7.87	1.13	8.20
40	1.95	6.67	1.66	7.30	0.81	7.60

^a Measured by Mr. B. B. Howard. ^b Measured by Dr. R. C. Miller. ^c May contain about 1% water.

Methods of Measurement.—Dielectric constants and losses at wave lengths of 1.24, 3.22 and 10.7 cm., the static dielectric constants, the refractive indices, the densities and the viscosities were measured by the methods described in earlier papers of this series,⁴⁻¹¹ some modifications and improvements having been made.¹² The measurements at 6.6 and 33.3 cm. and some of those at 10.7 cm. were made with a coaxial resonant cavity cell constructed by Mr. D. A. Pitt. Measurements were made at 1, 20, 40 and 60°, where possible. Quinoline and isoquinoline had too high a loss to permit measurement at 10.7 cm. with the apparatus available at the time.

All of the nitrogen-containing compounds were highly conducting as compared to other organic compounds. Some conducted too strongly to permit measurement of the

static dielectric constant with the bridge. Where possible, static dielectric constants were measured at 0.5, 5.0 and 50.0 kc. and extrapolated to infinite frequency in order to eliminate the effects of polarization of the cell electrodes. When this high conductance was observed during the course of the static dielectric constant measurements, the loss was corrected by means of the relation

$$\epsilon''_{\text{obs.}} = \epsilon''_{\text{cor.}} + 2k/f$$

where k is the d.c. conductance in electrostatic units and f is the frequency at which ϵ'' is determined. Conductances were measured at 1000 cycles by means of an ordinary conductance cell with 1 cm.² platinized platinum electrodes and a Serfass conductance bridge. All of the observed conductances were less than 5×10^{-6} mho, and, since the lowest microwave frequency employed was 9×10^8 cycles per second, the error in the observed dielectric loss due to conductance was never greater than 0.004.

(11) F. H. Branin, Jr., *J. Appl. Phys.*, **23**, 990 (1952).

(12) R. S. Holland, Ph.D. Thesis, Princeton University, 1954.

Experimental Results

The squares of the refractive indices, n^{20D} , the dielectric constants, ϵ' , and the dielectric losses, ϵ'' , for the pure liquids and for solutions of pyridine in heptane are given in Table I. It has been shown previously^{7,9} that, for dilute solutions, the slopes a of the linear plots of ϵ' and ϵ'' against mole fraction or weight fraction of polar solute may be used to obtain the relaxation times or critical wave lengths. Critical wave lengths calculated in the usual manner are given in Table III, together with values of the distribution coefficients α , densities d , viscosities η , macroscopic relaxation times τ_M , molar volumes V , and dipole moments μ . The moments are taken from the literature, using gas values where available. The viscosities for pyridine are taken from "International Critical Tables," those for γ -picoline and pyrrolidine have been measured by Dr. R. C. Miller, and those for pyrrole have been measured by Dr. Miller or corrected from the measurements of one of us.

TABLE II

SLOPES (a) FOR DEPENDENCE OF DIELECTRIC CONSTANTS AND LOSSES OF SOLUTIONS UPON MOLE FRACTION OF PYRIDINE IN HEPTANE

t , °C.	ϵ_1	a_{∞}	λ_0	a'	a''
1	1.948	0.20	1.24	3.50	1.26
			6.6	3.90	0.35
			10.7	4.10	.19
20	1.922	0.17	1.24	3.26	1.06
			6.6	3.66	0.25
			10.7	3.70	.15
40	1.895	0.17	1.24	3.00	.86
			6.6	3.32	.17
			10.7	3.40	.11
			33.3	3.38	.04

Discussion of Results

Pyridine and γ -picoline differ structurally only in that γ -picoline carries a methyl group in the 4-position. Since they have roughly equal dipole moments, densities and viscosities, the intermolecular forces should be of similar magnitudes in the two liquids. However, the critical wave lengths of γ -picoline are almost twice those of pyridine and show a greater rate of change with temperature, indicating that the protrusion of the methyl group from the ring hinders orientation of the dipole, while not interfering appreciably with the process of viscous flow. The relaxation time of γ -picoline depends on both the effect of the methyl group and the dipolar forces present in the liquid as evidenced by its macroscopic relaxation time, 1.33×10^{-11} sec. at 20°, being almost twice that of pyridine, 0.71×10^{-11} sec., and that of toluene, $0.73-0.77 \times 10^{-11}$ sec.,¹³ the latter molecule having a size and shape similar to that of γ -picoline, but without its large dipole moment.

The internal field should be considered¹⁴ in comparing the relaxation times of toluene and those of pyridine and γ -picoline, since the latter two sub-

TABLE III

DENSITIES, VISCOSITIES, CRITICAL WAVE LENGTHS, DISTRIBUTION COEFFICIENTS AND RELAXATION TIMES

t , °C.	d	η (cps)	λ_m (cm)	α	$\tau_M^M \times 10^{11}$ (sec.)	V (cc.)	$\mu \times 10^{18}$
Pyridine							
1	0.995	1.31	1.69	0.04	0.90	79.5	
20	.982	0.95	1.37	.0	.71	80.6	2.22
40	.962	.72	1.12	.0	.59	82.2	
60	.942	.58	0.90	.0	.48	84.0	
γ -Picoline							
1	0.971	1.27	3.2	0.08	1.7	95.7	
20	.954	0.94	2.51	.05	1.33	97.6	2.57
40	.936	.70	1.98	.03	1.05	99.4	
60	.917	.56	1.53	.00	0.81	101.5	
Pyrrole							
1	0.985	2.1	1.98 ^a	0.14 ^a	1.05 ^a	68.1	
20	.969	1.31	1.47	.09	0.78	69.2	1.84
40	.953	0.92	1.11	.05	.59	70.4	
60	.935	0.67	0.91	.03	.48	71.7	
Pyrrolidine							
1	0.887	1.34	4.0 ^a	0.18 ^a	2.1 ^a	80.2	
20	.868	0.92	2.45	.15	1.30	81.8	1.6
40	.850	.67	1.50	.11	0.80	83.6	
60	.829	.51	1.10	.07	0.58	85.7	
Quinoline							
1	1.108	6.72	14.5	0.11	7.7	116.5	
20	1.092	3.95	8.4	.09	4.5	118.2	2.18
40	1.077	2.55	5.63	.07	2.99	119.8	
60	1.062	1.78	3.72	.07	1.97	121.7	
Isoquinoline							
25	1.094	3.95	12.4	0.13	6.6	118.0	
40	1.082	2.75	8.52	.11	4.52	119.4	2.53
60	1.066	1.89	5.63	.08	2.99	121.1	
Thiophene							
1	1.084	0.840	0.60	0.01	0.316	77.6	
20	1.062	.652	.51	.01	.268	79.1	0.55
40	1.039	.517	.44	.01	.231	81.0	
60	1.014	.423	.38	.09	.20	82.9	
Furan							
1	0.963	0.470 ^a	0.41	0.0	0.22	70.7	0.72
20	0.937	0.380	.33	0.0	0.17	72.7	
Tetrahydrofuran ^a							
1	0.9085	0.636	0.73	0.03	0.39	79.4	1.70
20	.8886	.506	.54	.07	.29	81.2	
40	.8675	.416	.42	.09	.22	83.2	
Pyridine in heptane							
1			0.46	0.05	0.24		2.22
20			.42	.04	.22		
40			.36	.06	.19		

^a Measured and calculated by Dr. R. C. Miller.

stances have dielectric constants of 13.3 and 12.2, respectively, at 20°, implying possible large field corrections, while that of toluene is only 2.39, so that the internal field will have but negligible effect on the molecular relaxation time of the latter substance. In the original equations of Debye¹⁵ based on the Lorentz internal field the macroscopic

(13) D. H. Whiffen and H. W. Thompson, *Trans. Faraday Soc.*, **42A**, 114, 122 (1946).

(14) Cf. C. P. Smyth, *This Journal*, **52**, 580 (1954).

(15) P. Debye, "Polar Molecules," Chemical Catalog Co., New York, 1929, Chap. V.

relaxation time τ_M in Table III was replaced by a molecular or microscopic relaxation time, which may be called τ_μ , given by the relation

$$\tau_\mu = \frac{\epsilon_\infty + 2}{\epsilon_0 + 2} \tau_M \quad (1)$$

where ϵ_∞ is the optical or infinite frequency dielectric constant and ϵ_0 is the static dielectric constant given in Table I. Powles¹⁶ has obtained an approximate expression for the internal field which leads to

$$\tau_\mu = \frac{2\epsilon_0 + \epsilon_\infty}{3\epsilon_0} \tau_M \quad (2)$$

a relation which has been shown¹⁴ to be closer to reality than the Debye expression. A more exhaustive treatment by O'Dwyer and Sack¹⁷ has yielded this same expression as a first-order approximation and, as a second-order approximation, the supposedly more exact expression

$$\tau_\mu = \frac{3\epsilon_\infty\epsilon_0(2\epsilon_0 + \epsilon_\infty)}{2\epsilon_0^3 + \epsilon_\infty^3} \tau_M \quad (3)$$

The almost identical shapes and sizes of the γ -picoline and toluene molecules make this pair especially suited to test the field corrections. In Table IV are given the macroscopic relaxation times τ_M and the molecular or microscopic relaxation times τ_μ calculated by means of equations 1, 2 and 3.

TABLE IV

DEPENDENCE OF RELAXATION TIME ($\times 10^{11}$ SEC.) ON INTERNAL FIELD AT 20°

	ϵ_0	ϵ_∞	η	τ_M	(1)	τ_μ (2)	(3)
Pyridine	13.3	2.3	1.12	0.71	0.20	0.51	0.27
γ -Picoline	12.2	2.3	1.07	1.33	.40	.97	.53
Toluene	2.39	2.22	0.59	0.75	.72	.74	.73

Qualitatively, it would be expected that γ -picoline should have a relaxation time longer than that of toluene, since its viscosity is twice as high and dipole interactions should tend to hinder orientation in the pure polar liquid. The proper relationship exists in the relaxation times in column (2), where that of γ -picoline is one third longer than that of toluene, but it can be seen in column (3) that equation (3) overcorrects for the dipole interactions to the extent that the relaxation time of γ -picoline becomes shorter than that of toluene. The values in column (1) calculated by the Debye expression show an even greater overcorrection. The apparently overcorrected relaxation time 0.27 of pyridine in column (3) is slightly higher than the solution relaxation time of 0.22, which would not be significantly altered by correction, but it would be expected that the proper molecular relaxation time of the pure polar liquid would be longer than this because of the effect of viscosity and the interactions of neighboring dipoles. The Debye relaxation time in column (1) is even lower, again showing excessive overcorrection.

The relations between the molecular relaxation times may be considered quantitatively in terms of the Debye relationship¹⁵

$$\tau_\mu = \frac{4\pi\eta a^3}{kT} \quad (4)$$

where a is the molecular radius. Measurement of Stuart-Briegleb models set up for the molecules shows that the molecular diameters in which the nitrogen atom and the methyl group, hence the molecular dipoles, lie are approximately: 5.8 Å. for pyridine, 6.8 for γ -picoline, and 7.8 for toluene. The Debye relationship has often been shown¹⁴ to fail when the macroscopic or measured viscosity is used for η , particularly when the latter varies over a wide range. Pyridine and γ -picoline resemble each other so closely in dielectric constant and viscosity that their critical wave lengths and macroscopic relaxation times should be in the ratio of the cubes of their various radii, approximately 0.6. 0.6 of the critical wave length of γ -picoline at 1° is 1.92 as compared to the observed 1.69 for pyridine, as good agreement as is warranted by the accuracy of the radii. A similar calculation at 60° gives 0.92 for pyridine in fortuitously good agreement with the observed value 0.90. At 20°, the value of τ_M thus calculated for pyridine is 0.80×10^{-11} sec. as compared to 0.71×10^{-11} observed. The value of the molecular relaxation time τ_μ for pyridine similarly calculated from that for γ -picoline in column (2) of Table V is 0.58×10^{-11} as compared to 0.51 observed. The internal field correction is so nearly the same for the two liquids that its application while altering the value calculated for the relaxation time, does not materially alter the relative difference between the observed and calculated values. For toluene, which has a viscosity of only 0.59 centipoise at 20°, the molecular relaxation time calculated by multiplying that for γ -picoline in column (2) of Table V by the factor $\eta_{\text{tol.}} a^3_{\text{tol.}} / \eta_{\text{pic.}} a^3_{\text{pic.}}$ given by eq. (4) is 0.75, as compared to the value 0.74 in Table V. For these three liquids, not differing greatly in viscosity and having molecules differing little in size and shape, the Debye relationship (eq. 4) evidently applies satisfactorily.

Because of the protons carried by their respective nitrogen atoms, pyrrolidine and pyrrole should show hydrogen bonding effects. Indeed, pyrrole, the molecule of which is slightly smaller than pyridine and has a smaller dipole moment, has a longer critical wave length and higher viscosity than the latter, consistent with the effect of hydrogen bonding evidenced by its molecular association.¹⁸

At 60° the viscosities of the two five-membered ring compounds, pyrrole and pyrrolidine, and that of the six-membered ring compound, pyridine, are nearly equal, but the critical wave length or macroscopic relaxation time of pyrrolidine is considerably higher than those of the other two liquids. As the static dielectric constants of pyrrole and pyrrolidine are nearly the same, a correction for the effect of internal field would not significantly alter the ratio of the values for these two substances. The rate of increase of critical wave length with decreasing temperature is greater for pyrrolidine than for pyrrole, while the reverse is true for the viscosities, the result being that, at 1°, pyrrolidine

(16) J. G. Powles, *J. Chem. Phys.*, **21**, 633 (1953).

(17) J. J. O'Dwyer and R. A. Sack, *Australian J. Sci. Research*, **A5**, 647 (1952).

(18) S. N. Vinogradov and R. H. Linnell, *J. Chem. Phys.*, **23**, 93 (1955).

has the lowest viscosity and much the highest critical wave length.

Since pyrrole is aromatic, while pyrrolidine behaves chemically as an aliphatic secondary amine, it may be enquired whether the differences in their dielectric behavior are paralleled by similar differences between bromobenzene and cyclohexyl bromide. Cyclohexyl bromide has a longer critical wave length than the aromatic bromobenzene,⁶ but it also has a much larger viscosity.¹⁹ Greater molecular association through hydrogen bonding might account for the large critical wave length of pyrrolidine, but it should also raise the boiling point and the viscosity of pyrrolidine above those of pyrrole, which actually has the higher boiling point and viscosity. Consequently, until further information has been acquired, the critical wave length of pyrrolidine must be regarded as an anomaly, possibly attributable to an effect of hydrogen bonding. No such anomaly exists in the critical wave lengths of the somewhat analogous pair of substances, furan and tetrahydrofuran, in which there should be no hydrogen bonding.

Both quinoline and isoquinoline, as would be expected from consideration of the large and virtually equal sizes of their molecules, exhibit long critical wave lengths and high viscosities, isoquinoline having a considerably longer critical wave length, but a viscosity only slightly higher. The increase of critical wave length of isoquinoline over that of quinoline is greater than would be expected from the approximately equal viscosities. In quinoline the axis of the molecular dipole is nearly parallel to the short axis of the molecule in the plane of the rings, while, in isoquinoline, it makes an angle slightly less than 30° with the long axis in the plane of the rings. This effectively increases the radius of the orienting unit and, consequently, the observed critical wave lengths and relaxation times. The small distribution coefficients of these two unsymmetrical molecules are slightly larger than those for the seven more symmetrical molecules for which α hardly differs significantly from zero.

(19) W. M. Heston, Jr., E. J. Hennelly and C. P. Smyth, *J. Am. Chem. Soc.*, **72**, 2071 (1950).

Both thiophene and furan have low viscosities and short relaxation times, those for thiophene being slightly greater than the corresponding values for furan at the same temperatures. The two molecules are almost identical structurally. Both are aromatic five-membered rings, their only difference being that thiophene has a sulfur atom in the ring where furan has an oxygen atom. Furan has slightly the larger dipole moment of the two, but the considerably larger polarizability of the sulfur atom as compared to the oxygen may account for the higher viscosity and larger critical wave length of thiophene. The viscosities and critical wave lengths of both liquids are considerably lower than those of pyrrole, which has a molecule of very similar size, but a much larger dipole moment and some hydrogen bonding.¹⁸ The molecule of tetrahydrofuran differs from that of furan in the same way that the molecule of pyrrolidine differs from that of pyrrole. The liquid has a slightly larger molar volume, a larger viscosity, and a longer critical wave length. The molecular relaxation time remains somewhat longer after correction for the effect of internal field by means of equation 2, the values being 0.29 instead of 0.39 at 1° , 0.22 instead of 0.29 at 20° , and 0.16 instead of 0.22 at 40° . The values of the distribution coefficient α are, probably, too small to be significant.

The molar free energies, ΔF^\ddagger , enthalpies, ΔH^\ddagger , and entropies, ΔS^\ddagger , of activation for dielectric relaxation (ϵ) and viscous flow (V), calculated by the method previously described,⁵ are not given. The figures in the second decimal place have, at best, only relative significance. In general it has been found that $\Delta F_\epsilon^\ddagger$ is less than ΔF_V^\ddagger for long-chain compounds,^{6,20} in agreement with the idea that while viscous flow involves both translation and rotation of molecules, dipole orientation involves only rotation. The same relationship is followed for these compounds. The differences between the thermodynamic quantities are consistent with the previously discussed comparisons and differences of dielectric behavior.

(20) P. L. McGeer, Ph.D. Thesis, Princeton University, 1951.

THE REDUCTION OF Ce(IV) IN SOLUTIONS IRRADIATED BY Au¹⁹⁸ BETA-PARTICLES¹

By B. J. MASTERS AND G. E. CHALLENGER

Contribution from the University of California, Los Alamos Scientific Laboratory, Los Alamos, New Mexico

Received May 25, 1955

An automatically recording potentiometric technique has been applied to the study of Ce(IV) reduction and Fe(II) oxidation by Au¹⁹⁸ β -radiation. The observed cerous yield was in general agreement with the values obtained by other investigators using Co⁶⁰ as a radiation source. No significant change in cerous yield was observed during minor variations in irradiation intensity or in the concentrations of Ce(IV), Ce(III) and H₂SO₄. The yield was uninfluenced by the presence or absence of dissolved oxygen gas, and a slight positive temperature coefficient was noted. In contrast to the Co⁶⁰ results, dissolved hydrogen gas was found to cause only a small increase in cerous yield. The inhibition of the Ce(IV) reduction process by silver ion also was studied, and a rate expression for this effect was derived.

The radiation-induced reduction of Ce(IV) in aqueous sulfuric acid solutions has been subjected to study by several independent investigators. Most of the recent work has been performed using the gamma emitter Co⁶⁰ as a radiation source²⁻⁴ although some studies have been made with relatively soft X-rays⁵ and with S³⁵ β -particles of 45 kev. average energy.⁶ It was believed that a study of this system with more energetic β -particles would be of interest. Au¹⁹⁸, which emits β -particles of 0.96 Mev. maximum energy, appeared to be particularly attractive as a radiation source, since its average β -energy approximates the average energy of the secondary electrons formed in aqueous solutions by the passage of a Co⁶⁰ γ -ray.

In order that the course of the Ce(IV) reductions could be studied continuously throughout the irradiations, a potentiometric technique was developed for this work, and the method was found to be readily adaptable to this type of kinetic study.

Experimental Methods

Ferrous sulfate and ceric sulfate solutions were irradiated in the cell shown in Fig. 1. In each case, the course of the reaction was followed by measuring the changing e.m.f. of the Fe(II)-Fe(III) or Ce(III)-Ce(IV) couples relative to the mercurous sulfate electrode. Potentials were recorded on a Brown Recording Potentiometer equipped with a scale folding device.⁷ On this instrument one chart width was equivalent to 0.1 volt, and the total recordable e.m.f. change was 0.6 volt. Potentials could be read to within 0.1 mv. and were quite reproducible. The cell potentials were checked by standard potentiometric methods from time to time, and in no case did the potential obtained in this manner differ measurably from that given by the recording device.

Sources.—The sources consisted of hollow cylinders of 2 mil gold foil about 1.6 in. long and 0.6 in. in diameter. The weight of each source was approximately 2 g. Struts of 10 mil gold wire were welded without flux to the open ends of the cylinders and to small gold rings about 0.15 in. in diameter placed concentrically within the cylinder. After activation, the source was mounted on a glass supporting rod run through these rings.

The sources were activated to approximately 2 to 3 curies each by the reaction Au¹⁹⁷(n, γ)Au¹⁹⁸ in the "Glory Hole" of the Los Alamos Water Boiler reactor. Since the half-life of

Au¹⁹⁸ is only 64.5 hr.,^{8,9} it was necessary to make use of each source as soon as possible after the neutron irradiation. Runs were therefore made in quick succession with each source until the length of time required for the complete reduction of a ceric sulfate solution became excessively long (more than about 24 hr.). In this manner it was possible to make from 8 to 19 runs with each source.

In order to demonstrate that the activity of the sources was that of Au¹⁹⁸ uncontaminated by other radiation, source half-lives were determined from the change of Fe(II) oxidation rate with time. A value of 64.5 \pm 1.1 hr. was obtained, in excellent agreement with the 64.5 hr. value reported in the literature.^{8,9}

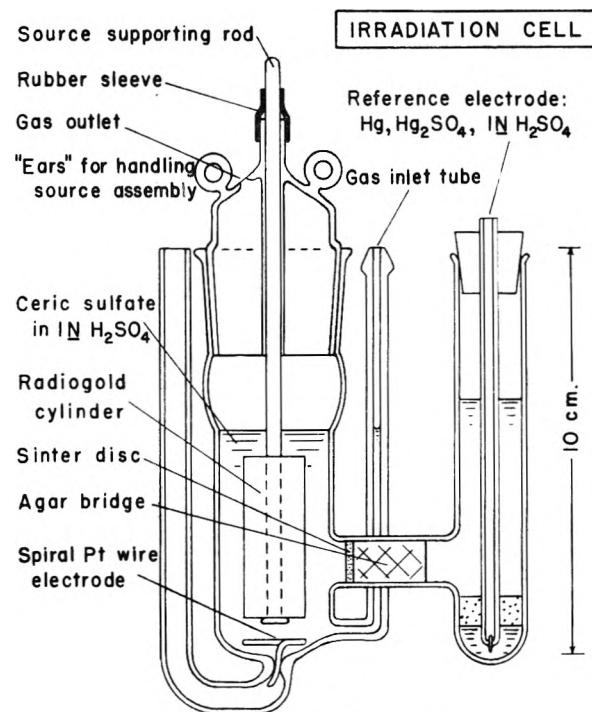


Fig. 1.—Irradiation cell.

The energy distribution of the β -particles emitted from the sources was measured,¹⁰ and the average energy was found to be 0.36 Mev., independent of the angle of emission from planar 2 mil gold foil sources. Beta intensity was found to vary as the sine of the angle of emission from the plane surface.

Thermostat.—This consisted of a hollow lead cylinder of 2 in. wall thickness, 11 in. high and 9 in. in diameter. The walls were provided with holes for electrical leads, thermocouples, and gas inlet and outlet tubes. Water of the desired temperature was circulated through a copper coil cast

(1) This work was performed under the auspices of the United States Atomic Energy Commission.

(2) T. J. Sworski, *J. Chem. Phys.*, **21**, 375 (1953).

(3) E. R. Johnson and Jerome Weiss, *ibid.*, **22**, 752 (1954).

(4) T. J. Hardwick, *Can. J. Chem.*, **30**, 23 (1952).

(5) C. L. Clark and W. S. Coe, *J. Chem. Phys.*, **6**, 97 (1937).

(6) T. J. Hardwick, *Can. J. Chem.*, **30**, 39 (1952).

(7) This instrument was designed and constructed by Group CMR-7 of this Laboratory.

(8) L. M. Silver, *Phys. Rev.*, **76**, 589 (1949).

(9) D. Saxon and R. Heller, *ibid.*, **75**, 909 (1949).

(10) We are indebted to M. Bunker of this Laboratory for determining these β -spectra.

within the walls of the cylinder. The irradiation cell was mounted centrally within the thermostat. In order to maintain thermal contact between the cell and thermostat walls, the lead cylinder was partially filled with water which was continually agitated by means of a bubbling air stream. Cell temperatures were thus controllable to within $\pm 0.1^\circ$.

In the case of the 0° runs, the irradiation cell was placed in a large Dewar filled with cracked ice and surrounded by lead sheets.

Reagents.—Water from the laboratory distilled water supply was further distilled from alkaline permanganate before being used to make up ferrous sulfate and ceric sulfate solutions.

Helium, oxygen and hydrogen used in the major portion of the work were of spectroscopic purity. Some runs were made with electrolytic hydrogen and with commercial grades of helium and oxygen. In each case, the purity of the gas appeared to have no influence upon the observed ceric reduction rate. All gases were bubbled through a 1 *N* H_2SO_4 solution *ca.* 0.01 *M* in $\text{Ce}(\text{SO}_4)_2$ before being passed through the solution in the irradiation cell.

Sulfuric acid was prepared by fractional distillation of J. T. Baker C.P. H_2SO_4 , to which a few crystals of $\text{K}_2\text{Cr}_2\text{O}_7$ had been added.

Cerium metal, 99.5% pure, was supplied by the Ames Laboratory of the Atomic Energy Commission. The principal impurities were: Na, 0.05%; Mg, 0.01%; Ca, 0.005%; La, 0.01%; C, 0.0090%; N, 0.0975%; O, 0.244%; H, < 0.001%. Other metallic impurities were present in amounts too small to be detected by the spectroscopic method used. Cerium sulfate stock solutions were made by dissolving the cerium metal in H_2SO_4 . Cerous sulfate obtained in this manner was oxidized to the ceric state by ozone, after which the solution was either heated or flushed with oxygen in order to remove the excess ozone.

Radiation Safety.—Although the lead thermostat provided adequate radiation protection during a run, additional precautions were needed while mounting, transferring or storing the source. This protection was secured by handling the source on the end of a three foot rod, and keeping the thermostat and source storage pig in a plywood box, measuring 3 ft. \times 2 ft. \times 2 ft. lined with $\frac{1}{4}$ in. lead sheet. As a result, radiation doses received by personnel during the manipulations were negligible.

Irradiation Procedure.—The reaction cell was first filled with 30 ml. of the solution to be irradiated. The cell dimensions were such that all of the β -energy from the source was absorbed by the solution before reaching either the cell walls or the platinum electrode, while 80% or more of the γ -radiation passed through the cell unabsorbed. The cell was then placed in the thermostat, and the gas (helium, oxygen or hydrogen) to be used in the particular experiment was allowed to bubble through the cell at the rate of 7 cc./min. It was found that variations in the gas bubbling rate of as much as 50% had no effect upon the rate of ferrous oxidation or of ceric reduction. After obtaining both temperature equilibrium and a steady potential on the recorder, usually within one-half hour, the source, mounted on a male ground glass joint and carried on the end of a three foot rod, was lowered into the cell. Reproducible irradiation geometry was achieved by mating the standard taper joints. The lead thermostat and the lead lined cave were then covered, and the reaction was allowed to go to completion. At the end of the run, the source was removed, washed with several changes of distilled water, and stored under distilled water within the cave until needed for the following run.

Results and Discussion

The average cerous yield values obtained from all experiments performed under each of the specific conditions are summarized in Tables I and II. Yields, $G_{(\text{Ce}^{+3})}$, are reported in terms of cerous ions produced per 100 e.v. absorbed, with energy absorption being measured by means of the ferrous sulfate dosimeter and using the value¹¹ of $G_{(\text{Fe}^{+3})} = 15.6$ ions/100 e.v.

It was found that, even in the absence of a radiation source, a very slow reduction of ceric ion oc-

TABLE I

AVERAGE CEROUS YIELD VALUES

All solutions 0.001 *M* in cerium except where specified.

Temp., ($^\circ\text{C}$.)	H_2SO_4 , (<i>N</i>)	Sweeping gas	$G_{(\text{Ce}^{+3})}$, (ions/100 e.v.)
0	1.0	He	2.11
15	1.0	He	2.25
25	2.0	He	2.20
25	1.0	He	2.36
25 ($^\circ\text{C}_e = 0.004 M$)	1.0	He	2.36
25	1.0	O_2	2.36
25	0.1	He	2.44
35	1.0	He	2.55
45	1.0	He	2.77
0	1.0	H_2	2.11
15	1.0	H_2	2.38
25	2.0	H_2	2.23
25	1.0	H_2	2.52
35	1.0	H_2	2.75
45	1.0	H_2	2.69

TABLE II

EFFECT OF SILVER AND CESIUM IONS UPON CEROUS YIELD

Temperature = 25° . All solutions 1.0 *N* in H_2SO_4 , 0.001 *M* in cerium, swept with helium gas.

Additive	$G_{(\text{Ce}^{+3})}$, (ions/100 e.v.)	Additive	$G_{(\text{Ce}^{+3})}$, (ions/100 e.v.)
None	2.36	$4.3 \times 10^{-5} M \text{Ag}^+$	2.11
$4.4 \times 10^{-3} M \text{Cs}^+$	2.35	$4.3 \times 10^{-4} M \text{Ag}^+$	1.64
$5.0 \times 10^{-2} M \text{Cs}^+$	2.34	$2.2 \times 10^{-3} M \text{Ag}^+$	1.31
$7.5 \times 10^{-1} M \text{Cs}^+$	2.20	$3.2 \times 10^{-2} M \text{Ag}^+$	1.10
		$5.8 \times 10^{-2} M \text{Ag}^+$	1.14

curred in the irradiation cell. This 'blank' reduction rate, which was found to be quite reproducible, amounted to only a few per cent. of the total reduction rate observed with a radiation source present in the cell. This small "blank correction" was always subtracted from the total amount of reduction in order to calculate the cerous yield values which appear in the tables.

An average value of $G_{(\text{Ce}^{+3})} = 2.36$ ions/100 e.v. was observed for a total of eleven ceric sulfate reduction experiments in 1.0 *N* H_2SO_4 solutions swept with helium gas at 25° . The average deviation from this mean value amounts to 5% in these experiments. Sworski² and Hardwick⁴ report cerous yield values of 2.52 and 2.48, respectively, for the Co^{60} -irradiation of 0.8 *N* H_2SO_4 solutions, again assuming a ferrous dosimeter yield of 15.6. It is apparent that, within the limits of accuracy of the determinations, the results obtained in the Au^{198} -irradiation system are in agreement with those obtained with Co^{60} sources. Since the cobalt γ -ray dissipates most of its energy in aqueous solutions *via* the formation of secondary electrons possessing energies similar to the β -particle energies of radiogold, one would probably expect to find little difference in the primary yield values of H_2 , H_2O_2 , H and OH produced by the two sources. On the other hand, a very great departure from the Co^{60} -irradiation geometry is realized in the present system, and it is gratifying to find that the cerous yield appears to be little influenced in this respect.

Effect of Radiation Intensity.—The rate at which energy was absorbed in the irradiated solutions (total volume 30 ml.) varied between

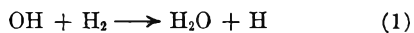
(11) C. J. Hochanadel and J. A. Ghormley, *J. Chem. Phys.*, **21**, 880 (1953).

about 3×10^{17} and 3×10^{18} e.v. per minute during the course of these measurements. Both the ferric and the cerous yields were found to be unaffected by this tenfold variation in irradiation intensity. It should be noted, however, that the energy absorption throughout the cell solution was strongly inhomogeneous, and that maximum specific dosage rates as high as 1×10^{22} e.v./l.-min. were probably attained in the immediate proximity of the radiogold surface.

Effect of H_2SO_4 Concentration.—Although a slight decrease in cerous yield was observed upon varying the sulfuric acid concentration from 0.1 to 2.0 *N* (see Table I), it appears that the value of $G_{(\text{Ce}^{+3})}$ is essentially independent of the acid concentration in solutions approximately 1 *N* in H_2SO_4 .

Oxygen Effect.—In Table I, it may be seen that no difference in the cerous yield value was observed between de-aerated (solutions through which helium gas was bubbled during irradiations) and oxygenated ceric sulfate solutions. Thus, if oxygen enters into the ceric sulfate reduction mechanism at all, it must be in such a way that the net reducing power of the irradiated solution remains unimpaired. This observation is in agreement with the results reported for Co^{60} -irradiations.^{3,4}

Hydrogen Effect.—It will be noted in Table I that the $G_{(\text{Ce}^{+3})}$ values obtained in the presence of H_2 gas average about 10% higher than the yields found with either helium or oxygen gas present. Other investigators^{3,4} have reported a doubling of the cerous yield in the presence of hydrogen gas, attributing the increased yield to the reaction



Although there is evidence¹² which seems to indicate that reaction (1) may indeed be of importance in the irradiated water system, there exists some doubt as to its occurrence in the presence of dissolved sulfuric acid. Allen¹³ has pointed out that in irradiated sulfuric acid solutions the OH species probably reacts with sulfuric acid or its ions to form complexes such as H_2SO_5^- , HSO_4 , etc. Such complexes presumably would be less likely to be reduced by H_2 in the manner of equation 1 than would free OH radicals. This concept seems to be in accord with the findings of the present study. Even with our technique of keeping the solution saturated with hydrogen by bubbling it through the irradiation solution at 580 mm. pressure (one atmosphere at Los Alamos), we were unable to approach the 100% increase in yield reported by the other workers. Further studies of the effect of hydrogen upon the cerous yield should be undertaken in order to resolve this point of difference.

Effect of Cerous and Ceric Ion Concentrations.—In Fig. 2, ceric ion reduction *versus* energy absorption is plotted for a typical run. The point at the origin actually represents about 10% reduction, because below this limit the potential change was too fast for the potentiometer to remain in balance. Throughout the measurable portion

of the reduction process it is apparent that the cerous yield is independent of the concentrations of cerous and of ceric ions. Furthermore, no change in cerous yield was observed during the irradiation of a solution in which the initial ceric ion concentration was 0.004 *M* rather than the usual 0.001 *M* value (see Table I).

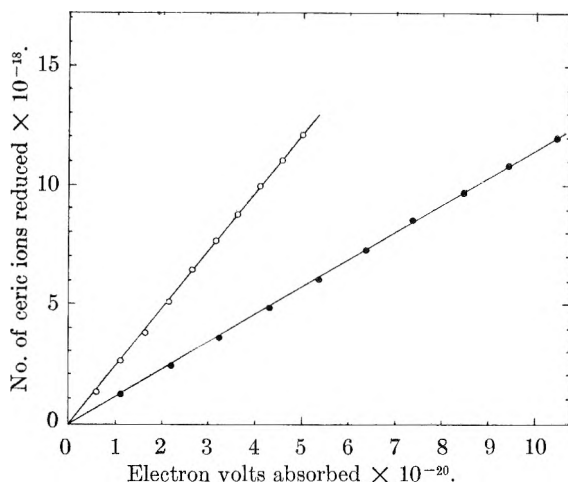


Fig. 2.—Reduction of ceric ion solutions at 25°. 0.001 *M* in $\text{Ce}(\text{SO}_4)_2$, 1 *N* in H_2SO_4 , swept with helium gas; O, without added Ag^+ ; ●, 5.8×10^{-2} *M* Ag^+ added.

Temperature Effect.—The temperature coefficient was found to be about +6% per 10° temperature rise, as compared with the value reported by Hardwick⁴ of about -1.5% per 10° rise for the reduction of ceric sulfate by Co^{60} -radiation. An activation energy of +1.1 kcal./mole may be calculated from the temperature plot of Fig. 3; however, this value is of little significance in view of the approximately 5% average deviation from the mean value of $G_{(\text{Ce}^{+3})}$ for each temperature.

Tests for Residual Oxidizing and Reduction Entities.—Ceric sulfate solutions which had been subjected to extended irradiations also were tested for residual oxidizing and reducing powers. This was done by permitting the reduction to proceed to 95–99% completion, then removing the radiation source from the cell. Any appreciable build up of reducing entities would have been evidenced by a continued drop in cell potential, and conversely, an increase in potential upon removing the source would have indicated an excess of oxidizing entities. However, it was found that the cell potential always remained constant at the instantaneous value it had reached at the time the source was removed. Furthermore, potentiometric titrations of the nearly reduced solutions indicated that the only oxidizing substance remaining in these solutions was residual Ce(IV).

There is also the possibility that persulfate ion, $\text{S}_2\text{O}_8^{2-}$, can be formed in irradiated sulfuric acid solutions along with other peroxy complexes of H_2SO_4 such as those previously mentioned in the discussion of the hydrogen effect. In the absence of silver ion catalyst, the oxidation of Ce(III) by persulfate ion proceeds very slowly, so that an appreciable concentration of persulfate ion could be built up during a lengthy irradiation. In order to test for such a build up of persulfate ion, ceric

(12) C. J. Hochanadel, *This Journal*, **56**, 587 (1952).

(13) A. O. Allen, *Radiation Research*, **1**, 85 (1954).

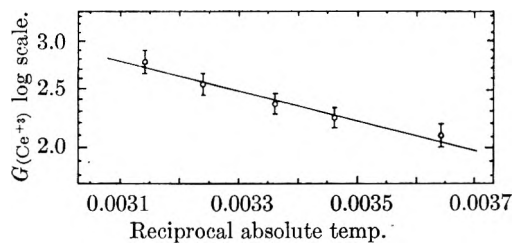


Fig. 3.—Temperature dependence, 0.001 M $Ce(SO_4)_2$ solutions, 1 N in H_2SO_4 , swept with He.

solutions free of Ag^+ were irradiated to about 99% reduction, the source removed, and silver ion added. In no case was an increase in potential noted. Small amounts of persulfate, amounting to about 1% of the cerous ion present, were then added, and an immediate increase in potential was observed. It is therefore evident that if persulfate ion is formed at all in the irradiated solutions, it can be present only in extremely small amounts.

Inhibition by Silver Ion.—Inhibition of the radiation-induced ceric reduction rate in solutions containing added silver ion was first noted by Clark and Coe.⁵ This effect was re-investigated in the present study, in hopes that some elucidation of the ceric sulfate reduction mechanism might result. The results, reported in Table II, are in substantial agreement with those of Clark and Coe.

In Fig. 2 is plotted the course of a typical ceric reduction in the presence of silver ion. It is seen that in this case, as well as in the one in which no added Ag^+ was present, the rate of reduction is independent of both ceric and cerous ionic concentrations. No measurable steady state ceric-cerous ratio was ever found in these or in any other runs, although with the potentiometric method used in this work, steady-state concentration ratios of 1000 to 1 would easily have been detected.

Just what the mechanism of the silver inhibition may be is not clear. That the effect probably is produced by the ability of silver ion to form other oxidation states, rather than merely by the presence of a heavy cation, was evidenced by adding cesium ion to the irradiation solutions in the place of silver ion. In the presence of cesium ion, the cerous yields were found to remain unchanged. In view of the results of the experiments in the preceding section, it also seems likely that the inhibition cannot be caused by any reaction involving persulfate ion, although the possibility that persulfate radical may be of importance cannot be eliminated.

A plot of $G_{(Ce^{+3})}$ versus added silver and cesium ion concentrations appears in Fig. 4. By assuming two reaction paths for the ceric reduction, only one of which is inhibited by Ag^+ , and making the standard steady state assumption, the following rate expression can be derived

$$G_{(Ce^{+3})} = 1.13 + \frac{1.23}{1 + 3.4 \times 10^3 [Ag^+]}$$

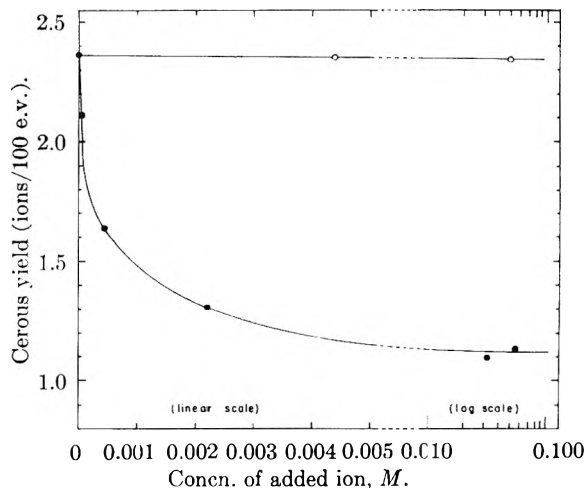


Fig. 4.—Effect of foreign ions: O, added Cs^+ ion; ●, added Ag^+ ion.

where $G_{(Ce^{+3})}$ is the number of cerous ions produced for every 100 electron volts absorbed by the solution and the silver ion concentration is given in moles per liter. This expression fits the data within the experimental error.

Actually, this rate law is of little aid in deducing the mechanism of the silver effect, since many different assumptions as to the specific reactions involved can be reduced to give this rate expression. The cause of the silver inhibition probably can be ascribed to one or more of the following four possibilities

- (1) A change in the primary yields of H, OH, H_2O_2 and H_2 as a result of the presence of Ag^+ ion.
- (2) Interference by Ag^+ in the peroxide reduction of Ce(IV).
- (3) Competition of Ag^+ with Ce(IV) for reducing radicals possibly to form Ag, which in turn could react with some of the primary water decomposition products.
- (4) Reaction of Ag^+ with oxidizing radicals to form Ag^{++} which in turn might either oxidize Ce(III) or react with some of the primary products.

Since the silver ion is present in such extremely low concentration, (1) appears to be a very unlikely explanation. The occurrence of (2) also does not seem probable, since we have been unable to affect the stoichiometry of the Ce(IV) titration with H_2O_2 by adding Ag^+ to the titrating solutions. This possibility cannot be eliminated entirely, however, since our titrations cannot duplicate the experimental conditions which prevailed during the irradiations. On the basis of the data obtained in this study, it is not possible to distinguish between the possibilities (3) and (4). However, direct measurements of the oxidation of Ce(III) to Ce(IV) in irradiated solutions recently have been made by the authors¹⁴ using tracer techniques, and the same methods applied to solutions containing added silver ion may prove to be of value in the determination of the silver inhibition mechanism.

(14) G. E. Challenger and B. J. Masters, *J. Am. Chem. Soc.*, **77**, 1063 (1955).

WETTING PROPERTIES OF ORGANIC LIQUIDS ON HIGH ENERGY SURFACES

BY H. W. FOX, E. F. HARE AND W. A. ZISMAN

Surface Chemistry Branch, Chemistry Division, Naval Research Laboratory, Washington, D. C.

Received June 2, 1955

An investigation has been made of the relation between the constitution of organic liquids and their ability to wet and spread on solids of high melting point (high free surface energy). Wettability was measured by the contact angle at 20° of each liquid on various metals, fused silica and α -alumina (sapphire). Large differences were found in the wettability of the various metals and the silica and α -alumina. These were caused by differences in the adsorption forces and by the existence of a firmly bound layer of water of hydration on the surfaces of the non-metallic crystals. A large variation in wettability could be caused in the latter by the partial dehydration resulting from baking treatments. For these reasons, a greater variety of liquids wet metals than non-metals. Few liquids exhibited non-spreading on all high energy surfaces. It was found that many carboxylic esters hydrolyze at ordinary temperatures upon being adsorbed on silica or α -alumina. When the products released by hydrolysis *in situ* formed adsorbed films having a low enough critical surface tension, the parent ester was nonspreading. It is concluded that the wettability of smooth high energy surfaces by organic liquids can be predicted approximately from knowledge of the orientation and packing of the molecules adsorbed from the liquid phase. The nature of the high energy solid surface is important only insofar as it affects the adsorptivity of the liquid or as it causes chemical changes during adsorption which change the nature of the most adsorbable molecular species present. Pure organic liquids spread completely on all high energy surfaces unless the liquid is (a) "autophobic" or (b) able to decompose on adsorption to release a more adsorbable product which converts the solid surface into one of low surface energy. The qualitative effects on the wettability of varying the temperature, humidity, and roughness of solid are discussed.

Introduction

High melting point solids such as diamond, sapphire, silica and most metals have free surface energies at ordinary temperatures which are believed to range from several thousand to several hundred ergs/cm.².¹ Low melting solids such as organic polymers, waxes and covalent compounds in general have free surface energies ranging from 100 to as low as 25 ergs/cm.². It is convenient to describe the former group of solids as having "high surface energy" and the latter as having "low surface energy."

Nearly all liquids other than liquid metals have free surface energies (γ_{LV}^0) of less than 75 ergs/cm.² at ordinary temperatures. Each such liquid would be expected to spread spontaneously on any clean "high energy surface" because there would thereby be expected to result a decrease in the free surface energy (F) of the system. The precise condition for the spreading of the liquid on the clean dry solid is that $(\partial F/\partial A)$ the free energy change per unit area wetted should be negative. If S_{LV^0/S^0} is the initial spreading coefficient of Harkins, the free energy change that takes place when a liquid spreads on a solid is

$$-\frac{\partial F}{\partial A} = S_{LV^0/S^0} = \gamma_S^0 - \gamma_{SL} - \gamma_{LV}^0$$

Here use is made of the convenient nomenclature of Boyd and Livingston,³ γ_S^0 being the free energy per unit area of the solid/vacuum interface and γ_{SL} the free energy of the solid/liquid interface. Evidently, the necessary condition for spreading is that S_{LV^0/S^0} be positive; this will occur only when $\gamma_S^0 > \gamma_{SL} + \gamma_{LV}^0$. Many years ago Harkins and Feldman,⁴ extrapolating from measurements of the spreading coefficients of liquids on water and mercury,^{5,6} concluded that practically all liquids

should spread on clean metals and other inorganic high melting solids.

Our research during the past ten years has shown that if the liquid in contact with a high energy surface is made up in whole or in part of polar-non-polar molecules of certain types, there will be produced through adsorption at the solid/liquid interface a low energy surface on which the liquid will not spread. When the adsorbed film comprises long-chain, unbranched, polar molecules, which are able to form a close-packed array with terminal $-\text{CH}_3$, $-\text{CF}_2\text{H}$ or $-\text{CF}_3$ groups,⁷⁻¹² the resulting surfaces permit spreading only by liquids having low surface tensions. When the adsorbed molecules are branched or cyclic structures,¹³ the resulting surfaces permit spreading by all liquids excepting those having high surface tensions. Recently it has been shown¹⁴ that many classes of pure liquids including the branched and unbranched aliphatic alcohols and acids are "autophobic," *i.e.*, each liquid is unable to spread on its own adsorbed film. When the solid is coated with a non-polar adsorbed film such as an n -alkane or perfluoroalkane, non-spreading occurs if the liquid has a higher surface tension than the critical surface tension (γ_c) of the adsorbed layer.¹³ We have defined γ_c of a solid surface as that value of the liquid surface tension above which liquids show finite contact angles (θ_E) on the given surface.^{2,15}

Provided that information is available on the over-all configuration and packing of the adsorbed molecules of liquid, it should be possible to explain

- (1) W. D. Harkins in Alexander's "Colloid Chem.," Vol. VI, Reinhold Publ. Corp., New York, N. Y., 1946, p. 4.
- (2) H. W. Fox and W. A. Zisman, *J. Colloid Sci.*, **5**, 514 (1950).
- (3) G. E. Boyd and H. K. Livingston, *J. Am. Chem. Soc.*, **64**, 2383 (1942).
- (4) W. D. Harkins and A. Feldman, *ibid.*, **44**, 2665 (1922).
- (5) W. D. Harkins and E. H. Grafton, *ibid.*, **42**, 2534 (1920).
- (6) W. D. Harkins and W. W. Ewing, *ibid.*, **42**, 2539 (1920).

- (7) W. C. Bigelow, D. L. Pickett and W. A. Zisman, *J. Colloid Sci.*, **1**, 513 (1946).
- (8) W. C. Bigelow, E. Glass and W. A. Zisman, *ibid.*, **2**, 563 (1947).
- (9) E. G. Shafrin and W. A. Zisman, *ibid.*, **7**, 166 (1952).
- (10) F. Schulman and W. A. Zisman, *ibid.*, **7**, 465 (1952).
- (11) A. H. Ellison, H. W. Fox and W. A. Zisman, *THIS JOURNAL*, **57**, 622 (1953).
- (12) E. F. Hare, E. G. Shafrin and W. A. Zisman, *ibid.*, **58**, 236 (1954).
- (13) H. W. Fox, E. F. Hare and W. A. Zisman, *J. Colloid Sci.*, **8**, 194 (1953).
- (14) E. F. Hare and W. A. Zisman, *THIS JOURNAL*, **59**, 335 (1955).
- (15) H. W. Fox and W. A. Zisman, *J. Colloid Sci.*, **7**, 428 (1952).

TABLE I
CONTACT ANGLES OF ALIPHATIC CARBOXYLIC ESTERS AND ETHERS
(Measurements at 20° and 50% R.H.)

No.	Compound obsd.	Source ^a	Surface tension, dynes/cm. at 20°	On metals, degree 18/8 Steel	Brass	On non-metals, degree Silica	Sapphire
Aliphatic diesters							
1	Dibutyl citraconate	a	30.4	0	0	10	0
2	Dibutyl pyrotartrate	a	29.3	0	0	11	0
3	Bis-(2-ethylhexyl) adipate	a	30.2	0	0	23	15
4	Dibutyl β -methyladipate	a	30.4	0	0	11	0
5	Bis-(2-ethylhexyl) β -methyladipate	a	30.1	0	0	22	8
6	Bis-(2-ethylhexyl) sebacate	a	31.1	0	0	16	11
7	Bis-(1-methylheptyl) sebacate	a	31.0	0	0	17	6
8	Dioctyl sebacate	a	32.2	0	0	13	11
9	Bis-(3,5,5-trimethylhexyl) sebacate	a	29.9	0	0	12	10
10	Bis-(2-ethylhexyl) glutarate	..	29.4	0	0	21	13
11	Bis-(3,5,5-trimethylhexyl) glutarate	a	28.4	0	0	26	22
12	Bis-(2-ethylhexyl) β,β' -thiodipropionate	a	31.3	0	0	33	24
13	Bis-(2-(2-ethylbutoxy)-ethyl) azelate	a	34.3	0	0	0	0
14	Diethylene glycol dicaproate	a	30.8	0	0	29	20
15	Dipropylene glycol dicaproate	a	29.5	0	0	15	5
16	Triethylene glycol bis-(2-ethylhexanoate)	a	30.3	0	0	23	15
17	Polyethylene glycol bis-(2-ethylhexanoate)	a	28.2	0	0	23	21
18	1,6-Hexanediol bis-(2-ethylhexanoate)	a	30.2	0	0	5	0
19	1,10-Decanediol bis-(2-ethylhexanoate)	a	31.4	0	0	0	0
Aliphatic monoesters							
20	Decyl acetate	f	28.3	0	0	0	0
21	Amyl caproate	g	27.0	0	0	0	0
22	Decyl caproate	f	28.8	0	0	11	0
23	Undecyl 2-ethylhexanoate	a	27.5	0	0	0	0
24	Methyl laurate	g	28.3	0	0	19	8
25	Amyl laurate	f	28.2	0	0	5	0
26	Decyl laurate	f	..	0	0	17	13
Aliphatic ethers							
27	Ucon (DLB-50-B)	1	28.3	0	0	0	0
28	Ucon (DLB-100-B)	1	29.9	0	0	0	0

^a For the meaning of the code letters, see Acknowledgments.

the essential features of the wetting behavior of each organic liquid on high energy surfaces. In determining the probable orientation of the adsorbed molecules, it is necessary, as deBoer and co-workers have pointed out,¹⁶ to recognize the essentially additive nature of the highly localized non-polar "dispersion forces" between the individual atoms of organic molecules and the solid surface.

Materials and Experimental Procedures

High energy surfaces investigated included small flat discs of platinum, brass (2 copper:1 zinc), 18-8 stainless steel, fused silica and colorless synthetic sapphire (α - Al_2O_3). The platinum and sapphire were polished on lead laps with diamond powder ($<0.5 \mu$) suspended in an organic vehicle; the quartz and stainless steel on a pitch lap using optical rouge suspended in water; and the brass on a pitch lap with γ - Al_2O_3 in an aqueous Aerosol-OT solution. These polishing procedures produced surfaces which were flat, specularly smooth, and scratch-free to the naked eye. The platinum was freed from organic contamination by heating it dull red; the discs of fused silica and sapphire by boiling in (1:2) nitric-sulfuric acid solution, rinsing copiously with hot freshly-distilled water, and drying at 120° for 5 minutes; brass and stainless steel discs were rinsed for 30 minutes and 2 hours, respectively, in continuously condensing benzene vapor. Freedom from organic surface contamination was shown by the ability of a drop of grease-free distilled water to spread on each surface and by the absence of a "water-break" during the subsequent evaporation.

Water failed to spread on stainless steel refluxed in benzene, indicating that not all organic contamination had been removed. A series of exhaustive experiments showed that no cleaning technique involving solvents—including a Bureau of Aeronautics specification method¹⁷—was completely satisfactory. The only method which produced surfaces comparable in cleanliness to freshly flamed platinum was one which involved polishing the stainless steel on a cloth lap impregnated with an aqueous slurry of γ - Al_2O_3 , the latter being removed on a second lap wet with distilled water; the specimen was then rinsed in hot freshly distilled water and dried in a clean oven at 110°. Water spreads freely on stainless steel surfaces prepared in this way.

Many of the pure esters and ethers studied were prepared by O'Rear.¹⁸ All liquids were freed of traces of volatile impurities by either molecular distillation or countercurrent stripping.¹⁹ Adsorbable impurities were removed before each measurement by repeated percolation of the liquid through a column packed with appropriate absorbents. The source and preparation of each liquid have either been given in previous publications⁷⁻¹⁵ or are indicated here under "Acknowledgments." All observations of the spreading properties of these liquids were usually made immediately after and always within 24 hours of purification of the compounds.

Since a number of the liquids had not been prepared before, it was necessary to measure their surface tensions. Where the receding contact angle of the liquid on platinum

(17) Bureau of Aeronautics Specification 14L1f, April 8, 1949.

(18) J. G. O'Rear, Naval Research Laboratory Report 3891, "Synthesis and Characterization of Esters and Ethers for Non-spreading Lubricants," December 14, 1951.

(19) R. W. Miller and J. K. Wolfe, U. S. Patent 2,522,529 (Sept. 17, 1950).

TABLE II
CONTACT ANGLES OF CYCLIC CARBOXYLIC ESTERS AND ETHERS
(Measurements at 20° and 50% R.H.)

No.	Compound obsd.	Source ^a	Surface tension, dynes/cm. at 20°	On metals, 18/8 Steel	degree Brass	On non-metals, Silica	degree Sapphire
Cyclic diesters							
29	2-Methyl-1,3-pentanediol bis-(phenylacetate)	a	39.4	8	10	11	4
30	Bis-(2-phenylethyl) β -methyladipate	a	41.3	9	15	8	7
31	Bis-(cyclohexane-ethyl) β -methyladipate	a	35.8	3	9	17	8
32	Dipropylene glycol bis-(hydrocinnamate)	a	40.1	14	17	9	4
33	Dibutyl phthalate	a	33.6	6	0	11	11
34	Bis-(2-ethylhexyl) phthalate	a	31.3	8	2	28	27
35	Bis-(2-ethylhexyl) tetrahydrophthalate	a	30.7	0	0	19	17
36	Bis-(2-ethylhexyl) isophthalate	m	30.8	0	0	19	11
37	Bis-(2-ethylhexyl) terephthalate	m	32.0	0	0	10	0
38	Dibutyl pinate	b	30.5	0	0	7	0
39	Diheptyl pinate	b	31.0	0	0	23	8
Cyclic monoesters							
40	Butyl phenylundecanoate	a	32.9	0	0	0	0
41	Benzyl phenylundecanoate	a	38.0	9	11	18	6
42	1-Methyl-4-ethyloctyl hydrocinnamate	a	31.7	0	0	21	19
43	2-Ethylhexyl β -(3-phenylpropylmercapto)-propionate	a	31.7	0	0	16	11
Cyclic ethers							
44	Benzyl phenylundecyl ether	a	36.5	3	12	14	3
45	1,9-Bis-(phenylmethoxy)-nonane	a	39.2	18	23	0	0
46	1,5-Bis-(3-phenylpropoxy)-pentane	a	38.7	9	20	0	0
47	1,4-Bis-(3-phenylpropoxy)-3-methylbutane	a	37.5	5	11	0	0
48	1,6-Bis-(2-phenylethoxy)-3-methylhexane	a	38.0	17	10	5	0
49	1,11-Diphenyl-6,10-dimethyl-1,5,8,11-butoxaundecane	a	38.5	7	7	0	0
50	1,5-Bis-(3-phenylpropoxymercapto)-pentane	a	43.2	12	12	6	5
51	Phenoxyphenylcetane	k	33.3	2	0	10	4
52	α -Naphthyl ethyl ether	g	39.3	10	7	5	4

^a For the meaning of the code letters, see Acknowledgments. ^b These materials discussed by C. M. Murphy, J. G. O'Rear and W. A. Zisman, *Ind. Eng. Chem.*, 45, 119 (1953).

was zero, the surface tension was measured by the ring method (precision of ± 0.03 dynes/cm.); and where the contact angle was not zero, either the differential maximum-bubble-pressure method of Sugden²⁰ or the pendant drop method of Andreas, Hauser and Tucker²¹ was used with a precision of ± 0.03 dyne/cm.

By exercising sufficient care the polished and cleaned specimens could be stored for four days in the observation cells without loss of surface cleanliness. Each cell was a rectangular parallelepiped of cemented plate glass ($3\frac{3}{4} \times 1\frac{1}{4} \times 2$ inches) covered by a flat plate of glass. Between the time of cleaning and use, the specimens were stored in covered, acid-cleaned, Parr weighing dishes. Of course, one liquid at a time was studied in each cell to prevent contamination by vapor-phase transfer, and the clean specimens were always handled with grease-free tongs.

Each liquid was usually applied to the surface with a "triple dropper" made of three parallel stainless steel pins (each 1 mm. in diameter) held rigidly together so that the tips formed the apexes of an equilateral triangle having sides 7 mm. long. These pins were cleaned by successive rinsings in A.C.S. grade benzene. A mechanical device was used to make the three pins gently and simultaneously touch the surface of the liquid. This resulted in the transfer of the test liquid to the pins as 3 nearly equal pendant droplets which then could be touched to the test surface without touching the ends of the pins to the leveled solid surface. Experiments showed that the liquid hanging from each pin and just touching the solid surface formed an hour-glass shaped drop. Liquid cohesive forces prevented the adhering drop from spreading to the diameter it would assume at equilibrium. Slowly withdrawing the pins caused

each drop to separate from the pin, advance slowly over the clean surface, and assume a new equilibrium configuration. The result was that three nearly equal drops were left on the solid which exhibited essentially equal advancing contact angles.

When the drops had been placed on the surfaces, the cell was covered, and the system was allowed to attain equilibrium in a constant temperature room at 20° and 50% relative humidity. Contact angles of the liquid drops were measured with a low-powered goniometer microscope described elsewhere.⁷ All contact angles produced in this way were independent of the drop diameter. Each contact angle reported represents the average of measurements on at least six different drops on a given surface, the precision of the measurements being $\pm 2^\circ$ at contact angles of 10° and $\pm 1^\circ$ at 40°. Measurements on each drop were made after apparent attainment of equilibrium (usually in about 15 minutes) and again about 24 hours later. No appreciable change in the contact angles of these liquids occurred after the first 24 hours.

Experimental Results

In Tables I through V will be found the measured contact angles for 97 liquids on the various high energy surfaces studied. The liquids are arranged in each table in groups according to homology, or to some similarity of molecular structure, and are consecutively numbered for reference. The source of each compound is given in the second column and the liquid surface tension at 20° is given in the third column.

In contrast to the results obtained by us previously on various low energy surfaces,⁹⁻¹⁵ the liquid surface tension alone did not determine whether spreading would occur on these surfaces; however, with the exception of one liquid out of the 97 studied, the surface tensions of all the liquids which were non-spreading on all four types of solid surfaces examined were greater than 33.5 dynes/cm. This was not

(20) S. Sugden, "The Parachor and Valency," Knopf, New York, N. Y., 1930.

(21) J. Andreas, E. Hauser and W. Tucker, *THIS JOURNAL*, 42, 100 (1938).

TABLE III
CONTACT ANGLES OF SATURATED HYDROCARBONS
(Measurements at 20° and 50% R.H.)

No.	Compound obsd.	Source ^a	Surface	On metals, degrees		On non-metals, degrees	
			tension, dynes/cm. at 20°	18/8 Steel	Brass	Silica	Sapphire
Open-chain compounds							
53	Hexadecane		27.6	0	0	0	0
54	V-120 polyethylene	^b	27.8	0	0	0	0
55	SS-903 polyethylene	^b	30.4	0	0	0	0
56	SS-906 polyethylene	^b	30.7	0	0	4	0
Cyclic compounds							
57	9-(α - <i>cis</i> -0-3-3-Bi-cycloöctyl)-methyl-heptadecane	^b	31.2	0	0	0	0
58	1,7-Dicyclopentyl-4-(3-cyclopentylpropyl)-heptane	^b	34.6	2	0	8	6
59	3,3'-Dicyclopentylidicyclopentane	^j ^c	^d	0	0	0	0
60	1,3-Dicyclopentylcyclopentane	^j ^c	34.6	0	0	0	0
61	1-Cyclohexyl-2-(cyclohexylmethyl)-pentadecane	^b	32.7	0	0	0	0
62	4-Cyclohexyleicosane	^b	31.6	0	3	0	0
63	9- <i>n</i> -Dodecylperhydrophenanthrene	^b	34.2	0	0	6	2
64	1- α -Decalylhendecane	^b	32.7	0	0	0	0
65	1,1-Di-(α -decalyl)-hendecane	^b	35.1	3	3	7	4
66	1- α -Decalyl-2-cyclohexylethane	^d	32.0	0	0	32	8
67	1,1-Dicyclohexylethane	^d	33.0	0	0	5	0
68	2,6-Dimethyl-4-(α -decalylmethyl)-heptane	^d	35.6	0	0	0	0
69	2,6-Dimethyl-4-cyclohexylmethylheptane	^d	27.0	0	0	0	0
70	Isoamyl-3,3,5-trimethylcyclohexane	^d	25.3	0	0	0	0
71	Decalin	^g	30.5	0	0	0	0
72	2-Ethyldecalin	^e	30.5	0 ^e	0 ^e	0 ^e	0 ^e

^a For the meaning of the code letters, see Acknowledgments. ^b These materials discussed by C. M. Murphy and C. E. Saunders in "German Synthetic Polyethylene Oils," *Petroleum Refiner*, May, 1947. ^c Unable to be satisfactorily cleaned. ^d Not enough material for surface tension determination. It should be slightly higher than #59 in surface tension. ^e Evaporated.

surprising since many liquids will adsorb on such solids to produce surfaces with free surface energies (and critical surface tensions) more characteristic of the adsorbates than the adsorbents.¹³

TABLE IV
CONTACT ANGLES OF AROMATIC HYDROCARBONS
(Measurements at 20° and 50% R.H.)

No.	Compound obsd.	Source ^a	Surface	On metals, degrees		On non-metals, degrees	
			tension, dynes/cm. at 20°	18/8 Steel	Brass	Silica	Sapphire
73	8- <i>p</i> -Tolylnonadecane	^b	30.7	0	0	0	0
74	<i>p</i> -Di- <i>sec</i> -amylbenzene	^c	28.1	0	0	0	0
75	<i>p</i> -Octadecyltoluene	^c	31.5	0	0	8	0
76	<i>p</i> -Dodecyltoluene	^c	29.9	0	0	0	0
77	1,1-Diphenylethane	^b	38.0	0	0	0	0
78	Amyldiphenyl	^g	34.6	0	0	0	0
79	α -Methylnaphthalene	^g ^b	36.4	0 ^c	3 ^c	0 ^c	3 ^c
80	<i>t</i> -Butylnaphthalene	ⁱ	33.7	3 ^c	4	3 ^c	4 ^c
81	Monoamyl-naphthalene	^j ^b	34.3	3 ^c	4	3 ^c	4 ^c
82	Nonylnaphthalene	^j ^b	32.5	6	0	9	10
83	Dinonylnaphthalene	^j ^b	31.5	2	0	18	12

^a For the meaning of the code letters, see Acknowledgments. ^b Unable to be satisfactorily cleaned. ^c Evaporated.

A. Open-Chain Aliphatic Esters.—Table I contains the results for 26 liquid esters containing only aliphatic structures. Every aliphatic ester exhibited a zero contact angle on each of the metal surfaces studied, but twenty-one of the twenty-six esters were non-spreading on silica while 15 were non-spreading on sapphire. It will be noted that the contact angle of each non-spreading liquid was always larger on silica than on sapphire.

Of the 7 monoesters studied, only decyl acetate (compound no. 20) and methyl laurate (no. 24) could conceivably adsorb as the unhydrolyzed ester to form oleophobic monolayers.⁷ However, that is most unlikely since T_w (the critical temperature of wetting oleophobic films of these esters) must be below 20°. Evidence for this conclusion

is the fact that T_w for the ester must be *much less* than the value of 50° observed for an alcohol of the same number of carbon atoms.⁸

The non-spreading property observed with most of these monoesters could arise from hydrolysis of each ester *in situ*, *i.e.*, immediately after adsorptive contact with the silica or sapphire surface. If it were due to hydrolysis products existing *before* contact with the surfaces, these liquids could not have exhibited zero contact angles on clean metals. The differences in spreading observed cannot be caused by the variation of the surface tension among these esters, since γ_{LV}^0 lies between 27.0 to 28.8 dynes/cm.; therefore, they must be due to differences in either the rates of hydrolysis or the nature of the hydrolysis products.

The three lauric acid esters (no. 24, 25 and 26) will each release lauric acid for which T_w is much above 20°.⁸ The ester will be unable to spread upon the resulting adsorbed film of lauric acid, because γ_c for a close packed surface of methyl groups is between 22 and 25 dynes/cm.,⁹ and the surface tension of each ester is about 28 dynes/cm. The observed contact angles range from 5 to 20°; these values are in reasonable accord with this theory, since the slope of the graph of $\cos \theta_E$ vs. γ_{LV}^0 in reference 9 is such that for liquids with surface tension only slightly greater than 24 dynes/cm., θ_E should be under 20°. If a greater degree of contact hydrolysis of the esters on silica than on sapphire is assumed, it accounts for the larger contact angles observed on the former. This assumption is reasonable, because the surface of silica is more hydrated and more difficult to dehydrate than that of sapphire.¹⁴ A lesser degree of hydrolysis on the sapphire surface would lead to a less closely packed film of adsorbed lauric acid. This means γ_c will be nearer 28 dynes/cm. than 25, and hence the contact angle will accordingly be smaller than on silica. The zero contact angle on sapphire observed for amyl laurate (no. 25) may have been caused by the accidental dehydration of the particular sapphire surface used,¹⁴ because the necessary precautions against intensive dehydration adopted in reference¹⁴ had not been recognized at that time.

Undecyl 2-ethylhexanoate (no. 23) exhibited zero contact angles on both silica and sapphire. We have recently demonstrated¹⁴ that γ_c for a solid coated with a monolayer

TABLE V
CONTACT ANGLES OF AROMATIC CHLORINE AND/OR PHOSPHATE COMPOUNDS
(Measurements at 20° and 50% R.H.)

No.	Compound obsd.	B.p. at 0.6 mm.	n_D^{20}	Source ^a	Surface tension, dynes/ cm. at 20°	Platinum, degrees	Silica, degrees	Sap- phire, de- grees
Phosphate esters								
84	Tricresyl phosphate			n	40.9	ca. 2	ca. 2	ca. 2
85	Tri- <i>o</i> -cresyl phosphate			g	..	7	14	18
86	Tri- <i>o</i> -chlorophenyl phosphate			h	45.8	7	19	21
87	Di-(<i>o</i> -chlorophenyl)-monophenyl phosphate			h	43.6	9	11	24
88	Biphenyl mono-(<i>o</i> -xenyl) phosphate			h	44.3	9	16	17
Chlorinated hydrocarbons								
89	<i>x</i> -Chlorobiphenyl ether			h	40.6	0	0	0
90	<i>x</i> -Dichlorobiphenyl ether			h	42.8	12	0	ca. 2
91	Chlorinated biphenyl (Aroclor 1242)			n	41.9	12	10	6
92	Chlorinated biphenyl (Aroclor 1248)			n	42.9	11	14	7
93	Chlorinated biphenyl (Aroclor 1254)			n	45.8	14	29	12
94	Aroclor 1248—Fraction I	130–143°	1.6259	u	..	5	19	5
95	Aroclor 1248—Fraction II	143–147°	1.6302	a	..	11	11	7
96	Aroclor 1248—Fraction III	147–152°	1.6340	a	..	13	14	6
97	Aroclor 1248—Fraction IV	152–156°	1.6385	u	..	15	13	22

^a For the meaning of the code letters, see Acknowledgments.

of 2-ethylhexanoic acid is between 28 and 29 dynes/cm.; as the acid is here the more adsorbable species generated by hydrolysis and as the surface tension of the ester (27.5 dynes/cm.) is less than γ_c , it is to be expected that the ester spreads on each surface. Since decyl acetate (no. 20) exhibited a zero contact angle on silica and sapphire, it is presumed that the acetic acid formed by surface hydrolysis had adsorbed either preferentially or in a mixed film with the decyl alcohol to form a film with a value of γ_c higher than the surface tension (28.3 dynes/cm.) of the ester. If the decyl alcohol formed by hydrolysis had been the only adsorbed species, the ester would have been unable to spread upon that film. Amyl caproate (no. 21) will release caproic acid on hydrolysis which upon adsorbing will form a low energy surface having a value of γ_c greater than 26.8 dynes/cm.¹⁴ Since the ester has a surface tension of 27 dynes/cm., it is to be expected that zero contact angles will be exhibited on silica and sapphire. Ester no. 22 releases both caproic acid and decyl alcohol. If this acid were the more adsorbable species, the ester would rest on a film having a value of γ_c of 26.8 dynes/cm.¹⁴ Because $\gamma_{LV}^\circ = 28.8$, the contact angles on silica and sapphire should be small. If the adsorbed species were decyl alcohol, γ_c would be between 25 and 22 dynes/cm.,⁹ and the contact angles would be much larger. Therefore, it is presumed the caproic acid is the more adsorbable of the two products of hydrolysis.

From the above discussion of the monoesters, it is evident that the observed spreading properties on silica and sapphire can be explained by: (i) surface hydrolysis following adsorption of the ester group on silica and sapphire, the effect on the former being more pronounced; (ii) formation of a low energy surface by adsorption of the more surface active species generated by hydrolysis (usually the acid product); and (iii) comparison of the relative values of the critical surface tension of the resulting low energy surface and the surface tension of the liquid ester. It is concluded that compounds with molecular weights as low as 2-ethylhexanoic and caproic acids can be effective in forming low energy surfaces on silica and sapphire; this conclusion is in full agreement with the results of experiments reported recently.¹⁴

Thirteen of the 19 aliphatic diesters were non-spreading on both silica and sapphire. A few exhibited zero contact angles on sapphire or on silica, but only compounds no. 13 and no. 19 had zero contact angles on both surfaces. Diesters no. 1, 2 and 4 will hydrolyze on the surface to release *n*-butanol and an aliphatic methyl-branched ester having a carboxylic acid terminal. The value of γ_c of a surface saturated with adsorbed butanol molecules is approximately 28 dynes/cm.¹⁴ and that of the ester-acid must be slightly greater. The acid product, being much less volatile and able to pack closely on adsorbing, is very probably the more

adsorbable hydrolysis product. The contact angles of these esters are only 10°, 11° and 11°, respectively, on silica; these are reasonable since the surface tension of each liquid (about 30 dynes/cm.) is not much greater than γ_c . The zero contact angle exhibited on sapphire is presumed to be further evidence of the smaller adsorptivity of each of these three esters on sapphire than on silica.

Diesters no. 3, 5, 6, 10 and 12 through surface hydrolysis generate 2-ethylhexanol and a monoester having an acid group at one end and a 2-ethylhexyl radical at the other. The acid will adsorb preferentially on silica and sapphire to form low energy surfaces¹⁴ for which γ_c will be about the same as that of a monolayer of 2-ethylhexanoic acid (*i.e.*, $\gamma_c = 28$); hence, liquids whose surface tensions are between 30 and 31 dynes/cm. would be expected to exhibit contact angles of 10 to 20° as can be seen by an inspection of the curve of $\cos \theta_E$ vs. γ_{LV}° (see Fig. 2 of reference 14). The same conclusions apply essentially to diesters no. 7, 8, 9 and 11 which generate 1-methylheptanol, *n*-octanol, or 3,5,5-trimethylhexanol. The acid-ester would appear to be the most surface-active species released by hydrolysis. However, it is conceivable that the diester completely hydrolyzes on the absorbing surface, since both hydrophilic ester groups might be adsorbed at the same time on the solid. The resulting dibasic acid would be the most adsorptive species generated by surface hydrolysis. But a closed-packed monolayer of dibasic acid would form a low-energy surface having a value of γ_c of about 35 dynes/cm.¹³; consequently, each of these four diester liquids would exhibit a zero contact angle on it. Since the diesters all did not spread on either silica or sapphire, the adsorbed film must not have been the dibasic acid. The acid-ester probably would adsorb by the carboxyl group, and the resulting film at closest packing would have essentially the same wetting properties as a closely packed monolayer of 2-ethylhexanol. In either case, the non-spreading of the five diesters on such a monolayer could then be explained by the same argument given at the beginning of this paragraph.

Diester no. 13 exhibited zero contact angles on both silica and sapphire. Here the numerous dipoles in the ether-alcohol hydrolysis product or in the half-ester will cause it to adsorb lying down to form a low energy surface with a critical surface tension above that of both polyethylene and sebacic acid films, *i.e.*, above 35 dynes/cm.^{13,15} As the surface tension of diester no. 13 is 34.3 dynes/cm., it would be expected to spread on the resulting low energy surface.

Diesters no. 14 through no. 19 are prepared from glycols esterified with monocarboxylic acids; surface hydrolysis of each compound will produce an adsorbable acid and a monoester terminated by an alcohol group. The former is the more adsorbable species. Thus diesters no. 14 and no. 15 will release *n*-caproic acid which will adsorb to form a low

energy surface having a value of γ_c of 26.8 dynes/cm.¹⁴ Since these esters have surface tensions of 30.8 and 29.5 dynes/cm., respectively, they should be non-spreading on the resulting low energy surface. Diesters no. 16 through no. 19 will release 2-ethylhexanoic acid on surface hydrolysis. The low energy surface resulting from the adsorbed close-packed monolayer will have a value of γ_c of about 28 dynes/cm.; hence, as in the discussion above of the diesters of 2-ethylhexanol and dibasic acids, esters with surface tensions of 30.5, 28.2, 30.2 and 31.4 dynes/cm., respectively, would not be expected to spread on silica or sapphire. This is precisely the behavior of diesters no. 16 and no. 17; however, no. 18 exhibited a zero contact angle on sapphire and no. 19 had zero contact angles on both silica and sapphire. While esters no. 16 and no. 17 were made from polyethylene glycols, diesters no. 18 and no. 19 were made from polymethylene glycol. It is possible that the greater wettability of these surfaces by the latter two esters is because the most adsorbable species released by their surface hydrolysis is polymethylene glycol instead of 2-ethylhexanoic acid, and hence γ_c is between 31⁹ and 35 dynes/cm.¹³

Therefore, the spreading behavior on silica and sapphire of all of these open-chain diesters can be explained on the basis of the same mechanisms proposed for the spreading behavior of the monoesters with the additional and reasonable assumption that when diesters adsorb on the surface of silica or sapphire both ester groups are not hydrolyzed.

These experiments have also led us to conclude that all of the aliphatic esters spread on clean, polished metal surfaces. Previous research^{7,8,13,14} demonstrated that a wide variety of aliphatic acids and alcohols (including the majority released in the hydrolysis of these esters) adsorbed on clean metals to form low energy surfaces having values of γ_c which ranged from 22 to 28.5 dynes/cm., depending on the existence and type of branching of the acid or alcohol. From the zero contact angles of all these pure esters, it is concluded that no significant amount of surface hydrolysis occurs following the adsorption of the esters on the metals at 20° and 50% relative humidity. Instead, the monoesters and diesters each adsorb with the principal chain of the molecule lying as flat as possible on the surface of the metal. The resulting low-energy surfaces must have critical surface tensions above that of polyethylene and probably about that of sebacic acid monolayers, *i.e.*, above 35 dynes/cm. Since every one of these esters has a surface tension which is well below 35 dynes/cm., it follows that each must exhibit a zero contact angle. However, each of these pure esters can be made non-spreading by adding a small concentration of a suitable acid or alcohol, which (in many instances) can be the very acid or alcohol used to prepare the ester.

B. Aliphatic Ethers.—The only aliphatic ethers studied were several alkyl-terminated polypropylene ethers.²² These exhibited zero contact angles on the metals and also on silica and sapphire (see Table I, no. 27 and no. 28). As these compounds do not hydrolyze, each must adsorb with the principal chain of the molecule lying in the plane of the surface. Because the resulting adsorbed film contains ether oxygen atoms, the value of γ_c must be greater than that of polyethylene, *i.e.*, greater than 31 dynes/cm.¹⁵ Since the liquids have surface tensions of only 28 to 30 dynes/cm., it is understandable why they spread on all the high-energy surfaces studied.

C. Cyclic Esters.—Experimental results for 15 monoesters and diesters containing either one or two rings are given in Table II. All five of the esters containing two rings per molecule were non-spreading on both metals and non-metals. These esters have the high surface tensions of from 35.8 to 41.3 dynes/cm. But of the ten esters containing a single hydrocarbon ring, all but two behaved like the aliphatic esters because they spread on metals and were non-spreading on silica and sapphire. Their surface tensions ranged from 30.5 to 34.7 dynes/cm. The two exceptions (no. 33 and no. 34) are diesters of orthophthalic acid; each was non-spreading on steel, silica and sapphire, the contact angle on silica being the greatest. The spreading behavior of the various cyclic esters on silica and sapphire will be discussed first. Essentially the same mechanisms postulated for the aliphatic esters will suffice. However, here the most adsorbable species released by surface hydrolysis may be an acid or alcohol containing a terminal hydrocarbon ring; and the critical surface tension of the re-

sulting low energy surface can be estimated as 35 dynes/cm. from the value of γ_c for an adsorbed film of aniline reported by us earlier.¹³

Thus, the hydrolysis of diesters no. 29, 30, 32, and monoester no. 41 will produce aromatic alcohols or acids which will be adsorbed to form this type of low energy surface. But the surface tensions of such esters are between 38 and 41 dynes/cm.; hence $\gamma_{LV} > \gamma_c$, and their non-spreading is understandable. We assume that diester no. 30 is non-spreading because the phenylethanol released adsorbs to form a low energy surface with γ_c equal to 35 dynes/cm. Diester no. 31 produces cyclohexylethanol which has a value of γ_c of considerably less than 35; here γ_{LV} is somewhat greater than 35 dynes/cm.

Each of the two pinate diesters (no. 38 and no. 39) will release on surface hydrolysis an ester having a carboxyl terminal and a *gem*-cimethylcyclobutane ring and also an aliphatic alcohol (butanol from no. 38 and heptanol from no. 39). The acid hydrolysis product is the more adsorbable species released by each ester. The much larger contact angles exhibited by no. 39 than no. 38 on both silica and sapphire are presumably due to the larger value of γ_{LV} of ester no. 39 and to a somewhat closer packing on the monolayer of acid released by no. 39.

Monocyclic diesters no. 34, 35, 36 and 37 will release by hydrolysis 2-ethylhexanol and also a monoester containing an acid terminal group and an adjacent six-membered hydrocarbon ring. Regardless of which is the more adsorbable species, the adsorbed film will contain a 2-ethylhexyl terminal group oriented outermost. The resulting low energy surface at closest packing will have nearly the same critical surface tension as a monolayer of 2-ethylhexanoic acid, *i.e.*, 28 to 28.5 dynes/cm.¹⁴ As the surface tensions of these four esters range from 30.7 to 32.0 dynes/cm., their appreciable contact angles on silica and sapphire are to be expected. Diester no. 33 will release on hydrolysis a monoester similar to its analog (no. 34) except that the terminal group will consist of a butyl instead of a 2-ethylhexyl group.

Previous research¹⁵ has shown that dodecyloxybenzoic acid, which is adsorbed similarly to these monoesters, will pack nearly as densely as hydrocarbon chains since its critical surface tension of 26 dynes/cm. is not much greater than the value of 22.5 dynes/cm. for a close-packed monolayer of octadecylamine.⁹ Therefore, it is to be expected that the monoester of no. 33 will have a critical surface tension slightly greater than 26 dynes/cm. The surface tension of 33.6 dynes/cm. of di-*n*-butyl phthalate is sufficient to account for its inability to spread on such a film. Both monoesters no. 40 and no. 41 hydrolyze to form phenylundecanoic acid, which is the more adsorbable species produced. The critical surface tension of 35 dynes/cm. of aniline¹³ should be quite close to that of phenylundecanoic acid. Hence, ester no. 40, which has a surface tension of 32.9 dynes/cm., spreads on the adsorbed film whereas ester no. 41, which has a surface tension of 38.0 dynes/cm., does not spread.

Monoester no. 42 will release an isomer of undecyl alcohol and also hydrocinnamic acid. If the acid were the more adsorbable species, spreading would result because of the terminal phenyl group and the fact that $\gamma_{LV} < \gamma_c$. Therefore, it is presumed the undecyl alcohol is the more adsorbable hydrolysis product on silica and sapphire. This alcohol has an ethyl side chain because of which its close packed adsorbed film should approximate the value of γ_c of 2-ethylhexanol (*i.e.*, 28.5 dynes/cm.). Since γ_{LV} is 31.7, the observed contact angles on silica and sapphire are reasonable. Monoester no. 43 will generate 2-ethylhexanol and 3-phenylpropylmercaptopropionic acid. If the latter were the more adsorbable species, the resulting low energy surface would have the phenyl group outermost, γ_c would be around 35 dynes/cm., and spreading on silica and sapphire would result. This is contradicted by the experimental results. If the alcohol were the more adsorbable species, γ_c would equal 28.5 dynes/cm. Because $\gamma_{LV} = 34.7$ dynes/cm., it would be expected that the contact angle would be large. Since this agrees with observations, it is concluded the alcohol is the more adsorbable species on silica and sapphire. Monocyclic diester no. 33 will generate *n*-butanol and a 12-carbon monoester of *o*-phthalic acid. The latter will certainly be the more adsorbable product of surface hydrolysis. Because of the structure of this monoester, the phenyl group cannot adsorb outermost; hence, the critical surface tension of the resulting low energy surface will be greater than 28.5 but less than 35 dynes/cm. Since

(22) W. H. Millett, *Ind. Eng. Chem.*, **42**, 2436 (1950).

γ_{LV}° is 35.6 dynes/cm., the observed contact angle of 11° on both silica and sapphire appears reasonable.

As regards their spreading behavior on metals, the cyclic esters can be divided into two groups: (i) compounds like no. 29, 30, 31, 32 and 41, which have dumb-bell shaped molecules containing two rings; and (ii) compounds like no. 33, 39, 42 and 43, which contain only one ring. Compounds in group (i) are all non-spreading on metals; compounds of group (ii), with the exception of the two *o*-phthalic acid diesters no. 33 and 34, spread on metals. All of the esters of group (i) are able to adsorb unhydrolyzed on metals to form oriented films on which the ester cannot spread because $\gamma_{LV}^\circ > \gamma_c$; *i.e.*, they are all autophobic liquids. As in the argument presented for the open-chain esters in section A, the esters of group (ii) which spread on metals did not hydrolyze upon adsorbing on the metal surfaces, and $\gamma_{LV}^\circ < \gamma_c$. *o*-Phthalate diesters no. 33 and 34 are believed the exceptions in group (ii) because they are known to exist in a resonance-stabilized state having a planar double-ring-shaped configuration. Such a molecular structure permits adsorption on the metal surface with the plane of the ring in the surface. If these ideas are correct, it would be expected that the ether analogs and aromatic hydrocarbon analogs of these esters would also behave as autophobic liquids (compare compounds no. 41 and 44).

D. Cyclic Ethers.—Nine ethers or thioethers containing cyclic groups have been studied (see Table II). Six of these ethers (no. 44 through 49) have molecular configurations like a dumb-bell, and each liquid exhibited zero contact angles on both silica and sapphire (no. 44 and 48 being exceptions). Compounds no. 50, 51 and 52 are sufficiently different to need special consideration. All nine cyclic ethers were non-spreading on metals like the analogous esters of section C.

Because of the absence of strong dipole forces, each ether chain and each terminal aromatic group must adsorb with as many covalent atoms in contact with the surface as possible. The critical surface tensions of the resulting low energy surfaces will be greater than that of a polyethylene surface and less than that of a surface of coplanar aromatic rings. Hence, γ_c must considerably exceed 31 dynes/cm. As liquids no. 44 through no. 49 have surface tensions of 36.5 to 39.2 dynes/cm., and as all exhibited zero contact angles, it follows that $\gamma_c > 39.2$ dynes/cm.

Compound no. 50, which contains two thioether atoms, has the high surface tension of 43.2 dynes/cm. In order to explain why this liquid is non-spreading on silica and sapphire it is assumed that $\gamma_{LV}^\circ > \gamma_c$. Compound no. 51 contains an oxygen atom connecting two phenyl groups both of which cannot adsorb in the same plane. Hence, γ_c should be lower than the value for the dumb-bell shaped ethers. The fact that no. 51 is non-spreading on silica and sapphire may be considered evidence that $31 < \gamma_c < 33.3$ dynes/cm. Compound no. 52 can be expected to adsorb on the silica and sapphire surfaces with the plane of the naphthalene group in the plane of the surface. The small proportion of paraffinic to aromatic hydrocarbon atoms in this molecule causes γ_c to be essentially that of the naphthalene portion. Since γ_{LV}° is 39.3 dynes/cm. and the liquid is observed to be non-spreading, it is concluded that for such a low energy surface $\gamma_c < 39.3$ dynes/cm. However, γ_c must exceed that of benzene or naphthalene groups adsorbed with the plane of the ring at right angles to the solid surface. Hence $35 < \gamma_c < 39.3$ dynes/cm. for compound no. 52 and similar structures.

The greater tendency of these cyclic dumb-bell shaped ethers to spread on non-metals than on metals can be explained if we start with several reasonable assumptions. First, the aromatic portion of the molecule is so much less strongly adsorbed by the metals than by the silica and sapphire surfaces that they need not be coplanar with the adsorbing surface. Second, when adsorbed on a metal, the molecular dipoles always remain in contact with the metal surface. Fisher-Hirschfelder atom models show that each molecule can adsorb with the planes of its two aromatic rings oriented perpendicularly to the surface. Also, the aromatic rings of adjacent adsorbed molecules can cohere in pairs through the action of the London "dispersion" forces. Therefore, it is assumed that such mutual cohesive forces serve to stabilize this adsorbed film on metals. Such a film would have a smaller critical surface tension (γ_\perp) than the value (γ_\parallel) of films of these close-packed molecules oriented with the benzene rings in the plane of the adsorbing surface.

The observed contact angles of each liquid is reasonable if $\gamma_\parallel > \gamma_{LV}^\circ > \gamma_\perp$. For example, the data of Table II will be consistent with these conclusions if in each case γ_\perp is less than 37.5 dynes/cm. and γ_\parallel exceeds 39.2 dynes/cm. This explanation of the wetting behavior is quite consistent with the contact angle data of Table II, for it is seen that the average θ_E for the two metals is greater the larger the excess of γ_{LV}° over the 37.5 dynes/cm. It is concluded that a satisfactory explanation of the wetting behavior of these ethers can be given by using reasonable assumptions about the orientation of the adsorbed films of such dumb-bell shaped molecules.

E. Saturated Hydrocarbons.—Each of the four high-boiling aliphatic hydrocarbons studied exhibited zero contact angles on the high energy surfaces studied (see Table III). The liquid surface tensions ranged from 27.6 for *n*-hexadecane to 30.7 dynes/cm. for the liquid polyethylenes. Each hydrocarbon molecule would be expected to adsorb with as many methylene groups as close to the solid surface as steric considerations permit, and hence the resulting low energy surface should have essentially the same value of γ_c as that of the solid polyethylene-air interface, *i.e.*, 31 dynes/cm.¹⁵ Evidently, these aliphatic hydrocarbons exhibited zero contact angles because their surface tensions are always smaller than the critical surface tension of the solid coated with the adsorbed liquid film.

Results obtained with sixteen cyclic saturated hydrocarbons are also given in Table III. Although the liquid surface tensions varied from 25.3 to 35.6 dynes/cm., only compound no. 70 had a surface tension below 27 dynes/cm. and only compounds no. 65 and no. 68 had values over 34.6 dynes/cm. Twelve of these compounds spread freely on all of the surfaces studied. The four exceptions (no. 58, 63, 65 and 66), which have surface tensions of 32 dynes/cm. or more, exhibited non-spreading on both silica and sapphire. Only no. 58 and no. 65 were non-spreading on metal surfaces. Evidently, non-spreading is observed with this class of naphthenic compounds only when γ_{LV}° exceeds 32 to 34 dynes/cm.; also, θ_E is usually greater the larger the excess of γ_{LV}° over that value. Although it is not certain how the molecular constitution of the liquid affects γ_c , it is to be expected that γ_c would not be very different from the value of 31 dynes/cm. of a surface of fairly closed-packed $-\text{CH}_2-$ groups. Certainly, γ_c would be greater the looser the packing in the adsorbed film, and the surface packing of $-\text{CH}_2-$ and $-\text{CH}_3$ groups should be loose for compounds no. 57, 58, 59, 60, 61, 64, 68 and 69. The observation that γ_{LV}° must exceed 32 to 34 dynes/cm. suggests that γ_c also ranges from 32 to 34, depending on the packing; this is a reasonable conclusion because of the constitution of the adsorbed film.

F. Aromatic Hydrocarbons.—The four alkyl-substituted benzene compounds studied (see Table IV), exhibited zero contact angles on all the high energy surfaces with one exception: *p*-octadecyltoluene ($\gamma_{LV}^\circ = 31.5$ dynes/cm.) did not spread on silica. However, *p*-dodecyltoluene ($\gamma_{LV}^\circ = 29.9$ dynes/cm.) did spread. Each of these four hydrocarbons will adsorb with as many aromatic and aliphatic hydrogen atoms located contacting the adsorbing surfaces as possible, and hence γ_c should be determined by the relative proportion of aliphatic and aromatic atoms. As *p*-octadecyltoluene and 8-*p*-tolylnonadecane have the greatest proportion of aliphatic atoms and *p*-*di*-*sec*-amylbenzene the least, γ_c should be greater for the latter and smaller for the former compound. Now, the relative surface tensions of these liquids is in the inverse order, *i.e.*, *p*-*di*-*sec*-amylbenzene has the lowest value of γ_{LV}° . Therefore, it should be most likely to spread on all surfaces; similarly, *p*-octadecyltoluene should be the least likely. The differences in spreading of the two long-chain substituted toluenes indicates that for *p*-octadecyltoluene $30.7 < \gamma_c < 31.5$ dynes/cm. This is reasonable from the relative areas covered by aliphatic chains and aromatic rings.

Compounds no. 77 and no. 78 were the only substituted diphenyls studied which spread completely on all the high energy surfaces. This is remarkable since their surface tensions were as high as 34.6 and 38.0 dynes/cm. Anyldiphenyl is assumed to adsorb with both aromatic rings in the plane of the solid surface. The zero contact angle observed on all surfaces means that $\gamma_c > 34.6$ dynes/cm.; this is a reasonable intermediate value between the low value of γ_c characteristic of adsorbed alkanes and the higher value of γ_c of adsorbed aromatic rings. 1,1-Diphenylethane is

sterically hindered from adsorbing with both aromatic rings in the plane of the adsorbent. Since the adsorbed molecule must have the plane faces of both benzene rings considerably exposed to wetting, and since the molecule has only one aliphatic carbon-carbon bond, γ_c must be greater than the value for benzene rings packed edgewise. Hence, γ_c should be greater than 35 dynes/cm., and it is probable that $\gamma_c > 38$ dynes/cm.

All five alkyl-substituted naphthalenes were difficult to purify and maintain pure. Measurements of θ_E with the naphthalenes of lower molecular weight were complicated by rapid evaporation of the liquid around the periphery of the drop; thus, drops of compounds no. 79, 80, 81 evaporated completely during the 24-hour test. Probably, the observed values of θ_E or 3 to 4° would become zero in the absence of evaporation. These compounds should adsorb on high energy surfaces with the planar naphthalene ring in the surface; and hence on closest packing $\gamma_c > 35$ dynes/cm. Since their surface tensions are less than 36.4 dynes/cm. these liquids should have $\theta_E = 0$. The two nonynaphthalenes studied (no. 82 and no. 83) exhibited small but reproducible contact angles on metals which may be caused by impurities. When pure, these liquids would be expected to behave the same on all four surfaces studied because the orientation of such adsorbed non-polar hydrocarbons would not be expected to vary among these high energy surfaces.

G. Chlorinated Aromatic Hydrocarbons and Ethers.—All five chlorinated aromatic hydrocarbons and ethers of Table V are mixtures of isomers which are difficult to separate. The average composition of the chlorinated diphenyls (Aroclors 1242, 1248 and 1254) corresponds to three, four and five atoms of chlorine per molecule, respectively, but in each liquid there are present molecules containing more or less chlorine. For this reason, Aroclor 1248 was distilled through a Vigreux column into four fractions, which are characterized by the boiling point, refractive index and contact angles given in Table V.

The large dipole moment of the carbon-chlorine bond and the relatively strong London "dispersion" or adsorption forces which must exist between covalent chlorine atoms and metal or other high energy surfaces^{23,24} will cause as many as possible of the chlorine atoms in each molecule to adhere to the adsorbent. Thus, in the low energy surface formed by the adsorption of the first monolayer of chlorinated diphenyl, the orientation will be such that the minimum possible number of chlorine atoms will be in the monolayer/air interface. From inspection of Stuart-Briegleb molecular models,²⁵ which accurately represent such aromatic structures, and from the fact that the preferred position for chlorine substitution in biphenyl is *ortho*, it will be seen that the two aromatic rings will not be coplanar. A surface of close packed covalent chlorine atoms has a critical surface tension of 43 dynes/cm.,²³ while a surface of benzene rings has a value of 35 dynes/cm. when oriented edgewise¹³ and a greater value when oriented coplanar. Hence, the adsorbed film of chlorinated diphenyl will have a critical surface tension between 35 and 43 dynes/cm. which will be closer to the upper limit. Of course, in working with mixtures of the chlorinated diphenyls, some homolog or isomer will be preferentially adsorbed.

Increasing the extent of chlorine substitution in diphenyl raises γ_{LV} (see Table V). This factor alone would cause the θ_E to increase with the chlorine content, and Table V shows this is true for each surface studied. Generally, the results obtained on silica and on platinum agreed reasonably well. The lower values of θ_E observed with sapphire may be evidence of a slightly looser packing of the adsorbed molecules.

Inspection of the molecular models of the two chlorinated diphenyl ethers (no. 89 and 90) reveals that such ethers are somewhat less sterically hindered than the biphenyls, and so are able to adsorb with one aromatic ring coplanar with the adsorbing surface. This may cause the value of γ_c an adsorbed film of such an ether to be higher than that of the chlorinated diphenyl, and it would explain why lower contact angles are observed with compounds no. 89 and 90 on silica and α -alumina than with no. 91 through 93.

(23) A. H. Ellison and W. A. Zisman, *THIS JOURNAL*, **58**, 260 (1954).

(24) R. C. Bowers, W. C. Clinton and W. A. Zisman, *Modern Plastics*, **31**, 131 (Feb. 1954); *J. Applied Phys.*, **24**, 1966 (1953).

(25) Anon., *Chem. Eng. News*, **32**, 2534 (1954).

H. Phosphates.—Because of the autophobic properties observed in carefully purified tricresyl phosphate, a study was made of five aromatic esters which are homologs of triphenyl phosphate. On the assumption that the strongly polar P=O group of the ester will physically adsorb on the high energy surface with its axis oriented normally to the surface, the most probable configuration of the adsorbed molecule of triphenyl phosphate is with the planes of the three aromatic rings all oriented as nearly normal as possible to the surface. This permits close packing of the molecules with the planar aromatic rings of adjacent molecules in contact. The critical surface tension of such a film-covered surface will approach that of an aniline monolayer (35 dynes/cm.) with certain difference peculiar to such phosphates. In the first place, such a large, branched molecule cannot adsorb with the aromatic rings packed as closely as those of aniline. This will decrease the population density of the aromatic-CH- groups in the outermost surface of the film and so will raise γ_c . Ball models of such phosphates all show that the ether oxygen atoms may be partially exposed to the liquid resting on the adsorbed layer, and that will also increase γ_c .

Methyl substituents on the phenyl groups of triphenyl phosphate will change γ_c by influencing the orientation of the aromatic groups, tending to make their planes more vertical to the adsorbing surface or less so depending on the position of substitution. Also, this will introduce methyl groups in the plane of the resulting low energy surface and thereby reduce γ_c . The methyl substituents will orient away from the adsorbing solid but will not completely shield the ether oxygen in the *meta* or *para* positions. When the methyl group is *ortho* to the ether oxygen, the oxygen atoms will be nearly completely shielded. The *meta* and *para* isomers of tricresyl phosphate are contained in commercial preparations in a ratio of approximately 80% *para* and 20% *meta*. It is assumed that the surface tension of tricresyl phosphate (40.9 dynes/cm.) is roughly equal to γ_c for the "parent" compound, triphenyl phosphate, since the contact angles are nearly zero for this mixture on each of the three solid surfaces listed in Table V. Tri-*o*-cresyl phosphate should have a lower value of γ_c because of (i) the shielding of the ether oxygen atoms by methyl groups and (ii) their presence in the outermost portion of the adsorbed monolayer. This surmise is confirmed by the experimental data of Table V for the contact angles of tri-*o*-cresyl phosphate on platinum, silica and sapphire.

In adsorbed films of diphenyl mono-(*o*-xenyl) phosphate, the xenyl (biphenyl) group would be expected to shield the ether oxygens somewhat. In addition, since the surface tension of this ester is considerably greater than that of tri-*o*-cresyl phosphate, this should cause the contact angles to be somewhat greater than those of tri-*o*-cresyl phosphate. The experimental results of Table V are in accord with this conclusion.

Chlorine substituents, such as in tri-*o*-chlorophenyl phosphate, will orient the phosphate molecule with the chlorine atoms next to the adsorbent because of the large electric dipole created by the carbon-chlorine bond. As a result of the much larger size of the chlorine than the hydrogen atoms, this substituent will tilt the benzene ring toward the phosphorus atom and thus will partly shield the adjacent ether oxygen. The surface tension of the liquid increases with the chlorine content so that the contact angles of the chlorinated esters should be larger than those of tricresyl phosphate. In particular, tri-*o*-chlorophenyl phosphate should have larger contact angles than tri-*o*-cresyl phosphate, and this is the case.

The larger phosphate contact angles on silica and α -alumina than on platinum are caused by the differences in the nature of the forces of attraction to the adsorbing surfaces. The molecular attraction to platinum is most probably the electrostatic attraction of the dipoles with their electrical images in the conducting surface; that of these esters to silica and α -alumina include dipole-ion attractions as well as hydrogen bonding to the adsorbed layer of water found on these oxides.¹⁴ Molecules adsorbed by such hydrogen bonds are probably more mobile than molecules adsorbed on a metal lattice and so closer packing is likely to occur.

General Discussion

All of the contact angles presented here were obtained on specularly polished solid surfaces. If

the surfaces were roughened, Wenzel's law²⁶ states that the contact angle will decrease, since it is always less than 90° for such systems. Roughening the surfaces will also introduce differences in the advancing and receding contact angles which will increase with the roughness.

Although the observations reported here were all made of 20° and 50% relative humidity, the effect of variations in the temperature and humidity can be outlined. It is well established that the surface tensions (γ_{LV^0}) of pure organic liquids decrease linearly with rising temperature until close to the critical temperatures. Hence

$$\gamma_{LV^0} = C_1 - C_2T$$

But we have shown that $\cos \theta_E = a - b\gamma_{LV^0}$, if the surface composition of the solid is constant. Here C_1 , C_2 , a and b are positive. Therefore

$$\cos \theta_E = (a - bC_1) + bC_2T$$

and $\cos \theta_E$ must increase (and θ_E decrease) with increasing temperature. In addition, the effect of raising the temperature will be to cause desorption of any physically adsorbed compounds. Temperature increase will therefore decrease the packing of the adsorbed film. This will raise the critical surface tension of the system and thus cause θ_E to decrease with rising temperatures.

When the temperatures become high, there may result chemical changes in the liquids such as hydrolysis, oxidation and pyrolysis, or there may develop surface-chemical changes in the solid due to oxidation, dehydration or crystallographic rearrangement. The products of chemical reaction in the liquids may be highly adsorbable and may cause the formation of new low energy surfaces on which the liquids will not spread. This effect may overbalance the above-mentioned normal decrease in θ_E with rising temperature. The oxidation or dehydration of these inorganic solid surfaces may greatly alter the wetting behavior of the liquids. But if the chemical reactivity or adsorptivity of the liquid is little changed thereby, no large change in wettability is to be expected.

Decreasing the relative humidity at ordinary temperatures will have little effect on θ_E unless the atmosphere is so dry as to dehydrate the solid surface (as in silica and α -alumina). But usually very long exposure to dry air will be required to significantly change the contact angles. As the relative humidity approaches 100%, increased condensation of water on the surfaces of both metals and metallic oxides will invite the hydrolysis *in situ* of adsorbed liquids, and so the wetting properties of these surfaces will become more like those of such highly hydrated surfaces as glass, silica and alumina.

Polymethylsiloxane liquids spread on all high energy surfaces because the surface tensions of 19 to 20 dynes/cm.²⁷ are always less than the critical surface tensions of their own adsorbed films. This follows because an adsorbed close-packed monolayer of the silicone molecules has an outermost surface of methyl groups which are not as closely

packed as the methyl groups in a single crystal of a paraffin. Since γ_c of hexatriacontane is about 21 dynes/cm.,¹⁵ the value of γ_c for the silicone monolayer must exceed 21. Hence, γ_{LV^0} must always be below γ_c and the silicones cannot be autophobic. A similar argument using the critical surface tension of polyethylene of 31 dynes/cm.,¹⁵ and the surface tensions of liquid aliphatic hydrocarbons, which are always less than 30 dynes/cm., leads us at once to understand why such hydrocarbons are not autophobic.

This study has added to the list of autophobic liquids reported earlier¹⁴; the various chlorinated diphenyls, the derivatives of triphenyl phosphate listed in Table V, certain aromatic hydrocarbons (Table III) and certain aromatic esters and ethers (Table II).

We have chosen to define the class of autophobic liquids as those compounds which are non-spreading by virtue of the fact that they adsorb unaltered to form low energy films on which the bulk liquid will not spread. Liquid compounds, which release polar decomposition products able to adsorb and form low-energy surfaces, behave like pure liquids which contain polar additives. As we have pointed out earlier (7-13), the non-spreading property can be produced in nearly all pure liquids by the addition to each of a minor concentration of a polar compound which preferentially adsorbs to form a suitable low energy surface.

The degree of hydration of the surfaces of silica and sapphire has a marked influence on the contact angles of the esters. It is reasonable to assume that the rate and extent of hydrolysis *in situ* increases with the amount of adsorbed water. We have previously shown¹⁴ that increased hydration favors the closer packing of adsorbed polar molecules.

In a number of instances, the value of the critical surface tension of the film of adsorbed polar molecules depended on the constitution of the hydrolysis fragments generated. Thus, esters having the same surface tensions will exhibit different contact angles depending on whether the adsorbed fragments are linear or are branched-chain monoacids or monohydric alcohols or are either dicarboxylic acids or dihydroxy alcohols. These conclusions agree with results obtained in previous studies^{13,14} in which the critical surface tensions of the adsorbed film were shown to depend on the composition and packing of the atomic groups uppermost in the surface.

Our results on the molecular mechanism of spreading can be generalized as follows: every organic liquid spreads freely on specularly smooth, clean, high energy surfaces at ordinary temperatures unless the film adsorbed by the solid is so constituted that the resulting film-coated surface is a low energy surface having a critical surface tension less than the surface tension of the liquid. This in turn is caused by the highly localized nature of the forces between each solid surface and the molecules of the organic liquid and also between the molecules of each liquid. The localization is so extreme that the influence of molecules or atoms beneath the first monolayer must be minor. A

(26) R. Wenzel, *Ind. Eng. Chem.*, **28**, 988 (1936).

(27) H. W. Fox, P. W. Taylor and W. A. Zisman, *ibid.*, **39**, 1401 (1947).

monolayer of adsorbed molecules is always found sufficient to give the high energy solid surface the same wettability properties with respect to all liquids as the low energy solid having the same surface constitution.

Applications of the results of this investigation are too numerous for presentation here. The mechanisms reported here account completely for the non-spreading properties observed in various mineral, animal and vegetable oils as well as in the synthetic liquids reported by many workers including Woog,²⁸ Bulkley and Snyder,²⁹ Barker, *et al.*,³⁰ and Bielak and Mardles.³¹ Clock oils, which have been troublesome and expensive for producers and users of watches and clocks as well as of timers, fuses, and other instruments, can now be synthesized and/or controlled adequately. In the production and use of paints, varnishes, plasticizers, cements and printing inks, hitherto unexplainable changes in adhesiveness, spreadability, or permeability can be understood and can be avoided by eliminating compounds capable of converting the solid surfaces involved

(28) P. Woog, *Compt. rend.*, **81**, 772 (1925), and "Contribution à l'étude du graissage onctuosité," Delagrave, Paris, France, 1926.

(29) R. Bulkley and J. Snyder, *J. Am. Chem. Soc.*, **55**, 194 (1933).

(30) G. E. Barker, U. S. Patent 2,355,616 (August 15, 1944); also G. E. Barker, G. E. Alter, C. E. McKnight, J. R. McKleven and D. M. Hood, A.S.T.M. Bull. No. 138, 25 (March 1946).

(31) E. B. Bielak and E. W. J. Mardles, *J. Colloid Sci.*, **9**, 233 (1954).

into ones having undesirably low adhesion or poor wettability. Also, it should now be established once and for all that high lubricity in a liquid need not be associated with ability to spread and wet surfaces completely, for poor boundary lubricants like polymethylsiloxanes spread over all metals and good boundary lubricants like tri-*o*-cresyl phosphate do not spread on such surfaces.

Acknowledgments.—The authors are pleased to acknowledge the following sources of the liquids used in this report which have been referred to by code letters in Tables I–V: (a) Mr. J. G. O'Rear of this Laboratory; (b) pure hydrocarbons prepared under the supervision of Dr. R. W. Shiesler of the Penn. State University in A.P.I. Project 42 for the American Petroleum Institute; (c) Prof. G. H. Hennion of the University of Notre Dame; (d) Dr. J. P. Kass of the University of Minnesota; (e) and (f) were prepared under the N.D.R.C. contract for Division B by Prof. Homer Adkins of the University of Wisconsin and Prof. C. S. Marvel of the University of Illinois, respectively. The remaining compounds were obtained from the following companies: (g) Eastman Kodak Company, (h) Dow Chemical Company, (i) Sharples Chemical Company, (j) Sun Oil Company, (k) Gulf Research and Development Company, (l) Carbide and Carbon Chemicals Corporation, (m) Genesee Research Corporation, and (n) Monsanto Chemical Company, respectively.

NOTES

SORPTION-HYSTERESIS PROPERTIES OF GASES ON CARBONYL IRON POWDER

BY P. L. WAIKER, JR., AND F. RUSINKO, JR.

Department of Fuel Technology, The Pennsylvania State University, University Park, Pennsylvania

Received February 23, 1955

Adsorption-desorption isotherms of argon, nitrogen, carbon monoxide and carbon dioxide have been determined on iron powder produced from iron carbonyl. The work was undertaken primarily to examine the effect of pretreatment of a relatively pure iron surface on the sorption hysteresis properties of the above gases.

Experimental

Apparatus and Procedure.—The apparatus and procedure used to determine the isotherms were comparable to those described by Emmett.¹

Materials.—The iron powder known as "HP" grade, was obtained from the General Aniline and Film Corp. The method of preparation of the iron was briefly as follows: iron was converted to $\text{Fe}(\text{CO})_5$ at a temperature of ca. 175° and a pressure of ca. 1000 p.s.i. The $\text{Fe}(\text{CO})_5$ was decomposed to iron powder at ca. 250° and atm. pressure. The iron powder was then reduced in H_2 at ca. 500°. The powder consisted of spherical particles having an average diameter on a weight basis of 10 μ . The impurity content of

the sample was less than the following: 0.002% N_2 , 0.30% O_2 , 0.04% C, 0.03% sulfide, 0.0005% As, 0.04% insoluble in H_2SO_4 , and 0.03% water soluble substances. An iron content of at least 99.6% by weight was guaranteed.²

The gases used were obtained from the Matheson Company. Argon, nitrogen and carbon dioxide had minimum purities of 99.8%. The carbon monoxide had a known purity of 97.1%, the impurities consisting of 2.1% N_2 , and 0.8% H_2 . Prior to entering the sorption apparatus, the gases were dried by passage over anhydrous magnesium perchlorate.

Results and Discussion

In one particular series of runs (shown in Fig. 1 up to a relative pressure of only 0.5 to expand the plots), iron was first reduced at 400° (standard reduction temperature used throughout) in flowing hydrogen (200 cc./min.) for 24 hours and then outgassed for 24 additional hours. The subsequent sorption of argon (run 1) at -195° up to a relative pressure of 0.88 resulted in a typical Type II isotherm and showed no hysteresis. Further successive treatments consisting of outgassing the iron at room temperature for 12 hours (run 2), reducing in hydrogen for 1 hour and outgassing for 12 hours at 400° (run 3), and outgassing at room tempera-

(2) A more detailed description of the iron can be obtained from the manufacturer. The same product, known as C.P. iron powder, is marketed by J. T. Baker Chem. Co.

(1) P. H. Emmett, *Am. Soc. Testing Materials*, **41**, 95 (1941).

ture for 12 hours (run 4) had a negligible effect on the three subsequent sorption isotherms of argon.

Similar pretreatment of the iron prior to nitrogen sorption runs at -195° also resulted in Type II isotherms (runs 5 and 6), running slightly higher than those of argon but again showing no hysteresis nor pretreatment effect.

The iron was next reduced in hydrogen for 2 hours, outgassed at 400° for 8 hours, and then at room temperature for 14 hours prior to carbon monoxide sorption at -195° . The adsorption isotherm (run 7) ran essentially parallel to that of argon but was 0.070 cc./g. higher. Even though this difference may be due completely to chemisorption of carbon monoxide on the iron powder,³ it amounts to only 27% of a complete monolayer, agreeing qualitatively with the findings of Podgurski and Emmett,⁴ who report that on a pure iron surface the chemisorption of carbon monoxide amounts to only a fraction of a monolayer. The desorption isotherm (run 7) also essentially paralleled but was 0.29 cc./g. higher than that of argon. The iron was next outgassed for 12 hours at -78° . In the subsequent sorption of carbon monoxide (run 8), the isotherm again paralleled that of argon but the adsorption and desorption volumes were still 0.035 and 0.10 cc./g. higher. This is thought to be indicative of the removal of a fraction of chemisorbed carbon monoxide when the iron was outgassed under the above conditions.

The sample was next reduced in hydrogen for 5 hours, outgassed at 400° for 5 additional hours, and then outgassed at room temperature for 10 hours. Free space determinations using helium agreed well with the original value, indicating the absence of carbides of iron and free carbon as possibly formed at elevated temperatures from the previously chemisorbed carbon monoxide. The subsequent sorption isotherm (-78°) of carbon dioxide (run 9) fell significantly below the argon curve but showed only slight hysteresis. After the sample was outgassed overnight at room temperature, run 10 not only found a slightly higher adsorption volume but also a considerably larger hysteresis than the preceding run. Next, the sample was reduced in hydrogen for 12 hours and cooled down to -78° with the hydrogen flow continuing. The subsequent carbon dioxide adsorption (run 11) is seen to parallel closely run 9 at low pressures but to continue to increase in divergence (greater adsorption) with increasing pressure. The desorption curve failed to close the isotherm, falling close to that of the preceding run.

The sample was next outgassed for 8 hours at room temperature and then exposed to a stream of oxygen for 16 hours. The subsequent sorption run (12) showed no marked effect of oxygen pretreatment over the three previous carbon dioxide isotherms, with the desorption curve agreeing particularly well with those of the two previous runs. It should be noted that the B.E.T. area for the four carbon dioxide runs was 0.76 ± 0.02 m.²/g. (using a molecular area of 17.0 \AA^2) compared to

(3) P. H. Emmett and S. Brunauer, *J. Am. Chem. Soc.*, **59**, 310 (1937).

(4) H. H. Podgurski and P. H. Emmett, *This Journal*, **57**, 159 (1953).

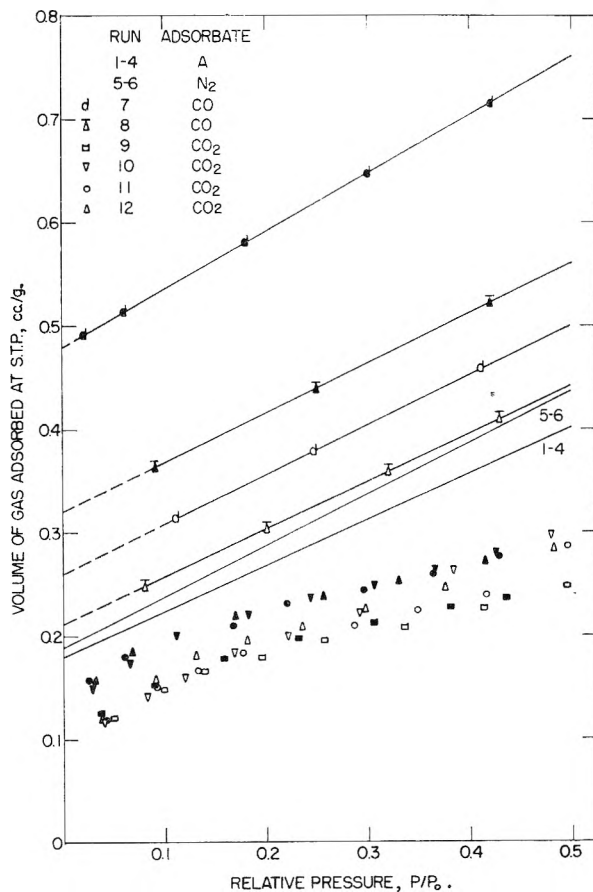


Fig. 1.—Sorption isotherms of gases on iron powder (closed symbols are desorption).

0.89 m.²/g. for argon adsorption (using a molecular area of 14.2 \AA^2). Therefore, the combined physical adsorption and possible chemisorption volumes of carbon dioxide still produced a B.E.T. area less than the physical adsorption volume of argon.

ON THE SUTHERLAND MODEL FOR THE VISCOSITY OF GASES

BY M. EL NADI AND F. ABU ZEID

Cairo University, Egypt

Received April 4, 1955

Assuming the gas molecules to be hard elastic spheres, interacting with an attractive field, Sutherland obtained for the coefficient of viscosity of a gas, the relation

$$\eta = \frac{CT^{1/2}}{1 + S/T} \quad (1)$$

where C and S are constants. η is the coefficient of viscosity of the gas, T the absolute temperature and S is called the Sutherland constant for the gas under consideration.

Although this equation was derived in non-rigorous way by Sutherland, it was found to hold successfully for many gases over a considerable range of temperatures. Some observers,¹ however, reported that equation 1 fits the experimental results

(1) Binkele, *Ann. Physik*, **9**, 839 (1931); Rilaud and Vasilescu, *Cempr. rend.*, **208**, 884 (1939).

TABLE I

Gas	$\sigma \times 10^8$, cm.	$C_1 \times 10^{60}$	S°	$C_2 \times 10^{76}$	S'	$C_3 \times 10^{92}$	S''	$S + S' + S''$	S obsd.
H	2.39	6.098	41.13						31
H ₂	2.22	11.4	119.71	31	59.2	45	16.83	195.74	234
He	1.82	1.23	42.54	1.89	17.69	1.65	4.5	64.73	173
Ne	2.25	4.67	45.26	6.9	11.84	5.3	1.38	58.48	128
		7.48	72.49	10.9	18.71			92.6	
A	2.99	55.4	97.46	120	21.17	136	2.59	121.22	142
		63.5	111.4	190	33.52			144.92	
Kr	3.22	107	120.67	275	26.81	370	3.36	150.84	188
		136	153.38					183.55	
Xe	3.55	233	146.33	710	31.71	1120	3.83	181.87	252
		273	171.45					207	
N ₂	3.22	57.2	64.51	120	11.71	130	1.18	77.39	105
O ₂	3.02	39.8	65.95	96	15.63	120	2.07	83.65	125
CO ₂	3.45	152	113.31	410	23.02	590	2.67	139	213
CH ₄	3.33	112	103.25	310	23.1	440	2.85	129.2	162
NH ₃	2.47	70	387.5	236	191.94	410	72.76	652.2	626
Cl ₂	3.68	321	162.47	1000	33.49	1630	3.89	199.85	351
HCl	2.96	111	207.46	320	61.18	480	10.11	278.75	362
HBr	3.16	185	233.56	600	67.99	1000	10.95	312.50	375
HI	3.55	370	232.37	1360	60.75	2700	9.17	302.29	390

over wide ranges of temperature if it is assumed that Sutherland's constant S be taken as varying somewhat with T .

It was shown later by London that at large distances, the forces between two molecules are attractive and the potential can be represented by the equation

$$\phi(r) = -\frac{C_1}{r^6} - \frac{C_2}{r^8} - \frac{C_3}{r^{10}} - \dots \quad (2)$$

in which the constants C_1, C_2, C_3, \dots , represent the dipole-dipole, dipole-quadrupole, quadrupole-quadrupole interactions, respectively.

It is the purpose of this note to calculate the Sutherland equation and constant of the potential (2), and then to compare the calculated with the experimental values.² Moreover, the large value of the factors³ C_2 and C_3 (as can be seen from Table I) makes it desirable to know their contributions to the values of the molecular constants, as in particular the value of Sutherland constant.

(2) Landolt-Bornstein, "Zahlenwerte und Funktionen aus Physik, Chemie, Astronomie, Geophysik und Technik," Springer-Verlag, 1950, Band I, pp. 325, 369-372.

(3) H. Margenau, *Rev. Mod. Phys.*, **11**, 1 (1939).

Following Chapman's⁴ treatment, it can be shown that the Sutherland equation for the interaction (2) is of the form (1), where now the constant S is given by

$$S = S^\circ + S' + S''$$

where

$$S^\circ = \frac{i(7)C_1}{6K\sigma^6} \quad S' = \frac{i(9)C_2}{8K\sigma^8} \quad S'' = \frac{i(11)C_3}{10K\sigma^{10}}$$

σ the molecular diameter and K is Boltzmann's constant. The function $i(\nu)$ is given by⁵

$$i(\nu) = 4 \int_0^1 v_{00}^{3-\nu} (2v_{00}^2 - 1)(1 - v_{00})^{1/2} \int_0^{\pi_{00}} v^{\nu-1} (1 - v^2)^{-3/2} dv dv_{00} \dots \quad (3)$$

The functions $i(7)$ and $i(9)$ are equal to $i(7) = 0.1736$; $i(9) = 0.1556$.

To get $i(11)$, the integral (3) was integrated and found to give $i(11) = 0.1502$.

In Table I we have calculated the values of S° ,

(4) Chapman, "Mathematical Theory of Non-Uniform Gases," Camb. Press, 1939, p. 182.

(5) S. Chapman, ref. 4, p. 184.

S' , S'' and their sum S , by using the constants C_1 , C_2 and C_3 calculated by Margenau.³

In Table I it is quite clear that while the contribution of the dipole-quadrupole part of the interaction potential is considerable, the contribution of the quadrupole-quadrupole term (and similarly the higher terms) is negligible.

From these calculations one observes that at higher temperatures when the dipole-quadrupole contribution becomes appreciable, the value of Sutherland constant increases. This has been observed experimentally by Rilaud and Vasilescu¹ and others.

Bearing in mind the fact that the above calculations are very sensitive to the values of σ , as they appear in high powers, the agreement between the calculated and observed values is reasonable with the exception of few gases. Some of these gases such as hydrogen and helium are known not to obey the Sutherland law; while the others such as CO_2 , Cl_2 and HCl which are polar gases require in their expression for the interaction potential a term depending on their dipole moments and varies inversely as r^3 .

SURFACE AREA MEASUREMENTS ON CARBON BLACK PRODUCED BY THE CATALYTIC DECOMPOSITION OF CARBON MONOXIDE OVER IRON

BY DONALD S. MACIVER AND PAUL H. EMMETT

Contribution from the Multiple Fellowship of Gulf Research and Development Company, Mellon Institute, Pittsburgh, Pennsylvania

Received April 25 1955

Various workers¹⁻⁴ have observed that when carbon monoxide is decomposed over iron at 450–600°, the carbon is deposited as minute, thread-like growths having thicknesses of the order of several hundred ångström units. The threads often appear to be twisted into rope-like formations and always seem to contain iron, usually in the form of carbides and usually to the extent of one such particle per thread. It is difficult to tell from electron micrographs whether the threads are tubular or flat ribbons. In view of the unusual nature of the carbon deposit, it seemed of interest to investigate the nature of the carbon threads by the standard gas adsorption technique using nitrogen and carbon monoxide as adsorbates at –195°.

Experimental

The carbon black used was prepared by Dr. E. Sterling⁴ by decomposing pure carbon monoxide over a finely divided iron catalyst at 400°. The portion of the carbon black powder passing through a 40-mesh sieve was taken for study after removing the massive catalyst particles initially present.

The volumetric adsorption apparatus employed in the present work was similar to the one described in the literature several times.⁵⁻⁷ The nitrogen used for adsorption

(1) L. V. Radushkevich and V. M. Luk'yanovich, *Zhur. Fiz. Khim.*, **26**, 88 (1952); known through *C.A.*, **47**, 6210 (1953).

(2) W. R. Davies, R. J. Slawson and G. R. Rigby, *Nature*, **171**, 756 (1953).

(3) V. J. Kehrer, Jr., and H. Leidheiser, Jr., *THIS JOURNAL*, **58**, 550 (1954).

(4) E. Sterling, L. J. Hofer and J. T. McCartney, to be published.

(5) P. H. Emmett, *Am. Soc. Testing Materials*, **41**, 95 (1941).

(6) P. H. Emmett, *Advances in Colloidal Sci.*, **1**, 1 (1942).

(7) P. H. Emmett and S. Brunauer, *J. Am. Chem. Soc.*, **56**, 35 (1934).

measurements was the prepurified tank grade; the helium, for calibration purposes, was a commercial grade and was purified by passage over degassed charcoal at –195°. Tank carbon monoxide from the Air Reduction Company was condensed at –195° and distilled, the middle portion being taken for the adsorption measurements.

The reduction and adsorptions were carried out in a sample tube equipped with an inlet and outlet, as well as a side-arm containing a manifold of thin-walled capillary tubes. By means of the latter, it was possible to remove small portions of the sample *in vacuo* for X-ray diffraction studies.

The carbon black was placed in the sample tube and degassed at 150° for 2 hours. A nitrogen adsorption isotherm was then run on the sample at –195°. From this, the surface area was calculated from the familiar BET plot.⁸ The sample was then reduced for 48 hours at 425° in a stream of hydrogen at 1 atmosphere. A small portion of the sample was removed for X-ray analysis and the surface area of the remainder measured by nitrogen adsorption. Following this, the adsorption of carbon monoxide at –195° was measured. The sample was then evacuated for one hour at –78° and another carbon monoxide isotherm run at –195°.

A portion of the original, unreduced carbon black was subjected to an X-ray analysis and to a wet analysis for total iron.

Results

According to electron microscope pictures by Dr. E. Sterling,⁴ the carbon black is thread-like in form, the threads having an apparent thickness of 500 to 1000 Å. An iron analysis indicated that the material contained 6.94% Fe. X-Ray analysis showed that the original sample contained 10–15% Hägg Fe_2C with a trace of Fe_3O_4 . The average crystallite size of the Fe_2C as estimated from the diffraction patterns appeared to be in the range of 150–250 Å.

The nitrogen adsorption-desorption isotherm obtained on the unreduced carbon black is shown in Fig. 1. The lack of a hysteresis effect suggests⁶ the probable absence of pores in the range 20 to 1000 Å. The BET surface area as calculated from the nitrogen isotherm was 145 m.²/g. This corresponds to a calculated diameter of 132 Å. for the carbon threads, and indicates that they have a roughness

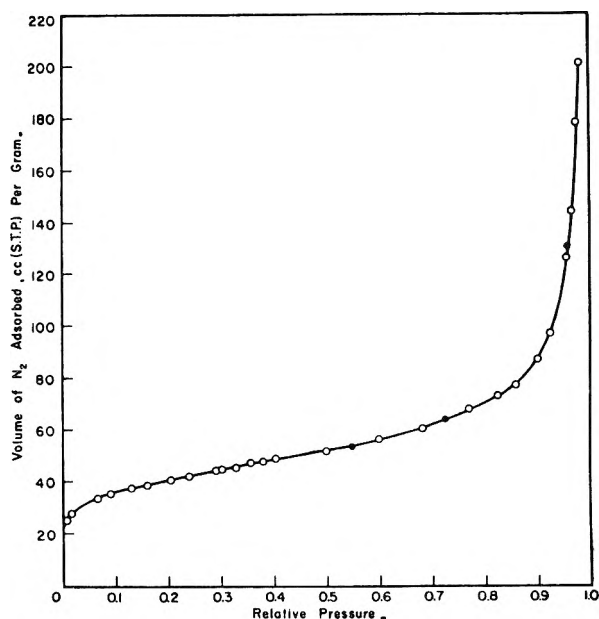


Fig. 1.—Nitrogen adsorption isotherm on carbon black at –195°: ○, adsorption; ●, desorption.

(8) S. Brunauer, P. H. Emmett and E. Teller, *ibid.*, **60**, 309 (1938).

factor of about five in the form of cracks and crevices too small to cause hysteresis.

The reduced carbon black had a BET surface area of 144 m.²/g. A comparison of the two carbon monoxide isotherms at -195° before and after an intervening evacuation at -78° in the manner suggested by Emmett and Brunauer,⁹ indicates a chemisorption of 2.4 cc. (STP) of carbon monoxide per gram of carbon black. Assuming a chemisorbed molecule of carbon monoxide occupies the same area as a molecule of physically adsorbed nitrogen, one can calculate that about 7% of the surface of the carbon black sample consists of iron. This corresponds to an average diameter of about 50 Å. for each particle of iron.

An X-ray analysis of the reduced sample showed particles of α -iron about 300 Å. in size. This is probably in satisfactory agreement with the 50 Å. size estimated from the adsorption measurements in view of the fact that the iron particles may have a roughness factor that makes the surface area several-fold greater (and the calculated particle size several-fold smaller) than would be deduced from X-ray analysis.

(9) P. H. Emmett and S. Brunauer, *J. Am. Chem. Soc.*, **59**, 310 (1937).

RADIATION-INDUCED EXCHANGE OF HYDROGEN ISOTOPES: CHAIN INHIBITION

By LEON M. DORFMAN¹ AND F. J. SHIPKO

Knolls Atomic Power Laboratory,² General Electric Company, Schenectady, N. Y.

Received May 2, 1955

Studies of the exchange reaction of hydrogen and deuterium initiated by α -particles^{3,4} and measurements of the hydrogen-tritium exchange⁵ have demonstrated the chain-character of these reactions. Yields on the order of 2×10^3 molecules/100 e.v. at one atmosphere pressure and lower yields at lower pressures have been obtained. The effect of minute quantities of oxygen in drastically lowering these yields has been shown.⁴

This note describes a brief continuation of these experiments in which yields as high as 2×10^4 molecules/100 e.v., at only 276 mm. total pressure, have been obtained for the hydrogen-deuterium exchange. These experiments, carried out in the absence of stopcock grease and with special care in heating and degassing the reaction cell prior to the runs, emphasize the high chain-length of the reaction, and indicate that earlier rate measurements represent the rates for inhibited chains.

Three runs on the hydrogen-deuterium exchange, initiated by β -particles at extremely low radiation intensities, were carried out at room temperature. In these runs the source of radiation, tritium gas,

was present at pressures below 0.09 mm. A single run on the hydrogen-tritium exchange, at very much higher radiation intensity, was completed.

Experimental

The reaction cell was a spherical Pyrex bulb, diameter 5.7 cm. The reaction bulb was closed off by a mercury cut-off to avoid any possible effect of stopcock grease, and analytical samples were taken by letting one or two bubbles of gas out through the cut-off. The analyses were performed on a General Electric analytical mass spectrometer. In the hydrogen-deuterium runs the pressure of tritium was so low that its presence did not significantly affect the analyses for the other two isotopes.

The reaction bulb was flamed and sparked to assist in degassing prior to the runs. The isotopic gases were purified on separate uranium beds. In the deuterium runs the tritium used (approximately 93% tritium, 7% hydrogen) was analyzed beforehand and introduced to the reaction cell at a low pressure. This pressure was then read on a sensitive McLeod gage. The first two hydrogen-deuterium runs were carried out in separate bulbs which were degassed simultaneously. The same batches of reactants and of tritium were used in these two runs. The third run and the hydrogen-tritium run were done at separate times.

In the hydrogen-deuterium runs the progress of the reaction was followed for two or three days, during which time five analytical samples were taken. The hydrogen-tritium run, at a much higher radiation intensity, was followed for three hours.

Results and Discussion

The data for each run gave good linear plots of the exponential equation

$$HD_{\infty} - HD_t = HD_{\infty} e^{-kt} \quad (I)$$

and the initial rates of formation of the mixed isotopic molecule were obtained from

$$\left(\frac{d(HD)_t}{dt} \right)_{t=0} = kHD_{\infty} \quad (II)$$

where $(HD)_t$ and $(HD)_{\infty}$ are the concentrations at time t and at equilibrium, and k is a constant. These equations have been discussed previously.⁵

The absorption of tritium β -particles in hydrogen has been measured⁶ and the fraction absorbed is known within a few per cent. at the higher pressures and within about $\pm 10\%$ at the lower pressures. The absorbed intensity is thus readily determinable from the measured concentration and the known nuclear constants for tritium: half-life 12.4 years,⁷ average energy 5.69 kev.⁸ The results of the runs are given in Table I.

The yields for the exchange reaction listed in Table I are substantially higher than those which have been obtained in any of the earlier work.^{4,5} The yields for the hydrogen-deuterium runs are approximately 20 times as high as those observed in the α -particle studies.⁴ The yield obtained in the hydrogen-tritium run is about 15 times as high as yields reported earlier.⁶ A yield of approximately 4×10^4 for the hydrogen-deuterium exchange initiated by polonium α -particles has recently been obtained.⁹

The yields for the hydrogen-deuterium runs in Table I increase with increasing pressure, consist-

(1) General Electric Research Laboratory, Schenectady, N. Y.

(2) The Knolls Atomic Power Laboratory is operated by the General Electric Company for the Atomic Energy Commission. The work reported here was carried out under Contract No. W-31-109-Eng-52.

(3) W. Mund, T. deMenten de Hornes and M. Van Meersche, *Bull. soc. chim. Belg.*, **56**, 386 (1947).

(4) W. Mund and M. Van Meersche, *ibid.*, **57**, 88 (1948).

(5) L. M. Dorfman and H. C. Matraw, *THIS JOURNAL*, **57**, 723 (1953).

(6) L. M. Dorfman, *Phys. Rev.*, **95**, 393 (1954).

(7) G. H. Jenks, F. N. Sweeton and J. A. Ghormley, *ibid.*, **80**, 990 (1950).

(8) G. H. Jenks, J. A. Ghormley and F. N. Sweeton, *ibid.*, **75**, 701 (1949).

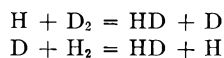
(9) S. O. Thompson and O. A. Schaeffer, private communication; *J. Phys. Chem.*, **23**, 759 (1955).

TABLE I

H ₂	Pressure (mm.)		HD _∞	k (min. ⁻¹ × 10 ⁶)	I_{abs} I_0	Yield (molec./ 100 e.v.)	Yield, Press. × 100
	D ₂	T ₂					
43.4	19.8	0.084	25.8	9.05	0.37	6.2 × 10 ³	0.98
39.8	55.6	0.084	44.1	7.97	0.46	7.5 × 10 ³	0.79
162.2	114.3	0.077	127.2	11.7	0.75	21.0 × 10 ³	0.76
63.7	...	26.6	35.4 ^a	1930	0.45	4.7 × 10 ³	...

^a For the hydrogen-tritium run, this represents HT_∞.

ent with the interpretation of Mund, *et al.*,⁴ that the chain is



From a qualitative comparison of the high intensity run with the hydrogen-deuterium runs, it would seem that the absorbed intensity does not markedly affect the yield. The over-riding factor in determining the observed yield is the level of trace impurity since chain inhibition occurs without the deliberate addition of inhibitors.

Continued rigorous purification of reactants and system may lead to even higher yields. But an upper limit should eventually be reached in which chain-termination occurs by recombination at the walls. It is not possible to say whether the yields observed, in excess of 10⁴, represent such an upper limit.

REVISION OF THE ELECTRODE-POTENTIAL DIAGRAM FOR TECHNETIUM¹

By G. H. CARTLEDGE AND WM. T. SMITH, JR.²

Contribution from The Oak Ridge National Laboratory, Oak Ridge, Tennessee

Received May 12, 1955

Values for the electrode potentials between different valence states of technetium have been reported by Cobble, Smith and Boyd.³ The potentials were calculated from the measured potential for the half-cell reaction and the measured heats of



formation of Tc₂O₇ and HTcO₄ (aq), together with estimated entropies. The earlier values of the potentials were obtained in the presence of air, but it was noted that a "drift" occurred when nitrogen was bubbled through the electrode solutions. In measurements by one of us of potentials involved in the use of the pertechnetate ion as a corrosion inhibitor it was found that although the TcO₂-TcO₄⁻ electrode is very sluggish at 25° the potentials obtained on sweeping out the air with nitrogen ultimately reached a constant value. Since the partial pressure of nitrogen in air did not result in a "drift," it is presumed that sweeping out with pure nitrogen only removed the more active oxygen from the system. The thermodynamic value for the reaction given above should then be that obtained in the absence of oxygen. The standard value ob-

tained in an atmosphere of nitrogen differs by about 45 mv. from the previous value.

Six TcO₂ electrodes were prepared by cathodic reduction of potassium pertechnetate on platinum and two on gold. The platinum electrodes included four wire coils, one foil of 2 cm.² area and one 0.7 × 1.0 cm. gauze. Gold wire was used in the form of a coil. These electrodes were made the cathodes in solutions of potassium pertechnetate acidified by sulfuric acid. Electrolysis was continued for from 30 to 90 minutes with a current of 1 to 2 ma. This gave dark brown, adherent deposits.

The TcO₂-TcO₄⁻ half-cell was closed by a rubber stopper carrying a thermometer, three electrodes, and inlet and outlet tubes for the passage of nitrogen or air. Cylinder nitrogen was bubbled continuously through the solution after passage through either chromium(II) chloride or alkaline pyrogallol or over pure copper at 450° to remove oxygen. The same e.m.f. was obtained with each purification train. To the bottom of the glass half-cell was sealed a tube connected to a three-way stopcock. One of the tubes beyond the stopcock dipped into a small beaker containing sulfuric acid of the same concentration as was present in the half-cell. Calomel half-cells of the Beckman type were dipped into the acid. The other tube beyond the stopcock was used for removing and replacing electrode solutions without exposing the electrodes to the atmosphere.

Freshly prepared electrodes which were transferred to the solution without prolonged exposure to solutions containing air became rapidly more noble for a time and then slowly approached a steady value. Electrodes that were first exposed to solutions saturated with air quickly became too noble, but slowly attained a steady potential in nitrogen. Cell solutions were made by mixing sulfuric acid and potassium pertechnetate solutions. The pH was determined initially and checked at the end of a series of measurements by using the Beckman Model G pH Meter. The potassium pertechnetate concentration was determined by measurement of the absorption spectrum, making use of the molar extinction coefficients recently determined.⁴ The rate of attainment of equilibrium was highly dependent upon the concentrations of the pertechnetate and hydrogen ions, and at a pertechnetate-ion concentration of approximately 10⁻⁴ *f* this rate was too low for reliable measurements to be made. Four calomel half-cells were compared among themselves, two of which had been in use and two taken freshly from stock. The greatest deviation among the four was less than 1 mv. The value of the potential of the saturated calomel electrode was taken as -0.242 v.⁵ referred to the normal hydrogen electrode. The potentials were measured by use of a vibrating-reed electrometer and Brown Recorder which was calibrated against a Rubicon high-precision Model B potentiometer. Table I summarizes the results obtained, the cell e.m.f. having the sign of the technetium electrode.

The dependence of the potential on the presence of oxygen was again demonstrated by switching from nitrogen to air after one series of measurements. In 20 minutes the gold electrode ennobled by 24 mv., the platinum coil by 21 mv., the gauze by 9 mv., and the foil by 19 mv.; the potentials were still increasing.

In calculating the *E*^o value the measured pH value was used together with an activity coefficient for TcO₄⁻ calculated from the ionic strength by the Debye-Hückel relation. The maximum correction on account of this activity coefficient was 1 mv.

In order to calculate the Tc-TcO₂ and Tc-TcO₄⁻ potentials, the Δ*F*_i^o for TcO₄⁻(aq) was taken as

(4) G. H. Cartledge, *Corrosion*, **11**, 335t (1955).

(5) W. M. Latimer, "Oxidation Potentials," Prentice-Hall, Inc. Second Ed., New York, N. Y., 1952, p. 177.

(1) This work was performed for the Atomic Energy Commission.
(2) Department of Chemistry, University of Tennessee, Knoxville, Tennessee.
(3) J. W. Cobble, Wm. T. Smith, Jr., and G. E. Boyd, *J. Am. Chem. Soc.*, **75**, 5777 (1953).

TABLE I
 ELECTRODE POTENTIAL, $\text{TcO}_2(\text{c})-\text{TcO}_4^-(\text{aq})$, 24°

Electrode	KTcO_4 f	H_2SO_4 f	$r\text{H}$	E.m.f., volt	E° , calcd.
Pt coil	1.00×10^{-3}	...	6.65	-0.091	-0.734 ^a
Pt coil	1.16×10^{-3}	0.5×10^{-3}	3.10	+ .198	- .741 ^b
Pt coil	1.16×10^{-3}	0.5×10^{-3}	3.10	+ .199	- .742 ^c
Pt coil	1.66×10^{-3}	2.0×10^{-3}	2.49	+ .250	- .743
Pt foil	1.66×10^{-3}	2.0×10^{-3}	2.49	+ .240	- .733
Pt gauze	1.66×10^{-3}	2.0×10^{-3}	2.49	+ .244	- .737
Au coil	$1.81_5 \times 10^{-3}$	2.0×10^{-3}	2.49	+ .244	- .736
Au coil	$1.03_7 \times 10^{-3}$	1.7×10^{-3}	2.69	+ .223 ₅	- .736 ^d

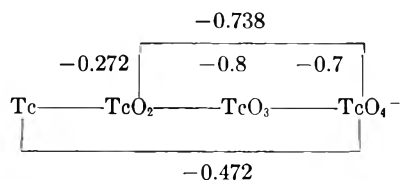
Av. - .738 = 0.003₁ volt

^a Still slowly ennobling. ^b Equilibrium approached from negative side. ^c Equilibrium approached from positive side. ^d This electrode was considerably more heavily coated with TcO_2 than the others. After equilibration had been obtained in nitrogen purified by heated copper, the measurements were continued for 24 hours in a stream of argon similarly purified. The e.m.f. remained unchanged.

-150.6 kcal. mole⁻¹.³ This, with the previously estimated entropies,³ gives -88.3 kcal. mole⁻¹ as the free energy of formation of technetium dioxide and -100.7 kcal. mole⁻¹ for ΔH_f° . Using these values the standard potential of the $\text{Tc}-\text{TcO}_2$ electrode is -0.272 v. According to these revised free energies $\Delta F^0 = -2.3$ kcal. for the disproportionation reaction



This confirms the observed instability previously reported.³ The revised potential diagram for technetium is



OAK RIDGE, TENN.

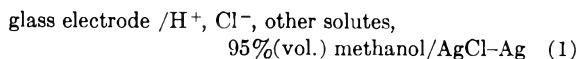
A REVERSIBLE SILVER-SILVER CHLORIDE ELECTRODE FOR 95% (VOLUME) METHANOL-WATER SOLUTIONS¹

By E. LEE PURLEE AND ERNEST GRUNWALD

Contribution from the Department of Chemistry, Florida State University, Tallahassee, Florida

Received May 23, 1955

Experimental difficulties with the silver-silver chloride electrode in organic solvents have been reported.² In the course of recent e.m.f. measurements with the cell



thermal silver-silver chloride electrodes prepared by the method of Anderson³ were observed to perform rather sluggishly and to require relatively long periods of time for equilibration, especially after exposure to dilute solutions of mixed electrolytes, e.g., sodium chloride-sodium benzoate mixtures.

(1) This work has been supported by a grant from the National Science Foundation.

(2) (a) P. S. Buckley and H. Hartley, *Phil. Mag.*, [7] **8**, 320 (1929).

(b) H. S. Harned and C. Calmon, *J. Am. Chem. Soc.*, **60**, 2130 (1938).

(3) N. J. Anderson, Ph.D. Dissertation, Dept. of Chemistry, Univ. of Chicago, Chicago, Ill., 1934.

E^* is defined as the reference e.m.f. of the silver-silver chloride electrode at 25.0°, i.e.

$$E^* = E + 0.05915 \log c_{\text{HCl}}/y^2 \quad (2)$$

where

E = measured e.m.f. in volts
 $c_{\text{HCl}}(\%)$ = stoichiometric hydrogen (chloride) concn.
 y = mean ionic activity coefficient

The equation

$$-\log y = 1.638 \mu^{1/2} / (1 + 2.426 \mu^{1/2}) \quad (3)$$

is employed to obtain activity coefficients.⁴ Although values of E^* differ for individual glass electrodes, E^* has been found to remain satisfactorily constant (± 0.2 mv.) and reproducible for a given glass electrode at the ionic strengths employed (up to ca. 0.025 M).

Experiments with the Thermal Electrolytic Silver-Silver Chloride Electrode (Anderson Type).

—With electrodes of this type E^* was found to be satisfactorily constant when cell (1) contained 0.001–0.007 M HCl. It was, however, necessary to age the electrodes in 0.001 M HCl for 24 hours prior to measurements. Equilibration of the electrodes in the HCl solutions was slow, requiring 30 to 45 minutes.

After 12 hours immersion in the mixture: HCl-(0.002 M)-KCl(0.005 M), 2.5 hours were required for the electrodes to equilibrate in 0.001 M HCl. After 6 hours immersion in the mixture: sodium benzoate (0.006 M)-benzoic acid (0.006 M)-sodium chloride (0.001 M), slightly over two hours were required for electrode equilibration in 0.001 M HCl. After 45 min. the e.m.f. was still 3.0 mv. from its equilibrium value. These results are perhaps not surprising since the silver-silver chloride electrode is extremely porous and the silver chloride coating relatively heavy. 30 to 35% of the thermally deposited silver was converted to silver chloride.

Experiments with a Silver Mirror Silver-Silver Chloride Electrode.—The silver mirror technique of depositing silver on platinum foil was employed. (See Experimental part.) A thin film of silver chloride was then electrolytically deposited on the silver surface.

Electrodes prepared in this manner proved to be very satisfactory. The e.m.f.'s for different silver mirror electrodes and different thermal elec-

(4) E. Grunwald, *Anal. Chem.*, **26**, 1696 (1954).

trolytic electrodes in cell (1) have been found to agree to within 0.2 mv. or less. In all measurements the equilibration time for the silver mirror electrode has been observed to be 10 to 15 minutes and virtually independent of exposure to mixed electrolytes. For example, the electrodes equilibrate readily in 0.003 *M* HCl after the following exposures

- 24 hr. in sodium benzoate (0.015 *M*)-benzoic acid (0.01 *M*)
- 8.5 hr. in KCl (0.012 *M*)
- 1 hr. in sodium formate (0.0014 *M*)-formic acid (0.028 *M*)-NaCl (0.006 *M*)
- 4.5 hr. in sodium acetate (0.005 *M*)-NaCl (0.0013 *M*)-acetic acid (0.0025 *M*)
- 24 hr. in distilled water

Some typical data for HCl and HCl-KCl mixtures are shown in Table I.

TABLE I

E^* VALUES FOR SILVER MIRROR-ELECTROLYTIC SILVER CHLORIDE ELECTRODE FOR HCl AND HCl-KCl MIXTURES IN 95% (VOL.) METHANOL AT 25.0°

HCl, <i>M</i>	KCl, <i>M</i>	$-E^*$ (v.)
0.001223	0.001602	0.6294
.001223	.005338	.6293
.002426	.001602	.6294
.004047	.005338	.6294
.004047	.01067	.6294
0.001223-	0.0000	0.6295 ±
.02219		0.0001 ^a (v.)

^a Average and standard deviation for 6 determinations at different concentrations in this range.

The applicability of this electrode was further tested by comparing pK_A values for formic and acetic acids in cell (1) with values based on the cell glass electrode/H⁺, other solutes, 95% (vol.) methanol/

KCl(sat., 95% (vol.) methanol AgCl-Ag (4)

The two sets of pK_A values in Table II are in good agreement. For comparison, Table II also contains some results for acetic acid with the thermal electrolytic silver-silver chloride electrode. The latter results, being of the correct order of magnitude, exhibit poor precision and actually decreased steadily with increasing degree of neutralization. In 80% methanol it has been readily possible to obtain a precision of ±0.02 in the pK_A 's for organic acids with the thermal electrolytic electrode. The drifts for acetic acid in 95% methanol appear significant and quite possibly resulted from difficulties in observing electrode equilibrium.

TABLE II

COMPARISON OF pK_A VALUES FOR FORMIC ACID AND ACETIC ACID IN 95% (VOL.) METHANOL, 25.0°

Acid	Cell 4	Cell 1: Ag-AgCl Electrode: Silver mirror electrolytic	Thermal electrolytic
Formic	6.548 ± 0.008	6.542
Acetic	7.863 ± .009	7.855 ± 0.003 ^a	7.90 to 7.79 ^b

^a Average and standard deviation for 5 determinations in which the % acid neutralized ranged up to 60%. ^b 6 determinations by Dr. A. L. Bacarella in this Laboratory in which the % acid neutralized ranged up to 8%.

Two important factors appear to influence the equilibration of the electrodes: (a) extreme porosity (and large surface area) of the electrodes;

(b) thickness of the silver chloride coatings. In Table III the equilibration times for different electrodes of varying silver chloride coatings are compared.

TABLE III

EQUILIBRATION TIMES FOR DIFFERENT ELECTRODES IN 0.001 *M* HCl AFTER 12 HR. IMMERSION IN HCl (0.001 *M*)-KCl (0.001 *M*) MIXTURES

Electrode Type	Fraction of Ag converted to AgCl	Equilibration time, min.
Thermal electrolytic	0.30	150
Thermal electrolytic	0.17	70
Thermal electrolytic	0.05	45
Mirror electrolytic	0.15-0.25	10-15

In the application of potentiometric titrimetry with cell (1) to solutions rich in organic solvent it is desirable to have a dependable electrode which equilibrates rapidly. The silver mirror electrode appears to offer this advantage.

Experimental.—E.m.f.'s were measured with a Beckman model GS pH meter and were accurate to within 0.1 mv. The cell consisted of a 180-ml. electrolytic beaker fitted with a rubber stopper which held a Beckman #1190-42 glass electrode. The volumes of the test solutions ranged from 25 to 50 ml. The cell was suspended in a large water thermostat maintained at 25.00 ± 0.02°. Stirring of the solutions was accomplished by manually agitating the cell.

The thermal-electrolytic silver-silver chloride electrodes (Harned's type 2)⁵ were prepared by the method of Anderson.³ The anodization time was 3 to 3.5 hours and resulted in the conversion of 30 to 35% of the thermally deposited silver to silver chloride.

Silver mirror silver-silver chloride electrodes consisted of platinum foil 0.001" thick welded to platinum wire. The total electrodes surface area was approximately 2 cm.². After cleaning with concentrated nitric acid, concentrated ammonia and doubly distilled water, silver was deposited on the platinum foil by the Rochelle salts silvering process.⁶ (Sodium tartrate was substituted for Rochelle salts.) The platinum foil was suspended vertically in the silvering mixture. Three depositions of silver, each requiring about one hour, were made. This procedure resulted in the deposition of ca. 0.8 mg. of silver per cm.² of platinum surface. The silver chloride coating was produced by anodization for 2 to 3 minutes in 0.05 *M* hydrochloric acid at a current density of ca. 1.0 ma./cm.². By these techniques 15 to 25% of the silver was converted to silver chloride.

The saturated KCl/AgCl-Ag reference electrode of cell (4) consisted of a silver wire-electrolytic AgCl electrode immersed in 95% (vol.) methanol saturated with KCl. The latter solution was contained in a Pyrex tube (10 mm. × 100 mm.) fitted with a standard-taper inner joint at the top. Liquid junction contact with the test solution in the cell was made *via* an asbestos fiber sealed in the bottom of the electrode container.

(5) H. A. Harned, *J. Am. Chem. Soc.*, **51**, 416 (1929).

(6) "Handbook of Chemistry and Physics," 29th Edition, Chemical Rubber Publishing Co., Cleveland, Ohio, 1945, p. 2492.

DIFFUSION IN THE SYSTEM METHANOL-BENZENE¹

BY C. S. CALDWELL AND A. L. BABB

Department of Chemical Engineering, University of Washington, Seattle Washington

Received May 23, 1955

Diffusion coefficients for the system methanol-benzene have been measured at 27° with a Mach-

(1) This work was supported in part by the Office of Ordnance Research, U. S. Army.

Zehnder interferometer described elsewhere.² The data of Lemonde³ for this system were available for 11°, but two widely separated values of D were reported at a concentration of 4 mole % methanol (1.30 and 1.89×10^{-5} cm.²/sec.). In order to clearly define the shape of the complete D - x curve at 11° two supplementary points were obtained for this system at methanol concentrations of 0.477 mole % ($D = 2.875 \times 10^{-5}$ cm.²/sec.) and 1.572 mole % ($D = 2.233 \times 10^{-5}$ cm.²/sec.). The data shown in Fig. 1 indicate that the lower value reported by Lemonde at 4 mole % methanol is the more reliable.

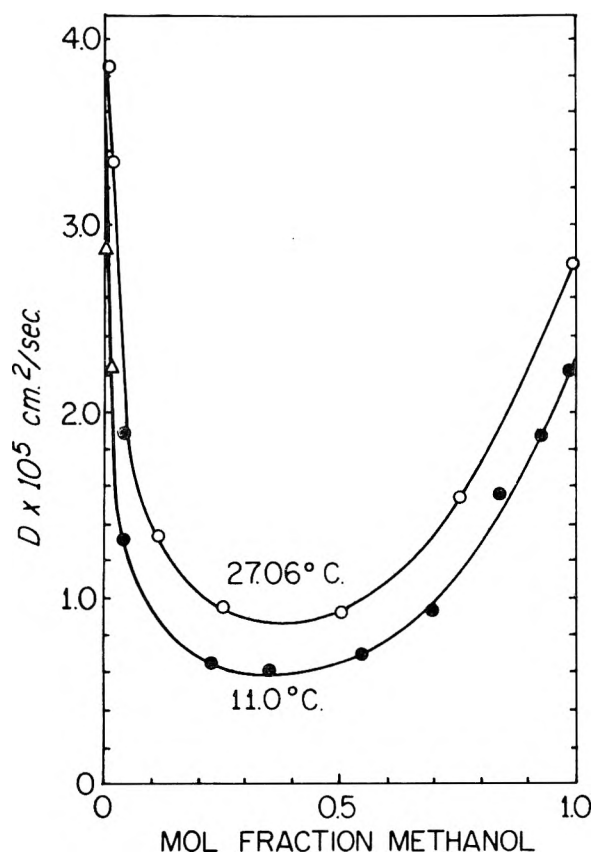


Fig. 1.—Mutual diffusion coefficients for the system methanol-benzene: Δ , \circ , at 11.0° and 27.06° (the authors); \bullet , at 11.0° (Lemonde).

The experimental activation energies E_D and E_η for diffusion and viscosity, respectively, have been calculated as a function of concentration and are shown in Fig. 2. It is evident that E_D is larger than E_η by about 50% for most of the concentration range, but that the two activation energies approach each other in the dilute regions. One is led to conclude that the rate of hole formation according to the Eyring theory is the limiting process only at high dilutions, and that in the concentrated region, additional energy must be acquired by an alcohol molecule before it can move from one equilibrium position to the next. The irregular shape of the E_D - x curve suggests that definite changes in the structure of the alcohol aggregates are taking place particularly in the region from 0 to 15% methanol.

(2) C. S. Caldwell, Ph.D. Thesis, University of Washington, 1955.

(3) H. Lemonde, *Ann. Phys.*, **9**, 539 (1938).

In the dilute methanol region in Fig. 1, a sharp drop in D from 4.05 to 1.8×10^{-5} cm.²/sec. occurs as the concentration changes from 0 to 6 mole % methanol. This probably is caused by a change in species from single methanol molecules of high mobility to polymers having greatly restricted translational freedom.⁴⁻⁶ In this same region, the activation energy for diffusion rises from 2.7 to 5.9 kcal./mole, indicating that energy equivalent to the breaking of a full hydrogen bond is involved. Further evidence that a high degree of ordering occurs in this region comes from the fact that the partial molal excess entropy of mixing for methanol drops abruptly from about 1.5 to -2.0 e.u. as the concentration of methanol changes from 0 to 10 mole%.^{5,6} It is also significant that E_D for 0% methanol (2.7 kcal./mole) is only slightly above E_D for self-diffusion of benzene (2.1 kcal./mole).⁷ The difference, 0.6 kcal./mole, might represent approximately the interaction energy between benzene and methanol.

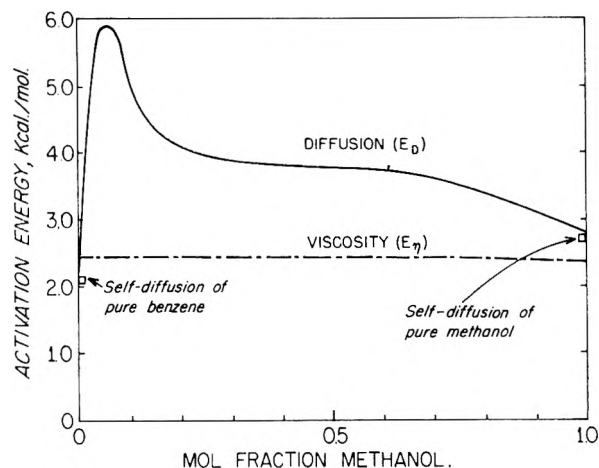


Fig. 2.—Variation of activation energies with composition for the system methanol-benzene.

In the concentrated region, in spite of the fact that a highly polymerized structure is known to exist in pure methanol, the diffusivity is moderately high, and the activation energy for diffusion is 2.8 kcal./mole. This is only slightly higher than the respective activation energies for self-diffusion and viscosity of pure methanol. Evidently the polymer structure is such that benzene and methanol can move past each other freely, and that a full H-bond need not be broken when transfer occurs from one aggregate to the other.

Further discussions of the benzene-methanol system will be presented in conjunction with the results of measurement of self-diffusion coefficients of radioactive components in benzene-methanol solutions.⁸

(4) G. Scatchard and C. L. Raymond, *J. Am. Chem. Soc.*, **60**, 1278 (1938).

(5) G. Scatchard, S. E. Wood and J. M. Mochel, *ibid.*, **68**, 1957 (1946).

(6) G. Scatchard, L. B. Ticknor, J. R. Coates and E. R. McCartney, *ibid.*, **74**, 3721 (1952).

(7) K. Graupner and E. R. S. Winter, *J. Chem. Soc.*, 1145 (1952).

(8) P. A. Johnson and A. L. Babb, *THIS JOURNAL*, in press.

ON THE ROLE OF DIFFUSION IN CATALYSIS

BY JUI H. WANG

Contribution No. 1303 from the Sterling Chemistry Laboratory, Yale University, New Haven, Conn.

Received May 23, 1955

In order to examine the role of diffusion in a general catalytic reaction, let us consider a spherical catalyst particle immersed in an infinite solution of substrate molecules, and consider the center of the catalyst particle as the origin of our system of moving spherical polar coordinates, r , θ and φ . The probability that a reaction will occur within a given time interval, dt in a volume element, dv , located at the point (r, θ, φ) should be an explicit function of the substrate concentration, c , and the coordinates at that point, and may be denoted by $P(r, \theta, \varphi, c)dvdt$. The change in c at that point due to the combined effect of diffusion and reaction is governed by the relationship

$$\frac{\partial c}{\partial t} = \nabla \cdot D_{12} \nabla c - P(r, \theta, \varphi, c) \quad (1)$$

where $D_{12} = D_1 + D_2$. In equation 1, D_1 and D_2 are the diffusion coefficients of the catalyst particle and substrate molecule, respectively, and D_{12} is the relative diffusion coefficient of the substrate molecules with respect to the catalyst particle.¹

For problems in catalysis only steady-state reaction rate when $\partial c / \partial t = 0$ is of practical importance. If we further assume that D_{12} is practically independent of c , and

$$P(r, \theta, \varphi, c) = 0, \text{ at } r > r_0 \quad (2)$$

$$c = c_\infty, \text{ when } r \rightarrow \infty \quad (3)$$

and the boundary condition which includes the saturation-effect at the "reaction surface", *i.e.*

$$D_{12} \frac{\partial c}{\partial r} - \frac{k'c}{1 + (c/K)} = 0, \text{ at } r = r_0 \quad (4)$$

where K and k' are constants characteristic of the system under consideration, then the steady-state solution of equation 1 becomes

$$c = c_\infty - \left(\frac{r_0}{r}\right) \left(\frac{K}{2\beta}\right) \left\{ \left(1 + \beta + \frac{\beta c_\infty}{K}\right) - \left[\left(1 + \beta + \frac{\beta c_\infty}{K}\right)^2 - \frac{4\beta c_\infty}{K} \right]^{1/2} \right\} \quad (5)$$

where

$$\beta = D_{12}/k'r_0$$

The turnover number n of the catalyst, which is defined as the number of substrate molecules transformed per unit time per catalyst molecule, may then be obtained with the help of equation 5 as

$$\begin{aligned} n &= 4\pi r_0^2 D_{12} \left(\frac{\partial c}{\partial r}\right)_{r=r_0} \\ &= 2\pi r_0 D_{12} \left(\frac{K}{\beta}\right) \left\{ \left(1 + \beta + \frac{\beta c_\infty}{K}\right) - \left[\left(1 + \beta + \frac{\beta c_\infty}{K}\right)^2 - \frac{4\beta c_\infty}{K} \right]^{1/2} \right\} \quad (6) \end{aligned}$$

The following two special cases are of particular importance.

(A) For $\beta \gg 1$, *i.e.*, for non-diffusion-limited reactions, equation 6 may be written as

(1) See, for example, S. Chandrasekhar, *Rev. Mod. Phys.*, **15**, 1 (1943).

$$\begin{aligned} n &= 2\pi r_0 D_{12} \left(\frac{K}{\beta}\right) \left(1 + \beta + \frac{\beta c_\infty}{K}\right) \\ &\quad \left\{ 1 - 1 + \frac{4\beta c_\infty}{2K \left(1 + \beta + \frac{\beta c_\infty}{K}\right)^2} - \dots \right\} \\ &\cong 4\pi r_0^2 \left(\frac{k'c_\infty}{1 + \frac{c_\infty}{K}}\right) \quad (7) \end{aligned}$$

which is formally identical with the Michaelis-Menten law for enzymes or the Langmuir formula for surface reactions.

(B) For $\beta \ll 1$, *i.e.*, for diffusion-limited reactions, equation 8 reduces to

$$n = \frac{4\pi r_0 D_{12} c_\infty}{1 + \beta + \frac{\beta c_\infty}{K}} \cong 4\pi r_0 D_{12} c_\infty \quad (8)$$

or

$$n = k_2 C$$

where

$$k_2 \cong 4\pi r_0 D_{12} \left(\frac{N}{1000}\right) \quad (9)$$

Homogeneous Catalysis.—For catalytic reactions involving only small molecules or ions in liquid solutions at room temperatures, we may conservatively estimate the second-order rate constant, k_2 , by putting $r_0 = 2 \times 10^{-8}$ cm., $D_{12} = D_1 + D_2 = 10^{-5}$ cm.²/sec. in equation 9 and obtain $k_2 = 1.5 \times 10^9$ moles per liter per sec.

Since this value is much larger than any of the observed second-order rate constants in homogeneous catalysis in liquids involving only small molecules or ions, we may conclude that none of these observed catalytic reactions is diffusion-limited. It is true that in many of these observed catalytic reactions neither the catalyst nor substrate molecules are spherical. But this simply means some average "collision diameter" should be used for r_0 . While the uncertainty in such an estimated value for r_0 can seldom exceed a factor of 10, the above calculated value of k_2 is greater than most observed values by a factor of 10^9 . Thus in spite of our unrealistic assumption of spherical symmetry, the above conclusion should still hold.

Heterogeneous Catalysis.—Practically all diffusion-limited catalytic reactions reported in the literature are heterogeneous. This is consistent with the above derivation of equations 6, 7 and 8. It is there shown that whether or not a given reaction is diffusion-limited depends on the value of $\beta = D_{12}/(k'r_0)$. For given values of D_{12} and k' , the reaction may become diffusion-limited if $r_0 \rightarrow \infty$, *i.e.*, in heterogeneous catalysis. Thus catalysis by a uniform planar surface is often diffusion-limited because a planar reaction surface can be considered as a small section of a spherical reaction surface with infinite radius r_0 . If, however, the small catalytic centers are sparsely dispersed on a large planar "carrier surface," then the value of r_0 for the individual catalytic centers may still be of molecular dimensions and consequently the reaction is unlikely to be diffusion-limited, even though the gross geometric surface is planar.

If it is possible to change the size of the catalyst particle continuously from molecular to macro-

scopic dimensions without appreciably changing the surface reaction rate constant k' , one may be able to observe a gradual transition from non-diffusion limited to diffusion-limited reaction according to (6). The change in $D_{12} = D_1 + D_2$ is often small, since usually D_2 is greater than D_1 and is not affected by the size of the catalyst particle. One of the possible ways to detect such a gradual transition is to investigate the isotope effect in catalytic reactions.

It was found by Dole and co-workers² that the oxygen gas liberated in the catalytic decomposition of hydrogen peroxide by various catalysts is often enriched in O^{18} . These workers explained the observed enrichment of O^{18} in the oxygen produced by assuming that the rate-determining step in these reactions involves the production of free radicals and that $HO^{16}O^{16}H$ reacts faster than $HO^{16}O^{18}H$. If it is possible to increase the size of catalyst particles gradually to macroscopic dimensions without appreciably changing k' so that the reaction gradually becomes diffusion-limited, the observed isotope-effect should gradually decrease and eventually disappear. This is because if the reaction becomes diffusion-limited, the H_2O_2 molecule, be it $HO^{16}O^{16}H$ or $HO^{16}O^{18}H$, reacts instantaneously as soon as it reaches the reaction surface and consequently the above described isotope effect should disappear.

Isotope effects in the catalytic decomposition of hydrogen peroxide by manganese dioxide and ferric hydroxide were studied in connection with this work. The procedure involves the mixing of $\sim 3\%$ H_2O_2 with equal volume of a suspension of MnO_2 or $Fe(OH)_3$ in an evacuated vessel, collecting and drying the liberated oxygen gas after the decomposition was completed, and analyzing the resulting oxygen gas for its atom per cent. of O^{18} by means of a Consolidated-401 mass spectrometer. The atom per cent. of O^{18} of the original H_2O_2 was determined by complete oxidation with acid ceric sulfate solution, followed by mass spectrometric analysis of the oxygen gas produced. The results found with MnO_2 as catalyst are summarized in Table I. The experimental details are not given since the procedure consists mainly of standard techniques in mass spectrometric analysis. The term "O¹⁸-enrichment Factor" in Table I is defined as the ratio of the atom per cent. of O^{18} in the liberated oxygen to that in the original hydrogen peroxide.

An earlier value obtained by Dole and co-workers² is included in Table I for comparison. It may be noticed from Table I that as the size of MnO_2 particles increase with their age, the measured enrichment factor decreases. This is suggestive of a gradual transition to diffusion-limited reaction, although more experimental data in this direction are necessary before definite conclusions can be drawn on this point.

When ferric hydroxide was used as the catalyst, it was found that the corresponding change in the enrichment factor was very small as the freshly precipitated $Fe(OH)_3$ was gradually aged by

TABLE I

ISOTOPE EFFECT IN THE CATALYTIC DECOMPOSITION OF HYDROGEN PEROXIDE BY MANGANESE DIOXIDE

Catalyst	No. of mass-spectrometric detmn.	O^{18} -enrichment factor
MnO_2 , freshly pptd. from Mn^{++} in soln. with OH^- and O_2H^-	7	1.020 ± 0.0023
MnO_2 , electrolytic, by Dole, <i>et al.</i>	6	(1.018 ± 0.0016)
MnO_2 , pptd. from Mn^{++} in soln. with OH^- and O_2H^- , boiled for 1 hr. and aged for 24 hr.	8	1.009 ± 0.0023
MnO_2 , native pyrolusite ($\sim 90\%$)	6	1.006 ± 0.0023

boiling. This observation seems to indicate that a phase-transition probably occurred when the freshly precipitated $Fe(OH)_3$ was boiled, so that the catalytic character of the surface was no longer the same. As a matter of fact while freshly precipitated $Fe(OH)_3$ is very efficient in catalyzing the decomposition of H_2O_2 , the aged precipitate is almost inert. Visually the decomposition of H_2O_2 took place very slowly only at a few particular spots of the aged precipitate. But for MnO_2 , there was no noticeable decrease in catalytic efficiency as the precipitate was aged.

These results suggest that the rate laws of heterogeneous and homogeneous catalysis can be brought under one formulation.

The Effect of Stirring.—It is a customary practice to conclude that a certain given reaction is not diffusion-limited if the introduction of stirring does not increase the reaction rate. That this reasoning is not generally sound can be shown by rather simple considerations. Thus for diffusion-limited catalytic reaction, $\beta \ll 1$ and equation 6 simplifies to

$$c = c_{\infty}[1 - (r_0/r)]$$

If the constant $r_{1/2}$ is so defined that

$$c = \frac{c_{\infty}}{2} \text{ at } r = r_{1/2}$$

then

$$r_{1/2} = 2r_0$$

and the "half-thickness" of the diffusion layer surrounding the catalyst particle is equal to $r_{1/2} - r_0 = r_0$. Thus for reaction surfaces with r_0 of macroscopic dimensions, one should be able to observe a pronounced stirring effect for diffusion-limited reactions. But for reaction surfaces with r_0 of molecular dimensions, say 2×10^{-8} cm., the half-thickness of the diffusion layer is so thin that one can hardly disturb the concentration gradients near the catalyst by an ordinary laboratory stirring device. This shows for homogeneous catalysis in liquids involving only small molecules or ions there should be no detectable effect of stirring on the observed reaction rate even if the reaction is diffusion-limited. The quenching of fluorescence in liquids appears to be a suitable example to test this conclusion.

(2) M. Dole, R. DeForest, G. Muchow and C. Compte, *J. Chem. Phys.*, **20**, 961 (1952).

THE SORPTION OF GASEOUS HYDROGEN CHLORIDE BY CRYSTALLINE INSULIN

By L. H. REYERSON AND LOWELL PETERSON

School of Chemistry, University of Minnesota, Minneapolis, Minnesota
Received May 31, 1955

Recent work completed in this Laboratory on the sorption of NH_3 and HCl by Nylon fibers indicated that the mechanism of the sorption of the two gases differed markedly. This work is being prepared for publication, but in the meantime it was deemed desirable to study the sorption of HCl by crystalline insulin. Earlier studies on the sorption of polar molecules by proteins have been reported.^{1,2} A very recent study³ indicated that the authors propose to investigate the sorption of NH_3 and HCl by proteins. This note presents the completed work on the sorption of HCl on crystalline insulin at 20 and -78.9° . The sensitive Mc-Bain quartz spiral balance used in these determinations together with the cryostatic temperature controls were of the same type as previously described.⁴ The sample of crystalline zinc insulin was supplied by the Lilly Research Laboratories, and it contained approximately equal parts of cubic crystals about 12μ on edge and rhombic crystals $8 \times 12 \mu$. The samples were dried to constant weight by evacuation for three days at room temperature. Carefully purified HCl was then admitted through a specially ground stopcock. Constant pressure was maintained by adding or withdrawing small amounts of HCl through the stopcock while keeping the reservoir of HCl in a Dewar surrounded by either solid CO_2 or liquid nitrogen.

The data obtained for the sorption of HCl by dry zinc insulin at 20° are shown graphically in Fig. 1. Three days were allowed for complete equilibrium at each sorption point, but the protein sorbed 90% of the equilibrium amount usually within 12 hours. Hysteresis was observed on desorption and about 51 mg. of HCl per g. of insulin remained permanently bound at near zero pressure. In these experiments as in those of Benson and Seehof,⁵ the HCl is regarded as being permanently bound when it desorbs at a rate of 0.03 millimole or less per gram of protein per day.

The data for the sorption at -78.9° are shown graphically in Fig. 2. Equilibrium was reached more slowly at this temperature, taking from three to ten days per point. Hysteresis was again observed and 215 mg. of HCl per g. of insulin remained permanently bound at this temperature. At the conclusion of this run, the sample was allowed to warm up to about 30° while pumping was continued for five days. After five days, 40 mg./g. remained permanently sorbed, as previously defined. This sample was then heated to 40° and at this temperature 33.2 mg./g. was found to be permanently bound. Another experiment was car-

(1) S. W. Benson, D. A. Ellis and R. W. Zwanzig, *J. Am. Chem. Soc.*, **72**, 2102 (1950).

(2) E. F. Mellon, A. H. Korn, E. L. Kokes and S. R. Hoover, *ibid.*, **73**, 1870 (1951).

(3) A. C. Zettlemoyer, J. J. Chessick and Amir Chand, *THIS JOURNAL*, **59**, 375 (1955).

(4) L. H. Reyerson and J. M. Honig, *J. Am. Chem. Soc.*, **75**, 3917 (1953).

(5) S. W. Benson and J. Seehof, *ibid.*, **75**, 3925 (1953).

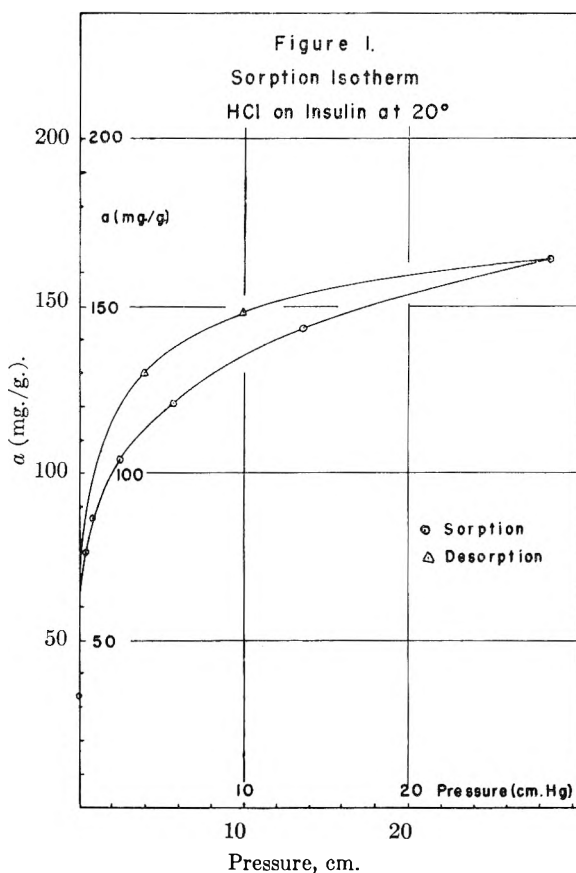


Fig. 1.—Sorption isotherm HCl on insulin at 20° .

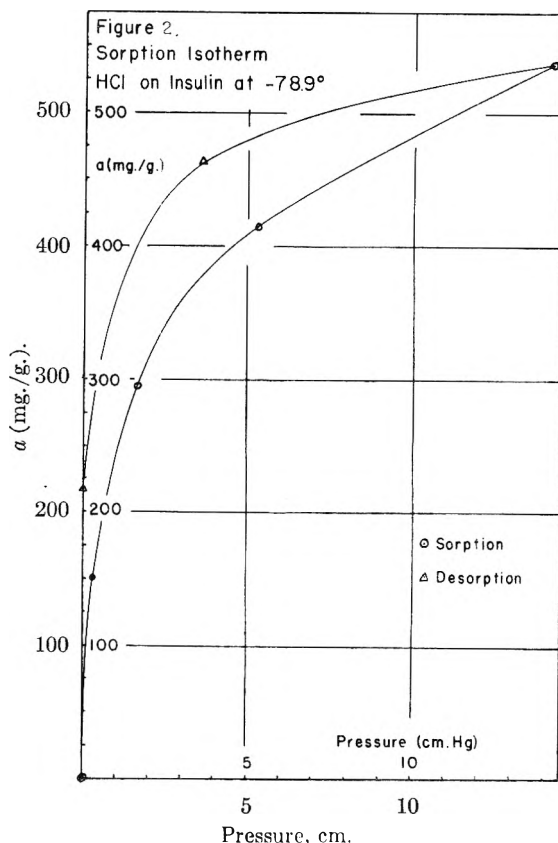


Fig. 2.—Sorption isotherm HCl on insulin at -78.9°

ried out at 0° and 72 mg./g. was permanently bound. These experiments indicate that the amount of HCl permanently bound by insulin is strongly temperature dependent. Table I illustrates this fact.

TABLE I
AMOUNTS OF HCl PERMANENTLY BOUND AT DIFFERENT TEMPERATURES

Temp., °C.	Amount bound, mg./g.
-78.9	215
0	72
20	51
30 (room temp.)	40
40	33.2

The sorption of HCl by insulin has little in common with the results obtained in this Laboratory for HCl sorbed by Nylon fibers. Whereas insulin has about 10% fewer amide links per unit weight than does Nylon, the sorption on the crystalline protein is far less than on Nylon. This suggests that many of the amide groups in the protein are unavailable as sorption sites for HCl while every amide link in Nylon sorbs an HCl molecule at room temperature. Possibly the only sorption sites in the protein are the polar groups present in the side chains. Further work is planned in an attempt to answer these differences. In view of the pronounced effect of temperature on the amount of permanently bound HCl, it seemed futile to attempt to identify the amount of irreversibly bound gas with the total number of free amino groups in the side chains of the protein, as was done by Benson and Seehof.⁵ There is no evidence that these authors studied the effect of temperature on the irreversible sorption of HCl by proteins since they mention only studies at room temperature. It would seem worthwhile to repeat their experiments on the same proteins at a series of different temperatures.

ON THE GERMANIUM-SILICON PHASE DIAGRAM

By F. X. HASSION, A. J. GOSS AND F. A. TRUMBORE

Bell Telephone Laboratories, Inc., Murray Hill, New Jersey

Received June 10, 1955

In their determination of the Ge-Si phase diagram, Stöhr and Klemm¹ reported anomalous thermal arrests at 930°, approximately ten degrees below the melting point of Ge. These heat effects were obtained upon cooling melts containing up to 60 atom per cent. Si. Thurmond² has pointed out that a heat effect would be expected at the melting point of Ge in the absence of solid state diffusion during the solidification of Ge-Si alloys, and that a true solidus point is obtained by thermal analysis only in the absence of coring. Consequently, he concluded that the temperature reported by Stöhr and Klemm may be in error by about ten degrees. The purpose of this note is to report the results of experiments which resolve

this discrepancy and which also provide additional information on the positions of both the liquidus and solidus curves in the germanium-rich region of the phase diagram.

Cooling curve measurements were run on two different Ge-Si melts, and the inflections corresponding to the liquidus point and the anomalous arrest were noted. The results are summarized in Table I. The general procedure and apparatus for these experiments and the visual observations referred to below are described elsewhere in detail.³ The melts were contained in a graphite crucible under an argon atmosphere and consisted of known amounts of extremely pure germanium and silicon of resistivities greater than 20 and 50 ohm-cm., respectively. The anomalous arrest is seen to occur at a temperature about 1-3 degrees above the melting point of Ge, $937.2 \pm 0.5^\circ$.^{3,4} (Stöhr and Klemm obtained a value of 940° for the melting point of Ge). The agreement of the values for liquidus points of Stöhr and Klemm and of the present study is considered good.

TABLE I

Atom % Si	Liquidus points, °C.		"Anomalous arrest"
	This study	Stöhr and Klemm	
7.4	1027 ± 2	1018 ^b	940.4 ± 2
7.4 ^a	1025 ± 2	1018	938.0 ± 2
33.5	1207 ± 2	1208	938.7 ± 2

^a This melt was not stirred; the other two melts were stirred as long as possible. ^b These values were obtained by interpolation using the very small scale diagram of Stöhr and Klemm. Since no estimates of experimental error were given, no errors are quoted here. The interpolation itself may involve an error of $\pm 4^\circ$.

Three Ge-Si alloys were prepared as single crystals or as samples containing large grains by the slow solidification technique previously discussed by Wang and Alexander.⁵ This method eliminates the very lengthy annealing procedure of Stöhr and Klemm. Small samples of these alloys were sealed into quartz tubes under helium and, after heating to the desired temperatures, were examined microscopically for the presence of liquid phase. By this method the solidus points were determined. The results, shown in Table II, are seen to be in good agreement with the data of Stöhr and Klemm.

TABLE II

Atom % Si	Solidus points, °C.	
	This study	Stöhr and Klemm
10 ± 1	963 ± 1.5	964 ± 3^a
13 ± 1	971 ± 3	973 ± 3
16 ± 1	987 ± 3	982 ± 3

^a This error is only that associated with an error of $\pm 1\%$ in composition of the alloy and does not include any error involved in interpolation from Stöhr and Klemm's small scale plot.

Lattice parameters calculated from X-ray powder patterns were determined for alloys containing 0-20 atom per cent. Si. These results are summarized in Table III in which also are tabulated

(3) F. X. Hassion, C. D. Thurmond and F. A. Trumbore, *ibid.*, **69**, 1076 (1955).

(4) E. S. Greiner and P. Breidt, Jr., *J. Metals*, **7**, 187 (1955).

(5) C. C. Wang and B. H. Alexander, A.I.M.E. Symposium on Semiconductors, New York, N. Y., Feb. 15-18, 1954 (unpublished).

(1) H. Stöhr and W. Klemm, *Z. anorg. allgem. Chem.*, **241**, 305 (1939).

(2) C. D. Thurmond, *This Journal*, **57**, 78 (1953).

some of the values obtained by Stöhr and Klemm. The latter data have been corrected assuming the values were reported in kX units. Microchemical analysis was used to determine the compositions of the alloys referred to in this table. Once this relation between composition and lattice parameter was established, the X-ray powder pattern provided a rapid method for measuring composition and homogeneity. The compositions in Table II were obtained in this way.

TABLE III

Atom % Si	a_0 (Å.)	
	This study	Stöhr and Klemm
0.0 (Ge)	5.657 ± 0.0005^a	5.659
8.3 ± 0.1	5.637	...
9.5 ± 0.1	5.634	...
10.0	...	5.631
12.5 ± 0.1	5.626	...
16.6 ± 0.1	5.614	...
19.7 ± 0.1	5.607	...
20.0	...	5.605

^a Straumanis and Aka [*J. Appl. Phys.*, **23**, 330 (1952)] report a value for a_0 of 5.6575 Å. for pure Ge.

In summary, while the anomalous arrest temperature of Stöhr and Klemm appears to be in error by about 10 degrees, and their melting point by about 2-3 degrees, the liquidus, solidus and X-ray data are in good agreement with the results of the present study.

The authors thank C. D. Thurmond for several helpful discussions and also Mrs. L. B. Eary and M. Kowalchik for their assistance in some of the measurements.

TABLE OF AXIAL RATIOS CALCULATED FROM THE PERRIN EQUATION

BY WILLIAM C. BOYD

School of Medicine, Boston University, Boston, Massachusetts

Received June 10, 1955

If we assume (Onley¹) the protein molecule is perfectly rigid, and that there is no penetration by the solvent, we can calculate its dimensions from its molecular weight and the frictional ratio f/f_0 . Perrin² showed that the frictional ratio of a prolate ellipsoid with the ratio of minor to major axis $b/a = \rho$ would be

$$f/f_0 = \frac{(1 - \rho^2)^{1/2}}{\rho^{2/3} \ln [1 + (1 - \rho^2)^{1/2}]/\rho}$$

where \ln means logarithm to the base e .

Tables of the values of f/f_0 for various assumed values of ρ have been given (Svedberg and Pedersen,³ Cohn and Edsall⁴), but in practice we are given f/f_0 as found experimentally and wish to know what axial ratio a/b the experimental value implies. For this a table of axial ratios corresponding to definite values of f/f_0 is useful. Such

a table has been computed by solving the above equation, for fixed values of f/f_0 , by Newton's method of approximation.⁵ The results are shown in Table I. The relation is sufficiently linear so that intermediate values of a/b can be obtained with all necessary accuracy by interpolation.

TABLE I

RELATION BETWEEN FRICTIONAL COEFFICIENT (f/f_0) AND RATIO OF MAJOR TO MINOR AXIS (a/b)

f/f_0	a/b ($1/\rho$)	f/f_0	a/b ($1/\rho$)
1.10	2.82	1.05	2.09
1.20	4.26	1.15	3.53
1.30	5.78	1.25	5.00
1.40	7.42	1.35	6.58
1.50	9.20	1.45	8.29
1.60	11.11	1.55	10.13
1.70	13.15	1.65	12.11
1.80	15.34	1.75	14.23
1.90	17.66	1.85	16.48
2.00	20.12	1.95	18.87
2.10	22.72	2.05	21.40
2.20	25.45	2.15	24.06

(5) For the benefit of those who might wish to calculate values of a/b not given in the table, it may be mentioned that the derivative $d(f/f_0)/d\rho$, which is needed in Newton's method, is rather tedious to derive. It is

$$\frac{\rho^{-1/3} - 2\rho^{-5/3}}{3(1 - \rho^2)^{1/2} \ln [1 + (1 - \rho^2)^{1/2}]/\rho} + \frac{\rho^{-2/3}}{\ln^2 [1 + (1 - \rho^2)^{1/2}]/\rho}$$

TRACER ELECTROPHORESIS. IV. MODIFIED BRADY METHOD¹

BY KAROL J. MYSELS AND HORST W. HOYER

Department of Chemistry, University of Southern California, Los Angeles 7, Cal.

Received June 20, 1955

In the first paper of this series² we have described in detail a method of measuring the electrophoretic mobility which uses tracers and has the advantages of avoiding boundary anomalies and obviating the use of porous membranes. For comparison we also reported at that time some results obtained using a modified Brady method³ which also uses tracers but employs porous membranes. In view of the success and basic advantage of the former method, the latter has not been further refined or studied as planned originally. It nevertheless may be worthwhile to present in this Note a brief description of the apparatus we developed and particularly to point out the real reason why Brady's and our method work.

Experimental

The apparatus used is shown in Fig. 1. The tagged solution is placed in the central compartment between two "medium" fritted glass plugs P. On both sides of it and extending to the level of stopcocks S is the same solution but untagged, beyond is an NaCl solution which makes

(1) J. L. Onley, Biol. Chem. Lecture Series, N. Y. Section, Am. Chem. Soc., April 15, 1953.

(2) F. Perrin, *J. phys. radium*, **7**, 1 (1936).

(3) T. Svedberg and K. O. Pedersen, "The Ultracentrifuge," The Clarendon Press, Oxford, 1940.

(4) E. J. Cohn and J. T. Edsall, "Proteins, Amino Acids and Peptides," 1943, Reinhold Publ. Corp., New York, N. Y.

(1) Presented at the 12th International Congress of Pure and Applied Chemistry, New York, September, 1951.

(2) H. W. Hoyer, K. J. Mysels and D. Stigter, *This Journal*, **58**, 385 (1954).

(3) A. P. Brady, *J. Am. Chem. Soc.*, **70**, 911 (1948).

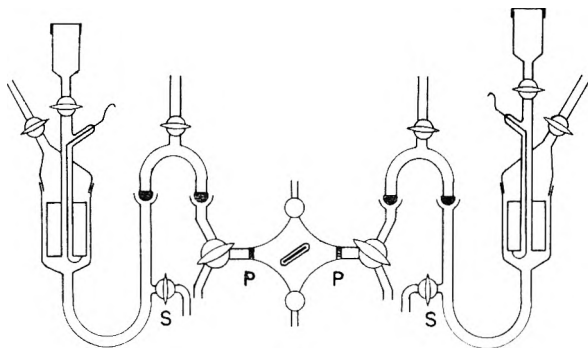


Fig. 1.

contact with Ag/AgCl electrodes. The essential distinction from Brady's method is that the tracer is confined between two membranes.

In principle, upon passage of current the tagged ions move across one membrane and are replaced by untagged ions entering through the other membrane. Hence analysis of the middle compartment after a known amount of current has passed gives the mobility. In practice, we found that unavoidable joule heating at the membranes causes convection currents throughout the middle compartment so that some of the untagged ions leave through the first membrane instead of the tagged ions and low results are obtained. This same effect presumably forced Brady to keep the movement of his ions to some 15% of the theoretically available distance. Large transports, however, are always advantageous, and in our case of colorimetric analysis they were indispensable. We obtained them by magnetically stirring the middle compartment so that the proportion of untagged ions leaving through the first membrane is always equal to their concentration in the compartment. Hence the concentration of tracer no longer increases linearly with time (at constant current) but logarithmically, and the mobility is given by

$$\mu = \frac{\kappa}{Q} V \ln (C_i/C_f)$$

where C_i and C_f denote the initial and final concentrations of tracer in the middle compartment whose volume is V . Q is the number of coulombs passing through the cell and κ the conductivity of the solution.

Theory

At first sight the method should not work because electroosmotic flow within the porous membrane should, and does, cause bulk flow of the solution. The fact that the apparatus is closed at one end simply nullifies the average flow and makes the solution near the walls of the pores flow in one direction and that near the center in the opposite. The method works, however, and closer examination shows that this is because diffusion of the ions across the pore is rapid compared to the flow along it. As a result, each ion finds itself on the average an equal length of time in any streamline and the liquid flow imparts to it only the average, *i.e.*, zero, velocity.

More quantitatively, the average pore radius in "medium" fritted glass is 3 microns.⁴ A particle having a diffusion coefficient of only 10^{-6} cm.²/sec. requires on the average 0.05 sec. to diffuse that distance according to Einstein's law ($D = x^2/2t$). If the potential gradient within the pores is taken as high as 10 v./cm. and the "zeta" potential as high as 100 mv., the average electroosmotic flow in either direction proceeds at a maximum velocity of 60 microns/sec. The thickness of the fritted glass plugs is at least 1 mm. Hence, the average particle will cross all the streamlines in about a thousandth of the time required for the fastest streamline to carry it through the plug.

Acknowledgment.—We are grateful to the Bristol Myers Co. for support which permitted the undertaking of this work and to the Office of Naval Research for supporting its development through Project ONR-356-254, for which this forms the Seventh Technical Report. Reproduction in whole or in part is permitted for any purposes of the United States Government.

(4) Kindly determined by mercury injection by Dr. I. Fatt of the California Research Corporation.

Number 6 in
Advances In Chemistry Series

compiled by
L. H. Horsley and coworkers at the
Dow Chemical Company

AZEOTROPIC DATA

Contains a 41-page formula index, 107 charts, a 247-page table of binary systems, and a 17-page table of ternary systems.

329 pages—cloth bound—\$4.00 per copy

order from:

Special Publications Department
American Chemical Society
1155 Sixteenth Street, N.W.
Washington 6, D. C.



**A challenging
opportunity for**

SCIENTISTS

- physicists
- mathematicians
- physical chemists
- experimental psychologists

to apply creative, scientific methods to vital problems in military operations research. To above-average scientists seeking above-average rewards, we can offer:

- a secure future
- freedom to think in a virgin field
- growth potential
- important results

Openings are filling rapidly. Send us your resume *now*.

Address: Mr. R. A. Langevin
TECHNICAL OPERATIONS INC.
777 14th Street, N.W.
Washington 5, D. C.



Reprint in Preparation:

JOURNAL OF PHYSICAL CHEMISTRY

Volumes 31-33, 1927-1929 (approx. 2,000 pages per volume)

Single volumes, paper bound, about \$40.00 each

Volumes 34-36, 1930-1932 (approx. 3,000 pages per volume)

Single volumes, paper bound, about \$50.00 each

Previously Reprinted:

Volumes 37-55, 1933-1951

(Slightly reduced format)

Paper bound set

\$475.00

Single volumes, paper bound

\$25.00 each

(Vols. 45, 49, 53 not available separately)

JOHNSON REPRINT CORPORATION

125 East 23 Street, New York 10, N. Y.



NUCLEAR AND RADIOCHEMISTRY

BY GERHART FRIEDLANDER, Brookhaven National Laboratory
and JOSEPH W. KENNEDY, Washington University

Written from the chemist's viewpoint and based on the widely used *INTRODUCTION TO RADIOCHEMISTRY* by the same authors, this new work offers a modern introduction to nuclear science. A large portion of the earlier book has been either rewritten or rearranged; approximately 65% of the material appears in this version for the first time. Greatly expanded reference lists at the end of each chapter include not only books covering the subject matter of the chapter and selected research papers, but also recent review articles and monographs.

NEW FEATURES:

- A new introduction to artificial radioactivity.
- A completely rewritten and expanded discussion of nuclear properties and nuclear systematics.
- Expanded material on reaction mechanisms, high-energy reactions, fission, cross section, neutrons, and neutron reactions.
- A modern treatment of new types of accelerators and a new section on target chemistry.
- An added section on equations of transformation in a neutron flux, making it possible to handle most difficult problems of transformations by decay and nuclear reactions.
- A rewritten and rearranged chapter featuring: a) survey of systematics of stationary states of nuclei from the viewpoint of single-particle and collective models, b) expanded treatment of gamma transitions isomerism and internal conversion, c) discussion of selection rules and ft values and some aspects of the Fermi theory in the section on beta decay, d) discussion of alpha decay systematics and spontaneous fission.
- More factual information in the form of graphs, tables, empirical formulas for use in obtaining energies from absorption measurements in nuclear radiation.
- Inclusion of recent developments in techniques and section on decay scheme study.
- Material on applications of tracers to chemical problems, including new material on isotope effects, activation analysis, and new actinide elements.
- Discussion of nuclear reactors and nuclear weapons.
- Section on energy production in stars, cosmic rays, geological and cosmological dating by nuclear methods, and the genesis of the elements.

1955

468 pages

\$7.50

Send today for an on-approval copy.

JOHN WILEY & SONS, INC., 440 Fourth Ave., New York 16, N. Y.